MOLECULAR BASIS OF HERBIVORE RESISTANCE IN *Brassica napus*

Kirsty Jamie McInnes

Submitted in fulfilment of the requirements for the degree of Doctor of Philosophy

College of Medical, Veterinary and Life Sciences
Institute of Molecular, Cell and Systems Biology
University of Glasgow

September 2015

Abstract

On account of their sessile natures, plants depend upon complex internal signalling pathways to monitor their surroundings and engage appropriate responses to adapt to them. The interplay between many environmental factors means the majority of response pathways in plants are activated or repressed by several biotic or abiotic stimuli. Such an overlap has been identified between invertebrate herbivore-induced signalling pathways, and those regulated by a component of sunlight, Ultraviolet-B (UV-B) radiation. UV-B (280-315 nm) is a small yet potent component of solar radiation that can result in the development of macromolecular damage in the majority of living organisms that are exposed to the short wavelength radiation over prolonged periods of time. Plants, on the other hand, seldom exhibit the negative effects of excessive UV-B exposure, but in fact depend on such components of sunlight as environmental signals for regulating their photomorphogenic and metabolic processes. In plants, the constituents of solar radiation are detected by specialised photoreceptor proteins that, upon recognition of specific qualities and/or quantities of light, initiate an array of downstream reprogramming events that can promote fundamental developmental processes, such as germination, or dictate the positioning of photosynthetic organelles in cells to maximise the rates of photosynthesis while protecting the apparatus from excessive illumination. UV-B radiation is perceived by a UV-B photoreceptor, UV RESISTANCE LOCUS8 (UVR8), via intrinsic UV-B-absorbing tryptophan chromophore residues that are embedded within the protein. UVR8 is present in the cytoplasm and nucleus as a homodimer when in the absence of UV-B, and upon detection of the short wavelength radiation, it undergoes monomerisation and accumulates in the nucleus, where it interacts with the E3 ubiquitin ligase, CONSTITUTIVELY PHOTOMORPHOGENIC1 (COP1), initiating subsequent UVR8-signalling cascades. UVR8-mediated responses include suppression of hypocotyl extension, activation of DNA damage repair mechanisms, and increased biosynthesis of UV-B-absorbing flavonoids, along with their accumulation in the epidermis.

Previous research has found that UV-B radiation can reduce the susceptibility of many species of plants to pathogen infection, invertebrate herbivory and invertebrate oviposition, in that plants placed under UV-B-excluding filters in controlled experimental conditions or in the field sustaining higher levels of tissue damage to pests and pathogens. Microarray studies have identified genes differentially regulated by herbivory and UV-B radiation, including genes involved in the biosynthesis of the wound response phytohormone,

jasmonic acid (JA). It has been suggested that plant sensitivity to JA is heightened, possibly due to regulation in expression or the stability of components involved in downstream JA signalling events. As such, the exact molecular mechanisms of UV-B-enhanced plant defence against invertebrate pests and necrotrophic pathogens are somewhat elusive, although the use of Arabidopsis mutants or over-expressing lines has identified certain genes and pathways that may be involved in this response.

This study aimed to better understand the transcriptomic and metabolic basis of UV-B-mediated defence in the commercially important crop, oilseed rape (*Brassica napus*), against two destructive invertebrate pests, the grey field slug (*Deroceras reticulatum*) and larvae of the Diamondback moth (*Plutella xylostella*). Choice chamber bioassays conducted under controlled experimental conditions revealed that both invertebrates displayed a feeding preference for WT Arabidopsis and *B. napus* plants maintained under minus UV-B conditions, while use of Arabidopsis *uvr8-1* mutants and *35S*pro:GFP-UVR8 over-expressing lines found that a UV-B-mediated reduction in plant susceptibility is not regulated by UVR8. Several early-induced *B. napus* transcription factors were identified in RNA-seq as being commonly regulated by UV-B radiation, MeJA treatment, slug herbivory or *Plutella* herbivory, including *WRKY40, ANAC102, ZAT6* and *ERF104,* while a selection of chlorine-containing metabolites, putative lipid-based molecules and compounds associated with the phenylpropanoid pathway were found to accumulate in response to UV-B- radiation and invertebrate herbivory using reversed-phase HPLC.

Two genes were selected from the RNA-seq data for over-expression in Arabidopsis, based on their increased expression in response to separate UV-B radiation and herbivory treatments in *B. napus*. One of these genes was predicted to encode VITAMIN C DEFICIENT 2 (VTC2), a GDP-L-galactose phosphorylase involved in the first committed step of L-ascorbate biosynthesis from D-glucose. The second is a putative aromatic alcohol dehydrogenase *ELICITOR-ACTIVATE GENE 3-2* (*ELI3-2*), which is part of a family of 9 proteins in Arabidopsis typically involved in the phenylpropanoid pathway. Despite not being identified as differentially regulated in the RNA-seq data, an additional gene, *CAFFEATE O-METHYLTRANSFERASE 1* (*COMT1*), was also over-expressed in Arabidopsis, due to its presence in a branch of the phenylpropanoid pathway previously thought to be important in conferring UV-B-mediated resistance against the necrotrophic fungus, *Botrytis cinerea*. Mutants impaired in the expression of either of these genes retained the ability to deter invertebrate herbivores in a UV-B-dependent manner, while Arabidopsis *COMT1* over-expressing lines treated with UV-B radiation were not only less susceptible to slug and *Plutella* herbivory than non-UV-B-treated plants of the same

genotype, but noticeably more resistant than UV-B-treated Col-0 progenitor lines.

This study obtained extensive information on the genetic and metabolic overlaps in *B. napus* following UV-B radiation and invertebrate herbivory, and the data presented from these studies, along with the results from the over-expressing Arabidopsis lines, will hopefully provide some insight into the possible mechanisms of UV-B-mediated defence against herbivore pests, and facilitate future research into this area of study.

TABLE OF CONTENTS

LIST OF FIGURES

Chapter 1

Chapter 2

Chapter 3

Chapter 4

Chapter 5

Chapter 6

Chapter 7

LIST OF TABLES

Chapter 2

Chapter 3

Chapter 4

Acknowledgements

Firstly, I'd like to thank my supervisor, Prof. Gareth Jenkins. Thank you for having faith in me and for your words of wisdom over the years. You provided me with advice and support when I needed it most, gave me the opportunity to overcome my fear of slugs, and refrained from telling me to leave the lab and never return. I would also like to thank everyone else in the Brian lab, especially those who provided educational and/or whimsical conversations. That also includes the voices in my head, both the good, the bad, and the ones that nearly got me into trouble on multiple occasions. A large thank you goes to Dr's Catherine Cloix, Katherine Baxter and Lisa Blackwood, three wonderful people who were there for me throughout my whole PhD. Well, at least until they all got jobs elsewhere and effectively abandoned me in the lab during my final year. Not that I'm holding any grudges. Seriously, though, I really appreciate everything you did for me, and for just being my friends. Thank you to Dr. Bobby Brown, not just for helping me during my Ph.D, but also for looking out for me during my Honours project as an undergraduate student. Thank you also to the other members of the Brain lab, both past and present, who offered me friendship, advice (some of it useful), and jolly good banter: Prof. John Christie, Kirsten Findlay, Dr's Ashutosh, Bhavana Sharma, Monika Heilmann, Chris Velanis, Stuart Sullivan and Jan Petersen. Thank you also to Dr's Pawel Herzyk, Graham Hamilton and Justin Van der Hooft at the Glasgow Polyomics facility, who made Chapter's 4 and 5 of this thesis possible by helping me with the data analysis and teaching me how to make sense of all the information from the transcriptomics and metabolomics. Thank you also to Prof. Anna Amtmann for her time helping me to better interpret the RNA-seq data.

Thank you to my Co-PI's at Norwich, Dr. Chris Ridout and Prof. Lars Østergaard, who helped me throughout this project, and let me visit them at the John Innes Centre on numerous occasions. I'd also like to acknowledge other members of staff at the JIC, who helped me figure out what to do with a bunch of insects and a big plant that, until recently, had no sequenced genome: Dr. Ian Bedford and Mr. Gavin Hatt in the Entomology department provided invaluable guidance on conducting invertebrate bioassays, Dr. Martin Trick and Dr. Andrea Harper (University of York) introduced me to the joys of working with the Brassica Unigene and 'R', and Dr's Henk-Jan Schoonbeek, Ruth Bryant and Simon Llyod always provided great conversations and fun nights out in Norwich whenever I visited. My funding body, the BBSRC Crop Improvement Research Club (CIRC) also deserves a big mention here, as they financially fuelled this project, and opened up numerous doors to my future by introducing me to life outside of academia. Thanks to the CIRC, I've met so many wonderful people, including fellow PhD students Harriet Benbow, Mike Rugan and Max Newbert, and I have had some truly spectacular experiences. Oh yeah, did I ever mention that I won the poster prize competition at the dissemination events? Twice? Cause, you know, I did...

I know she probably won't read this, but I can't write this thesis without acknowledging the woman who gave me confidence in myself from the very start. Thank you Miss Crosson, my biology teacher at Williamwood High School. You really looked out for me when things got tough, and took the time just to sit and blether with me whenever I had a bad day. I got the award that year for Human Biology, not just because I rocked that essay on the lymphatic system, but because you kept encouraging me to aim for what I wanted in

life. It was amazing to see that despite everything life threw at you, you just kept that smile on your face and embedded all those contextual cues in our heads to help us with our exams (The Mighty Mitochondria!!). Thank you for being an inspiration.
My final thanks go to my family, starting with my girls, Sonata and Aria. It really is nothing short of a miracle that I didn't slaughter at least one of you over the past four years. But you were, are and always will be my motivation to keep working hard in life. As for the cats, Storm, Rory, Scampi, Sandy, Fionn, Rowan, Rhum, Sithean, Islay, Jura, Tiree, Coll, Bruce and the two interlopers, Tux and Rufus, I say a big, heart-felt 'Meaow.' Thank you also to the human members of my family, for always being there for me, and then obligingly not being there when I told you to go away and leave me alone to write up my thesis. The one person who deserves the biggest acknowledgement has to be my mum. I'm sorry. I know I'm pain. But thank you for being a rock for me, and I appreciate everything that you've gone through for us, not just in the past 4 years, but since the beginning. You kept us safe and got me to school every morning, and also put up with my slightly bizarre thought processes (I still regard them as historical breakthroughs, but lets agree to disagree…). For the record, I still stand by my beliefs that a 'shepherd' should be called a 'sheepherd,' and that relocating Ayr to the East coast of Scotland would help help my geographical capabilities immensely. Thank you mum, I love you.

Author's declaration

I declare that, unless otherwise stated, the work presented in this thesis is entirely of my own work and has not been submitted for any other degree at another institution.

This project was funded by the BBSRC Crop Improvement Research Club, to which I am eternally grateful.

Kirsty Jamie McInnes

Abbreviations

35S	Cauliflower mosaic virus *35S* promoter
-UV-A/B	illumination conditions lacking UV-A or UV-B radiation
+ UV-A/B	illumination conditions supplemented with UV-A or UV-B radiation
$\mu mol\ m^{-2}\ s^{-1}$	the quantity of light photons reaching one meter squared per second
ANAC	NAC domain-containing protein
ANOVA	ANalysis Of VAriance
AOS	ALLENE OXIDE SYNTHASE
ARR	ARABIDOPSIS RESPONSE REGULATORS
ATP	Adenosine TriPhosphate
bHLH	beta Helix-Loop-Helix domain
BSA	Bovine Serum Albumin
bZIP	basic leucine Zipper
CAD	CINNAMYL ALCOHOL DEHYDROGENASE
CCoAOMT	CAFFEOYL CoA *O*-Methyltransferase
cDNA	complimentary DeoxyriboNucleic Acid
CGA	Chlorogenic Acid
CHS	CHALCONE SYNTHASE
CO	CONSTANS
COI-1	CORONATINE INSENSITIVE 1
Col-0	Columbia-0
COMT1	CAFFEATE *O*-METHYLTRANSFERASE
COP1	CONSTITUTIVELY PHOTOMORPHOGENIC1
CRY	Cryptochrome
CYP	Cytochrome P450 hydroxylase family members
DAMPs	Damage Associated Molecular Patterns
DAVID	Database for Annotation, Visualisation and Integrated Discovery
dNTP	deoxyriboNucleotide TriPhosphate
EF1a	ELONGATION FACTOR 1a
ELI3-2	ELICITOR ACTIVATED 3-2
ERD5	EARLY RESPONSE TO DEHYRDRATION 5
ERF	ETHYLENE RESPONSIVE FACTOR
EST	Expressed Sequence Tag
ET	Ethylene
EtOH	Ethanol

FAD	Flavin Adenine Dinucleotide
FC	Fold Change
FDR	False Discovery Rate
FLS	FLAVONONE SYNTHASE
FMN	Flavin Mononucleotide
F5H	FERULIC ACID 5 HYDROXYLASE
GFP	Green Fluorescent Protein
GO	Gene Ontology
3xHA	3xHaemagglutinin tag
HAMPs	Herbivore Associated Molecular Patterns
HPLC-MS	High Pressure Liquid Chromatography-Mass Spectrometry
HSD	Honest Significant Difference
HYH	ELONGATED HYPOCOTYL HOMOLOG
HY5	ELONGATED HYPOCOTYL5
JA	Jasmonic Acid
JA-Ile	JAsmonyl-Isoleucine
JAZ	JASMONATE ZIM-DOMAIN PROTEINS
JIN1	JASMONATE INSENSITIVE 1
kDa	kilo Dalton
L*er*	Landsberg *erecta*
LOX2	LIPOXYGENASE 2
LOV	Light, Oxygen, Voltage
MBP	Maltose binding protein
MeJA	Methyl JAsmonate
MS	Murashige and Skoog salts
MYB	MYB-related transcription factor
MYC2	MYC-related transcription factor
m/z	Molecular mass; mass over charge
$M\text{-}H^-$	Molecular mass in negative ionisation mode
NASC	The European Arabidopsis Stock Centre
O/X	Over eXpressing
PAL	Phenylalanine Ammonia-Lyase
PAMPs	Pathogen Associated Molecular Patterns
PAR	Photosynthetically Active Radiation
PCR	Polymerase Chain Reaction

PHOT	Phototropin
PHY	Phytochrome
PIs	Proteinase Inhibitors
Pr	red light-absorbing form of phytochrome
PR	PATHOGENESIS-RELATED
Pro	Promoter
rbcL	Ribulose-1, 5-bisphosphate carboxylase large subunit
RCC1	Regulator of Chromatin Condensation1
qRT-PCR	quantitative Real-Time Polymerase Chain Reaction
RNA-seq	RNA-sequencing
ROS	Reactive Oxygen Species
RPKM	Reads Per Kilobase per Million
RSRE	Rapid Stress Response Element
RT	Retention Time
RWR	Rapid Wound Responsive
SA	Salicylic Acid
SCF	Skp1-Cull-F-box ubiquitin E3 ligase
SD	Standard Deviation
SDS-PAGE	Sodium Dodecyl Sulfate PolyAcrylamide Gel Electrophoresis
SE	Standard Error
sq-PCR	semi-quantitative Polymerase Chain Reaction
TAE	Tris-Acetate EDTA
TAIR	The Arabidopsis Information Resource
TBS-T	Tris Buffered Saline Triton-X
TBS-TT	Tris Buffered Saline Triton-X Tween
TEMED	N,N,N',N'-TetraMethylEthane-1, 2-Diamine
T-DNA	Transfer DNA
TF(s)	Transcription Factor(s)
TMV	Tobacco Mosaic Virus
Tris	Tris(hydroxymethyl)aminomethane
UN65	Surfac-UN65
UV	UltraViolet
UV-A	UltraViolet-A
UV-B	UltraViolet-B
UV-C	UltraViolet-C

UVR8	UV RESISTANCE LOCUS 8
VOCs	Volatile Organic Compounds
VTC2	VITAMIN C DEFICIENT 2
v/v	Volume/Volume
WRKY	WRKY transcription factor family member
WT	Wild Type
w/v	Weight/Volume
ZAT	Zinc transporter-related gene
ZTL	Zeitlupe

Chapter 1: Introduction

1.1 Solar radiation and plants

As sessile organisms, plants rely on internal signalling networks to detect changes in their environment and regulate their biochemical and physiological processes accordingly to promote growth and survival. On a daily basis, plants are bombarded with a plethora of biotic and abiotic factors, some of which promote developmental processes, such as germination and leaf positioning to maximise photosynthetic processes (Inouea et al., 2008), while others can have negative effects on their survival, such as the transmission of disease or subjection to drought. Undoubtedly, one of the most important environmental factors required for sustaining plant life, and subsequently all life on earth, is solar radiation. Sunlight is not only intrinsic for photosynthetic processes, but also serves as an external signal that can reprogram approximately 20% of a plant's genome (Jiao et al., 2007) leading to an array of photomorphogenic and metabolic modifications in plants, such as seedling emergence, phototropism, inhibition of hypocotyl elongation, and development of reproductive organs (Kami et al., 2010). The biologically relevant range of solar radiation that reaches the planet encompasses the long wavelengths of far-red light (~700-800 nm) to the short wavelengths of Ultraviolet-B (UV-B) radiation at 280-315 nm (Figure 1-1), with the spectrum of visible light between 400-700 nm classed as photosynthetically active radiation (PAR). As the name suggests, constituents of PAR are essential for promoting plant photosynthetic processes, and subsequently sustaining their survival. The different components of solar radiation can have different and overlapping effects on plants, with red light promoting germination and shade avoidance (Aphalo et al., 1999, Kami et al., 2010) and blue light regulating plant growth towards the light source (phototropism), chloroplast accumulation and leaf expansion (Kinoshita et al., 2001, Takemiya et al., 2005, Christie, 2007). Due to the complexity of plant signalling cascades, it is unsurprising that many light-induced responses in plants converge with one another, and also with those regulated by other abiotic and biotic factors, such as temperature and nutrient availability (Jiao et al., 2007, Kilian et al., 2007, Franklin, 2009). Such convergences in signalling pathways are thought to confer cross-tolerance to plants that are exposed to multiple stresses or anticipate subjection to factors typically associated with a "primary" stress (Pastori and Foyer, 2002). A particularly interesting cross-communication event occurs between the UV-B- and wound-induced signalling pathways,

the latter of which is activated by insect and pathogenic pests. Studies have so far illustrated genetic and metabolic overlaps between these two signalling pathways, and it has been shown with numerous plant species that removal of UV-B from their growing environment can increase susceptibility to insect herbivory and oviposition (egg-laying; (Izaguirre et al., 2003)(Caputo et al., 2006, Roberts and Paul, 2006, Demkura and Ballaré, 2012, Mewis et al., 2012). While the ability of UV-B radiation to mediate plant defence against herbivore pests has received much attention over the past two to three decades, the exact molecular mechanisms underpinning this phenomenon remain elusive.

The introductory chapter of this thesis provides a brief overview of plant responses to components of visible and UV-A radiation, followed with a more detailed report of UV-B- and herbivore pest-induced signalling pathways. Overlaps between these light- and wound-responsive pathways will then be presented, along with an introduction to the overall aims of this study.

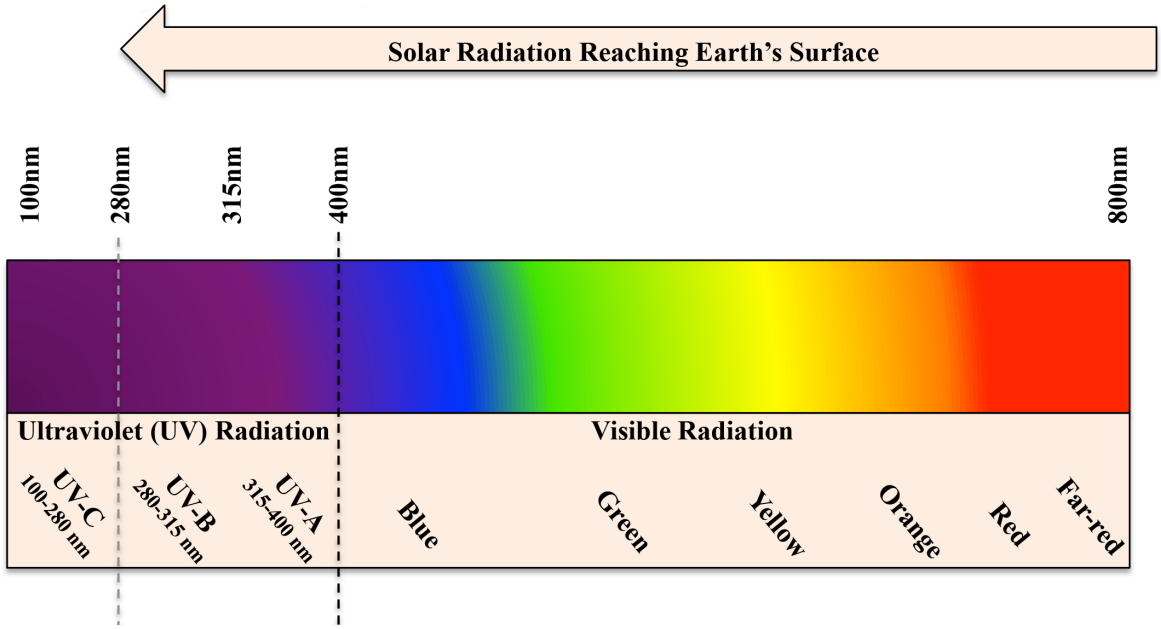

Figure 1-1. Components of the solar spectrum. The visible spectrum and part of the UV spectrum of sunlight (~290-800 nm) reaches the earth's surface, while the stratospheric ozone layer removes the majority of UV-B from the spectrum, along with all UV-C radiation.

1.2 Plant responses to visible radiation

1.2.1 Perception of light via photoreceptor proteins

As previously mentioned, light not only drives photosynthetic processes, but also promotes a wide range of developmental processes in plants. Dark grown seedlings exhibit a variety of skotomorphogenic phenotypes, which include elongated hypocotyls, unopened apical hook, unexpanded cotyledons and lack of pigmentation. Upon detection of light, seedlings undergo major biological reprogramming events that adjust their growth and development. These photomorphogenic plants possess shorter hypocotyls, opened apical hooks, expanded cotyledons and are pigmented (Kim et al., 1998). The detection of sunlight and activation of subsequent signalling pathways is facilitated by a series of photoreceptor proteins that are responsive to the quality of radiation (the wavelengths of light, nm) and the quantity of radiation (the number of moles of photons reaching a given area within a specific time, usually referred to as the fluence rate, μmol m^{-2} s^{-1}). To date five photoreceptor families have been characterised in plants, including red- and far-red light-absorbing phytochromes, blue/UV-A-responsive cryptochromes, phototropins and zeitlupe proteins, and the UV-B-specific UV RESISTANCE LOCUS 8 (UVR8) photoreceptor (Figure 1-2). The phytochromes, cryptochromes, phototropins and zeitlupe proteins absorb photons of light via organic non-protein cofactors called chromophores that typically associate with the apoprotein photoreceptor at the N-terminal region. Upon absorption of light, the chromophores undergo isomerization or reduction that induces a physical change in the structure of the photoreceptor, allowing subsequent activation of light-induced signalling responses (Taiz and Zeiger, 2002). Although each photoreceptor detects specific wavelengths of light, signal integration exists where two or more photoreceptors can activate overlapping genetic and physiological responses.

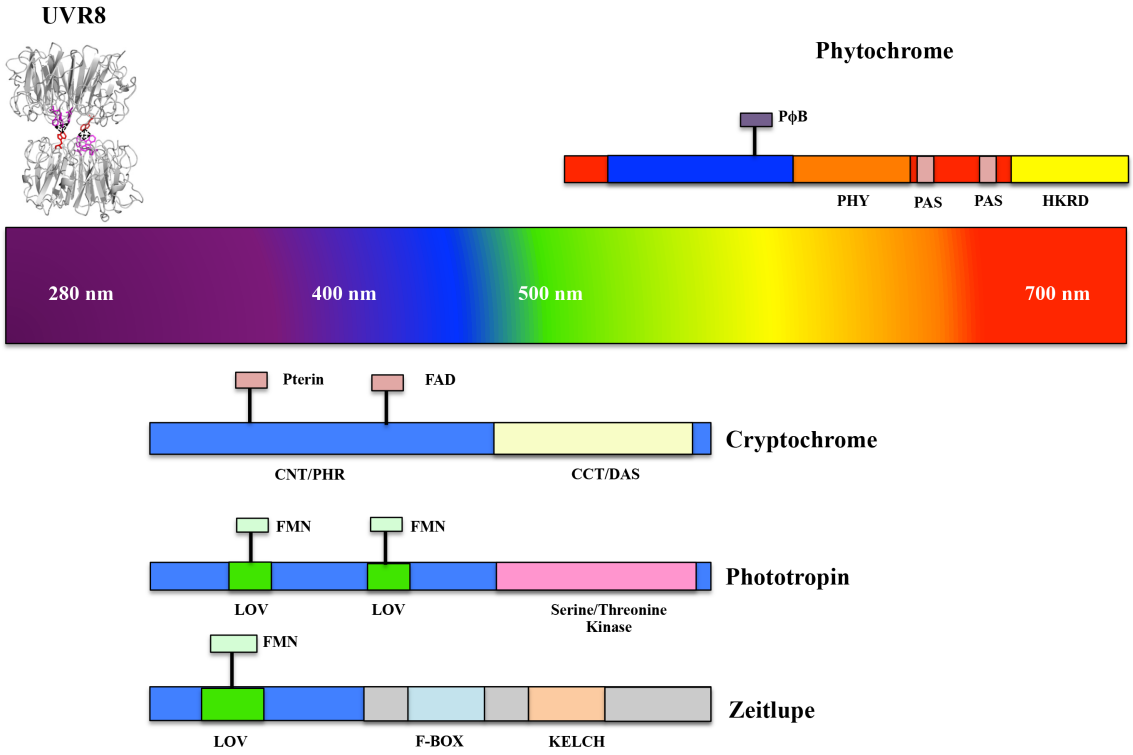

Figure 1-2: Plant photoreceptor proteins and the wavelengths of light they detect. Phytochromes detect red/far-red light, cryptochromes, phototropins, zeitlupe proteins absorb blue/UV-A radiation and UVR8 is a UV-B-specific photoreceptor. **Phytochromes** possess an N-terminal sensory domain that binds covalently to a light-absorbing chromophore, phytochromobilin (PϕB). The C-terminus contains various motifs involved in signalling pathways: Per-ARNT-Sim (PAS) domains and Histidine Kinase-Related Domain (HKRD). **Cryptochromes** contain a Cryptochrome N-terminal Photolyase-Related Domain (CNT/PHR) and less conserved, intrinsically unstructured C-terminal DAS Domain (CCT/DAS); FAD, Flavin Adenine Dinucleotide chromophore. **Phototropins** possess a photosensory N-terminal domain consisting of two light-oxygen-voltage (LOV) domains with flavin mononucleotide (FMN) chromophores. C-terminal contains serine/threonine kinase domain for signalling processes. **Zeitlupe proteins** possess a photosensory N-terminal region with a LOV domain and FMN chromophore, along with an F-Box motif and 6x Kelch repeats (KELCH) in C-terminal region. **UVR8** is a WD40 homodimeric photoreceptor with intramolecular tryptophan chromophores that detect UV-B radiation. Image adapted from (Jiao et al., 2007), UVR8 structure derived from (Jenkins, 2014).

1.2.2 Plant responses to far-red/red light

Red and far-red light-induced plant responses are regulated by the phytochrome photoreceptors, of which there are 5 members in Arabidopsis (phyA-phyE). Each phytochrome contains a photosensory N-terminal domain to which the phytochrombilin (PϕB) chromophore covalently binds, and a regulatory C-terminal region that includes a Histidine Kinase-Related Domain (HKRD) and dimerisation and localisation domains

(Figure 1-2)(Chen and Chory, 2011). The ability of phytochromes to differentiate between red and far-red light is facilitated by the photoreceptor existing in two physical states: the biologically inactive red light-absorbing Pr state, and the biologically active far-red light-absorbing Pfr state (Lagarias and Rapoport, 1980, Briggs and Huala, 1999). Upon detection of red light, the Pr state undergoes a conformational change into the bioactive Pfr form, and its subsequent translocation from the cytoplasm to the nucleus enables the photoreceptor to direct light-responsive processes. This photoconversion is reversible, and Pfr can return to the Pr state upon detection of far-red light or after prolonged exposure to dark conditions (dark reversion)(Rockwell et al., 2006). The phytochromes phyB-phyE are light-stable in Arabidopsis, and regulate responses to low-fluence red light and the red:far-red light ratio. The light-labile phyA, on the other hand, regulates plant responses to very low fluence rates of light and high irradiance, and is rapidly degraded in its active Pfr form (Rockwell et al., 2006).

Phytochrome activity and photoconversion promotes the transition of plants from skotomorphogenic to photomorphogenic growth and development, and regulates the shade avoidance reaction and a series of photoperiodism responses, which lead to flowering and bud dormancy. In addition, the ratio of Pfr:Pr in plants has been implicated in affecting plant susceptibility to pathogenic and herbivore pests, with plants reared under high ratios of far-red:red light, typical in a shaded environment, suffering higher rates of insect consumption and sustaining larger lesions from the nectrotrophic fungus *Botrytis cinerea* (Izaguirre et al., 2006, Cerrudo et al., 2012).

1.2.3 Plant responses to blue light and UV-A radiation

Plant responses to blue light are numerous, with the three blue light photoreceptors, phototropins, cryptochromes and members of the zeitlupe family, controlling various developmental and biochemical responses (Briggs and Huala, 1999).

The cryptochrome family of photoreceptors is made up of three members in Arabidopsis, 2 of which (cry1 and cry2) are involved in entraining the circadian clock and regulating plant developmental processes such as inhibition of hypocotyl elongation (Cashmore et al., 1999, Lin et al., 2002), while the third, cry3, belongs to a cry-DASH (Drosophila, Arabidopsis, Synechocystis and Homo) class of cryptochromes and demonstrates DNA-binding and repair activities (Pokorny et al., 2008). All members of the cryptochrome family possess an amino-terminal photolyase-related (Shinkle et al., 2004) domain that serves as the site of chromophore binding (Figure 1-2). The chromophores include a primary/catalytic

Flavin Adenine Dinucleotide (FAD) along with a light-harvesting pterin (Liscum et al., 2003, Jiao et al., 2007), and also possess a C-terminal (CCT) domain that has been shown to mediate protein-protein interactions and activate downstream signalling events (Liscum et al., 2003). The cry family of photoreceptors regulate entrainment of the circadian clock, seedling de-etiolation and stomatal opening (Liscum et al., 2003), and is known to overlap slightly with phytochrome-regulated responses, such as cell elongation and flowering (Li and Yang, 2007). While cry2 is constitutively localised in the nucleus, cry1 is located in the cytoplasm in dark conditions and undergoes nuclear localisation following detection of light (Liscum et al., 2003). Here, these photoreceptors were shown to interact with the RING E3 ubiquitin ligase and repressor of light signalling, CONSTITUTIVELY PHOTOMORPHOGENIC1 (COP1) to inhibit its suppression of light-mediated responses following photoexcitation of cry by blue/UV-A light (Liscum et al., 2003).

A selection of responses elicited by cryptochromes has been shown to be influenced by phytochromes, with studies on *phya* mutants reporting a loss of several blue light-dependent responses, such as hypocotyl inhibition, cotyledon opening and expansion, and regulation of the circadian clock (Lin, 2000). Yeast two-hybrid screens additionally demonstrated that cryptochromes and phytochromes interact with one another (Ahmad et al., 1998), revealing signal integration between red/far-red light- and blue/UV-A-responsive pathways.

Phototropins, a second blue/UV-A light photoreceptor, possess two Light-Oxygen-Voltage domains (LOV1 and LOV2) at the N-terminal region and a C-terminal serine/threonine kinase domain (Figure 1-2). Detection of blue light is facilitated by flavin mononucleotide (FMN) chromophores, which upon excitation, activate a reversible photocycle by covalently bonding with a cysteine residue in the LOV domain, inducing subsequent conformational changes in the protein and allowing kinase activity of the C-terminal region (Christie, 2007). Several substrates of phot kinases have been identified, for including phototropin itself in a process of autophosphorylation (Briggs and Christie, 2002). Two phototropins have been identified in Arabidopsis (phot1 and phot2) that mediate a variety of rapid light responses including chloroplast relocalisation, stomatal opening, leaf positioning and phototropism (Briggs and Huala, 1999, Christie, 2007). Phototropins have little influence on plant responses to blue light at the transcriptomic scale (unlike phytochromes and cryptochromes)(Jiao et al., 2007), although several proteins intrinsic to phototropin-regulated signalling have been identified, including NON-PHOTOTROPIC HYPOCOTYL3 (NPH3), which is essential for phototropism and lateral auxin redistribution (Demarsy and Fankhauser, 2009).

A third class of blue light photoreceptors, ZEITLUPE proteins, also utilise LOV domains and flavin mononucleotide chromophores for blue light detection. Three members of this family are known to exist in Arabidopsis, namely Zeitlupe (ZTL), Flavin-binding Kelch Repeat F-box 1 (FKF1) and LOV Kelch Protein 2 (LKP2)(Miyazaki et al., 2015). These proteins consist of a single N-terminal LOV domain and FMN chromophore, along with an F-box and several Kelch repeats on the C-terminus (Figure 1-2). Members of the ZEITLUPE family are involved in entrainment of the circadian clock (hence their name) by controlling the proteasome-dependent degradation of a key central clock protein, TIMING OF CAB EXPRESSION1 (TOC1)(Kim et al., 2007b).

1.3 Effects of UV-B radiation on terrestrial plant development

1.3.1 UV-B radiation as an environmental signal for plants

Three components of light make up the UV spectrum: UV-A (315-400 nm), UV-B (280-315 nm) and UV-C (≤ 280 nm; Figure 1-1). All UV-C radiation emitted from the sun, along with the majority of UV-B (below ~ 295 nm), is absorbed by the stratospheric ozone layer (McKenzie et al., 2003), with further fluctuations on the quantity of UV-B reaching various global locations attributed to the angle of the sun's rays, altitude, seasonal positioning of the earth in relation to the sun, the albedo effect of the planet's surface, atmospheric aerosols and cloud cover (Caldwell and Flint, 1994, Schwander et al., 1999, McKenzie et al., 2003, Jenkins, 2009). UV-B radiation is a small yet highly energised component of sunlight that reaches the earth's surface (≤ 0.5% of terrestrial radiation from the sun)(Caldwell et al., 1994), and as such can act as a potentially damaging agent to living organisms by inducing the development of cataracts, chronic sunburn, melanoma and macromolecular damage via the formation of pyrimidine dimers (Norval et al., 2007). Plants on the other hand, despite their sedentary nature, seldom exhibit negative effects of UV-B exposure, a trait attributed to the presence of protective mechanisms that minimise the extent of UV-B-induced damage in cells by promoting an array of genetic, metabolic and photomorphogenic responses (Flint et al., 2008, Jenkins, 2009, Tilbrook et al., 2013). These UV-B-induced responses can be broadly divided into two categories based on the nature of the activated signalling pathways: "photomorphogenic" responses and "stress-related" responses. The activation of one response category over another is determined by the duration, quality and quantity of radiation, but whether or not a plant has received a period of adaptation or acclimation to UV-B can also influence its degree of tolerance. For

instance, plants that have been grown in the absence of UV-B (particularly under controlled, laboratory conditions) are more likely to develop stress-related responses when introduced to UV-B radiation for the first time than plants that have been maintained under low UV-B fluence rates for at least several days. These plants tend to tolerate higher fluence of UV-B radiation better than non-acclimatised plants, and exhibit constant, steady-state expression of many UV-B-responsive genes following the transition from low to high fluence rate conditions, indicating continuous activation of basal plant protective mechanisms (Jenkins, 2009).

Photomorphogenic responses are induced by low fluence rates of UV-B radiation that serve as informative environmental signals to bring about a range of developmental and biochemical changes within plants, such as inhibition of hypocotyl elongation (Barnes et al., 1996, Kim et al., 1998) and the production of UV-absorbing phenolic compounds (Lois, 1994)(Brosche and Strid, 2003). High fluence rates of UV-B, on the other hand, lead to the development of tissue necrosis, reduced plant growth and crop yield, and can also induce a series of stress-related responses that are also regulated by other environmental stresses (A-H-Mackerness et al., 1999, Brosche and Strid, 2003, Frohnmeyer and Staiger, 2003, Jenkins, 2009).

1.3.2 UV-B photomorphogenic signalling pathways

Low doses of UV-B radiation serve as informative signals to plants and regulate a range of developmental processes, such as the promotion of cotyledon opening and the decreased rate of hypocotyl elongation and primary root growth (Ballaré et al., 1995, Kim et al., 1998 , Boccalandro et al., 2001, Shinkle et al., 2004), and the activation of DNA-damage repair mechanisms and antioxidant scavengers of reactive oxygen species (ROS)(S.A.-H.-Mackerness et al., 1999)(A.-H.-Mackerness et al., 2001). UV-B also induces a variety of protective mechanisms, such as the deposition of UV-reflecting epicuticular wax layers and accumulation of UV-absorbing phenolic compounds in the epidermis, which serves to reduce the extent of UV-B penetration into the leaf and potential damage it may cause to macromolecules and photosynthetic organs (Holmes and Keiller, 2002, Jenkins, 2009). These photomorphogenic and biochemical responses to UV-B radiation are regulated by a UV-B-specific signalling component, UV RESISTANCE LOCUS 8 (UVR8), which was identified over a decade ago (Kliebenstein et al., 2002) and recently confirmed as a UV-B-specific photoreceptor (Rizzini et al., 2011).

1.3.2.1 UV-B photomorphogenic signalling pathways are regulated by UVR8

UVR8 is encoded at the *UV RESISTANCE LOCUS 8* locus, which was first identified by Kliebenstein and co-workers in 2002 utilising a forward genetics approach to screen Arabidopsis mutants displaying UV-B-hypersensitive phenotypes. The isolation of a mutant displaying increased UV-B sensitivity in the form of leaf necrosis and stunted growth in the presence of UV-B led to the discovery of *uvr8-1* (Kliebenstein et al., 2002). This mutant was also unable to regulate the biosynthesis of UV-absorbing flavonoid compounds in the phenylpropanoid pathway, with transcript and protein levels of CHALCONE SYNTHASE (CHS), the enzyme involved in the first committed step of the flavonoid biosynthesis pathway, being significantly lower in the *uvr8-1* mutant compared to wild type (WT) plants. The presence of stress-related proteins (e.g. PR1) and ROS scavengers in *uvr8-1* plants implied that reduced transcript and protein levels of CHS was not caused by a general loss of stress-induced responses (Kliebenstein et al., 2002), but was later shown to be a UV-B-specific response as both WT, *uvr8-1* and *uvr8-2* Arabidopsis lines displayed similar levels of *CHS* expression in response to far-red light and UV-A radiation, along with sucrose and cold temperature treatments (Brown et al., 2005).

Transcriptomic studies with *uvr8-1* and additional alleles identified a large subset of UV-B-responsive genes that were regulated in an UVR8-dependent manner (Brown et al., 2005, Favory et al., 2009). Several of these genes encoded transcription factors, with one in particular, the basic leucine-zipper (bZIP) protein ELONGATED HYPOCOTYL5 (HY5), serving as an intrinsic regulator of the expression of UV-B-responsive genes (Ulm et al., 2004, Brown et al., 2005). Inclusion of the *hy5* mutant in an Arabidopsis microarray revealed that approximately 50% of UVR8-responsive genes are transcribed by HY5, indicating its role downstream of UVR8 in the UV-B-response pathway (Brown et al., 2005). HY5 was found to share functional redundancy with its homologue, HYH, another bZIP transcription factor shown to be responsive to UV-B radiation. Gene expression analysis of *hy5* and *hyh* mutants revealed HY5 to have a more dominant role in transcribing UV-B-responsive genes that HYH, as expression of select UV-B-responsive genes, including *CHS* and *ELIP1* (*EARLY LIGHT-INDUCIBLE PROTEIN1*), was significantly reduced in the *hy5* and *hy5hyh* mutants, but not in *hyh* (Brown and Jenkins, 2008).

HY5 is not a UV-B-specific transcription factor, but is also known to regulate a number of signalling pathways governed by red- and blue-light photoreceptors (Osterlund et al., 2000,

Oravecz et al., 2006). Activity of HY5 is regulated by the E3 ubiquitin ligase, COP1, a repressor of light-signalling events that targets components of light-response pathways for degradation in the dark, but is itself targeted for inactivation and nuclear exclusion in the presence of visible light (Osterlund et al., 2000). However, COP1 was reported as being a positive regulator of UV-B photomorphogenic responses in plants and an essential component required for UV-B-dependent expression of *HY5* and subsequent activation of the UV-B-signalling pathway (Oravecz et al., 2006). Photomorphogenic responses to UV-B are absent in *cop1*, *uvr8* and *cop1 uvr8* double mutants (Oravecz et al., 2006), suggesting that both proteins are intrinsic components in the regulation of UV-B responses.

The use of GFP-UVR8 constructs revealed that UVR8 is predominantely located in the cytosol under minus UV-B conditions, but undergoes rapid nuclear localisation upon irradiation (Brown et al., 2005, Kaiserli and Jenkins, 2007, Jenkins, 2009). The presence of UVR8 in the nucleus suggested some sort of transcriptional regulatory role for this protein, a hypothesis that was supported when ChIP analysis revealed that UVR8 associates with the *HY5* promoter region (Brown et al., 2005). In addition, CFP-UVR8 and YFP-COP1 constructs were found to interact with one another in a UV-B-dependent manner in mustard plants, indicating that these two signalling components can directly influence transcription of UV-B-responsive genes (Favory et al., 2009).

While the regulation of UV-B-responsive signalling pathways by UVR8 was being extensively studied soon after its discovery in 2002 (Kliebenstein et al., 2002), details of the structure and regulation of UVR8 were not published until fairly recently (Rizzini et al., 2011, Christie et al., 2012, Wu et al., 2012). UVR8 is a seven-bladed β-propeller WD40 protein of 440 amino acids (Christie et al., 2012, Wu et al., 2012) that is predominantly present in the cytosol as homodimer in the absence of UV-B radiation, and undergoes rapid monomerisation following UV-B exposure. Structurally, the UVR8 protein was shown to share 35% identity to that of the human REGULATOR OF CHROMATIN CONDENSATION 1 (RCC1) protein, a guanine nucleotide exchange factor (GEF) for the G-protein, Ran (Brown et al., 2005, Jenkins, 2009). UVR8 was not found to share functional similarity to RCC1, however, as the UV-B-signalling component lacks several amino acids required for maximal GEF activity in RCC1 and its interaction with Ran, was shown to possess under 10% GEF activity on human Ran compared to RCC1 in *E. coli* cells, and failed to interact with Arabidopsis Ran proteins in yeast two-hybrid experiments (Brown et al., 2005). The rapid monomerisation and nuclear localisation of UVR8 in response to UV-B radiation, along with the enhanced sensitivity and stressed-induced phenotypes of UV-B-irradiated *uvr8* mutants, indicated that UVR8 might possess a UV-B-

photoreception role in plants. The role of UVR8 as a UV-B-specific plant photoreceptor was recently confirmed (Rizzini et al., 2011), with the mode of detection of UV-B photons detailed shortly thereafter. Unlike the far-red/red and blue/UV-A photoreceptors previously mentioned in section 1.2, UVR8 does not depend on a non-protein chromophore for UV-B photon absorption. Photoreception of UVR8 is instead dependent on intramolecular tryptophan (W) residues that possess an absorption maximum of 280nm (UV-B; 280-315nm), and serve as the light-absorbing chromophore in the activation of UVR8 (Christie et al., 2012, Wu et al., 2012). The UVR8 dimer possesses 14 tryptophan residues along its dimer interface, with three of them from one monomer, W233, W285 and W337, forming the base of a pyramid with the W94 residue from the second monomer as its apex. Mutagenic studies revealed, however, that only residues W285 and W233 are critical for UV-B perception (Christie et al., 2012, Wu et al., 2012). The $UVR8^{W285A}$ mutant, which has an alanine residue in place of a tryptophan residue, appeared to be constitutively monomeric and associated with COP1 in the presence or absence of UV-B radiation, while mutating tryptophan to phenylalanine resulted in a constitutive UVR8 dimer that failed to monomerise in response to UV-B, and subsequently was unable to interact with COP1 (O'Hara and Jenkins, 2012, Heijde et al., 2013). It was thus confirmed that the UV-B photoreceptor UVR8's mechanism of photon detection was achieved through specific intramolecular tryptophan residues on the dimer interface of the protein.

1.3.2.2 UV-B photomorphogenic responses

Upon detection of UV-B radiation by intrinsic tryptophan residues, UVR8 regulates a variety of genetic reprogramming events via transcription factors, such as HY5, to initiate an array of photomorphogenic and metabolic responses. One of the most obvious phenotypic responses to UV-B radiation is the reduction in hypocotyl elongation in seedlings. Near-ambient levels of UV-B radiation were found to rapidly reduce hypocotyl elongation of tomato (*Lycopersicon esculentum*) seedlings, with an approximate 45% reduction in the length of UV-B-treated seedlings over minus UV-B-treated seedlings detected 4 hours after the start of irradiation (Ballare et al., 1995). Inhibition of hypocotyl elongation was also observed in response to less than 0.1 μmol m^{-2} s^{-1} UV-B (Kim et al., 1998), indicating that the molecular mechanisms for this physiological adaptation are very sensitive to UV-B radiation.

An additional UV-B-sensitive molecular response that provides tolerance to short wavelength radiation is the accumulation of UV-absorbing phenolic compounds in the

epidermis of plants. Components of the flavonoid biosynthesis pathway, a branch of the phenylpropanoid pathway involved in the production of anthocyanins, flavones and flavonols (Winkel, 2006), have received much attention with regards to their responsiveness to UV-B radiation (Li et al., 1993, Frohnmeyer et al., 1999, Jenkins et al., 2001, Warren et al., 2003, Tattini et al., 2004). *CHS* transcripts have been shown to be sensitive to low doses of UV-B, with *CHS* gene expression rapidly increasing following millisecond exposures to UV-B radiation in parsley cell cultures (Frohnmeyer et al., 1999) or after ≤ 5 min exposures to UV-B in Arabidopsis (Jenkins et al., 2001, Jenkins, 2009). Studies on Arabidopsis mutants with reduced or no pigmentation on the seed coat (testa) identified 11 loci referred to as *transparent testa* (*tt*) that are required for the biosynthesis of flavonoids (Shirley et al., 1995). Two mutants, *tt4* and *tt5*, impaired in CHS and CHALCONE ISOMERASE (CHI) activity, respectively, were found to be completely deficient in flavonoids and highly sensitive to UV radiation (Li et al., 1993). Interestingly, studies on Arabidopsis mutants impaired in the biosynthesis of sinapate esters, an alternative branch of the phenylpropanoid pathway involved in lignin production, have likewise been shown to be highly sensitive to UV-B radiation, and in some cases more susceptible to UV-B-induced damage that *tt* mutants (Landry et al., 1995). One mutant impaired in the activity of FERULIC ACID HYDROXYLASE, *fah1*, displayed upward leaf curling when exposed to low fluence rates of UV-B radiation (0.4 kJ m^{-2} h^{-1}) for 72 hours, while *tt5* mutants only developed similar phenotypes indicative of UV-B-induced stress under slightly higher fluence rates (0.6 kJ m^{-2} h^{-1}). Regardless of the difference in degree of sensitivity these mutants have to UV-B radiation, it is evident that the phenylpropanoid pathway plays a major role in conferring plant tolerance and protection to UV-B radiation.

The molecular mechanisms underlying these physiological responses are regulated at the genetic and biochemical level (Jenkins, 2009), with studies on plant cell suspension cultures revealing that regulation of *CHS* expression requires calcium ions, calmodulin and protein phosphorylation (Christie and Jenkins, 1996b, Frohnmeyer et al., 1997). Application of 50 μM of the voltage-dependent calcium channel blocker nifedipine to cell cultures inhibited the expression of *CHS* in response to blue light, UV-A and UV-B radiation, as did incubation of cell cultures with serine/threonine protein kinase inhibitors. Addition of the calmodulin antagonist W-7 also impaired accumulation of *CHS* transcripts to levels observed in untreated cell cultures following UV-B radiation but not UV-A or blue light, implying that UV-B-regulation of *CHS* expression is slightly distinct from UV-A/blue light-regulation of flavonoid biosynthesis (Christie and Jenkins, 1996a).

In addition to mutation screens, microarray studies have expanded our knowledge on the genetic mechanisms of UV-B-induced plant responses (Ulm et al., 2004, Brown et al., 2005, Kilian et al., 2007, Morales et al., 2010). In a study conducted by Ulm and co-workers (2004), a total of 107 Arabidopsis transcripts were identified as being differentially regulated (with a minimum fold change in expression of 2) by low wavelengths of UV-B radiation (≤ 305 nm). Approximately 20 of these transcripts encoded transcription regulators, including those involved in developmental processes (CIA2 and MYB13) and abiotic stress responses (ZAT10, ZAT12, ABF3 and AZF2), along with the known light-responsive transcription factors, HY5 and HYH (Ulm et al., 2004, Brown et al., 2005, Kilian et al., 2007). Some of the identified transcription factors were found to positively regulate UV-B-induced signalling pathways, while others serve as repressors of UV-B-induced responses. Members of various transcriptional regulator families, such as MYB-related proteins, WRKY DNA-biding proteins, and NACs, have been suggested to play roles in the regulation of plant responses to UV-B radiation, with HY5 still remaining the most important and well-studied transcription factor involved in the UV-B response pathway. Indeed, the expression of several genes encoding UV-B-responsive transcription factors has previously been shown to be regulated by HY5, with expression of *MYB12* and *MYB111*, two genes encoding R2R3-MYB transcription factors important in the production of flavonoid compounds, being lower in *hy5* Arabidopsis mutants than WT and *hyh* mutants (Stracke et al., 2010a).

Expression of MYB34/ATR1, a MYB transcription factor proposed to regulate expression of genes in the tryptophan pathway, was found to decrease in response to UV-B radiation, as was the gene encoding a known repressor of UV-B-induced responses, *MYB4* (Jin et al., 2000, Ulm et al., 2004). Other MYB-encoding genes have been shown to increase in expression following UV-B radiation, such as *MYB13*, encoding a transcription factor involved in developmental processes, and *MYB111*, which functions alongside *MYB12* to regulate flavonoid biosynthesis in Arabidopsis seedlings (Ulm et al., 2004, Stracke et al., 2007). Expression of *MYB1*, the main regulator of the phenylalanine ammonia-lyase gene (*PAL1*) in suspension-cultured cells of carrot (*Daucus carota*), was found to peak 2 hours into treatment with UV-B radiation, with levels of *PAL1* starting to increase approximately 1 hour afterwards (Maeda et al., 2005). These studies revealed multiple rapid responses in plants to UV-B radiation, and further highlighted the importance of the phenylpropanoid pathway in promoting plant protection against UV-B.

1.3.3 "Stress-related" responses in plants induced by high fluence rates of UV-B radiation

Prolonged exposure to UV-B radiation, especially short wavelengths and high fluence rates that are above typical ambient levels, can induce a myriad of biochemical and physical changes in plants that are reminiscent of those induced by other environmental stresses, such a drought, low temperatures, and invertebrate pest attack. These responses include activation of DNA-damage repair mechanisms and an accumulation of ROS scavenging agents and antioxidants (Britt et al., 1993, Jansen et al., 1998, Jenkins, 2009).

DNA damage from UV radiation primarily takes the form of cyclobutane pyrimidine dimer (CPD) formation, and to a lesser degree the production of pyrimidine [6-4] pyrimidinone dimers (6-4 photoproduct)(Britt et al., 1993, Britt, 2004). These photoproducts can inhibit transcriptional processes and subsequently lead to the growth arrest and death of cells. To counteract UV-induced DNA damage, plants initiate rapid DNA-damage repair mechanisms, such as nucleotide excision repair and homologous recombination, to remove the majority of photoproducts before a mutation arises (Strid et al., 1994). In addition, pyrimidine dimers are primarily repaired in a process known as photoreactivation, which is mediated by photolyase proteins in the presence of blue/UV-A light (Britt, 2004).

An additional nonspecific UV-B response seen in plants is the accumulation of ROS, which commonly accumulate in response to numerous biotic and abiotic stresses and cause oxidative damage to cellular components. The origin of ROS produced by UV-B is not obvious, however the inhibition of photosynthetic electron transport as a result of the damaging effects of UV-B on photosystem II may be one source of ROS production (Jansen et al., 1998)(A-H.-Mackerness, et al., 2001). To counteract the effects of ROS, plants increase the biosynthesis and accumulation of ROS scavengers and antioxidants in cells. Several transcriptomic reports have identified various genes associated with reducing oxidative stress as being UV-B-responsive (Ulm et al., 2004, Brown et al., 2005, Kilian et al., 2007). Likewise, metabolic studies have found that the abundance of particular antioxidants, such as ascorbic acid (AsA)(Landry et al., 1995, Conklin et al., 1996, Kusano et al., 2011), increases in response to UV-B radiation in Arabidopsis. AsA has been documented as reversing some of the responses elicited in plants by UV-B radiation. For example, cotyledon curling in *B. napus* was found to occur in response to UV-B radiation, but inhibited by AsA (Gerhardt et al., 2005). Two mutants impaired in the biosynthesis of phenolics, *tt5* and *fah1*, were found to possess higher levels of ascorbate peroxidase activity than L*er* controls in the presence of UV-B, indicating that

these two mutants experience increased oxidative stress due to UV-B (Landry et al., 1995). This enhanced level of oxidative stress was thought to be partly a result of the decreased levels of UV-absorbing phenolics in the epidermis, subsequently allowing for greater penetration of UV-B photons to cellular organelles. Mutants impaired in the biosynthesis of AsA, such as *vtc1*, are highly sensitive to UV-B radiation, as following exposure to UV-B radiation, *vtc1* mutants exhibit oxidative damage through increased levels of hydrogen peroxide and thiobarbituric acid reactive substances (TBARS). In addition, activity of the main ROS scavenging enzymes, such as superoxide dismutase, catalase and ascorbate peroxidase, was insufficient to confer protection to the *vtc1* mutants, indicating the importance of AsA for plant survival under UV-B conditions (Gao and Zhang, 2008).

1.3.4 UV-B signalling pathways overlap with other biotic and abiotic pathways

UV-B radiation has been found to integrate into other biological signalling pathways regulated by several environmental stimuli such as cold temperatures, drought and wounding (Takeuchi et al., 1993, Chalker-Scott, 1999, Stratmann et al., 2000, Alexieva et al., 2001, Gitz and Liu-Gitz, 2003, Maeda et al., 2005, Kilian et al., 2007, Demkura and Ballaré, 2012, Mewis et al., 2012). The convergence between UV-B-regulated pathways and those typically associated with other environmental factors has been studied at the genetic and metabolic scale, as well as on a physiological level. In many cases UV-B has been demonstrated to alleviate the effects of several environmental stresses on plant fitness and development, particularly from drought (Alexieva et al., 2001) and invertebrate herbivory (Stratmann et al., 2000, Izaguirre et al., 2003, Izaguirre et al., 2007, Demkura and Ballaré, 2012, Mewis et al., 2012).

Drought and UV-B have been shown to induce similar physiological and biochemical responses in plants, albeit to different degrees of intensity (Alexieva et al., 2001). Both environmental factors can stimulate a reduction in plant growth rate, stem elongation and leaf expansion (Gitz et al., 2005), although this response is greater in pea (*Pisum sativum*) and wheat plants subjected to UV-B radiation than drought stress (Alexieva et al., 2001). Combining both treatments to pea plants reduced both the extent of UV-B-induced stem growth inhibition and the drought-induced reduction of relative leaf water content (RWC) in plant cells, suggesting that these two environmental signals integrate with one another to lessen the effects of drought stress on plant growth and water loss. This hypothesis was further supported when UV-B was shown to induce accumulation of osmolytes (e.g. proline) and stress proteins, such as superoxide dismutase and catalase, quicker than

drought stress in wheat and pea plants, which provided a possible explanation for the improved RWC observed in plants subjected to both treatments simultaneously (Alexieva et al., 2001). Biologically effective levels of UV-B radiation were also found to reduce stomatal density and aperture in rice, decrease stomatal conductance in pea plants, and reduce stomatal density and conductance in soybean (*Glycine max*)(Gitz and Liu-Gitz, 2003), in an attempt to reduce water loss from plants.

UV-B radiation has also been shown to increase expression of many wound-responsive genes that are normally induced following pathogenesis or insect herbivory (Izaguirre et al., 2003, Kilian et al., 2007, Mewis et al., 2012). Bioassay experiments with invertebrates demonstrated that plants reared under attenuated or no levels of UV-B sustain greater levels of consumption and increased use as an oviposition platform than those maintained under UV-B conditions (Rousseaux et al., 1998, Rousseaux et al., 2004, Caputo et al., 2006, Kuhlmann and Muller, 2009a, Demkura et al., 2010, Mewis et al., 2012). The involvement of UV-B radiation in promoting plant defence against herbivore pests and select pathogens has received much attention over the past two to three decades, however the exact molecular mechanisms underpinning the convergence in these signalling pathways remain elusive. The remainder of this introduction describes our current knowledge on UV-B-mediated plant defence mechanisms against herbivore and pathogen pests obtained from transcriptomic, mutagenic and metabolic studies.

1.4 Plant defence against invertebrate pests

As primary producers, terrestrial plants are susceptible to attack from pathogen and herbivore pests, both of which have the potential to destroy an entire crop through the transmission of disease or tissue loss from consumption. Invertebrate pests, which include insect and gastropod organisms, not only depend on plants as a food source but also as a shelter from predators and a site for oviposition. Plants can detect the presence of invertebrate pests through the use of several surveillance mechanisms that recognize physical and chemical characteristics of invading pests, however our understanding of the modes of detection is poor in contrast to our knowledge of plant recognition of pathogens (Jones and Dangl, 2006). Chemical elicitors present in invertebrate saliva or oviposition fluid can be transferred to the plant host upon contact, and contain invertebrate-derived compounds or invertebrate-modified plant-derived compounds (Howe and Jander, 2008). These effectors are thought to be detected by disease resistance (R) proteins in plants, that

subsequently induce appropriate defence response against the attacking invertebrate (Jones and Dangl, 2006). In addition, detection of physical characteristics of invertebrates (Damage/Herbivore Associated Molecular Patterns (DAMPs/HAMPs)(Erb et al., 2012)) or wound trauma sustained from grazing invertebrates can also serve as a trigger for plant defence responses, inducing the establishment of structural barriers, release of chemical deterrents, or production of toxic compounds as defence mechanisms. Plant defence against invertebrate and pathogenic pests is regulated by several plant phytohormones, mainly salicylic acid (SA), ethylene (ET) and jasmonic acid (JA). These hormones can work synergistically and antagonistically to regulate pathogen and pest defence responses in very complex signalling pathways, with SA and associated derivatives crudely considered as the predominant pathogen-response signalling molecules, while JA and derivatives are regarded as the main defence regulators against invertebrate pests (Farmer and Ryan, 1992, Bari and Jones, 2009).

1.4.1 Plant defence is regulated by the interplay of phytohormones

The interplay of SA, JA and ET and associated derivatives in mediating plant defence is believed to be an evolutionary tactic that broadens the protective capabilities of plants to the numerous attacking pests they are subjected to on a daily basis (Penninckx et al., 1998, Reymond and Farmer, 1998, Vos et al., 2005). The molecular basis of this overlap between signalling molecules remains somewhat elusive, however it is known that different pathogen and invertebrate species can induce varying degrees of SA-, JA- and ET-regulated responses, demonstrating the complexity of plant defence.

Inoculation of Arabidopsis with the biotrophic pathogen *Pseudomonas syringae* was found to increase SA, JA and ET production, which was complemented with heightened expression of marker genes associated with each hormone (*PR-1* for SA*, VSP2, PDF1.2* for JA and *HEL* for ET)(Vos et al., 2005). In contrast, the necrotrophic fungal pathogen *Alternaria brassicicola* only elicited JA- and ET-responses, with no immediate change in SA levels or expression of associated marker genes observed (Penninckx et al., 1998, Vos et al., 2005). Levels of JA and ET were also found to increase in Arabidopsis subjected to *P. rapae* herbivory, while the aphid species *Myzus persicae* induced no change in levels of any of the phytohormones (Vos et al., 2005), an observation also seen in *N. attenuata* (Heidel and Baldwin, 2004). Despite this, *M. persicae* did elicit the expression of two SA-responsive genes, *PR-1* and *BGL2*, in WT Arabidopsis, an observation that was lost in the *npr1* mutant impaired in SA signalling (Moran and Thompson, 2001), indicating that aphid

herbivory targets SA-regulated pathways in host plants. Indeed, increased expression of SA-responsive genes was also observed in tomato, sorghum and *N. attenuata* subjected to aphid herbivory (Heidel and Baldwin, 2004, Zhu-Salzman et al., 2004, Bruce and Pickett, 2007), while levels of SA were shown to heighten in wheat, soybean, tomato and barley exposed to phloem-feeding pests (Thompson and Goggin, 2006), indicating that the role of particular phytohormones against specific plant pests varies across plant species.

JA and SA are typically known to antagonize one another, with heightened expression of SA-mediated defences against *P. syringae* in Arabidopsis shown to increase susceptibility of these plants to necrotrophic pathogens, while JA-responses induced by *P. rapae* herbivory were down-regulated by the biotrophic pathogen, *Hyaloperonospora parasiticaa* (Spoel et al., 2007). Studies with mutant and over-expressing lines affected in JA- or SA-induced signalling revealed convergence points between these two hormones. Over-expression of the SA-responsive glutaredoxin (GRX480)-encoding gene in Arabidopsis abolished expression of MeJA-responsive *PDF1.2*, but did not affect abundance of *LOX2* or *VSP2* transcripts, indicating that SA may work in tandem with a particular branch of the JA-response pathway (Koornneef and Pieterse, 2008).

Likewise, JA and ET are suggested to work both antagonistically and in synergy with one another to promote plant defence against microbial and invertebrate pests as well as regulate several development processes, such as apical hook formation and ozone-induced cell death (Penninckx et al., 1998, Rojo et al., 1999, Stotz et al., 2000, Lorenzo et al., 2003, Rehrig et al., 2014). The ability of locally synthesized ET to repress JA-induced systemic expression of wound-response genes maintains the correct spatial pattern of systemic wound responses across the whole organism (Rojo et al., 1999), while positive interactions between these hormones facilitates the expression of PI-associated genes in wounded tomato plants, which were found to not be regulated by JA or ET alone (O'Donnell et al., 1996). Integration of JA- and ET-induced signalling pathways is mediated by the pathogen-responsive transcription factor ETHYLENE RESPONSE FACTOR1 (ERF1), with transcripts of this gene increasing in response to individual or combined treatments of ET and JA, and over-expression of *ERF1* in Arabidopsis increasing transcript abundance of select wound-responsive genes, including JA-biosynthetic-encoding genes (e.g. *LIPOXYGENASE, LOX*) and genes associated with glucosinolate and phenolic biosynthesis (e.g. *CY979B2, CCoAOMT* and *CAD*)(Lorenzo et al., 2003). The repression of other known JA-responsive genes in *ERF1* over-expressing lines (including *VSP2*) suggests that, like SA, ET overlaps with a particular branch of JA-signalling. Interestingly, ET and SA appear to have differential effects of the expression of certain JA-responsive

genes (such as *LOX* and *VSP2*), indicating that these three phytohormones operate very complex, finely tuned defence strategies against herbivore and pathogen pests.

Despite the interplay between these three phytohormones in conferring plant defence against pests, JA and its derivatives are still regarded as the predominant wound-responsive signalling molecules against herbivore invertebrates (Farmer and Ryan, 1992, Bari and Jones, 2009) and necrotrophic pathogens (Vijayan et al., 1998). As such, an in depth description of JA signalling pathways and subsequent induced defences shall be discussed in the following sections of this chapter.

1.4.2 Jasmonic acid (JA)

Jasmonic acid is an oxylipin derived from α-linolenic acid (18:3) via the octadecanoid pathway (Vick and Zimmerman, 1984), and serves as an important developmental hormone regulating a diverse range of biological processes, such as seed germination, root growth, tuber formation, fruit ripening, stomatal opening, leaf senescence and defence against pests (Farmer and Ryan, 1992, Koda and Kikuta, 1994, He et al., 2002, Bari and Jones, 2009). The octadecanoid pathway contains at least 7 catalytic steps involving a variety of enzymes, such as lipoxygenases (LOX), allene oxide synthase (AOS) and allene oxide cyclase (Wei et al.), that mediates peroxidation of linolenic acid to OPDA (12-oxo-*cis,cis*-10,15-phytodienoic acid), a breakdown product of the hydroperoxide fatty acid of linolenic acid by hydroperoxide cyclase (Zimmerman and Feng, 1978, Vick and Zimmerman, 1984), and the precursor of JA. OPDA undergoes a series of reduction and β-oxidation steps to shorten its acid side chains, leading to the production of the active (+)-7-iso-jasmonic acid, which is quickly converted to the stable stereoisomer, (-)-jasmonic acid (Wasternack and Parthier, 1997) (Vick and Zimmerman, 1984). JA can subsequently undergo further enzymatic modifications to form numerous derivatives, such as methyl-jasmonate (MeJA) and JA-amino acid conjugates collectively termed as jasmonates (Chesney et al.), many of which play important roles in mediating plant defence along with additional precursors of the octadecanoid pathway.

Initial studies investigating the effects of MeJA application on tomato plants reported increased levels of proteinase inhibitors (PIs) which impair invertebrate gut digestive processes (Farmer and Ryan, 1990), while the over-expression of *S*-adenosyl-L-methionine:jasmonic acid carboxyl methyltransferase (JMT), the enzyme responsible for the production of MeJA, led to constitutive expression of wound-responsive genes such as *VEGETATIVE STORAGE PROTEIN* (*VSP*) and *PLANT DEFENSIN1.2* (*PDF1.2*) and

reduced susceptibility of Arabidopsis to infection from the necrotrophic fungus, *Botrytis cinerea* (Seo et al., 2001). MeJA was therefore regarded as an effective inducer of plant defences, although was found to not be the main bioactive form of JA involved in regulating these defences. Instead, a JA-amino acid conjugate jasmonyl-L-isoleucine (JA-Ile) was identified as the bioactive form of JA (Staswick and Tiryaki, 2004).

The conjugation of JA to amino acids was found to occur in the presence of JASMONIC ACID RESISTANT1 (JAR1), a JA-amino synthetase structurally related to adenylate-forming enzymes of the firefly luciferase family. JAR1 adenylation of JA was shown to produce bioactive derivatives of the hormone, with *jar1-1* and *jar1-8* mutants failing to accumulate levels of JA-Ile. Interestingly, levels of JA-Val, JA-Leu and free JA were similar in WT and mutant plants, while JA-Phe and JA-ACC levels increased over 2-fold in mutants compared to WT (Staswick and Tiryaki, 2004), implying that JAR1 is important in the formation of JA-Ile conjugates while other enzymes may be involved in the production and/or regulation of additional JA-derivatives. Application of JA-Ile to *jar1-1* mutants complemented the jasmonate insensitive phenotype, while transgenic lines over-expressing *JAR1* in the *jar1-1* mutant background had restored levels of JA-Ile, further supporting the role of this protein in the synthesis of JA-Ile (Staswick and Tiryaki, 2004). JA acts in both a local and systemic manner when conferring plant resistance against pests, meaning that unchallenged regions of an attacked plant will express defence related genes. The rapid transduction of JA-regulated signalling across an entire organism enables plants to mount effective defence responses, as well as prime unchallenged tissue for an impending attack.

1.4.3 Important regulators of JA-induced defence

Three additional components were identified as being intrinsic to JA-signalling events through a series of mutagenic screens and microarray studies. The first component was identified by Feys and co-workers in 1994 as a Skp1-Cul1-F-box (SCF) ubiquitin E3 ligase complex, CORONATINE INSENSITIVE 1 (SCF^{COI1} or COI1). Arabidopsis *coi1* mutants were shown to be insensitive to both MeJA and a chlorosis-inducing toxin produced by several pathovars of the plant pathogen *Pseudomonas syringae,* coronatine, by retaining root and shoot growth in the presence of these agents while such developmental processes were arrested in WT lines. These mutants were unable to accumulate anthocyanins in response to coronatine and MeJA, and lacked two jasmonate-induced proteins, all of which were observed in WT plants (Feys et al., 1994). In addition, *coi1* mutants were less

susceptible to a coronatine-producing strain of *P. syringae* (Atr1) than WT plants, exhibiting fewer lesion areas, less chlorosis and a lower rate of Atr1 colonisation on leaf tissue over a 6-day period (Feys et al., 1994). However, the mutant was more susceptible to certain necrotrophic fungi that are known to activate JA-regulated defence responses (Lorenzo et al., 2004). These findings, along with the male sterility of *coi1* plants, indicated a role for COI1 in mediating a variety of JA-regulated developmental and defence-related pathways in plants. A microarray study of Arabidopsis WT and *coi1* lines indicated the influence of COI1 on the JA signalling pathway, with 85% of the 212 JA-inducible genes and ~ 44% of the 153 genes up-regulated by wounding shown to be regulated by COI1 (Devoto et al., 2005). In addition, COI1 was also shown to be required for repressing approximately 50% of genes likewise suppressed by JA or mechanical wounding, demonstrating that COI1 is an intrinsic component of JA-regulated signalling events. Several of the JA-responsive, COI1-dependent genes were found to encode transcription factors implicated in promoting plant defence responses, including *MYB34,* which encodes a putative component of tryptophan-biosynthetic processes, and various ethylene responsive factors such as *ERF1,* which translate into transcription factors critical for promoting synergistic interactions between MeJA- and ET-regulated pathways (Lorenzo et al., 2003, Devoto et al., 2005). COI1 was subsequently regarded not only as an important mediator of JA-induced plant defences, but also as a regulator of cross-communication events between MeJA and ET in Arabidopsis, an important convergence of phytohormones that was found to fine tune plant defence mechanisms to different invertebrate and pathogen attackers (Rojo et al., 1999, Lorenzo et al., 2004).

While attempting to better understand the interplay between JA and ET signalling events, a second important component of JA-regulated defence, a bHLH transcription factor, MYC2, was identified. The *jasmonate insensitive1* (*jai1*/*jin1*) Arabidopsis mutant was found in a genetic screen to be insensitive to JA treatment, displaying no inhibition of shoot or root growth in the presence of 50 μM JA, while development of WT Arabidopsis and ET-insensitive *ein3-3* mutants was arrested (Lorenzo et al., 2004). Characterisation of the *JAI1* loci revealed the *MYC2* gene, which was shown to be responsive to JA in a COI1-dependent manner and encode a basic helix-loop-helix-leucine zipper transcription factor. Unlike the *coi1* mutants, *jin1* retained male fertility and, interestingly, appeared more resistant to two necrotrophic fungi, *B. cinerea* and *Plectosphaerella cucumerina,* than Col-0, *coi1* and *ein3-3* lines (Lorenzo et al., 2004). Gene expression analysis of several defence-related markers in WT and *jin1* mutants found that expression of *PR4*, *PR1* and *PDF1.2*, which are known to be positively regulated through the collaborative effort of JA

and ET in an ERF1-dependent manner, increased in *jin1* mutants but not in WT plants treated with JA. On the other hand, a set of genes found to decrease in the *jin1* mutant, but not in WT upon treatment with JA, included the wound-responsive *VSP2*, which encodes an insect-deterring phosphatase enzyme, and *LOX3*, encoding a component of JA-biosynthesis (Lorenzo et al., 2004). These results collectively indicated that two branches of the JA signalling pathway existed: the first promoted plant defence against invertebrate pests was positively regulated by MYC2 but negatively by ERF1, while the second branch conferred defence against necrotrophic pathogens and was negatively regulated by MYC2 and positively regulated by ERF1 (Rojo et al., 1999, Reymond et al., 2000, Lorenzo et al., 2004). The interplay between MYC2 and ERF1 is believed to enable plants to fine-tune their defence mechanisms against particular pests in an elegant mechanism that promotes protection against invertebrate or necrotrophic attackers.

The final components of JA signalling were identified through mutagenic (Chini et al., 2007) and microarray studies (Thines et al., 2007), presenting themselves as the final link in understanding the molecular mechanisms of JA-signalling in plants. An Arabidopsis microarray identified several early-induced JA-responsive genes that were found to encode previously uncharacterised proteins containing a conserved 37-amino acid ZIM domain motif, and were as such assigned the name of JAZ (JASMONATE ZIM-DOMAIN) proteins. Twelve JAZ proteins have been discovered in plants (Chini et al., 2007), all belonging to the TIFY family, on account of possessing a conserved TIFYXG sequence within their ZIM motif. The ZIM domain is located at the N-terminal region of these proteins, with an additional highly conserved Jas domain found on the C-terminus of JAZ proteins. Unlike other ZIM and ZIM-like proteins identified in Arabidopsis, which contain zinc-finger DNA-binding domains (e.g. CONSTANS, CO), the JAZ proteins were not found to possess a characterised DNA-binding domain, despite transient expression of GFP-tagged JAZ1 and JAZ6 demonstrating nuclear localisation of these proteins (Thines et al., 2007).

JAZ proteins exhibit functional redundancy in plants, and as such no obvious phenotype could be detected in JAZ T-DNA insertion mutants. Interestingly, over-expression of JAZ-encoding genes revealed no evident phenotype, but targeted deletion of conserved domains and expression of such constructs in WT Arabidopsis plants under the control of the constitutive *35S* promoter identified one line, *35S-JAZ1*Δ*3A* (residues 202-228), that possessed a male-sterile phenotype reminiscent of that seen in *coi1*, which could not be rescued with the application of JA. These plants were also shown as being JA-insensitive, failing to undergo JA-induced root elongation inhibition, possessing weak expression of

JA-responsive genes and displaying slightly more resistance to *P. syringae* that WT plants (Thines et al., 2007). It was hypothesised from the JA-insensitive nature of this line, along with the inability of JA to rescue these phenotypes and the nuclear localisation of JAZ, that these proteins acted as negative regulators of JA signalling events.

To further assess any role of JAZ proteins in JA-signalling, pull-down assays were conducted with JAI3, a member of the JAZ family, and additional components of the JA-signalling pathway, starting with COI1. [^{35}S]JAI3 was found to interact with maltose binding protein (MBP)-COI1, and likewise [^{35}S]COI1 interacted with MBP-JAI3 (Chini et al., 2007), with repeats of this study using truncated versions of JAI3 identifying the site of interaction on JAI3 at the N-terminal region, where the ZIM motif is located. This finding implied that COI1 may be involved in the degradation of JAZ proteins, a hypothesis that was confirmed with transient expression studies using transgenic Arabidopsis *35S*-JAZ1-GUS lines and GFP-JAI3 constructs in tobacco (Thines et al., 2007, Chini et al., 2007). Arabidopsis *35S*-JAZ1-GUS lines displayed weaker signals than "control" lines expressing the *35S*-GUS construct alone, and treatment with 100 μM JA revealed complete loss of GUS activity 1 hour later, indicating degradation of these constructs in a JA-dependent manner (Thines et al., 2007). Likewise, transient expression of GFP-JAI3 revealed a JA-dependent loss of fluorescence in nuclei (Chini et al., 2007), an observation that was lost in both the JAI3ΔC and *coi1* mutants, indicating the importance of the C-terminal region of JAZ proteins for their degradation, that is dependent on COI1. The addition of 10 or 100 μM MG132, a 26S proteasome inhibitor, maintained GUS activity and GFP fluorescence respectively following treatment with JA, implying that the repressive nature of JAZ on JA-signalling is abolished by its polyubiquitination by COI1, and subsequent degradation via the 26S proteasome. Yeast two-hybrid analysis revealed that JAZ-COI1 interaction is dependent on presence of the JA-derivative JA-Ile, with MeJA and the JA precursor, OPDA, unable to promote yeast growth (Thines et al., 2007).

The exact mode of JAZ repression on JA-signalling was elucidated using *in vitro* pull-down assays, which identified a direct interaction between JAI3 and MYC2 (Chini et al., 2007). This interaction was found to occur at the C-terminal of JAI3 and the N-terminal region of MYC2, implying that the Jas domain is an intrinsic motif for promoting JAZ-MYC2 interaction. Unlike for COI1, this interaction is not dependent upon the presence of JA-Ile, further supporting a role for JAZ proteins in repressing JA-responses in the absence of this phytohormone.

Genetic studies revealed that the regulatory roles of COI1, JAZ and transcription factors such as MYC2 on JA-responses operate in a negative feedback loop, as eight JAZ-

encoding genes were identified as being constitutively over-expressed in *35S*:MYC2 lines, while their expression was significantly reduced in *myc2* mutants compared to WT plants (Chini et al., 2007). Investigation of the promoter regions of *JAZ* genes revealed the presence of G- and/or T/G-box motifs, which are target binding sites of MYC2. Therefore, JA-induced signalling pathways were found to operate via an auto-regulatory mechanism, where the repressive nature of JAZ proteins prevented transcription of wound-induced genes by directly inhibiting activity of JA-responsive transcription factors in the absence of JA-Ile, but were rapidly degraded via the 26S proteasome in a COI1-dependent manner to promote JA-induced defence upon detection of JA-Ile (Figure 1-3).

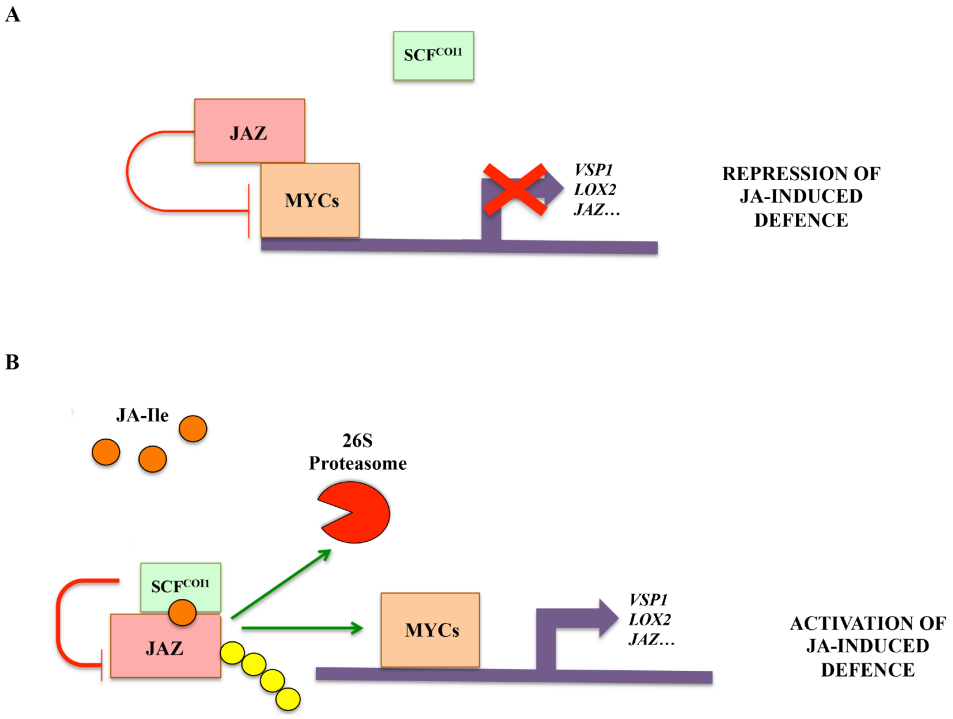

Figure 1-3: Schematic overview of invertebrate-induced defence responses in plants mediated by JA. **A**, in unchallenged tissue JAZ proteins interact with MYC transcription factors to repress expression of JA-responsive genes, however in the presence of the bioactive form of JA, JA-Ile, in **B**, the SCF^{COI1} E3 ubiquitin ligase interacts with JAZ to mark for degradation via the 26S proteasome, subsequently alleviating repression of MYC transcription factors and promoting JA-responsive defence mechanisms. Figure adapted from (Chico et al., 2008).

1.4.4 Plant defence mechanisms

Activation of MYC2 and additional JA-responsive transcription factors gives rise to increased abundance of various defence-related transcripts, and subsequent accumulation of defensive compounds and structural barriers. Some of these plant defence mechanisms can be constitutively present in plant tissue or induced upon recognition of physical and/or chemical characteristics of the attacking invertebrate or microbe, and further categorised into two strategic groups depending on whether these responses function in a direct or indirect manner against the pest (Figure 1-4)(Kessler and Baldwin, 2002).

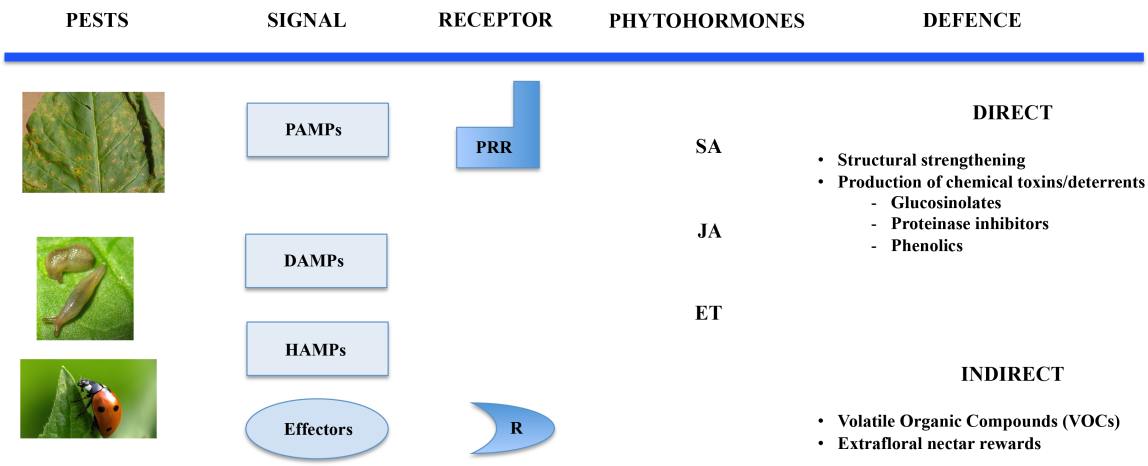

Figure 1-4: Brief overview of pathogen- and invertebrate-induced direct and indirect defences in plants. Plant receptors can detect invertebrate pests via their Pathogen/Damage/Herbivore Associated Molecular Patterns (PAMPs, DAMPs or HAMPs, respectively) or effectors from invertebrate saliva and/or ovipositon fluid to mount a series of phytohormone-regulated direct and indirect defence against them. Image adapted from (Ballaré, 2014). Image of *P. syringae*-infested *Nicotiana tabacum* extracted from Forestry Images (http://www.forestryimages.org/browse/detail.cfm?imgnum=5368884).

Constitutive plant defences are present in tissue regardless of an invertebrate attack, while inducible defences are activated upon detection of an invertebrate threat (Chen, 2008). Both forms of defence include structural and chemical protective mechanisms, with those of a constitutive nature being more metabolically expensive to plants and potentially less effective than induced responses, as they divert specific resources away from photosynthetic processes towards the biosynthesis of defensive compounds and pose the risk of not being specific to the attacking pest (Reymond and Farmer, 1998). Constitutive defence is commonly seen in select plant organs, with reproductive tissues tending to

possess large quantities of defensive proteins and metabolites at all times to deter grazing pests and promote plant species survival (Bostock, 2005).

Direct defences actively deter or destroy pests, while indirect defence mechanisms instead act as attractants to natural predators of the attacking pest. Direct defences include the development of physical barriers, such as thorns, trichomes, and lignification of tissue to reduce the ease of invertebrate consumption and tissue digestibility (Wittstock and Gershenzon, 2002), along with the production of chemical defences that serve as anti-nutritive compounds and deterrents such as phenolics, proteinase inhibitors (PIs) or toxic compounds such as glucosinolates (Leon et al., 2001). Indirect defence mechanisms that attract the attention of invertebrate predators and parasites include the emission of volatile organic compounds (VOCs) and the provision of nectar and nutritional rewards to the predator. The production and activation of these defence mechanisms has been found to vary across plant species and in relation to the attacking pest, with conflicting arguments suggesting that invertebrates may be able to elicit different defence responses in plants or respond differently to defence mechanisms based on their physical feeding mechanism and/or dietary preferences (Bidart-Bouzat and Kliebenstein, 2011, Ali and Agrawal, 2012). The main feeding mechanisms possessed by invertebrate species are leaf chewing, leaf mining, piercing-sucking and phloem feeding, while invertebrates classed as generalist feeders graze upon a broad range of plant families (polyphagous), and specialist feeders have a more restricted diet limited to only a few plant families or members within the same family (mono- or oligophagous). Examples of generalist feeders include the aphid species *Myzus persicae*, the Egyptian Cotton Leafworm, *Spodoptera littoralis*, and the grey field slug *Deroceras reticulatum*, while the diamondback moth, *Plutella xylostella*, and the *Brevicoryne brassicae* aphid species are classed as specialists due to their diet comprising of members from the Brassicaceae family.

It has been reported that leaf-chewing and phloem-feeding invertebrates can induce different wound responses in plants (Heidel and Baldwin, 2004, Zhu-Salzman et al., 2004, Vos et al., 2005), with the puncture-feeding pest *Tupiocoris notatus* shown to repress the expression of some JA-responsive PI-encoding genes in *N. attenuata,* which are known to increase in response to grazing caterpillars, and inducing expression of many SA-related genes (Heidel and Baldwin, 2004). In addition, aphid attack and exogenous SA application induced similar responses in *N. attenuata*, with both JA- and SA-responsive genes being up-regulated in expression following either treatment. Herbivory from the caterpillar, *Manduca sexta*, however, induced a transcriptomic response reminiscent of that generated by JA-application (Heidel and Baldwin, 2004), indicating that phloem-feeders

and leaf-chewing invertebrates may spark different wound-responses predominantly regulated by different phytohormones.

In addition to different plant responses being induced by invertebrates from separate feeding guilds, a specialist/generalist paradigm exists which implies that specialist feeders have more tolerance to plant defence mechanisms than generalist feeders on account of evolving various adaptations to counteract the negative effects of these defences (Agrawal and Kurashige, 2003). This paradigm has subsequently been expanded to state that generalist and specialist feeders may trigger different plant defences, however controversy exists around whether or not these differences do indeed exist (Bidart-Bouzat and Kliebenstein, 2011). Examples of varying plant defence mechanisms towards specific invertebrate pests, and the subsequent responses of these herbivores to the defence responses, shall be discussed further on.

Despite variation in the exact molecular defence mechanisms activated in plants by different invertebrate pests, the overall responses to herbivory include heightened levels of ROS scavengers, modification in Ca^{2+} fluxes, differential expression of JA-responsive genes and accumulation of various defence-related compounds. These defence-related compounds include glucosinolates, alkaloids (e.g. caffeine, nicotine and morphine), tannins, saponins, cyanogenic glycosides and terpenoids, the latter family being one of the most diverse in plants, possessing over 40,000 known structures. In addition, components of the phenylpropanoid pathway have a major role in conferring plant defence against invertebrate and microbial pests, by providing both chemical deterrents and structural barriers, along with the signalling molecule, SA (Dixon et al., 2002a). In light of the diverse roles possessed by various components of biological pathways in plant defence, clusters of defence compounds shall be discussed individually in the following sections, starting with phenylpropanoids.

1.4.4.1 The phenylpropanoid pathway

A number of defence-related compounds originate from the phenylpropanoid pathway and are directed towards reinforcing structural barriers against pests and pathogens (e.g. lignin), serving as signalling molecules in defence-associated pathways (such as SA), or presenting themselves as feeding deterrents or toxins (e.g. phenolics). Phenylpropanoids can be divided into three categories, namely phytoalexins (e.g. stilbenes, coumarins and isoflavonoids), phytoanticipins (such as chlorogenic acid, CGA) and signal molecules (SA). The phenylpropanoid pathway is also home to the biosynthesis of UV-absorbing

flavonoids, and monolignols which are the building blocks of the architectural biopolymer, lignin. The smooth running of this complex pathway depends on a number of enzymes, including the afore-mentioned PAL, cytochrome P450 hydroxylases and *O*-methyltransferase (OMTs), along with input of amino acid substrates and intermediates derived from the shikimate pathway (Yao et al., 1995).

The responsiveness of components in this pathway to JA treatment or invertebrate/microbial attack has been identified via "omics"-based studies (Yao et al., 1995) (Daayf et al., 2000) (Dixon et al., 2002b) (Shadle et al., 2003) (Lattanzio and Cardinali, 2006, Ralph et al., 2006) (Izaguirre et al., 2007) (Konig et al., 2014), with metabolic analysis on *B. rapa* subjected to MeJA treatment revealing increased levels of the phenylpropanoids 5-hydroxyferuloyl-, coumaroyl-, caffeoyl-, feruloyl- and sinapoyl-malates, along with hydroxyl-feruoyl (Liang et al., 2006b).

Several studies on transgenic and mutant plants have highlighted the importance of phenylpropanoids in conferring plant defence against pests, with tobacco mutants impaired in the production of the first committed enzyme of the phenylpropanoid pathway, PAL, appearing more susceptible to infection from the necrotrophic plant fungus *Cerospora nicotianae,* and transgenic tobacco lines over-expression *PAL* displaying increased resistance to the pathogen (Shadle et al., 2003). These findings were attributed to the modified levels of various downstream phenylpropanoids, particularly levels of CGAs such as caffeoyl-quinic acid, which were found to increase considerably in tobacco plants over-expressing PAL, indicating that these compounds are efficient at reducing plant susceptibility to invading microbial pests. CGA is derived from caffeic acid and quinine, which are synthesised from phenylalanine and dehydroquinate intermediates, respectively, derived from the shikimate pathway. A study by Yao and co-workers (1995) further highlighted the importance of CGAs and additional phenylpropanoids in promoting potato tuber defence against the hemi-biotrophic oomycete *Phytophthora infestans*, by expressing in this plant a gene from *Catharanthus roseus* encoding tryptophan decarboxylase (TDC), which redirects tryptophan into tryptamine. The authors observed decreased levels of tryptophan, phenylalanine and phenylalanine-associated derived phenolic compounds, with levels of CGA (the major soluble phenolic ester in potato tubers) falling by 2-3-fold, and soluble phenolic compounds such as ferulic acid-derivatives and *p*-coumaric acid decreasing by 30-40% in transgenic tubers compared to WT. In addition, transgenic tubers were noticeably more susceptible to *P. infestans* than WT, indicating the importance of phenylpropanoids in plant defence, along with the high demand for products derived from the shikimate pathway for facilitating plant defence (Yao et al., 1995). The extent of

phenylpropanoid accumulation in response to herbivory can vary across plant species, with *N. longiflora* showing overall higher levels of select CGA compounds but lower concentrations of dicaffeoylspermidine compounds than *N. attenuata* following simulated herbivory (Izaguirre et al., 2007).

Studies with *coi1-1* and WT Arabidopsis lines identified several wound- and *P. rapae*-responsive genes encoding components of the phenylpropanoid pathway that increase in expression in a COI1-dependent (*CCR, CHS, 4CL* and *COMT*) and COI1-independent manner (*PAL1* and *CM1*)(Reymond et al., 2000), suggesting that regulation of the expression of various phenylpropanoid-associated genes by herbivory and/or wounding can take place via the JA-Ile-signalling pathway outlined in Figure 1-4, and by an additional pathway.

In addition to chemical defence mechanisms, components of the phenylpropanoid pathway have also been suggested to provide structural barriers against invading pests. One branch of the phenylpropanoid pathway leads to the biosynthesis of sinapate esters and lignin, the latter compound being the second most abundant plant polymer on the planet, that serves as a waterproofing and strengthening agent in specific plant tissues (Halpin et al., 1994). Lignin is an inconvenient plant product in various commercial and agricultural systems by affecting cell wall polysaccharide degradation to simple sugars for fermentation in the biofuel industry, preventing use of woody material in the pulp and paper industry without its initial removal from cellulose, (Whetten and Sederoff, 1991), and limiting digestibility of forage crops for livestock (Jung and Vogel, 1986). Despite this, lignin's ability to strengthen cell walls has been implicated in plant defence against microbial pests (Lim et al., 2001). Tobacco antisense lines of COMT, CCoAOMT, CCR and CAD, enzymes active in the biosynthesis of lignin precursors, display decreased quality and quantity of lignin, with one tobacco line expressing the double antisense construct CCoAOMT/COMT being the most affected, both in relation to its development and resistance to TMV made evident by sustaining larger TMV-induced necrotic lesions than WT lines (Camera et al., 2004). A diverse role for members of the phenylpropanoid pathway in promoting plant defence against a myriad of invertebrate and microbial pests is therefore evident, and increased expression of several genes associated with this pathway in a COI1-independent manner suggests that phenylpropanoid-associated plant defence may be activated through multiple biological signalling events.

1.4.4.2 Glucosinolates

Glucosinolates are specialised, sulphur-rich defence compounds predominantly found in members of the Brassicaceae family, and have received a great deal of attention over the years in relation to their defence-promoting properties and diversity in cruciferous plants. These compounds can be characterised as being aliphatic, aromatic or indolic based on the nature of their amino acid side chains (of which over 120 different side chain structures are known to exist)(Hopkins et al., 2009). Indole glucosinolates are derived from tryptophan, and make up approximately 10% of known glucosinolates found in vegetative tissue, such as leaves and roots. Aromatic glucosinolates (synthesised from phenylalanine or tyrosine) likewise make up a small proportion of glucosinolates in plants (~10%), while aliphatics derived from methionine make up approximately 50% of glucosinolates in plants, particularly in seeds, flowers and siliques (Hopkins et al., 2009). The requirement for substrates derived from the shikimate pathway means that, like phenylpropanoids, glucosinolate biosynthesis and subsequent plant defence can be affected by mutations in the shikimate pathway, with the redirection of tryptophan into tryptamine reducing the quantity of indole glucosinolates in transgenic plants expressing TDC (Yao et al., 1995). The biosynthesis of glucosinolates generally takes place over three steps involving amino acid chain elongation, core glucosinolate biosynthesis and side chain modification, with key enzymes including methylthioalkyl-malate synthase (MAM) and a myriad of cytochrome P450 enzymes from the CYP79 and CYP83 subgroups (Sasaki-Sekimoto et al., 2005, Zang et al., 2009). In Arabidopsis, seven members of the CYP79 family have been identified (Mikkelsen et al., 2003), with CYP79A2, CYP79F1 and CYP79F2 targeting chain-elongated methionine derivatives and phenylalanine for metabolism, while CYP79B2 and CYP79B3 convert tryptophan to indole-3-acetaldoxime (Hull et al., 2000, Mikkelsen et al., 2000, Mikkelsen et al., 2003). The function of the remaining two members of this family, CYP79C1 and CYP79C2, remains somewhat elusive (Mikkelsen et al., 2003). Glucosinolates are constitutive defences as they are always present in plant cell vacuoles in an inactive form. Upon invertebrate herbivory and tissue damage, glucosinolates are released from their compartments into the cytosol where they are hydrolysed by myrosinase proteins, resulting in the accumulation of toxic by-products including isothiocyanates, nitriles and thiocyanates (Mithen, 2001). The nature and degree of toxicity of these final products are largely dictated by the specific side chain of the glucosinolate, however additional factors, such as cellular pH and the concentration of ferrous ions, also influence the characteristics of the final product (Mithen, 2001).

Glucosinolates appear to be regulated in response to specific herbivore pests and/or defence-related signalling molecules, as application of MeJA to Arabidopsis plants was found to increase the abundance on indole glucosinolates by approximately 3 to 4-fold along with expression of tryptophan-metabolizing genes, *CYP79B2* and *CYP79B3*, while levels of aliphatic glucosinolates were not largely affected by MeJA (Mikkelsen et al., 2003). Likewise, the mustard beetle *Phaedon cochleariae* increased levels of certain indole glucosinolates in 12-day old broccoli sprouts while *M. persicae* and *P. brassicae* did not invoke any noticeable change in levels of these compounds in comparison to untreated controls (Mewis et al., 2012).

The effects elicited on invertebrate pests by glucosinolates is also thought to vary across pest species, with some invertebrates being negatively affected by the consumption of these compounds, while others utilize glucosinolates as feeding and oviposition stimulants. For example, *P. rapae* larvae were found to use the glucosinolate sinigrin as a feeding stimulant, while adult *P. rapa* and *Pieris napi oleracea* regarded the same compound as a cue for egg laying (Huang and Renwlck, 1994, Renwick and Lopez, 1999). Additionally, *P. rapae* larvae were shown to be unaffected by ingesting toxic glucosinolates defence compounds from Brassicaceae plants, instead sequestering these secondary metabolites for their own use (Huang and Renwlck, 1994, Renwick and Lopez, 1999). A conflicting study in 2003, however, observed reproducible reductions in the performance on *P. rapae* maintained on artificial diets containing toxic alkyl isothiocyanate breakdown products of glucosinolates, with *P. rapae* mortality reaching approximately 40% with increasing concentrations of the toxin (0-1.69 μmol/g fresh weight in diet, resembling naturally occurring concentrations in plant tissue) and 0% on the control diet, while the relative growth rate of survivors (g/g/day) was negatively affected by increased concentrations of glucosinolates (Agrawal and Kurashige, 2003).

Molecular studies have been conducted to assess whether or not a specialist/generalist paradigm exists in relation to invertebrate responses to glucosinolate defences. One study investigating glucosinolate content in Arabidopsis plants subjected to herbivory from two specialist and 2 generalist feeders (one phloem-feeding aphid and one leaf-chewing caterpillar from each dietary group) found that while there was little difference between the levels of aliphatic glucosinolates induced by the generalist and the specialist aphid species, significant differences existed between the accumulation of aliphatic and indole glucosinolates in response to *P. rapae* and the generalist caterpillar *Spodoptera exigua* (Mewis et al., 2006). A separate study investigating the effects of glucosinolates on the specialist moth *P. xylostella* and generalist snail *Helix pomatia* found that both

invertebrates were able to attenuate the ill-effects of glucosinolate breakdown products by possessing a sulfatase enzyme in their guts which deactivated these toxic compounds (Hopkins et al., 2009). The combined results from both studies suggests that plant defences induced by various invertebrate pests and their subsequent responses to these mechanisms may not primarily be a result of invertebrate dietary specifications, but down to species-specific evolutionary developments that have facilitated each herbivore species to compete in its own arms' race against specific plant hosts. As a result, the effectiveness of glucosinolates against invertebrate pests is variable, with some able to regard these compounds as toxins or deterrents, while others view them as biological cues to commence grazing or egg laying.

1.4.4.3 Additional chemical and structural defences

Additional defensive compounds that have not been explored in depth in this introductory chapter include PIs, VOCs, alkaloids and terpenoids. While these defences are important in promoting plant survival against herbivore pests, they shall not be focused upon in this study, therefore are only briefly described.

PIs are potentially fatal compounds for invertebrates on account of their ability to inhibit protein hydrolysis in the digestive tract by tightly binding to proteolytic enzymes (such as serine, cysteine, aspartic- and metallo-proteinases), an interaction which prevents the invertebrate from assimilating amino acids from food sources, negatively impacting their growth and developmental processes and potentially leading to starvation and death (Kuhlmann and Muller, 2011). Growth of larvae from the meal worm *Tribolium confusum* was found to be inhibited when fed on a protein fraction obtained from soybean, while trypsin inhibitors were toxic to *M. sexta* larvae when incorporated into an artificial diet. Although the toxic effects of trypsin inhibitors were shown to be reversible with the addition of methionine to the diet of *M. sexta*, reduced fitness of invertebrates following excessive consumption of PIs can lead to long-term health effects due to a reduction in the efficiency of their digestive tract (Ryan, 1990).

Volatile organic compounds (VOCs), which function as indirect defence mechanisms, are composed predominantly of terpenoids, alkanes, aldehydes, esters and aromatics (Leitner et al., 2005), with the exact concentrations of each compound dependent upon the attacking invertebrate. For example, levels of alkanes, alkenes and homoterpenes in *M. truncatula* vary in response to *S. littoralis* caterpillars or the spider mites *Tetranychus urticae,* with the differences in VOC constituents proposed to be attributed to the different

hormone pathways regulated by each herbivore, as *S. littoralis* rapidly increases levels of JA following herbivory, while *T. urticae* instead induces an accumulation of SA, both locally and systemically (Leitner et al., 2005). Terpenoids additionally contribute towards direct plant defences, and are regarded as one of the most diverse group of defence compounds in plants. The effects of particular terpenoids are again dependent on the attacking invertebrate; for example, isoprene was found to deter *M. sexta* caterpillars, have little effect on *P. rapae* or *P. xylostella* behaviour, and additionally serve as an indirect defence by attracting the attention of the parasitic wasp, *Diadegma semiclausum* (Mithofer and Boland, 2012).

The diverse collection of plant defence mechanisms highlighted in the above sections of this chapter demonstrates the complexity of the plant-pest evolutionary arms' race, and the inability of one defence strategy to deter all invaders explains the presence of so many defence compounds in plants. It is plausible that the anthropogenic categorization of invertebrates based on their feeding mechanisms and dietary preferences does not necessarily reflect their effects on plant defence or response to such defence mechanisms, and that other (specific?) properties of individual invertebrate species may determine how they interact with plant hosts.

1.5 UV-B-induced responses overlap with those regulated by JA/herbivore pests

So far in this chapter, plant responses to either UV-B radiation or JA/invertebrate pests have been discussed, with several compounds or biological pathways being described in relation to both stimuli. Indeed, previous studies have observed overlapping regulatory roles of UV-B and JA/herbivory on plant biology (A-H-Mackerness et al., 1999, Izaguirre et al., 2003, Stratmann, 2003, Caldwell et al., 2007, Izaguirre et al., 2007, Demkura et al., 2010), with microarray data revealing an approximate 20% overlap in the regulation of herbivore-response by UV-B in *N. longiflora* (Izaguirre et al., 2003), and multiple bioassays observing the ability of UV-B radiation to enhance plant defence against invertebrate and necrotrophic pests. This final section of the introductory chapter introduces our current knowledge on the overlap between UV-B- and wound-responses in plants, before discussing the aims of this project

1.5.1 UV-B reduces plant susceptibility to invertebrate and necrotrophic pests

Outdoor and laboratory-based studies have shown that removal of UV-B from plant growing environments increases their susceptibility to invertebrate consumption (Rousseaux et al., 1998, Izaguirre et al., 2003, Rousseaux et al., 2004, Caputo et al., 2006), their use as an oviposition platform (Caputo et al., 2006, Foggo et al., 2007) and reduces their tolerance to necrotrophic fungi (Demkura and Ballaré, 2012). These findings have been documented in several plant species, including members of the Brassicaceae family (Caputo et al., 2006, Kuhlmann and Muller, 2009a, Mewis et al., 2012), Nicotiana (Izaguirre et al., 2003, Izaguirre et al., 2007) and beech trees (Rousseaux et al., 2004), in response to thrips (Kuhlmann and Muller, 2009a), aphids (Kuhlmann and Muller, 2009b) and *Plutella* (Caputo et al., 2006).

When maintained under terrestrial levels of UV-B radiation, Arabidopsis plants sustain up to 3 times less damage from invertebrate pests compared to plants grown under attenuated levels of UV-B radiation (Caputo et al., 2006), a finding that extends to shrub plants, with *Gunnera magellanica* plants exposed to UV-B radiation sustaining ~ 70% less tissue damage from Lepidopteran pests than plants maintained under attenuated levels of UV-B radiation (Rousseaux et al., 2001). Arabidopsis plants were also shown as being less susceptible to infection from *B. cinerea* following exposure to UV-B (Demkura and Ballaré, 2012), sustaining smaller lesion areas compared to –UV-B-treated plants, and also compared to a UV-B- and -UV-B-treated mutant impaired in the phenylpropanoid pathway. The observed reduction in plant susceptibility to pests in a UV-B-dependent manner is not uniform across all members of the plant kingdom, however, as the mountain birch *Betula pubescens* was shown to be largely unaffected in its interaction with the autumnal moth *Epirrita autumnata* under elevated levels of UV-B radiation (Anttila et al., 2010).

The effects of UV-B radiation on the biology of plants have also been suggested to impact invertebrate fitness, with the weight of *P. brassicae* caterpillars and *M. persicae* aphids fed on minus –UV-B broccoli sprouts being approximately 40-70% higher compared to larvae fed on +UV-B plants (Mewis et al., 2012). Likewise, the growth rate of *M. sexta* fed on UV-B-treated *N. attenuata* and *N. longiflora* was lower than the weight of those maintained on –UV-B-treated plants, although the weight of caterpillars fed on -/+UV-B-treated *N. attenuata* was lower than those fed on -/+UV-B-treated *N. longiflora*, indicating varying effects of these two closely related species on invertebrate growth in general (Izaguirre et al., 2003). However, an alternative study reported no difference in *Plutella*

larval weight on –UV-B or +UV-B Arabidopsis (Caputo et al., 2006), highlighting the varying indirect effects of UV-B radiation on the fitness of invertebrate pests.

In addition to modifying plant attractiveness to herbivore pests, UV-B radiation is proposed to directly affect the behaviour of invertebrate pests via their perception of the component of sunlight. UV assists invertebrates with orientation, navigation, feeding and mating, and various studies have shown that whiteflies and aphids detect and move towards areas of UV-A and UV-B light (Kuhlmann and Muller, 2011), while the thrip species *Caliothrips phaseoli* is attracted to UV-A, but actively moves away from areas of high UV-B to those of low UV-B (Mazza et al., 2002). While the majority of investigations demonstrating that UV-B radiation reduces plant susceptibility to herbivory claim that this response of invertebrates is due to the effects of UV-B radiation on the physical and/or chemical profile of the plant, one particular study presented evidence to suggest that the feeding preferences of *Plutella* larvae was not determined by the effects of UV-B on plant quality but by insect perception of UV-B. Caputo and co-workers (2006) conducted choice chambers under –UV-B conditions in a glasshouse and found no significant difference in the area of leaf tissue consumed from plants pre-exposed to UV-B or maintained under –UV-B conditions. However, as these choice chamber bioassays were only conducted for 3 hours, it is possible that the visual effects of UV-B-treated plants on invertebrate behaviour are apparent after a set period of time that exceeds 3 hours.

The exact evolutionary basis for the overlap between light- and JA/herbivore-induced responses in plants, or the effects of solar radiation on plant attractiveness to invertebrate pests remains unknown, however it is conceivable that the integration of UV-B-signalling into plant defence pathways promotes “cross-tolerance" (section 1.1), to prime plants for impending attacks. However, the kinetics of these responses into the subjective night (e.g. when UV-B radiation is absent from the plant’s growing environment) has not been elucidated, therefore it is unknown how effective UV-B-induced plant defences are against nocturnal pests, such as molluscs.

1.5.2 Assessing the overlaps between UV-B- and wound-response pathways

Genetic and metabolic studies have attempted to pinpoint where UV-B- and wound-responsive pathways intercept in plants, with several reports indicating that the effects of UV-B radiation on JA are highly species-specific. An accumulation of both JA and ET was observed in Arabidopsis plants exposed to supplementary UV-B radiation, which also induced expression of several stress-related genes such as *PR-1* and *PDF1-2*. Studies with

UV-B-treated JA (*jar1*) and ET (*etr1-1*) mutants demonstrated that ET was required for UV-B-dependent accumulation of *PR-1*, while both hormones worked synergistically with UV-B to induce expression of *PDF1-2* (A-H-Mackerness et al., 1999). In contrast, UV-B was not found to increase JA levels in tomato plants (Stratmann et al., 2000) or *N. attenuata* (Izaguirre et al., 2003, Demkura et al., 2010). The importance of JA in promoting UV-B-enhanced defence in Arabidopsis was demonstrated with WT and *jar1-1* lines, where the reduction in *Plutella* oviposition on UV-B-treated Col-0 plants compared to individuals of the same ecotype grown under attenuated levels of UV-B was lost in the *jar1-1* mutant, with adult moths being unable to differentiate between UV-B- and attenuated UV-B-treated *jar1-1* plants for egg laying (Caputo et al., 2006). These *jar1-1* mutants also displayed decreased levels of UV-absorbing compounds, which could be indicative of the differences observed between the two Arabidopsis lines. Interestingly, this apparent requirement of JA for UV-B-dependent phenolic accumulation in Arabidopsis is absent in *N. attenuata* anti-sense LOX3 mutants (*as-lox3*), as this study reported no change in levels of flavonoids in the *as-lox3* mutant impaired in the biosynthesis of jasmonates (Izaguirre et al., 2007).

UV-B radiation alone is not known to have a direct effect on the activity of PI, however evidence suggests that it may be able to enhance activity of PIs already induced by wounding or herbivory (Stratmann et al., 2000, Izaguirre et al., 2003). Varying effects of UV-B radiation on PI accumulation and activity have been observed in members of the Solanaceae family, with UV-B radiation increasing expression of PI-related genes in *N. attenuata*, but decreasing levels in *N. longiflora* (Izaguirre et al., 2003), suggesting that UV-B can differentially affect plant-invertebrate interactions across closely related plant species.

Glucosinolates do not offer any UV-protection to plants, however the expression of several genes encoding components of glucosinolate biosynthesis (e.g. *MAM1, MYB51, CYP79*'s and *CYP81*'s) were shown to increase in response to UV-B radiation, while levels of aliphatic glucosinolates increased significantly (~2-fold) in broccoli sprouts subjected to a 2-hour irradiation period under ecologically relevant levels of UV-B (Mewis et al., 2012). Indole glucosinolate levels remained unchanged in the same plants, however, indicating that UV-B exerts differential effects on different glucosinolate compounds. Interestingly, herbivory from *P. brassicae, M. persicae* or *P. cochleariae* did not affect levels of aliphatic glucosinolates in broccoli sprouts compared to untreated controls, and while a combination of UV-B radiation and herbivory increased the content of these compounds compared to the individual herbivore treatments, no difference was seen between the

combined treatments and UV-B-alone (Mewis et al., 2012). Levels of indole glucosinolates were similar in *M. periscae*- and *P. brassicae*-treated plants as seen in control and UV-B-treated plants, although *P. cochleariae* elicited an increase in the levels of two glucosinolates in particular, 1-methoxy-indol-3ylmethyl and indol-3ylmethyl, which was repressed slightly upon combining treatment of broccoli with this herbivore and UV-B radiation (Mewis et al., 2012). Therefore, not only are the effects of UV-B on different glucosinolates variable, but the combined effects of UV-B and invertebrate herbivory can elicit different chemical profiles in the same plant.

The importance of the phenylpropanoid pathway in conferring protection against UV-B radiation (section 1.3.2.2.) and resistance against invertebrate pests (section 1.4.4.1) has been previously outlined in this introductory chapter. Many compounds, including CGA and dicaffeoylspermidine isomers, accumulate in response to wounding and UV-B radiation in *N. attenuata* and *N. longiflora*, albeit to varying degrees across the two plant species (Izaguirre et al., 2007). Flavonoids have been described as functioning as feeding and oviposition deterrents, as well as anti-nutritive agents, however the exact effects they elicit on invertebrate pests varies, with incorporation of flavonoids into insect artificial diets impacting the fitness and survival of several Lepidopteran species, while some specialist invertebrates are attracted to these metabolites, using them as stimulants for feeding and ovipositing (Harborne and Williams, 2000).

An enzyme of the phenylpropanoid pathway involved in the biosynthesis of lignin and sinapate precursors, FERULIC ACID 5-HYDROXYLASE (F5H), has been implicated in promoting UV-B-mediated plant defence against *B. cinerea* in Arabidopsis. The Arabidopsis F5H mutant, *fah1-7*, was shown as being unable to reduce *B. cinerea*-induced lesion area in the presence of UV-B, an observation that was seen in WT plants and *tt4* mutants impaired in the production of *CHS* (Demkura and Ballaré, 2012). This finding implied that one branch of the phenylpropanoid pathway (i.e. the sinapate/lignin biosynthetic branch) exerts a larger influence in mediating UV-B-enhanced defence against necrotrophic pests over the branch involved in the biosynthesis of anthocyanins. As this study did not include invertebrate pests, it is unknown whether or not this particular component of the phenylpropanoid pathway or similar enzymes are potentially important in regulating UV-B-mediated defence against invertebrate herbivores, and as such warrants further attention.

The effects of UV-B radiation on enforcing structural defences are unclear, however lignin does not appear to be involved in UV-B-mediated plant defence. Levels of this biopolymer were not shown to increase in response to UV-B radiation in soybean crops,

and as such were not attributed to the UV-B-induced reduction in susceptibility of these plants to caterpillars of *Anticarsia gemmatalis* (Zavala et al., 2001). However, increased deposition of cuticular waxes and lignification was observed in transgenic rice (*Oryza sativa*) over-expressing the UV-B- and MeJA-responsive *OsWRKY89* gene, with these lines also possessing decreased levels of soluble and cell-wall-bound phenolic compounds and higher levels of SA. These lines were more resistant to attack from the rice blast fungus (*Magnaporthe grisea*) and white-backed planthopper (*Sogatella furcifera*), and appeared less attractive to female planthoppers for ovipositing than WT or RNAi-silenced *WRKY89* rice lines (Wang et al., 2007). It is therefore possible that UV-B and JA pathways can converge to heighten structural defences against invertebrate and microbial pests, however more work is required to test this theory.

1.5.3 UVR8 in UV-B-enhanced plant defence

A role of the UV-B photoreceptor, UVR8, in mediating UV-B-enhanced plant defence in Arabidopsis against *B. cinerea* was recently reported using the *uvr8-6* mutant (Demkura and Ballaré, 2012). Following a 4-hour exposure to UV-B radiation, Col-0 plants possessed smaller lesion areas induced by *B. cinerea* compared to control plants maintained under white light-only conditions. This enhanced resistance to *B. cinerea* was absent from *uvr8-6* mutants exposed to UV-B radiation, indicating that UV-B-mediated defence against necrotrophic microbes is dependent upon UVR8 (Demkura and Ballaré, 2012). A requirement for UVR8 in promoting plant defence against invertebrate pests in a UV-B-dependent manner has not yet been reported, and due to the evident complexity in plant defence signalling pathways, it cannot be assumed that UVR8 is also required for enhancing pest defence in the presence of UV-B, despite being the UV-B-photoreceptor. As only one study to date has investigated the role of UVR8 in regulating UV-B-mediated plant defence, further research is required to assess whether UV-B-mediated defence operates through the UV-B photoreceptor or if it is independent of UVR8.

1.6 The aims of this study

The overall aim of this study was to elucidate the molecular basis of UV-B-induced invertebrate resistance in a commercially important crop, *Brassica napus* (oilseed rape), by utilising a transcriptomic and metabolic approach to study the whole genome and metabolome modifications of this crop in response to UV-B radiation, invertebrate herbivory, or exogenous application with MeJA. To this end, two leaf-chewing invertebrate pests were used, the first being a generalist mollusc, the grey field slug (*Deroceras reticulatum* (Limacoidea: Agriolimacidae)), the second, larvae of the specialist feeder the diamondback moth (*Plutella xylostella*). These invertebrates are referred to simply as slugs and *Plutella* throughout this study. *B. napus* was selected as the model organism for this project for several reasons. It is accepted that plant defence responses may vary across plant species, therefore it seemed logical to investigate the effects of UV-B radiation on enhancing defence responses in a commercially important crop. In saying that, the close family relationship between *B. napus* and Arabidopsis (Brassicaceae family) allowed knowledge on genetic, metabolic and physiological aspects of Arabidopsis to be transferred (to some extent) to *B. napus*, and several Arabidopsis mutants were incorporated into this project. Access to the Arabidopsis genome also proved very beneficial during transcriptomic analysis of *B. napus*, as combining the sequenced Arabidopsis genome with either the 95K Brassica Unigene (Trick et al., 2009) or the recently sequenced *B. napus* genome (Chalhoub et al., 2014) allowed putative gene annotations to be assigned to *B. napus* transcripts (Chapter 4). In addition to *B. napus'* close relationship to Arabidopsis, its use in this project was also due to the degree of overlap between UV-B- and wound-induced responses in this crop having not yet been investigated, although convergences between these two signalling pathways have been studied in another member of the Brassicaceae family, broccoli (Mewis et al., 2012).

The first goal of this project was to assess any effect of UV-B radiation on modifying the attractiveness of *B. napus* to slug and *Plutella* herbivory (Chapter 3). To achieve this, invertebrate choice-chamber bioassays were set up where *B. napus* or Arabidopsis plants previously irradiated under minus UV-B (-UV-B) or plus UV-B (+UV-B) conditions were presented to a known number of invertebrates, and the area of leaf tissue consumed over a 48-hour period was reported to indicate invertebrate feeding preferences. The influence of another component of UV radiation (UV-A) on plant susceptibility to pests was also studied in similar bioassay experiments, before regulatory roles of the UV-B photoreceptor,

UVR8, on UV-B-enhanced defence was assessed by measuring leaf area consumed by invertebrates on Arabidopsis *uvr8-1* and *35Spro*:GFP-UVR8 lines.

Transcriptomic analysis of *B. napus* plants subjected to individual treatments of UV-B radiation, exogenous MeJA treatment, slug herbivory or *Plutella* herbivory via RNA-seq (Chapter 4) allowed identification of early-induced transcriptional regulators that increased in expression by multiple treatments. Several genes identified in this experiment were selected for over-expression in Arabidopsis, to assess any roles they may have in promoting UV-B-enhanced plant defence against slugs and *Plutella* (Chapter 6). To compliment the findings obtained from this study, a global metabolic profile of *B. napus* plants exposed to the same 4 treatments mentioned above was acquired using reversed-phase HPLC (Chapter 5), to identify key signalling pathways and their associated components that facilitate the convergence of UV-B- and wound-response pathways in *B. napus.*

Chapter 2: MATERIALS AND METHODS

2.1 Materials

2.1.1 Chemicals

Unless otherwise stated, all chemicals were obtained from Sigma-Aldrich Company Ltd. (Poole, Dorset, UK), Fisher Scientific UK Ltd. (Loughborough, Leicestershire, UK).

2.1.2 Antibiotics

Ampicillin and gentamycin were obtained from Melford Ltd. (Ipswich, Suffolk, UK) and kanamycin from Sigma-Aldrich. All were dissolved in sterile distilled water. Working concentrations of all antibiotics used are shown in Table 2-1.

Antibiotic	Working Concentration
Ampicillin	100μg/ml
Gentamycin	30μg/ml
Kanamycin (*E.coli*)	50μg/ml
Kanamycin (plants)	75μg/ml (agar plates) or 100μg/ml (silicon dioxide plates)

Table 2-1: Working concentrations of antibiotics.

2.1.3 Enzymes

Enzymes used for DNA and RNA modifications, cDNA synthesis, PCR, ligations and restriction digests were obtained from Promega (Southampton, Hampshire, UK), New England Biolabs (Hitchin, Hertfordshire, UK) and Life Technologies Ltd. (Paisley, UK). All were used according to the manufacturer's instructions.

2.1.4 Plasmid vectors

Plasmid vectors used for the generation of transgenic Arabidopsis plants are shown in Table 2-2.

Plasmid Vector	Properties of Plasmid Vector	Source
pEZR(K)L-C	35S promoter and a GFP tag on N-terminus region of the inserted gene	Dr. Gert-Jan de Boer, University of Amsterdam (Schnurr et al., 2002)
pEZR(K)L-N	35S promoter and a GFP tag on C-terminus of inserted gene	Dr. Gert-Jan de Boer, University of Amsterdam (Schnurr et al., 2002)
pGWB15	35S promoter and 3-HA tag on N-terminus of inserted gene	Dr. Nakagawa Shimane, University of Japan (Nakagawa et al., 2007)

Table 2-2: Plasmid vectors used throughout this study.

2.1.5 Bacterial strains

E.coli TOP10 cells (Agilent Technologies, California, USA) were transformed with the plasmid vector constructs for sub-cloning. Arabidopsis transformation with pGWB15, pEZR(K)L-C and pEZR(K)L-N containing either *VTC2, ELI3-2* or *COMT1* was carried out with *Agrobacterium tumefaciens* strain GV3101.

2.1.6 Additional reagents and materials

Methyl jasmonate (MeJA) ≥ 95% was purchased from Sigma-Aldrich Company Ltd. (W341002-25G-K), as was silicon dioxide ($Si0_2$ purum p.a.; acid purified; 40-200 mesh; 84880). A wetting agent, Surfac UN65, was a kind gift from Dr. Ian Bedford at the John Innes Centre, Norwich, from a stock supply purchased from Surfachem.

2.1.7 Equipment

Centrifugations were conducted with an Eppendorf 5415 D bench-top centrifuge (up to 2 ml tubes), SORVALL LEGEND RT Centrifuge (15-50 ml Falcon centrifuge tubes).

2.2 Preparation of media and solutions

2.2.1 Measurement of pH

The pH of solutions and media was carried out using a glass electrode attached to a Jenway 3320 pH meter (Jenway, Felsted, Essex, UK).

2.2.2 Autoclave sterilization

Solutions, media and equipment were sterilized using a benchtop autoclave (Prestige Medical, Model 220140) for 15 minutes at 120°C, 1atm.

2.2.3 Filter sterilization

Heat sensitive solutions wee filter sterilized through a 0.2μm pore diameter Nalgene filter using a needleless syringe.

2.3 Plant material

2.3.1 Seed stocks

Brassica napus RV31 seeds were purchased from the John Innes Centre (Norwich). *Arabidopsis thaliana* Landsberg *erecta* (L*er*) and Columbia-0 (Col-0) wild type seeds were from stocks established in the Jenkins lab. The segregating and homozygous T-DNA mutants (Table 2-3), all of which are in a Col-0 background, were obtained from The European Arabidopsis Stock Centre (NASC, Nottingham, UK). The *uvr8-1* mutant (in the L*er* background) was provided by Professor Daniel Kliebenstein (UC Davis, California, USA). The *35S*pro:GFP-UVR8 over-expressing line in a L*er* background was generated by a previous member of the Jenkins lab. Chinese cabbage var. Apex and lettuce seeds were obtained from Sea Spring Seeds (http://www.seaspringseeds.co.uk) and Dobbies Garden Centre, respectively, as a food source for the invertebrates.

T-DNA Mutant	NASC (SALK) Accession Name
comt1	N25167 (SALK_135290C)
eli3-2	N696708 (SALK_206866C)
jar1-1	N8072
vtc2	N656047 (SALK_146824C)

Table 2-3: NASC T-DNA Arabidopsis mutant lines used in this study.

2.3.2 Growth of plants on soil

B. napus, cabbage, lettuce and Arabidopsis seeds were sown in pots on the surface of compost dampened with tap water. Pots were covered with cling film and given a period of vernalisation at 4°C in the dark for 2-4 days before being transferred to 20°C growth chambers for germination. Unless stated otherwise, Arabidopsis and *B. napus* were kept under approximately 70 μmol m^{-2} s^{-1} constant white light in growth chambers until treatment. Plants for floral dip transformation and seed collection were maintained under these conditions until flowering or dried out.

2.3.3 Surface sterilization of seeds

Arabidopsis seeds to be sown on ½ MS agar plates were surface sterilized using 70% ethanol for 2 minutes, 50% (v/v) sodium hypochlorite for 5 minutes, then rinsing several times with sterile distilled water under all bleach was removed.

2.3.4 Growth of plants on agar plates

Surface sterilised Arabidopsis seeds were sown on ½ Murashige and Skoog salts (2.15 g/L) containing 0.8% agar with the pH adjusted to 5.7. 75 μg/ml kanamycin was added for segregating Arabidopsis transgenic lines. After seeds were sown on the surface of the agar, plates were sealed with micropore tape, wrapped in tin foil, inverted and kept at 4°C for 2 days in the dark. Seeds were germinated under approximately 70 μmol m^{-2} s^{-1} constant white light, and grown for the desired period of time.

2.3.5 Growth of plants on silicon dioxide plates

Segregating Arabidopsis transgenic lines were initially studied on ½ MS agar plates as described in section 2.3.4. An alternative method was also used, where non-sterilised Arabidopsis seeds were sown on top of non-sterile silicon dioxide as described by Davis *et al*. (2009). The silicon dioxide was initially poured into petri dishes, where it was dampened in ¼ MS solution (1.1 g/L MS salts, 0.5 g/L MES, pH adjusted to 5.7) containing 100 mg/ml of kanamycin. The plates were swirled then the bases were tapped to remove air bubbles from the sand, and allowed to sit in the media for several minutes before all liquid was removed with a pipette. Plates were again sealed with micropore tape, wrapped in tin foil, and kept upright in the darkness at 4°C for 2 days before being transferred to 70 μmol m^{-2} s^{-1} constant white light for germination and growth (Davis et al., 2009).

2.4 Invertebrate material

2.4.1 Invertebrate sources

Two invertebrates were studied during this project, larvae of the Diamondback moth, *Plutella xylostella*, and grey field slugs, *Deroceras reticulatum* (Figure 2-1). The initial invertebrate stocks maintained at the University of Glasgow were given as a kind gift from Mr. Gavin Hatt from the Entomology department at the John Innes Centre, Norwich. Slugs were collected around the Norwich area, while *Plutella* larvae were from a long

generation of captured moths held in the entomology facilities at the John Innes Centre. Subsequent slug colonies were established in the laboratory by collecting adults and eggs of the specific slug species (*Deroceras reticulatum*) from fields in Carluke, South Lanarkshire.

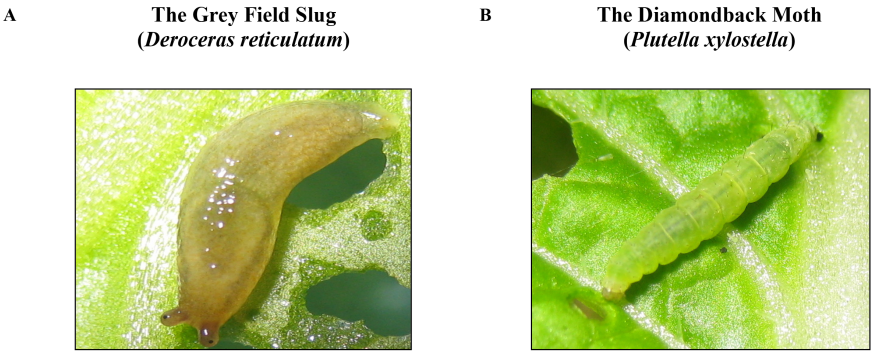

Figure 2-1: Images of the two invertebrates used in this study. The indirect effects of UV-B radiation on the feeding preferences of **A,** juvenile grey field slugs (*Deroceras reticulatum*) and **B,** larvae of the Diamondback Moth (*Plutella xylostella*) was investigated in this project. Pictures courtesy of staff at the Entomology department, the John Innes Centre.

2.4.2 Invertebrate maintenance

Plutella were kept in mesh-covered cages on a diet of Chinese cabbage (var. Apex), in a growth chamber set at 22°C in a 16h:8h light:dark cycle. Slugs were separated into small groups and kept in large petri dishes with dampened blue roll as a base. They were fed on a mixture of Chinese cabbage and lettuce, and kept in the shade under a bench top in the laboratory. Cages and petri dishes were cleaned out or replaced as required, and fresh food added when regularly.

2.5 Treatments

2.5.1 Light sources

Light treatments were carried out in growth chambers at 20°C. White light treatments (-UV-B) were conducted using warm white fluorescent L36W/30 tubes (Osram, Munich, Germany). UV-B radiation was provided with two sources: narrowband UV-B tubes (Philips TL20W/01RS; Philips, Aachen, Germany, Figure 2-2A) and broadband UV-B tubes (UVB-313; Q-Panel Company, USA; Figure 2-2B). The broadband tubes were covered with a cellulose diacetate filter (Cat. No FLM400110/2925, West Design Products, London, UK) to remove short wavelength radiation below approximately 290 nm from the emitted spectrum of light reaching the plants. Cellulose acetate was replaced every 24

hours. As narrowband tubes do not emit these short wavelengths, they were not covered in cellulose diacetate. Broadband tubes have a maximum emission at 313nm, and narrowband at 311nm. Both sources can also emit very low levels of UV-A and blue light, however they have not been found to induce a UV-A/blue light specific response (Ulm *et al.,* 2004). Removal of UV-A and UV-B from light sources in certain invertebrate bioassays was achieved using a Lee 130 clear filter (Lee Filters, Hampshire, UK), which removes wavelengths below approximately 400 nm.

The narrowband UV-B source was used to irradiate SDS-PAGE gels before conducting Western blots. Broadband UV-B was used for plant illuminations.

White light fluence rates were measured using a LI-250A light meter attached to a LI-190 quantum sensor (LI-COR, Lincoln, NE, USA). UV-B fluence rates were measured using a Spectro Sense 2 SKL904 meter and a UV-B sensor, SKU 430/SS2 (Skye Instruments, Powys, UK). Spectral measurements of wavelengths between 200-800nm were measured using a Macam Spectroradiometer model SR9910 (Macam Photometrics Ltd., Livingston, UK).

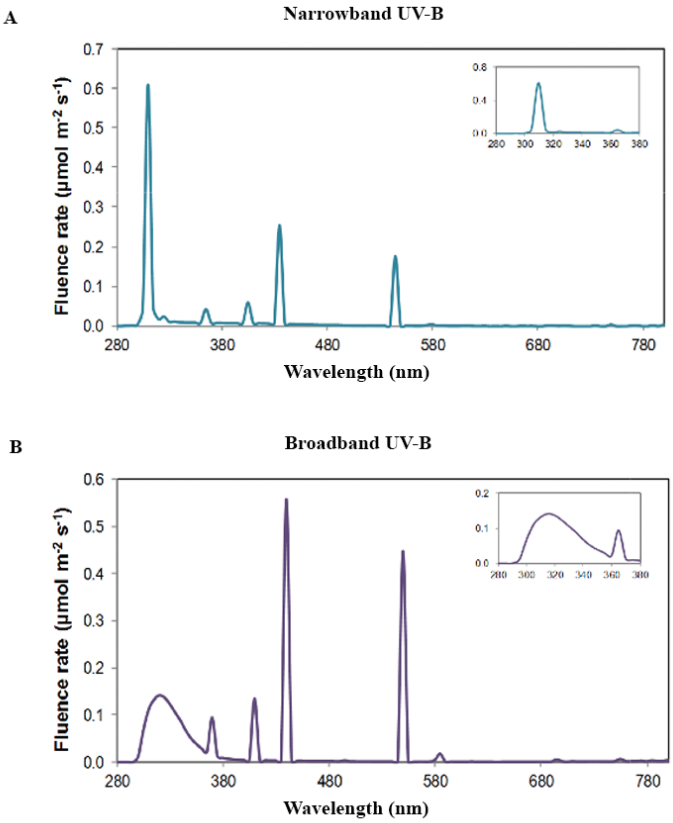

Figure 2-2: Spectra of light emitted from the two UV-B sources used in this study. The spectrum of light emitted from **A,** narrowband UV-B tubes, Philips TL20W/01RS and **B,** broadband UV-B tubes, UVB-313, Q-Panel. From Monika Heilmann's Ph.D thesis, University of Glasgow, 2013.

2.5.2 Invertebrate bioassays at the University of Glasgow

Invertebrate assays were conducted on three week old Brassica and Arabidopsis plants. *B. napus* were germinated and grown under approximately 70 μmol m^{-2} s^{-1} of constant white light for 2 weeks, then either maintained under these conditions for a further week or moved to 70 μmol m^{-2} s^{-1} white light supplemented with either 3 μmol m^{-2} s^{-1} broadband UV-B or 70 μmol m^{-2} s^{-1} of UV-A. The same protocol was followed for Arabidopsis, however they were grown under white light conditions for 17 days before being either maintained under these conditions for a further 4 days, or exposed to 70 μmol m^{-2} s^{-1} white light supplemented with 1.5 μmol m^{-2} s^{-1} broadband UV-B.

All bioassays were choice chamber assays, where invertebrates were presented with two plants that had received different light treatments for 4-7 days prior to the bioassay, and were allowed to choose which plant they preferred to graze upon over a 48-hour period. The feeding preferences of slugs and *Plutella* larvae were studied separately.

The assays took place in the *Plutella* growth chamber, where only warm white light is illuminated. Invertebrates underwent a period of fasting before the assay began. Second instar *Plutella* larvae were removed from their mesh cages carefully using a dampened paintbrush to a plastic container lined with dampened tissue paper that contained no food. The larvae were kept here for 1-2 hours before the start of the experiment. Juvenile slugs were moved carefully using the flat end of a spatula to a petri dish lined with dampened tissue paper. The petri dishes were sealed with micropore tape, and the slugs left overnight without food.

For all assays, intact plants were used. In order to calculate the leaf area consumed by the invertebrates, each leaf from the plants were photographed against a piece of white paper that had cm ruler markings drawn on it before the start of the experiment. For leaves that were slightly curled at the edges (a more prominent trend seen in UV-B treated *B.napus* plants), the side to which it curled towards was carefully pressed against the paper. This appeared to be effective at flattening the leaf without wounding it. Photographs were uploaded to a computer, and leaf area was measured using ImageJ 1.47v software.

On the day of the bioassays, dampened tissue paper was put on the base of the invertebrate cages, and one white light plant (-UV) and one UV treated plant (+UV-A/B) was positioned randomly in the cages. Invertebrates larvae were deposited in the centre of the cages, and allowed to move towards the plant of their choosing. Ten second instar *Plutella* larvae or 2 juvenile slugs were used in each bioassay.

At the end of the 48-hour herbivory period, invertebrates were removed, and leaves were detached from each plant at their petioles and stuck to white A4 paper using double-sided tape. The leaves were then scanned onto a computer alongside a ruler with cm markings on it, and the areas of leaf tissue was measured using ImageJ 1.47v software. The area of tissue remaining on each leaf could be compared to the starting leaf area, which subsequently revealed the total area of leaf tissue consumed by the invertebrates.

Several independent replicates of each bioassay were carried out on different occasions, with at least two biological replicates included examined on each occasion. As invertebrates can themselves be a source of variation, it was important to conduct as many replicates as possible over the course of the project.

Results were presented as bar charts to display the total area or average area of leaf tissue consumed (cm^2) by each invertebrate, and boxplots were also generated to display the spread of areas of tissue consumed across several replicates. For the boxplots, the middle line represents the median data point, while the 1st and 3rd quartile (the lower section and upper section of the box, respectively) each contain 25% of the data. The two vertical lines indicate the outliers that are 1.5 times the interquartile range (IQR). A white circle on the boxplot shows the position of an extreme outlier that is not within the 1.5x limit of the IQR.

Standard error of the mean (Willis et al.) error bars are included on bar charts to show the spread of variation of the sample means. Statistical analysis of the results was executed on R using Analysis of Variance (ANOVA) and Tukey's Honest Significant Difference (HSD) post-hoc test.

2.5.3 Treatments for gene expression analysis

For gene expression analysis, *B.napus* and Arabidopsis plants were grown under constant warm white light for three weeks prior to treatment. For *B.napus*, the youngest and second youngest true leaves were harvested for all treatments. All Arabidopsis leaves were harvested following light and methyl jasmonate treatment, while only those leaves showing signs of herbivory were collected following invertebrate treatment.

2.5.3.1 UV-B treatment

All plants were transferred under low white light (approximately 20 μmol m^{-2} s^{-1}) the night before treatment was due to commence. Plants were exposed to 3 μmol m^{-2} s^{-1} of broadband UV-B, and individual plant samples were harvested at various time points over a 24 hour period. Each time point had three biological repeats. For *B.napus*, the youngest

and second youngest true leaves were harvested. For Arabidopsis, all leaf tissue was harvested.

2.5.3.2 Methyl jasmonate treatment

A stock solution of 1 M methyl jasmonate in 100% ethanol was kept at 4°C. Working concentrations of 10 μM, 100 μM and 1 mM methyl jasmonate 0.01% ethanol were made fresh on the day of treatment, and a wetting agent, Surfac UN65, was added to a final concentration of 0.01% (v/v), to enable methyl jasmonate to penetrate through the waxy epidermal layer of the plant leaves.

Using a cosmetic spray bottle, 3 week old plants were sprayed with either water, 0.01% ethanol 0.01% UN65, or the working concentrations of methyl jasmonate (plus 0.01% ethanol and 0.01% UN65). The water and ethanol/UN65 treatments acted as additional controls, to confirm that the changes in gene expression were due to methyl jasmonate, and not another component of the solution.

After treatment, plants were put into pot trays and stored under low white light (20 μmol m^{-2} s^{-1}). Propagators were placed on top of the trays to prevent volatile organic compounds from treated plants coming into contact with other plants. All plants, including the white light (no treatment) controls received this precautionary measure. Individual plants were harvested over a 24-hour period, three biological replicates harvested at each time point.

2.5.3.3 Invertebrate treatments

Initial invertebrate treatments took place in the Entomology department of the John Innes Centre, and later at the University of Glasgow. In both cases, 3-week old *B. napus* plants were used. The two invertebrates received a period of starvation immediately before the bioassays began. Juvenile slugs were transferred to petri dishes lined with dampened tissue and sealed with breathable surgical tape, then stored in a cool room out of direct sunlight for approximately 16 hours with no food. Enough slugs were collected to ensure that two for each individual plant would be available. Second instar *Plutella* larvae were collected with a fine paintbrush and deposited in small, transparent plastic boxes. These boxes were again lined with dampened tissue, and no food source was provided. Experts at the Entomology department recommended a starvation period of 1-2 hours for *Plutella* larvae, to reduce cases of cannibalism within the boxes and/or death of invertebrates. Ten larvae for each plant were used, and the boxes were stored at 20°C under white light (-UV-B) during the starvation period.

To restrict the movement of invertebrates during the experiment, transparent, plastic clip boxes were used to house individuals leaves (Figure 4. A). These boxes possessed a 1 cm diameter circular hole on one side for the petioles of in tact plants to sit in. To prevent invertebrates from escaping through these holes, small sponge slices were inserted along with the petiole, filling the surplus gap while protecting the petiole.

At 3 weeks old, the *B. napus* plants had relatively long petioles, which meant they were liable to breaking easily. Many petioles were snapped due to the strain imposed by the clip boxes, therefore it was important to rest boxes on top of the plant pots, or a ledge of similar height, to reduce the strain on the petioles.

Invertebrate grazing took place for 1 hour. The boxes and pests were then removed from the plants, and samples were harvested at regular intervals over a 25-hour period, with time point 1 (T=1) being the time at which the invertebrates were removed from the plants.

These experiments were later replicated at the University of Glasgow, with one minor difference: plastic drinks cups and fine mesh netting were used to confine invertebrates to one leaf instead of the plastic boxes used at the John Innes Centre. Squares of fine mesh were cut out, and a ~ 1 cm diameter hole was punched through the middle of them. A straight line was then cut from this hole to one side of the square using a pair of scissors, to create a slit. 2 juvenile slugs or 10 second instar *Plutella* larvae were deposited in the bottom of the cup, and one *B. napus* leaf was then inserted into the cup. A mesh square was gently pulled around the stem via the cut slit, until the stem sat in the 1 cm diameter hole in the middle. The mesh was then taped to the side of the cup, and a piece of tape was put along the length of the cut slit. The cup was rested in such a position that prevented the stem or plant from being damaged.

2.6 DNA and RNA methods

2.6.1 Isolation of genomic DNA from Arabidopsis and *B. napus*

Genomic DNA was extracted from Arabidopsis and *B.napus* using the Qiagen Dneasy® Plant Mini Kit (Qiagen, Crawley, West Sussex, UK) according to the manufacturers instructions. Extractions were carried out on approximately 100 mg of leaf tissue, which was ground to a fine powder in liquid nitrogen using a mortar and pestle. Tissue was transferred to a 1.5 mL Eppendorf tube, where cell lysis and DNA extraction took place as described in the Qiagen Dneasy® Plant Mini Kit handbook. Purified genomic DNA was eluted from the Dneasy membrane in 50 µl of sterile distilled water, and stored at 4 °C.

2.6.2 Isolation of plasmid DNA

Small-scale plasmid DNA purifications from *E. coli* were carried out using the Qiagen® Plasmid Mini Kit following the manufacturers instructions. A single bacterial colony was inoculated in 10 mL LB medium containing the appropriate antibiotics for plasmid selection, and incubated at 37 °C overnight with constant shaking at 200 rpm. Cells were pelleted at 4, 000g for 10 mins, and the supernatant was discarded. Cell lysis and plasmid DNA purification was carried out as detailed in the Qiagen® Plasmid Mini Kit protocol, and plasmid DNA was stored at -20 °C.

2.6.3 Isolation of RNA from Arabidopsis and *B. napus*

RNA was extracted from both Arabidopsis and *B.napus* using TRIzol® Reagent from Invitrogen (Life Technologies) and following the manufacturer's instructions with one minor modification. RNA precipitation was carried out using pre-chilled isopropyl alcohol at either 4 °C or 20°C overnight. Samples were stored at -80°C after redissolving RNA in 30 μl of sterile DEPC'ed water.

2.6.4 Quantification of DNA and RNA

The quality and quantity of DNA and RNA was carried out using a spectrophotometer (Eppendorf Bio Photometer) by adding 2 μl of sample to 98 μl of dH_2O and measuring the absorbance at 230, 260 and 280nm.

2.6.5 Dnase treatment of RNA from Arabidopsis and *B. napus*

Dnase treatment of RNA was conducted using the DNA-*free*™ DNA removal kit from Life Technologies (cat. Number AM1906) following the manufacturers instructions. Approximately 2 μg of RNA was Dnased at 37 °C for 1 hour with 2 units of the Dnase I enzyme and 1 x Dnase buffer in a 25 μL reaction volume. The reaction was terminated using 3.5 μL of Dnase Inactivation Reagent and incubating at room temperature for 5 min, and the efficiency of the Dnase treatment was tested using a 35 cycle PCR reaction and *ACTIN2* primers.

2.6.6 Reverse transcription of Arabidopsis and *B. napus* RNA

First strand cDNA was synthesised from Dnased RNA using SuperScript® II Reverse Transcriptase from Life Technologies following the manufactures protocol. 1 μg of Dnased RNA was reverse transcribed in a 30 μL reaction volume with 4 μM oligo-dT

primers (dTTP20) at 65 °C for 5 min. The mixtures were briefly cooled on ice, and 1x Reverse Transcriptase Reaction Buffer, 1 mM dNTPs, and 50 units of Rnase inhibitor (Promega) were added. Reaction mixtures were then incubated at 42 °C for 2 minutes, before adding 200 units of SuperScript® II to the mixture. Samples were then incubated at 42 °C for 50 min, and the reaction inactivated by heating at 70 °C for 15 min. The cDNA samples were then stored at -20 °C.

2.6.7 Semi-quantitative and quantitative PCR

Semi-quantitative RT-PCR was conducted using GoTaq® G2 Flexi DNA Polymerase (Promega cat no. M7801). Equivalent quantities of cDNA, estimated using reactions with *EF1a* primers, were used as templates for semi-quantitative RT-PCR. Each reaction contained 1x Green GoTaq® Flexi buffer, 0.1 mM dNTPs, 0.5 μM of each gene specific primer and 0.625 units of GoTaq® G2 Flexi DNA Polymerase in a 25 μL reaction volume.

Primers for Arabidopsis and *B. napus* were designed using CLC Genomics Workbench (version 7.0, Qiagen), except those for genotyping, which were obtained from the SALK T-DNA primer design website (http://signal.salk.edu/tdnaprimers.2.html). Primers were synthesised by Invitrogen and are listed in Table 2-4. As sequencing of the *B. napus* genome was not completed and published until late 2014 (Chalhoub et al., 2014), the Arabidopsis genome, Brassica 95K Unigene, and sequenced genome of the *B. napus* progenitor species, *B. rapa* and *B. oleracea,* were used as platforms for primer design.

Transcript abundance measurements using quantitative RT-PCR (qPCR) was carried out on a StepOnePlus™ Real-Time PCR machine (Life Technologies), using Brilliant III Ultra-Fast SYBR master mix (Agilent Technologies Cat No. 600882) while adhering to the MIQE guidelines (Bustin et al., 2009).

PCR products of whole gene fragments were subcloned into the pCR™2.1 TOPO vector (Life Technologies) according to the manufacturers instructions to generate suitable standards for gene expression analysis. Six 1/10 serial dilutions of each construct where made, the highest concentration being 10 pg/μL, and analysed on every qPCR plate to generate a standard curve. Satisfactory standard curves possessed a 95-105% efficiency of amplification, and the equation of the standard curve was used to calculate the DNA quantity of each Ct value, providing the Ct values were not higher than that of the most diluted standard sample. An absolute target copy number could subsequently be calculated from this DNA quantity. Three technical replicates of each sample were run on each plate. The cycling conditions were as follows: 95 °C 2 min, (95 ° 10 sec, 60 °C 20 sec) x 40

cycles, 95 °C 1 min, 60 °C 30 sec, 95 °C 5min, with data collection at every +0.3 °C increment on the final ascent to 95 °C.

Expression changes in the genes of interest are presented as relative fold changes with regards to the reference gene, *EF1a*. Results are also presented with standard deviation (SD) error bars, to indicate the degree of variability across three technical replicates or several biological replicates. ANOVA was performed using R to assess the statistical significance of the results.

***B. napus* gene primers for semi-quantitative RT-PCR**			
Arabidopsis Gene ID	**Arabidopsis Gene Name**	**Brassica ID**	**Primer Sequence**
At5g60390	*EF1a*	Bra010178	For – 5' ATACCAGGCTTGAGCATACCG 3' Rev – 5' GCCAAAGAGGCCATCAGACAA 3'
AT3G45140	*LOX2*	Bra003526	For – 5' ACCATCACCACTCATCAACC 3' Rev – 5' TATGCAGCAAAGATGACAGC 3'
AT5G08640	*FLS*	Bra009358	For – 5' ATGGAGATCGAGAGAGTCCAAG 3' Rev – 5' TCAGTCCAGAGGAAGCTTATTGAGC 3'
AT5G54160	*COMT1*	Bra029041	For – 5' ATGGGATCAACGGCGGAGACAC 3' Rev – 5' TTACATCTTTTTGAGCAGCTCAATAACG 3'
AT4G26850	*VTC2*	Bol006503	For – 5' ATGCTGAAAATCAAGAGGGTTCC 3' Rev – 5' TCACTGAAGAACAAGGCACTCAGAG 3'
AT5G13930	*CHS*	Bol034259	For – 5' TCAAGCGCATGTGCGATAAGTCG 3' Rev – 5' TGCTGGTACATCATGAGACG 3'
AT1G32640	*MYC2*	Bra010178	For – 5' ATGAATCTCTGGACCACCGACG 3' Rev – 5' AGATTAAACTCGCCCGGAGC 3'
AT4G37990	*ELI3-2*	Bol032749	For – 5' ATGGTCAGCTCATGCGGGT 3' Rev – 5' TTAAGGACTAGGCTTCAAGGTG 3'
AT4G39950	*CYP79B2*	Bra011821	For – 5' GAGATACTCAAGCAACAAGACG 3' Rev – 5' TCTCTTCTGGTGAAGCCACC 3'
AT3G45640	*MPK3*	Bra038281	For – 5' GAGATGTGGTTCCTCCACCA 3' Rev – 5' ACTTGAGCCCTCGAAGAAGC 3'
AT2G38470	*WRKY33*	Bra017117	For – 5' ATGTTGAGAGGGCATCAAATGA 3' Rev – 5' GATCTTGTGCCAGTCTGTTTGTAGA 3'
AT5G42650	*AOS*	Bra035320	For – 5' ATGGCCTCTGCTTCACCTCATTTCC 3' Rev – 5' CTAAAAGCTAGCCTTCCTCAGAGACG 3'
AT5G09810	*ACT7*	Bra028615	For – 5' TGGAACTGGAATGGTGAAGG 3' Rev – 5' ATACCTCTCTTGGACTGAGC 3'

***B. napus* gene primers for qPCR**		
Arabidopsis Gene ID	**Brassica homologue ID**	**Primer Sequence**
AT4G37990 (*ELI3-2*)	Bol032749	For – 5' TTCCCCGATGAAGTATCACG 3' Rev – 5' CCATAGTACCCATTGCATCC 3'
AT4G26850 (*VTC2*)	Bol006503	For – 5' CTTGATGCCACAGTGTTACG 3' Rev – 5' CTTTCCTCTGACAGAGAAGC 3'
AT5G54160 (*COMT1*)	Bra029041	For – 5' TCTCACGTCTTACTCCATCC 3' Rev – 5' ACCAGCTTTCCATGAGAACC 3'
AT1G32640 (*MYC2*)	Bra010178	For – 5' TCGATCCAGTTTGAGAATGG 3' Rev – 5' TGCTGAATTTCGGATTCTGG 3'
AT4G01370 (*MPK4*)	Bol010768	For – 5' TCAGCCAATGTGTTACACCG 3' Rev – 5' AGATATCGATCGCTGCTGTG 3'
AT3G45140 (*LOX2*)	Bra003526	For – 5' GTTATGATGCTACCTCCTGC 3' Rev – 5' TACAGCAATGAGTCCTCAGC 3'

Primers for NASC genotyping		
Arabidopsis Gene ID	**NASC ID**	**Primer Sequence**
VTC2	SALK_146824c	For – 5' GTGTTCTTGACTGCTTGCCTC 3' Rev – 5' CCAAGAAGCTTCAAATGCAAC 3'
COMT1	SALK_135290c	For – 5' TTGAAACTAGCTTGGTCGGTG 3' Rev – 5' AATTCTTGATGGTGGGATTCC 3'
COMT1	SALK_020611c	For – 5' TCCGGTTTGCAAGTATTTGAC3' Rev – 5' CTAGGGTCAGTCCCGTGGTAC3'
AOS	SALK_017756c	For – 5' GTTCTTCAAATCACGAATCC 3 Rev – 5' AAAACTCGTAGAGTCTCTGG 3'
ELI3-2	SALK_206866c	For – 5' ATGGGAAAGGTTCTTCAGAAAGAGG 3' Rev – 5' TAGGATTAGGCTTCAATGTGTTGGC 3'
	LBb1.3 (T-DNA INSERT)	5' ATTTTGCCGATTTCGGAAC 3'

***B. napus* and plasmid primers for cloning**	
***B. napus* Gene and Plasmid**	**Sequence**
COMT1 pGWB14	For – GGGGACAAGTTTGTACAAAAAAGCAGGCTTCATGGGATCAACGGCGGAGACAC Rev – GGGGACCACTTTGTACAAGAAAGCTGGGTTTTACATCTTTTTGAGCAGCTCAAT AACG

COMT1 pGWB15	For - GGGGACAAGTTTGTACAAAAAAGCAGGCTTCATGGGATCAACGGCGGAGACAC Rev – GGGGACCACTTTGTACAAGAAAGCTGGGTTCATCTTTTTGAGCAGCTCAATAA CG
VTC2 pEZRLC	**PstI Restriction enzyme:** For - AAACTGCAGATGCTGAAAATCAAGAGGGTTCC **BamHI Restriction enzyme:** Rev - AAAGGATCCTCACTGAAGAACAAGGCACTCAGAG
ELI3-2 pERZLC	**EcoRI Restriction enzyme:** For - AAAGGATCCGCCATCTTTTTGAGCAGCTCAATAACG **BamHI Restriction enzyme:** Rev – AAAGAATTCATGGTCAGCTCATGCGGGT
ELI3-2 pERZLN	**EcoRI Restriction enzyme:** For - AAAGGATCCGCCATCTTTTTGAGCAGCTCAATAACG **BamHI Restriction enzyme:** Rev – AAAGGATCCGCAGGACTAGGCTTCAAGGTG

Arabidopsis gene primers for semi-quantitative RT-PCR	
Arabidopsis Gene ID	**Primer Sequence**
AT5G60390 (*EF1A*)	For - 5’ TGAGCACGCTCTTCTTGCTTTCA 3’ Rev - 5’ GGTGGTGGCATCCATCTTGTTACA 3’
AT4G37990 (*ELI3-2*)	For - 5' AGTCGGAGTTGGGTGTTTGG 3' Rev - 5' ACCATGTGGTCGGAGTAACC 3'
AT4G26850 (*VTC2*)	For - 5' CTTGATGCCACAGTGTTACG 3' Rev - 5' CTTTCCTCTGACAGAGAAGC 3'
AT5G54160 (*COMT1*)	For - 5' GATGGTGTTTCCATTGCTGC 3' Rev - 5' AACGCGCTCATTCCATAAGC 3'
AT1G32640 (*MYC2*)	For – 5’ GATGAGGAGGTGACGGATACGGAA Rev – 5’ CGCTTACCAGCTAATCCCGCA
Arabidopsis gene primers for semi-quantitative RT-PCR	
Arabidopsis Gene ID	**Primer Sequence**
AT5G60390 (*EF1A*)	For - 5’ TGAGCACGCTCTTCTTGCTTTCA 3’ Rev - 5’ GGTGGTGGCATCCATCTTGTTACA 3’
AT4G37990 (*ELI3-2*)	For - 5' AGTCGGAGTTGGGTGTTTGG 3' Rev - 5' ACCATGTGGTCGGAGTAACC 3'
AT4G26850 (*VTC2*)	For – 5’ GGACTTGCCCTAAAGAACGA Rev – 5’ GTGTTCTCGGTCCCATATCC
AT5G54160 (*COMT1*)	For - 5' GATGGTGTTTCCATTGCTGC 3' Rev - 5' AACGCGCTCATTCCATAAGC 3'

Table 2-4: Primers used for semi-quantitative and quantitative RT-PCR with *B. napus* and Arabidopsis cDNA/DNA. Brassica ID correspond to the Brassica gene that was used for primer design (*B. rapa,* “Bra.” *B. oleracea*, “Bol.”). For = forward primer, Rev = reverse primer.

2.6.8 Electrophoresis of DNA and RNA

Gel electrophoresis of DNA and RNA was carried out on agarose gels with 1:10,000 dilution of SYBR® Safe DNA gel stain (Invitrogen). The percentage of agarose gel varied depending on the size of amplicons/products being analysed (0.8% (w/v) for large

amplicons, 2.5% (w/v) for large amplicons). RNA and PCR products generated using KOD reagents were mixed with 6 x loading buffer (Promega), and all samples were separated by agarose gel electrophoresis in TAE buffer (40 mM Tris-HCl, 1 mM EDTA) at 100 V.

2.6.9 Extraction and purification of DNA from agarose gels

DNA was separated on 1% agarose gels stained with SYBR® Safe. Bands of the desired size were visualized and excised under a UV-illuminator. DNA was purified using the QIAquick® Gel Extraction Kit (Qiagen) and following manufacturers instructions.

2.6.10 Restriction digest

Restriction digests of 0.5 to 1 µg of DNA were carried out using the appropriate restriction enzymes and buffers at concentrations and incubation conditions according to the manufacturer's instructions.

2.6.11 DNA ligation

Digested and purified DNA obtained from PCR reactions and plasmid DNA with appropriate restriction sites were used for DNA ligations. An aliquot of plasmid vector and DNA insert was separated on an agarose gel to estimate quantities. An approximate 3:1 ratio of insert:vector was calculated. Reactions were set up in a total volume of 10 µl containing 1 x ligation buffer and 1 µl of T4 DNA ligase (Promega). The ligation mix was incubated either at room temperature for 3 hours, and then 2-5 µl of the mix was used for transformation of competent *E. coli* TOP10 cells.

2.6.12 DNA sequencing

To confirm the DNA sequence of plasmids and constructs generated for sub-cloning and use as qPCR standards, nucleotide sequencing was carried out by GATC Biotech (Konstanz, Germany), according to the service's instructions.

2.6.13 Genotyping

Arabidopsis mutants obtained from NASC were genotyped as described in the SALK T-DNA primer design website (http://signal.salk.edu/tdnaprimers.2.html). Two combinations of primers were used for each template, one set to target genomic DNA of the gene in question (primers LP and RP), the other set comprising of a gene-specific primer (RP) and a T-DNA-specific primer (LBb1.3). The former primer set indicates if the

T-DNA insertion is absent if a band appears on an agarose gel, the latter will yield a PCR product if the insert is present.

2.7 Protein methods

2.7.1 Protein extraction from Arabidopsis and *B. napus*

Arabidopsis and *B.napus* plants were freshly ground up in micro-extraction buffer (20 mM HEPES pH 7.8, 450 mM NaCl, 50 mM NaF, 0.2 mM EDTA, 25% (v/v) glycerol, 0.5 mM PMSF, 1 mM DTT and protease inhibitor mix (Complete Mini, Roche)) using a mortar and pestle kept on ice. The homogenate was centrifuged at 16,000g for 10 minutes at 4°C, and the supernatant transferred to a fresh 1.5 ml tube. Protein was stored at -80°C.

2.7.2 Quantification of protein concentrations

Protein concentration was measured using the Bradford colorimetric method, with bovine serum albumin (BSA) used as a standard. Bradford assay solution (Bio-Rad, UK) was diluted five-fold with distilled water and filter sterilized. 2 µl of protein extract was added to 1 ml of Bradford solution and mixed to obtain a homogenous colour. The absorbance at 595 nm was recorded with a spectrophotometer (Eppendorf, Germany) against a blank sample (Bradford assay solution without any protein sample). The concentration of each sample was calculated based on the equation of a standard curve obtained using a serial dilution of BSA standards of known concentrations (1, 2, 4, 6, 8, 10 µg/µl).

2.7.3 SDS-PAGE

The volume of protein sample required to load 25 µg on an SDS gel were calculated, and enough 4 x SDS protein sample buffer (250 mM Tris-HCl pH 6.8, 2% (w/v) SDS, 20% (v/v) β-mercaptoethanol, 40% (v/v) glycerol, 0.5% (w/v) bromophenol blue) was added to achieve a final volume of 20 µl. The samples were boiled for 5 min at 95°C.

For studying UVR8, 12.5% polyacrylamide separating gels with a 4% polyacrylamide stacking gel were used (Separating: 12.5% (w/v) polyacrylamide, 0.38 M Tris-HCl pH 8.8, 0.1% (w/v) SDS, 0.05% (w/v) APS, 0.07% (v/v) TEMED; Stacking: 4% (w/v) polyacrylamide, 132 mM Tris-HCl pH 6.8, 0.1% (w/v) SDS, 0.05% (w/v) APS, 0.15% (v/v) TEMED). Proteins were separated according to their size in SDS running buffer (25 mM Tris-HCl pH 8.5, 190 mM glycine and 0.1% (w/v) SDS) at 150V for approximately 120 minutes. Protein molecular weights were determined using a prestained molecular

weight marker (P7708, New England Biolabs). SDS-PAGE gels were then irradiated under a high flounce rate of narrowband UV-B radiation for 10 minutes.

2.7.4 Western blot transfer

Proteins separated by SDS-PAGE were transferred onto nitrocellulose membranes (Bio-Rad, Hertfordshire, UK) at 400 mA for 45 minutes in transfer buffer (25 mM Tris-HCl pH 8.5, 190 mM glycine and 20% (v/v) methanol). Membranes were stained in Ponceau solution (0.1% (v/v) Ponceau S, 1% (v/v) acetic acid) to allow visualisation of Rubisco protein bands, and evaluate if protein samples were loaded equally. Images of the membranes were taken using either a scanner or the Fusion FX7 Advance SUPER-BRIGHT instrument (Peqlab c/o VWR International, Leicestershire, UK). Membranes were rinsed with TBS (25 mM Tris-HCl pH 8, 150 mM NaCl, 2.7 mM KCl) and then blocked overnight at 4°C with 10% non-fat dried milk in TBS-T (25mM Tris-HCl pH 8, 150mM NaCl, 2.7 mM KCl, 0.1% (v/v) Triton-X) to prevent non-specific binding of the antibodies on the membrane.

2.7.5 Immunolabelling

Primary and secondary antibodies (Table 2-5) were diluted to the stated concentrations in TBS-T with 10% non-fat dried milk. Incubation with the primary antibody was done for 1 hour with gentle rotating at room temperature. Primary antibodies were rescued after use, and stored at -20°C for multiple incubations with membranes. Following removal of the primary antibody, the membrane was washed 4 times with TBS-TT (25mM Tris-HCl pH 8, 150mM NaCl, 2.7 mM KCl, 0.1% (v/v) Triton-X, 0.05% (v/v) Tween) and once with TBS for 5 minutes each time. The membrane was then incubated for 1 hour at room temperature with the appropriate HRP-conjugated secondary antibody (Sigma-Aldrich), which was diluted in 10% dried milk TBS-T. This was followed with five washes in TBS-TT and 2 washed in TBS, for 5 minutes each time.

Primary antibody and dilution	Primary antibody Source	Secondary antibody and dilution
Anti-GFP (1:10,000)	Clontech	Anti-mouse (1:10,000)
Anti-UVR8 polyclonal (1:10,000)	Fisher Scientific	Anti-rabbit (1:20,000)
Anti-UVR8 C-terminal (1:5000)	E. Kaiserli (Kaiserli and Jenkins, 2007)	Anti-rabbit (1:5000)

Table 2-5: Antibodies used for immunolabelling.

2.7.6 Immunodetection

Chemiluminescent detection of protein bands was achieved using SuperSignal West Femto Substrate (Thermo Scientific, Product No. 34094) according to the manufacturer's instructions. After incubation with the reagents, the membrane was visualised with the Fusion instrument.

2.8 Bacterial transformation

2.8.1 Production of chemically competent *E. coli* cells

One colony of *E. coli* TOP10 cells was grown overnight in 5 ml of Luria Broth (LB) medium at 37°C with constant shaking at 200 rpm. The 5 ml subculture was then inoculated in 250 ml of LB medium and grown until it reached an OD_{600} of approximately 0.4. Cells were then pelleted at 4,000 g for 10 minutes at 4°C. After discarding the supernatant, the pellet was washed 3 times with 50 ml of ice-cold water and once with 20 ml of CCMB80 buffer (10mM KOAc pH 7.0, 80mM $CaCl_2 \cdot 2H_2O$, 20mM $MnCl_2 \cdot 4\ H_2O$, 10mM $MgCl_2 \cdot 6\ H_20$, 10% glycerol, pH adjusted to 6.4 with 0.1 N HCl). The pellet was then resuspended in 5 ml of CCMB80 buffer, and aliquots of 100 µl were snap frozen in liquid nitrogen and stored at -80°C.

2.8.2 Transformation of chemically competent *E. coli* cells

100 µl aliquots of chemically competent *E. coli* TOP10 cells were transformed according to the manufacturer' instructions. The transformation process included 30 minutes on ice, a 42°C heat shock for 45 seconds, followed by constant shaking at 37°C for 1 hour. The cells were then plated on LB agar plates containing the appropriate antibiotic for selection of the plasmid. Plates were incubated overnight at 37°C.

2.8.3 Production of chemically competent *A. tumefaciens* cells

Agrobacterium strain gv3101 was inoculated in a 10 ml subculture of LB medium with 30 µg/ml gentamycin, and grown for 20-24 hours with constant shaking (200 rpm) at 28°C. The subculture was then inoculated in 1 litre of LB medium with rifampicillin and gentamycin, and grown to an OD_{600} of 0.5-0.8. Cells were pelleted at 2,000 g for 10 minutes at 4°C. After the supernatant was discarded, the pellet was resuspended in 100 ml of cold sterile 10% (v/v) glycerol. The cells were pelleted and resuspended two more

times, with the volume of 10% glycerol being reduced to 10 ml then 1 ml. Aliquots of 50 µl were snap frozen in liquid nitrogen then stored at -80°C.

2.8.4 Transformation of chemically competent *A. tumefaciens* cells

Aliquots of 0.1 mL chemically competent Agrobacterium cells were removed from -80°C, and thawed until almost liquid. 1-2 µg of plasmid DNA was added to aliquots, and the contents were mixed gently but thoroughly, then snap frozen in liquid nitrogen. Cells were thawed at 37°C for 5 min, 150 µL YEP liquid media added and incubated at 28°C for approximately 3 hours with constant shaking at 200 rpm. The cells were then spread on YEP plates containing appropriate antibiotics, and incubated for 2-3 days at 28°C. Positive colonies were confirmed by colony PCR using one gene-specific primer and one plasmid-specific primer.

2.9 Generation of transgenic plants

2.9.1 Generation of constructs for over-expression in plants

Three *B.napus* genes were selected for over-expression in Arabidopsis, their putative Arabidopsis orthologues being *COMT1, ELI3-2* and *VTC2*. Initial attempts to insert the genes into two binary vectors, pGWB14 and pGWB15 (containing an HA tag to the C- and N-terminal region of the insert, respectively) were not overly successful, with pGWB15-*COMT1* the only construct generated. As a result, the other two genes were inserted into pEZR(K)L-C and pEZR(K)L-N, which possess a GFP tag at the N- and C-terminal regions of the insert, respectively. Both the pGWB and pEZR(K)L vectors contain the constitutive *35S* promoter of the Cauliflower Mosaic Virus (CaMV) to over-express levels of the inserted genes.

2.9.2 Transformation of Arabidopsis by floral dipping

Transgenic lines of Arabidopsis were created in the Col-0 WT background and in NASC homozygous *comt1*, *eli3-2* and *vtc2* mutants. Plants for transformation were grown under constant white light (~100 µmol m^{-2} s^{-1}) until flowers began to develop (4-5 weeks).

One colony of Agrobacterium containing the desired plasmid construct was inoculated in 500 ml LB medium with appropriate antibiotics and grown at 28°C with constant shaking (200 rpm) until an OD_{600} of 1.5-2.0 was reached. The cells were pelleted at 2,000g for 15 minutes and resuspended in infiltration medium (2.2 g/l MS salts, 50 g/l sucrose, 0.5 g/l

MES and 200 µl./l Silwet L77) to an OD_{600} of approximately 0.8. The upper region of the plants were submerged and gently swirled in the infiltration medium for around 20 seconds. Plants were kept inside transparent bags to create humid conditions for no more than 24 hours, and then kept under high white light for 3-4 days before being re-dipped.

2.9.3 Screen for Arabidopsis homozygous lines

Seeds collected from transgenic lines 4-5 weeks after floral dipping were surface sterilised and sown on ½ MS agar plates or not surface sterilised and sown on silicon dioxide plates as described in sections 2.3.4 and 2.3.5, respectively. Seedlings that showed antibiotic resistance (Zaller et al.) were rescued on soil and grown until they set seed (T2). These seeds were subsequently grown on silicon dioxide pre-wetted with ¼ MS and scored for antibiotic resistance segregation. Lines displaying a 3:1 segregation were identified, rescued on soil, and their levels of GFP or HA expression were checked by Western blotting with the GFP- and HA-antibody, respectively, and by gene expression analysis. The lines with satisfactory levels of GFP or HA were carried on to the T3 generation, and those exhibiting 100% resistance to antibiotic selection and possessing satisfactory GFP/HA levels were used for further analysis.

2.10 Transcriptome profiling of *B. napus* by RNA-seq

Transcriptomic changes in leaf tissue of 3-week old *B. napus* plants treated with UV-B radiation, MeJA treatment, slug herbivory or *Plutella* herbivory (as in section 2.5.3) was investigated with RNA-seq at the Glasgow Polyomics Facility. Sequencing took place in a NextSeq™ 500 (Illumina) desktop machine, and reads were aligned to either the Brassica 95K Unigene (Trick et al., 2009) or *B. napus* genome (Chalhoub et al., 2014). Alignment of reads against the reference sequences was achieved using TopHat v 2.1.12, and differential expression analysis was conducted with Cufflinks v 2.2.1 (Trapnell et al., 2012). Arabidopsis gene annotations were donated to the RNA-seq transcripts based on their sequence similarity to the Arabidopsis genome (TAIR10). As sequence similarity between two genes from different species does not necessarily mean that the encoded gene products are functionally similar (therefore, not homologous to one another), the assigned Arabidopsis gene functions are described as being putative homologues to the RNA-seq transcripts. Functional analysis of the RNA-seq transcripts was carried out using the online bioinformatics resource, DAVID (the Database for Annotation, Visualization and Integrated Discovery (Huang, 2009 #87)). As DAVID did not recognize the Brassica Unigene or *B. napus* gene ID's, the TAIR ID's of the putative Arabidopsis homologues

were used instead to identify gene ontology (GO) groups enriched in the dateset. Enrichment scores highlight the GO terms that are most represented in the list of genes submitted to DAVID, which subsequently allows the investigator to identify the biological processes that are most significant in the study at hand.

2.11 Global metabolite analysis of *B. napus* by reverse-phased chromatograph

Reverse-phased chromatography MS was employed to conduct global metabolomics on *B. napus* leaf tissue treated with UV-B radiation, MeJA treatment, slug herbivory or *Plutella* herbivory (as in section 2.5.3). Plants were harvested 24 hours after the onset of treatment for metabolomic analysis. HPLC-grade acetonitrile was acquired from Fisher Scientific, Loughborough, UK. HPLC grade H2O was purchased from VWR Chemicals, Fountenay-sous-Bois, France. Formic acid (for mass spectrometry) was acquired from Fluka Analytical (Sigma Aldrich), Steinheim, Germany. Samples were injected onto an Acquity UPLC BEH 2.1 x 150 mm column with 1.7 µm particle size (Waters, Elstree, UK), equipped with the corresponding pre-column, operated by an UltiMate 3000 RSLCnano liquid chromatography system (Dionex, Camberley, Surrey). The LC mobile phase was a biphasic linear gradient from 5% B to 50% B over 30 min, followed by an 4.5 min wash with 90% B, and an 15 min re-equilibration with 5% B, where solvent B is 0.1% formic acid in acetonitrile and solvent A is 0.1% formic acid in water. The flow rate was 150 µL/min, column temperature was held at 35 °C, injection volume was 10 µL, and samples were maintained at 5 °C in the autosampler. An Orbitrap™ Elite (Thermo Scientific) mass spectrometer was calibrated using Thermo calibration mix in negative ionization mode and tuned on m/z 514.28 (MFRA). Source mass spectrometry settings were as follows: a HESI probe was used with AGC 1 × 106 (full scan mode) and 5 × 104 (MSn mode), sheath gas 10 a.u., auxiliary gas 3 a.u., sweep gas 3 a.u., capillary temperature 275 °C, source voltage 5 kV, source current 100 µA, S-lens RF 67.3%, skimmer offset 0 V, maximum ion times of 500 ms (full scan mode) and 100 ms (MSn mode), and all scans consisted of 1 microscan. Data was obtained in profile mode, for full scans the m/z window was 70.00 – 1000.00 and the resolution was set to 240.000. For fragmentation experiments, key settings were: isolation width of 1.0 Da, minimum signal required of 500, first mass fixed at 50.00 m/z (HCD), and a dynamic exclusion of 48 seconds. A rejection list was included with the 4 most intense ions encountered in blank injections. HCD fragmentation spectra of the most intense ion (data dependent acquisition) in the full scan were obtained at 30, 70, and 110 normalized collision energies (NCE). CID-MSn ($n \leq 3$) fragmentation was performed as in (van der Hooft et al., 2012). Chromatograms and data analysis was carried out using

Xcalibur™ software (Thermo Scientific), and putative compound annotations were assigned based on chemical formulas using online resources including KEGG.

Chapter 3: UV-B Radiation Decreases *Brassica napus* and *Arabidopsis thaliana* Susceptibility to Invertebrate Herbivory

3.1 Introduction

Select components of solar radiation have already been found to affect plant interactions with pathogens or invertebrates. Plants exposed to higher ratios of far-red:red light (i.e. conditions found under a shaded vegetation canopy) appear more susceptible to invertebrate consumption (Izaguirre et al., 2006), while UV-B radiation can instead promote plant defence mechanisms against invertebrates and select pathogens. Outdoor and laboratory-based studies have shown that removal of UV-B from plant growing environments increases their susceptibility to invertebrate consumption (Rousseaux et al., 1998, Izaguirre et al., 2003, Rousseaux et al., 2004, Caputo et al., 2006), their use as an oviposition platform (Caputo et al., 2006, Foggo et al., 2007) and reduces their tolerance to necrotrophic fungi such as *Botrytis cinerea* (Demkura and Ballaré, 2012). This finding has been documented across several plant species, including members of the Brassicaceae family (Caputo et al., 2006, Kuhlmann and Muller, 2009a, Mewis et al., 2012), Nicotiana (Izaguirre et al., 2003, Izaguirre et al., 2007), tomatoes (Stratmann et al., 2000), and beech trees (Rousseaux et al., 2004), with thrips (Kuhlmann and Muller, 2009a), aphids (Kuhlmann and Muller, 2009b) and *Plutella xylostella* (Caputo et al., 2006) employed as the infesting pests of interest. While the molecular basis of UV-B-mediated defence is not fully understood, it has been suggested that the UV-B photoreceptor, UVR8, is required for enhancing Arabidopsis defence against *B. cinerea* (Demkura and Ballaré, 2012), as the reduction in lesion area on inoculated WT leaves in the presence of UV-B is lost in the *uvr8-6* null mutant. However, no studies have been conducted to investigate any role of UVR8 in promoting plant defence against invertebrates.

This chapter examines the effects of UV-B and an additional component of the UV-spectrum, UV-A, on the susceptibility of the commercially important crop oilseed rape (*Brassica napus*) to two destructive agricultural pests (*Plutella xylostella* and juvenile grey field slugs, *Deroceras reticulatum*). Bioassays were conducted under controlled laboratory conditions, with plants exposed to or sheltered from either UV-A or UV-B radiation, and invertebrate feeding preferences evaluated by measuring the leaf area consumed of -UV and +UV pre-treated plants. With the use of Arabidopsis mutants impaired in UV-B- or

JA-signalling, the importance of UVR8 and the bioactive form of jasmonic acid, JA-Ile, in regulating UV-B-induced defence was also investigated.

3.2 UV-B-treated *Brassica napus* are less susceptible to invertebrate herbivory

The effects of a 7-day UV-B pre-treatment on the area of *Brassica napus* leaf tissue consumed by *Plutella* larvae and juvenile slugs was assessed. Plants were grown for two weeks under 70 μmol m^{-2} s^{-1} constant white light, then either maintained under these conditions for a further 7 days (-UV-B treatment), or moved to white light supplemented with broadband UV-B at 3 μmol m^{-2} s^{-1} (+UV-B treatment). The broadband UV-B source encompasses a wide range of the UV-B spectrum and overspills slightly into the UV-A spectrum (Figure 2-1B, section 2.5.1 of Materials and Methods).

Second instar *Plutella* larvae and juvenile slugs were collected from their growth enclosures, and given a period of starvation for 1 and 12 hours, respectively (as described in section 2.5.2 of Materials and Methods). Following starvation, the invertebrates were distributed in the centre of mesh choice chamber cages and presented with two *B. napus* plants, one pre-treated under -UV-B conditions, the other under +UV-B conditions. The feeding preferences of *Plutella* larvae were studied separately from those of juvenile slugs. Bioassays were carried out with at least three paired replicates (in separate cages), and several independent bioassays were conducted on different dates. The position of the plants in each cage varied across all replicates to eradicate any influence of plant location on the results. Leaf area was measured before and after the bioassay as previously described (section 2.5.2 of Materials and Methods) to calculate the leaf area consumed by invertebrates.

3.2.1 *Plutella xylostella* prefer grazing upon –UV-B-treated *Brassica napus*

Bioassays conducted with *Plutella* larvae revealed a clear-cut difference in the levels of susceptibility between –UV-B and +UV-B pre-treated plants, both visually (Figure 3-1A) and upon leaf area measurements (Figure 3-1B). Examination of the plants following herbivory revealed that –UV-B and +UV-B pre-treated plants are both susceptible to invertebrate grazing, but to different extents (Figure 3-1A).

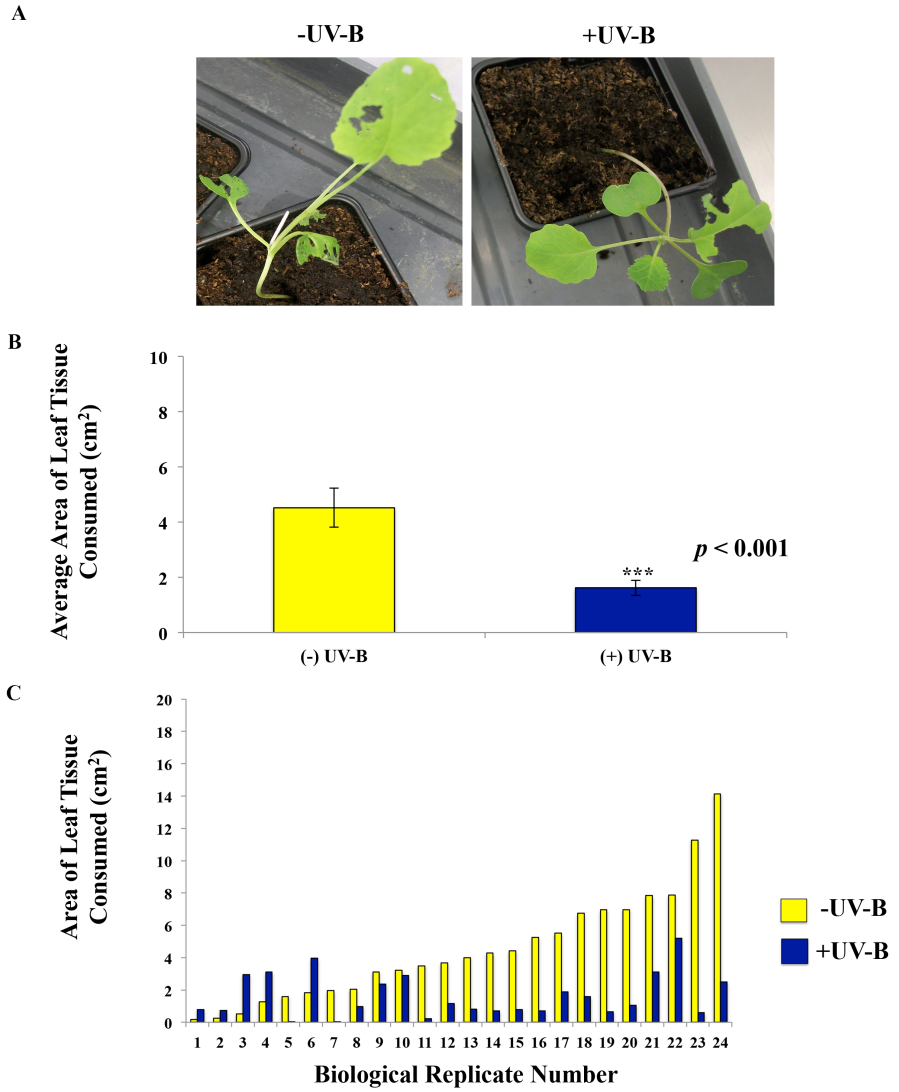

Figure 3-1: UV-B-treated *Brassica napus* show reduced susceptibility to *Plutella xylostella* larvae. Seven-day exposure to UV-B radiation reduces *B. napus* susceptibility to second instar *Plutella* larvae grazing, which is evident both visually, **A**, and upon measuring the average area of leaf tissue consumed (cm^2) over a 48-hour period, **B**. Variation in total tissue area consumed in the -UV-B and +UV-B plants across the 24 biological replicates is shown in **C.** Plants were reared under 70 µmol m^{-2} s^{-1} constant white light for 14 days, then either maintained under these –UV-B conditions for a further 7 days or exposed to +UV-B conditions (70 µmol m^{-2} s^{-1} white light + 3 µmol m^{-2} s^{-1} broadband UV-B). Choice chambers contained one -UV-B and one +UV-B plant side by side. Ten 2nd instar larvae were transferred to the cage with a fine paintbrush following a 1-hour period of starvation, being deposited an equal distance between the two plants. Bioassays ran for 48 hours under a long day photoperiod (16h light:8h dark). N=24. Bars for **B** represent estimated mean ± SEM. Significance of the +UV-B treatment against the –UV-B treatment was calculated using ANOVA and Tukey's Honest Significant Difference (HSD) post-hoc test. $p < 0.00041$.

The difference in average area of leaf tissue consumed in the –UV-B-treated and +UV-B-treated *B. napus* is statistically significant, with the –UV-B plants being preferred by *Plutella* larvae for consumption. This general trend can also be seen across each individual replicate (Figure 3-1C), where higher levels of consumption on –UV-B plants is observed

in approximately 80% of replicates. There is also noticeable variation in the total leaf area consumed in both –UV-B and +UV-B *B. napus* plants across all 24 replicates in Figure 3-1C, a finding that is most probably due to larval feeding behaviour.
Despite the variation in leaf area consumed across the replicates, the findings support the hypothesis that UV-B radiation reduces *B. napus* susceptibility to *Plutella* larvae.

3.2.2 Slugs prefer grazing upon –UV-B-treated *Brassica napus*

Slugs, on the other hand, do not appear to respond to UV-B-treated *B. napus* in the same manner as *Plutella* larvae (Figure 3-2). Visually, differences in leaf area consumed between –UV-B and +UV-B plants can be seen across most replicates (Figure 3-2A), however when combining the results from all replicates, no statistically significant difference in slug feeding preferences can be found with ANOVA (Figure 3-2B). This result implies that pre-treating *B. napus* with UV-B radiation does not induce slug-deterring mechanisms, but when the ten replicates are examined individually, a slightly different story emerges (Figure 3-2C). There is an indication that slugs generally prefer feeding upon –UV-B plants, as greater levels of consumption of –UV-B tissue is seen in 70% of the replicates. While this trend is not as intense for slugs as it is for *Plutella,* it can be concluded that UV-B is capable of reducing *B. napus* susceptibility to these two invertebrate pests to varying degrees.

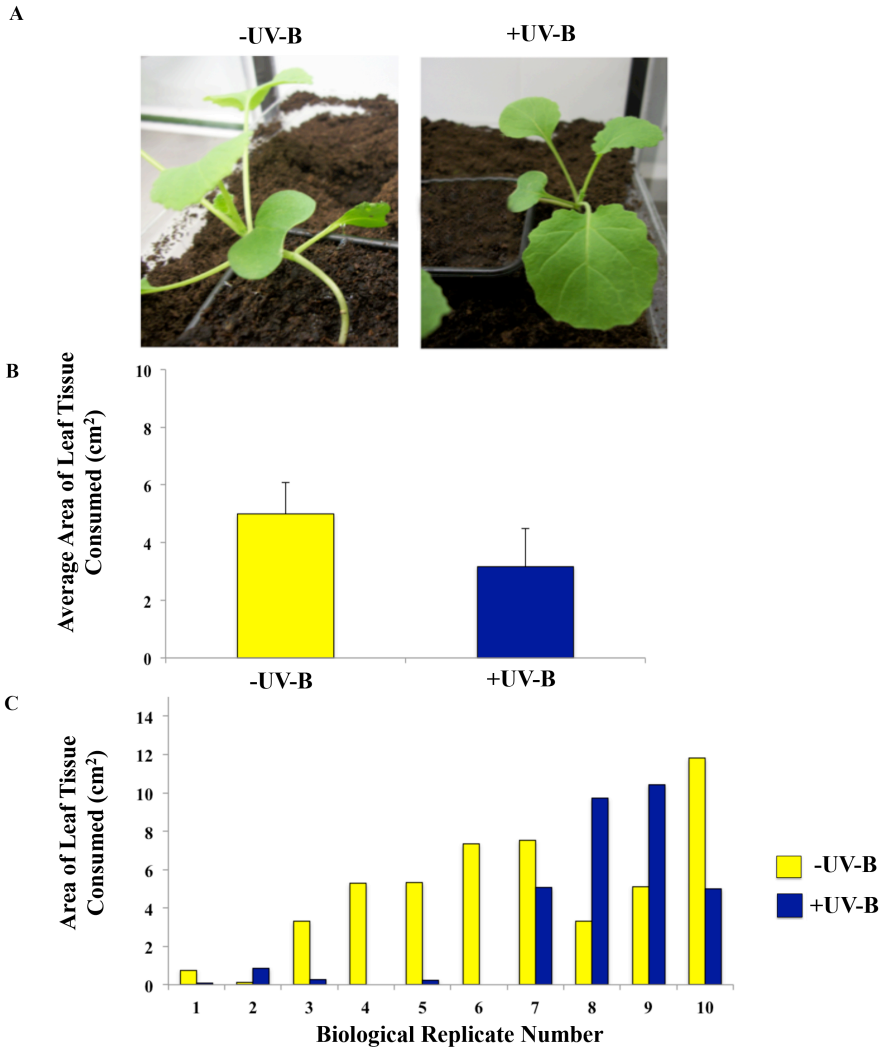

Figure 3-2: UV-B pre-treated *B. napus* are not significantly less susceptible to juvenile slugs. Seven-day exposure to UV-B radiation did not significantly reduce *B. napus* susceptibility to juvenile slugs. **A,** images of –UV-B and +UV-B *B. napus* following a 48-hour bioassay, **B,** the average area of leaf tissue consumed (cm^2), and **C,** variation in total tissue area consumed in the -UV-B and +UV-B plants across the 10 biological replicates**.** Plants were reared under 70 μmol m^{-2} s^{-1} constant white light for 14 days, then either maintained under these –UV-B conditions for a further 7 days or exposed to +UV-B conditions (70 μmol m^{-2} s^{-1} white light + 3 μmol m^{-2} s^{-1} broadband UV-B). Choice chambers contained one -UV-B and one +UV-B plant side by side. 2 juvenile slugs measuring approximately 20-30 mm in length were starved overnight and then moved to choice chambers lined with dampened soil using a pair of blunt-ended forceps. Slugs were deposited an equal distance between the two plants. Bioassays ran for 48 hours under a long day photoperiod. N=10. Bars for **B** represent estimated mean ± SEM. Significance of the +UV-B treatment against the –UV-B treatment was calculated using ANOVA and Tukey's Honest Significant Difference (HSD) post-hoc test. $p = 0.297$.

3.3 UV-A has different effects on *Brassica napus* susceptibility to *Plutella* and slugs

Another component of the solar UV-spectrum that reaches the Earth's surface is UV-A. The effects of terrestrial levels of UV-A on expression of several UV-B- and JA-regulated genes has been reported previously (Morales et al., 2013), but to the best of my knowledge, its effects on plant-invertebrate interactions have not been directly investigated before. Several in-field bioassays examining plant susceptibility to invertebrate consumption in the presence or absence of UV-B radiation retained UV-A in the spectrum of light received by both +UV-B and –UV-B plants (Ballaré et al., 1996, Izaguirre et al., 2003, Izaguirre et al., 2007). As the removal of UV-B increased plant susceptibility to herbivory in these studies, if UV-A is capable of promoting plant defence against invertebrate pests, it is not to the same extent as UV-B radiation.

To investigate if UV-A radiation can induce an invertebrate-deterring response in plants, bioassays were performed using *B. napus* and Arabidopsis plants illuminated with 70 μmol m^{-2} s^{-1} white light for two weeks, and then a further week with either white light only (-UV-A) or white light supplemented with 70 μmol m^{-2} s^{-1} UV-A radiation (+UV-A). The feeding preferences of *Plutella* larvae or juvenile slugs were then investigated with these plants, following the same procedures outlined in section 3.2.

3.3.1 UV-A-treated *B. napus* are significantly less susceptible to *Plutella* herbivory

Plutella larvae appear to be deterred by –UV-A-treated *B. napus* in a statistically significant manner, although the difference in the average area of –UV-A- or +UV-A-treated *B. napus* leaf tissue consumed by larvae may not appear significant at a glance (Figure 3-3A). The range of leaf area consumed by *Plutella* across the 8 replicates is depicted in a boxplot, with the areas of +UV-A-treated plants spanning a larger area than that of –UV-A-treated plants (Figure 3-3B).

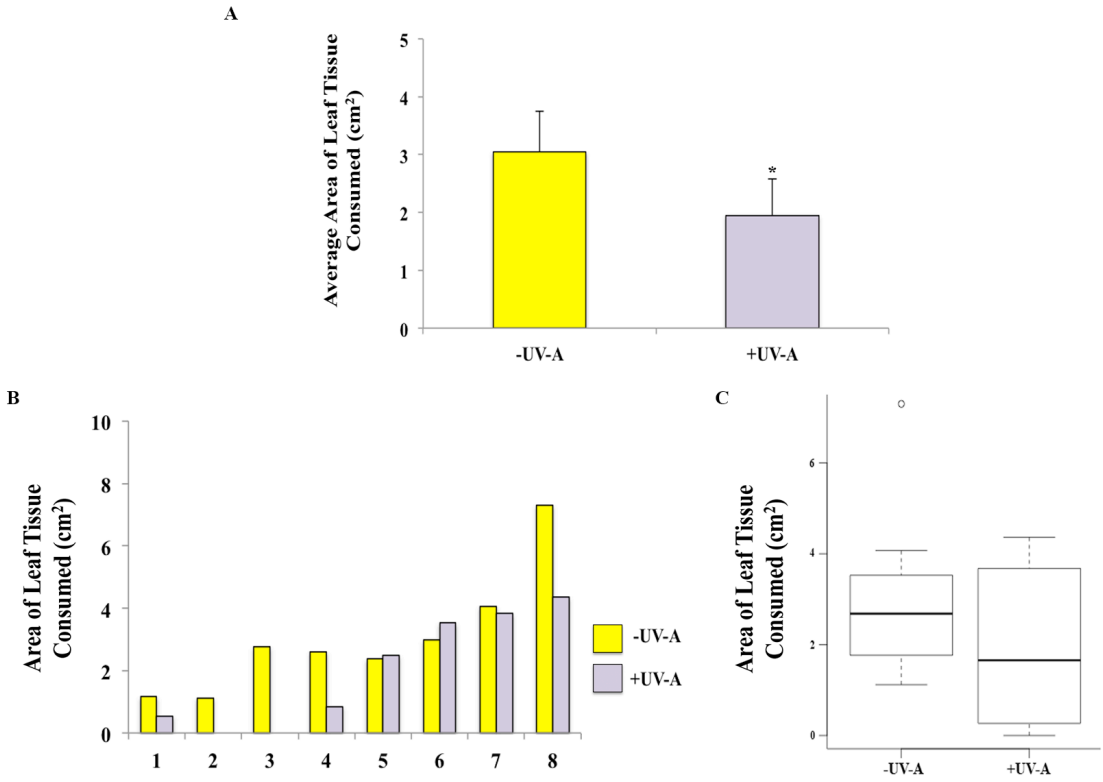

Figure 3-3: UV-A-treated *B. napus* are significantly less susceptible to *Plutella* larvae grazing. **A,** the average area of leaf tissue consumed by *Plutella* larvae on white light (-UV-A) and white light plus supplementary UV-A radiation (+UV-A) treated *B. napus*, **B**, the range of leaf tissue consumed by *Plutella* in plants from both light treatments across all replicates and **C,** the area of leaf tissue consumed in each of the 8 replicates**.** Plants were reared under 70 μmol m^{-2} s^{-1} white light for 14 days and either maintained under these –UV-A conditions for a further 7 days, or exposed to white light plus 70 μmol m^{-2} s^{-1} UV-A for 7 days (+UV-A). Invertebrate choice chambers were set up with one –UV-A and one +UV-A plant positioned side by side in a cage with a layer of dampened tissue roll lining the base. Ten 2nd instar *Plutella* larvae were starved for 1 hour, then placed at an equal distance between the two plant pots in each bioassay. The bioassay ran for 48 hours under a long day photoperiod (16h light:8h dark). N=8. Bars for **A** represent mean ± SEM. Significance of the +UV-A treatment against the –UV-A treatment was calculated using ANOVA and Tukey's Honest Significant Difference (HSD) post-hoc test. $p = 0.04$.

The black line that runs horizontally through each box represents the median (middle) value of the replicates. The median separates the boxes into two sections, with the bottom section referred to as the 1st quartile, and the top section, the 3rd quartile. Each quartile covers the area of leaf tissue consumed across 25% of the replicates, with the two vertical lines protruding from each quartile representing the spread of values that are up to 1.5-times that of the values in the 1st and 3rd quartile (also called the interquartile range, IQR). The white circle in the –UV-A column marks one replicate that has an area of tissue consumed exceeding 1.5-times that of the IQR.

At least 50% of the –UV-A replicates lose an area of leaf tissue to larvae that corresponds to the area covered by 3rd quartile of the +UV-B samples, with the median value for +UV-B, 1.65 cm^2, lying just below the 1st quartile of –UV-A which starts at 1.9 cm^2. This indicates that in some replicates, *Plutella* larvae consumed a smaller area of +UV-A leaf tissue and a larger area of –UV-A-treated *B. napus*, which is represented both in Figure 3-3A, and in Figure 3-3C. Here, the area of tissue consumed in both plants of the individual replicate can be seen, and it is clear that the larvae do show a clear preference of –UV-A plants over the +UV-A plants in several replicates. This trend, however, is not consistent, and in some cases little to no difference in leaf area consumed is measured between plants of the two light treatments. The statistics suggest that UV-A radiation does improve *B. napus* defence against *Plutella* larvae in a slightly significant manner.

3.3.2 Slugs are deterred by UV-A-treated *B. napus*

Slugs show a statistically significant preference for –UV-A-treated *B. napus* over +UV-A (Figure 3-4A), which is consistently seen over all 6 replicates. When the spread of leaf areas consumed in –UV-A- and +UV-A-treated plants is studied on a boxplot (Figure 3-4B), it is clear that there is no overlap in areas consumed between the two light treatments, and that slugs prefer to consume *B. napus* plants that have not been exposed to UV-A radiation.

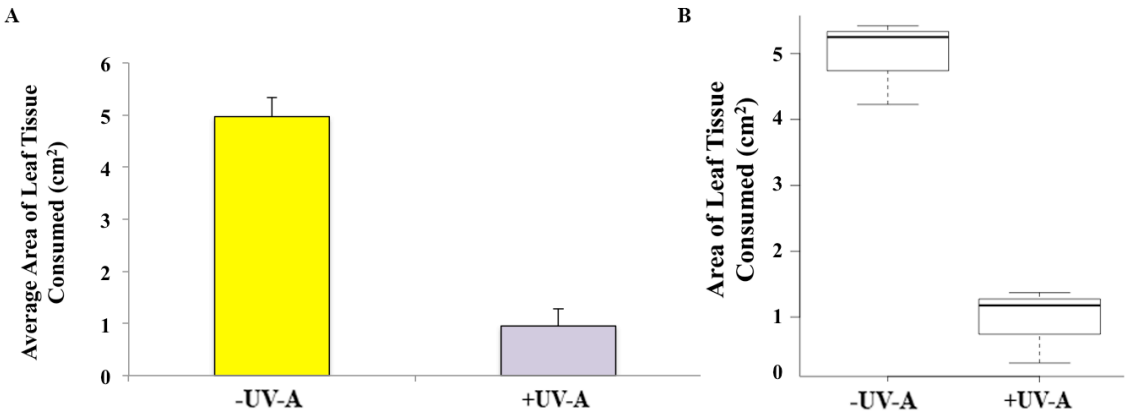

Figure 3-4: UV-A treatment reduces *B. napus* susceptibility to slug herbivory. A, the average area of leaf tissue consumed by slugs on white light (-UV-A) and white light plus supplementary UV-A radiation (+UV-A) treated *B. napus* and **B**, the range of leaf tissue consumed by slugs in plants from both light treatments across all replicates. Plants were reared under 70 μmol m^{-2} s^{-1} white light for 14 days and either maintained under these –UV-A conditions for a further 7 days, or exposed to white light plus 70 μmol m^{-2} s^{-1} UV-A for 7 days (+UV-A). Invertebrate choice chambers were set up with one –UV-A and one +UV-A plant positioned side by side in a cage with a layer of dampened soil on the base. 2 juvenile slugs, that were previously starved overnight, were placed at an equal distance between the two plant pots in each bioassay. The bioassay ran for 48 hours under a long day photoperiod (16h light:8h dark). N=6. Bars for **A** represent mean ± SEM. Significance of the +UV-A treatment against the –UV-A treatment was calculated using ANOVA and Tukey's Honest Significant Difference (HSD) post-hoc test. $p = 0.00127$.

3.4 UVR8 is not essential for UV-B-mediated invertebrate resistance in Arabidopsis

It is now known that UV-B radiation can promote *B. napus* defence against *Plutella* larvae and juvenile slugs, but it has not been investigated whether the UV-B photoreceptor, UVR8, is required for regulating this response against invertebrates. Recent studies using an Arabidopsis UVR8 null mutant, *uvr8-6*, and the necrotrophic fungus, *Botrytis cinerea*, demonstrated that UVR8 is required to promote UV-B-enhanced Arabidopsis defence against the fungus, as mutants developed larger lesion areas compared to the Col-0 WT (Demkura et al., 2012). To assess any role of UVR8 in promoting UV-B-enhanced defence against *Plutella* larvae and slugs, a UVR8 null mutant, *uvr8-1*, a UVR8 over-expressing line, *35S*pro:GFP-UVR8, and the wild type progenitor, L*er*, were pre-treated in the absence or presence of UV-B and used in invertebrate bioassays.

The *uvr8-1* mutant is characterised by a 15-bp deletion that encompasses residues 196-200, and is deficient in both levels of UV-induced flavonoids, along with transcript levels of flavonoid biosynthetic genes such as *CHS* (Brown et al., 2005). Mutants also display a

hypersensitive phenotype in response to UV-B radiation, including stunted growth and the development of necrotic lesions on leaves (Kliebenstein et al., 2002, Brown et al., 2005). The *35S*pro:GFP-UVR8 over-expressing line was developed by a previous lab member of the Jenkins group in the L*er* background, with UVR8 levels found to be considerably higher than that in WT plants (Figure 3-5).

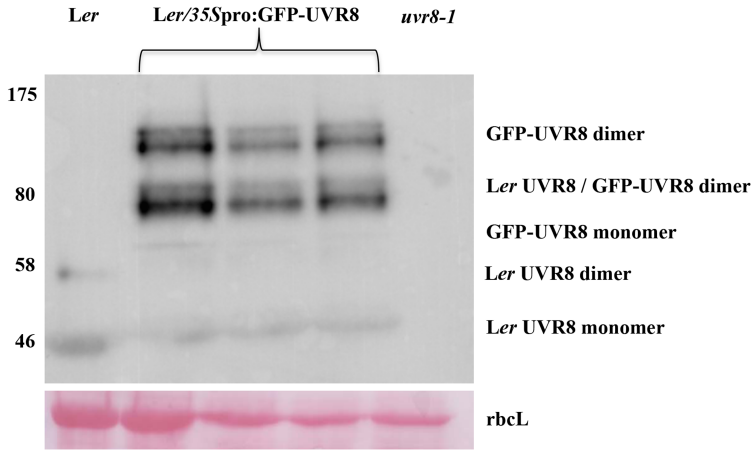

Figure 3-5: Levels of UVR8 over-expression in *35S*pro:GFP-UVR8 over-expressing plants. Polyclonal anti-UVR8 antibody immunoblots on protein extracts of 10-day old Arabidopsis L*er*, *35S*pro:GDP-UVR8 and *uvr8-1*. L*er* protein extracted from plants exposed to 1.5 μmol m^{-2} s^{-1} broadband UV-B radiation for 24 hours, while *uvr8-1* and *35S*pro:GFP-UVR8 plants were maintained under –UV-B conditions for 10 days. Protein from the L*er* plants was extracted on a separate occasion from protein originating from the *uvr8-1* and *35S*pro:GFP-UVR8 plants. Ponceau staining of the large RuBisCO subunit (rbcL) is presented as a loading control. Size markers (kDa) are indicated on the left hand side of the image, while the states of UVR8 are indicated on the right hand side. As the over-expressing line is in a L*er* background, GFP-tagged UVR8 can form a heterodimer with WT UVR8 ("L*er* UVR8 / GFP-UVR8 dimer").

The sensitivity of *uvr8-1* mutants to UV-B resulted in the period of irradiation being reduced from 7 to 4 days, and the fluence rate being halved to 1.5 μmol m^{-2} s^{-1}. By reducing the UV-B dose and exposure period, mutants developed fewer lesions and appeared healthier than those grown under 3 μmol m^{-2} s^{-1}. For comparison purposes, L*er* and *35S*pro:GFP-UVR8 plants were also treated in the same conditions. It was hypothesised that, if UVR8 is required for UV-B-enhanced defence in Arabidopsis, the null mutant would not display a UV-B-enhanced defence response, while the over-expressing plants would show heightened levels of resistance following UV-B radiation by sustaining far lower levels of tissue area consumed compared to L*er*.

3.4.1 UVR8 does not significantly mediate UV-B-enhanced defence against *Plutella* in Arabidopsis

The adjusted UV-B fluence rate and treatment period (1.5 μmol m^{-2} s^{-1} over 4 days) was found to effectively reduce L*er* susceptibility to *Plutella* larvae, as the average area of leaf tissue consumed by the pests was over 50% less on the +UV-B plants than on the –UV-B plants (Figure 3-6A). Likewise, the *uvr8-1* mutant also appeared less susceptible to *Plutella* grazing following a UV-B pre-treatment (Figure 3-6B), with the different ranges of leaf areas consumed by *Plutella* on -/+UV-B-treated *uvr8-1* plants indicating a clear preference of *Plutella* larvae for consuming –UV-B *uvr8-1* plants (Figure 3-6C). Despite this finding lying just outwith the range of statistical significance (*p*-0.0562; findings were considered statistically significant when $p \leq 0.05$), it can be concluded that +UV-B-treated *urv8-1* plants are less attractive to *Plutella* larvae as a food source compared to -UV-B-treated plants of the same genotype.

The *35S*pro:GFP-UVR8 over-expressing plants grown under –UV-B conditions also sustained higher levels of *Plutella* consumption compared to +UV-B plants (Figure 3-6D), with 100% of +UV-B *35S*pro:GFP-UVR8 replicates losing up to approximately 1 cm^2 by *Plutella* herbivory, while around 3 cm^2 was lost from –UV-B plants across at least 50% of replicates (Figure 3-6E). However, as this result is not statistically significant (*p*-0.32), it is clear that there is no significant difference in *Plutella* feeding preference between –/+UV-B-treated *35S*pro:GFP-UVR8 Arabidopsis plants.

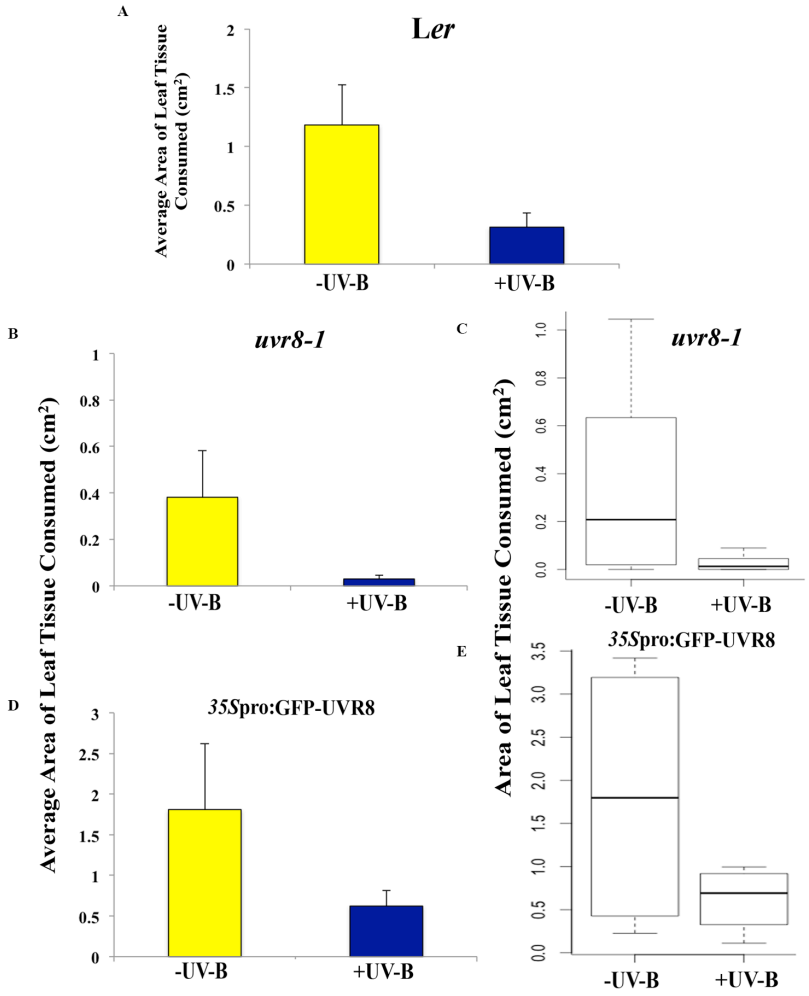

Figure 3-6: A role of UVR8 in promoting UV-B-induced defence in Arabidopsis is not evident in bioassays with *Plutella* larvae. The average area of leaf tissue consumed by *Plutella* in L*er*, **A**, *uvr8-1*, **B**, and *35S*pro:GFP-UVR8, **C**, and boxplots of area of leaf tissue consumed in *uvr8-1*, **D**, and *35S*pro:GFP-UVR8, **E**. Arabidopsis previously grown for 17 days under 70 µmol m^{-2} s^{-1} of continuous white light received 70 µmol m^{-2} s^{-1} of white light (-UV-B) or white light plus supplementary UV-B at 1.5 µmol m^{-2} s^{-1} (+UV-B) for 4 days before conducting bioassays with 2nd instar *Plutella* larvae. *Plutella* larvae were starved for 1 hour, and 10 were placed at an equal distance between one –UV-B and one +UV-B plant in each bioassay. Bioassays ran for 48 hours under a long day photoperiod (16h light:8h dark). Bars for **A** represent mean ± SEM. Significance of the +UV-B treatment against the –UV-B treatment was calculated using ANOVA and Tukey's Honest Significant Difference (HSD) post-hoc test. L*er*: $p = 0.03$, n=16. *uvr8-1*: $p = 0.12$, n=8. *35S*pro:GFP-UVR8: $p = 0.203$, n=5.

In comparison to L*er* and *35S*pro:GFP-UVR8, *uvr8-1* mutants possess a smaller average area of leaf tissue consumed by *Plutella* larvae, for both –UV-B and +UV-B plants. L*er* and *35S*pro:GFP-UVR8 plants sustain very similar average areas of leaf tissue consumption, especially the +UV-B plants from both lines. Unfortunately, it cannot be concluded if one line is more susceptible to *Plutella* herbivory than another following white light or supplemented UV-B treatment, as no such bioassays were conducted. With the results obtained from the bioassays, differences in the average area of tissue consumed

by *Plutella* in the *uvr8-1* and *35S*pro:GFP-UVR8 bioassays were calculated as a percentage of that consumed in L*er* (Table 3-1). It is evident that while *Plutella* consume a small area of tissue from *uvr8-1* mutants, high levels of consumption are seen in the *35S*pro:GFP-UVR8 over-expressing plants. These plants were not bigger than L*er,* and initial leaf area was not found to affect total area consumed when statistical analysis when ANOVA was conducted. It can be concluded, however, that UV-B radiation is capable of reducing the susceptibility of L*er*, *uvr8-1* and *35S*pro:GFP-UVR8 over-expressing plants to *Plutella* larvae herbivory under controlled conditions.

Table 3-1: Percentage of the average area of *uvr8-1* and *35S*pro:GFP-UVR8 tissue consumed by *Plutella* larvae in relation to that of L*er* (%).

	-UV-B	+UV-B
L*er*	100	100
uvr8-1	32.28	9.40
***35S*pro:GFP-UVR8**	153.24	198.25

3.4.2 UVR8 does not significantly mediate UV-B-enhanced defence against slugs in Arabidopsis

To investigate if UV-B-enhanced defence against slugs in Arabidopsis is regulated by UVR8, bioassays with –UV-B- and +UV-B-treated *uvr8-1* null mutants and *35S*pro:GFP-UVR8 over-expressing lines were conducted with juvenile slugs (Figure 3-7). As seen in the *Plutella* bioassays (Figure 3-6A), exposure of L*er* to 1.5 μmol m^{-2} s^{-1} UV-B for 4 days is sufficient to elicit a statistically significant UV-B-induced decrease in leaf area consumed by slugs (Figure 3-7A). Slugs also display a preference for consuming *uvr8-1* leaf tissue maintained under –UV-B conditions over +UV-B conditions (Figure 3-7B). The difference in the quantity of tissue consumed in –UV-B and +UV-B *uvr8-1* is statistically significant, and upon examining the spread of areas consumed across the 6 replicates (Figure 3-7C), it is clear that +UV-B *uvr8-1* mutants are less attractive to slugs as a food source.

The *35S*pro:GFP-UVR8 over-expressing line appears to be slightly less susceptible to slug herbivory following a 4-day period of UV-B radiation (Figure 3-7D), a finding that is not statistically significant, probably due to variation in the areas of tissue consumed at each replicate (Figure 3-7E boxplot). The largest area of tissue consumed by slugs on +UV-B-treated *35S*pro:GFP-UVR8 plants is 1.4 cm^2, but the position of the median value for –UV-

A-treated *35S*pro:GFP-UVR8 plants lies at 1.87 cm^2. As the median represents the middle area of tissue consumed by slugs across the 8 replicates, 50% of replicates possess a loss of tissue over 1.87 cm^2. This implies that UV-B radiation can lower the susceptibility of *35S*pro:GFP-UVR8 plants to slug herbivory, as higher levels of tissue consumption in at least 4 replicates is seen in the –UV-B-treated *35S*pro:GFP-UVR8 plants. With more repetitions of this bioassay, the statistical significance may become more evident.

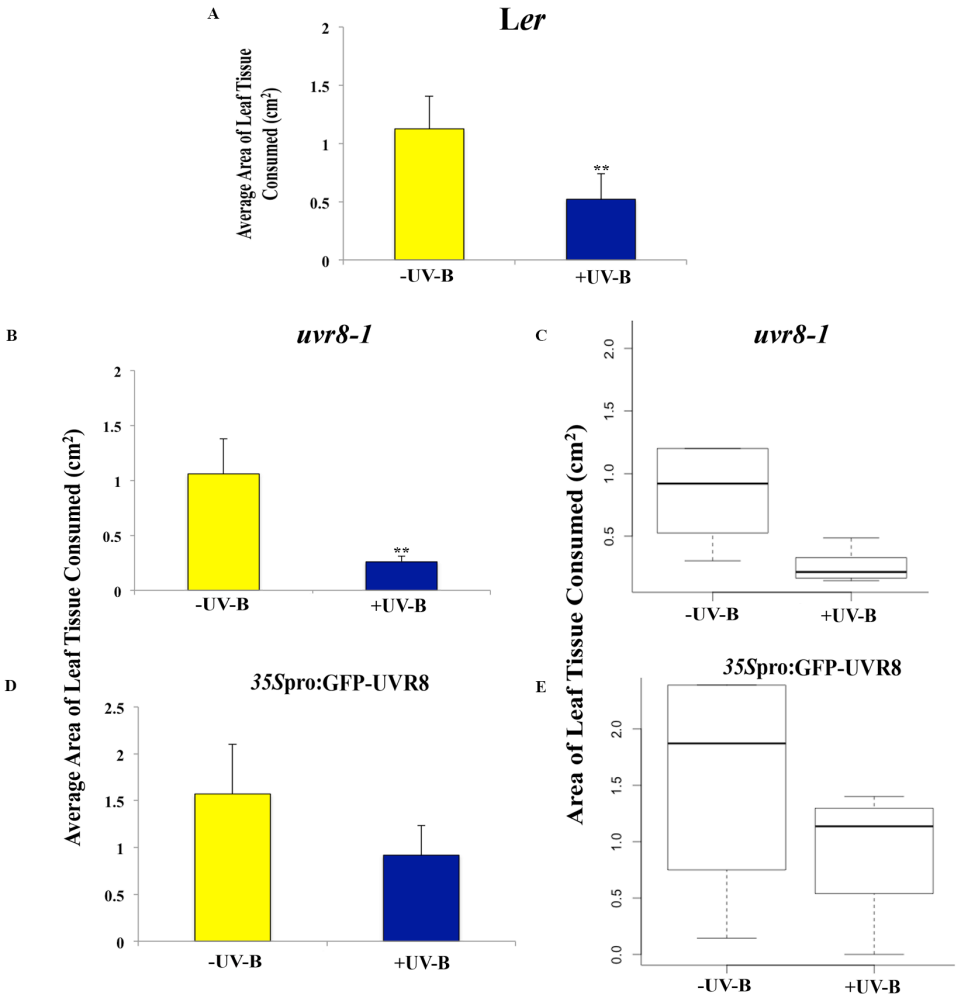

Figure 3-7: The effect of UV-B radiation on slug preference of Arabidopsis. Average area of leaf tissue consumed by slugs in L*er*, **A**, *uvr8-1*, **B**, and *35S*pro:GFP-UVR8, **C,** and boxplots of area of leaf tissue consumed in *uvr8-1*, **D**, and *35S*pro:GFP-UVR8, **E**. Arabidopsis previously grown for 17 days under 70 µmol m^{-2} s^{-1} of continuous white light received 70 µmol m^{-2} s^{-1} of white light (-UV-B) or white light plus supplementary UV-B at 1.5 µmol m^{-2} s^{-1} (+UV-B) for 4 days before conducting bioassays with juvenile slugs. Slugs were starved overnight. Two were placed at an equal distance between one –UV-B and one +UV-B plant in each bioassay. Bioassays ran for 48 hours under a long day photoperiod (16h light:8h dark). Bars for **A** represent mean ± SEM. Significance of the +UV-B treatment against the –UV-B treatment was calculated using ANOVA and Tukey's Honest Significant Difference (HSD) post-hoc test. L*er*: $p = 0.016$, n=16. *uvr8-1*: $p = 0.032$, n=6. *35S*pro:GFP-UVR8: $p = 0.33$, n=8.

The average area of leaf tissue consumed by slugs on –UV-B and +UV-B L*er* plants is similar to the areas consumed on the on –UV-B and +UV-B *uvr8-1* mutants. The over-expressing line sustained slightly more tissue loss than the WT and mutant line, however, as mentioned in section 3.3, no bioassays were conducted to investigate whether or not slugs preferred consuming one line over another, therefore it is unknown if the difference in average tissue area consumed across the lines has any significant meaning. The percentage average area consumed by slugs on *uvr8-1* and *35S*pro:GFP-UVR8 plants in relation to L*er* following either treatment was calculated (Table 3-2).

Table 3-2: Percentage of the average area of *uvr8-1* and *35S*pro:GFP-UVR8 tissue consumed by juvenile slug in relation to that of L*er* (%).

	-UV-B	**+UV-B**
L*er*	100	100
uvr8-1	93.94	49.76
***35S*pro:GFP-UVR8**	139.22	176.34

The levels of consumption on –UV-B-treated L*er* and *uvr8-1* mutants are very similar, however the area of tissue lost on +UV-B-treated null mutants is approximately half of that sustained by the wild type plants. The *35S*pro:GFP-UVR8 over-expressing line loses a higher area of tissue to herbivory than the other two lines, an observation also noticed in the *Plutella* bioassays (Table 3-1). The results from bioassays presented in Figure 3-6 and Figure 3-7 suggest that UVR8 is either not a key regulator or not the only regulator involved in mediating UV-B-enhanced defence in Arabidopsis, and that over-expression of the photoreceptor does not reduce the susceptibility of the plants to invertebrate herbivory following UV-B-treatment.

3.5 UV-B does not confer resistance to mutants impaired in JA-signalling

To assess the extent of UV-B-induced plant defence, it was asked whether or not UV-B radiation could compensate for a lack of JA-induced defence mechanisms in plants. Previous studies with *Nicotiana attenuata as-lox* mutants, that have reduced levels of jasmonic acid-regulated defence responses due to antisense silencing of a JA biosynthetic gene, *LIPOXYGENASE 3* (*LOX3*), found that terrestrial levels of UV-B radiation were unable to reduce the susceptibility of these mutants to thrip herbivory, while wild type *N. attenuata* displayed UV-B-induced defence (Demkura et al., 2010).

The effects of UV-B radiation on the levels of *Plutella* consumption on a JA-insensitive Arabidopsis mutant impaired in the biosynthesis of several JA-amino acid conjugates, *jar1-1*, was assessed during invertebrate bioassays. The *jar1-1* mutant and its progenitor line, Col-0, were reared under 70 μmol m^{-2} s^{-1} of white light for 17 days, then either maintained under these conditions (-UV-B) or irradiated with white light plus 1.5 μmol m^{-2} s^{-1} UV-B (+UV-B) for 4 days. Bioassays lasted 48 hours with 10 *Plutella* larvae each in each replicate.

Larvae consumed less leaf tissue on Col-0 plants previously exposed to UV-B radiation (Figure 3-8A), while the *jar1-1* mutant did not appear less susceptible to herbivory (Figure 3-8B). This result is in accordance with what has already been reported (Demkura et al., 2010), and suggests that, despite UV-B radiation's ability to promote plant defence against a selection of invertebrate pests, it is unable to compensate for the loss of JA-regulated defences in Arabidopsis mutants.

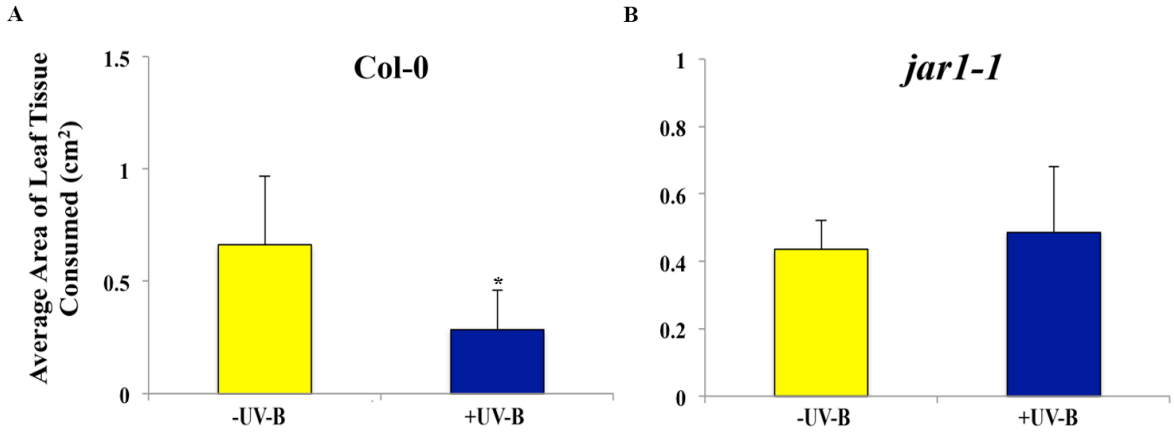

Figure 3-8. UV-B is unable to promote defence in the JA-insensitive Arabidopsis mutant, *jar1-1*. Average area of leaf tissue consumed by *Plutella* larvae in **A,** Col-0 and **B** *jar1-1*. Arabidopsis previously grown for 17 days under 70 μmol m^{-2} s^{-1} of continuous white light received 70 μmol m^{-2} s^{-1} of white light (-UV-B) or white light plus supplementary UV-B at 1.5 μmol m^{-2} s^{-1} (+UV-B) for 4 days. 2nd instar *Plutella* larvae were starved for 1 hour, then 10 were placed at an equal distance between one –UV-B and one +UV-B plant in each bioassay. Bioassays ran for 48 hours under a long day photoperiod (16h light:8h dark). Bars represent mean ± SEM. Significance of the +UV-B treatment against the –UV-B treatment was calculated using ANOVA and Tukey's Honest Significant Difference (HSD) post-hoc test. Col-0: $p = 0.04$, n=6. *jar1-1*: $p = 0.819$, n=8.

3.6 Direct effects of UV-B on invertebrate behaviour

The results presented up until now were derived from bioassays conducted in controlled growth rooms were UV-B is absent from light sources. These conditions enabled the indirect effects of UV radiation, i.e. UV-induced plant signalling pathways, on invertebrate feeding preferences to be examined. However, in uncontrolled environments outwith the laboratory, plants and invertebrates are likely to interact with one another under UV conditions, meaning both direct and indirect effects of UV on invertebrate behaviour may influence their feeding preferences. Previous research has indicated that invertebrates not only perceive UV radiation, but use it as an important environmental signal to assist with orientation, navigation, feeding and mating, with the propagation rate of *Myzus persicae* aphids decreasing up to 2-fold in the absence of UV-B (Raviv and Antignus, 2004), and the thrip species, *Caliothrips phaseoli,* detecting UV-B radiation and actively moving away from areas of high UV-B to those of low UV-B levels (Mazza et al., 2002). The same thrip species were later shown to be attracted to components of the UV spectrum against a low PAR background when kept in confinement in the laboratory, and it was suggested that they are highly sensitive to wavelengths between 290-330nm (Mazza et al., 2009). However, the direct effects of UV-B radiation on *Plutella* larvae and slug feeding behaviour have not, to my knowledge, been investigated before, and while it is apparent that UV-B radiation is capable of promoting a deterring quality in *B. napus* and Arabidopsis towards these two pests, it was of interest to investigate the direct effects UV radiation may have on slug and *Plutella* behaviour, if any.

To achieve this, bioassays were set up under white light plus supplementary UV-A conditions (70 μmol m^{-2} s^{-1} of each light) or white light plus UV-B conditions (70 μmol m^{-2} s^{-1} of white light plus 3 μmol m^{-2} s^{-1} of UV-B), and with the use of cut-off filters to remove components of the UV spectrum, the area of –UV-treated *B. napus* leaf tissue consumed under each light condition was monitored. In total, three filters were employed, the first being a cellulose diacetate filter, the second, a filter impenetrable to UV-A radiation, and the third filter removed UV-B radiation from the spectrum of light emitted from the tubes reaching the plants. Cellulose diacetate has been used throughout this project as a matter of course to remove short wavelengths of UV radiation below approximately 290 nm from the broadband UV-B source (Materials and Methods, section 2.5.1). In this experiment, plants positioned under this filter were regarded as 'control' plants, as they received unattenuated levels of UV radiation from the light source.

To create the appropriate illumination conditions inside the invertebrate cages, one side of the cages were covered with either a UV-A or UV-B filter, while the other sides were wrapped in cellulose diacetate. Light and UV meters were used to ensure that the desired light conditions had been met under each filter in the cages. Two 3-week old *B. napus* plants previously grown under –UV-A/B conditions were positioned in the cages, 1 under each filter. Two slugs or 10 *Plutella* larvae were placed in the centre of the cages, underneath the interface between the two filters. They were allowed to migrate to their preferred side of the cage, a decision that was theoretically based on the presence or absence of UV radiation, and not on attractiveness of the plants. Bioassays were run for 24 hours, to prevent the accumulation of UV-induced defence mechanisms in *B. napus*.

3.6.1 *Plutella* larvae feeding preferences do not change in the presence or absence of UV-A or UV-B radiation

Plutella larvae feeding behaviour did not appear to be influenced by UV-B (Figure 3-9A) or UV-A (Figure 3-9B), as similar levels of consumption were measured between the UV-treated and –UV-treated plants. This finding indicates that neither UV component of solar radiation can directly affect *Plutella* feeding behaviour. Interestingly, *Plutella* larvae consumed higher areas of leaf tissue on *B. napus* plants used in the UV-A bioassays (Figure 3-9B).

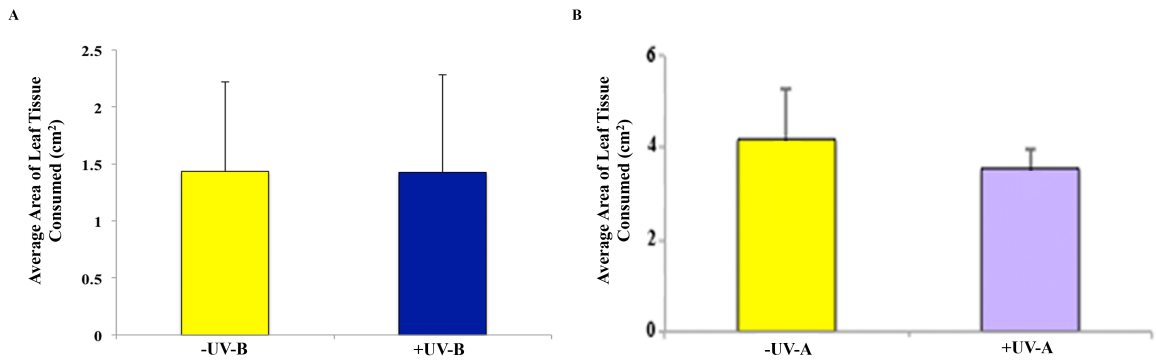

Figure 3-9: *Plutella* larvae feeding is not directly affected by UV-B or UV-A radiation. The area of leaf tissue consumed by *Plutella* larvae on *B. napus* positioned under **A,** –UV-B or +UV-B conditions or **B,** –UV-A or +UV-A conditions in an invertebrate choice chamber. Light conditions were created in either side of an invertebrate cage by covering it with two different filters, one removing either UV-B or UV-A, the other transmitting both components of UV. One 3-week old *B. napus* plant previously reared under 70 μmol m^{-2} s^{-1} white light was placed under each filter, and 10 *Plutella* larvae which were starved for 1 hour were deposited in the centre of cage under the filter interface. Bioassays were run for 24 hours under white light supplemented with either 3 μmol m^{-2} s^{-1} broadband UV-B radiation or 70 μmol m^{-2} s^{-1} UV-A. Significance of the +UV-A or UV-B treatment against the –UV-A or UV-B treatment was calculated using ANOVA and Tukey's Honest Significant Difference (HSD) post-hoc test. UV-B: $p = 0.99$. UV-A: $p = 0.61$. n=6. Bars represent mean ± SEM.

3.6.2 Slug behaviour appears to be slightly influenced by the presence of UV-B

The direct effects of UV-B radiation on slug grazing were examined using the same experimental set-up for as *Plutella* larvae. Due to a shortage of juvenile slugs, UV-A bioassays could not be performed.

At first glance, it would seem that slug feeding is influenced by the presence of UV-B radiation, as higher consumption of *B. napus* plants positioned under +UV-B conditions is observed (Figure 3-10). While this result does not appear to be statistically significant, the spread of tissue areas consumed across the replicates indicates that plants positioned under +UV-B conditions are more prone to higher levels of slug consumption (Figure 3-10B).

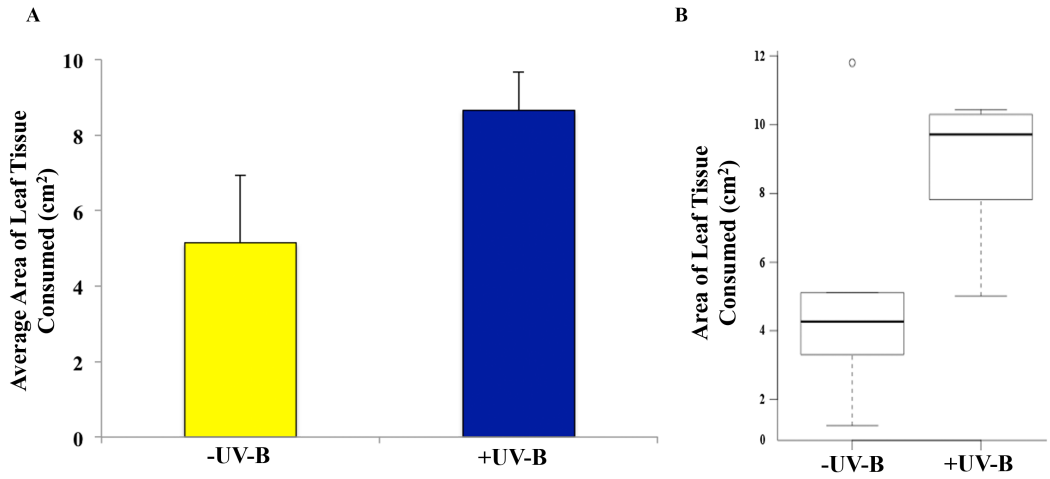

Figure 3-10: UV-B radiation does not directly affect slug feeding on *B. napus*. A, the average area of leaf tissue consumed by juvenile slugs on *B. napus* positioned under –UV-B or +UV-B conditions in an invertebrate cage, and **B,** a boxplot displaying the spread of areas consumed across all replicates. –UV-B and +UV-B conditions were created in two halves of the invertebrate cages by covering cages in two different filters, one of which filters out UV-B, the other transmits UV-B. One 3-week old *B. napus* plant previously reared under 70 μmol m^{-2} s^{-1} white light was placed under each filter, and 2 juvenile slugs, which were starved overnight, were deposited in the centre of cage under the filter interface. Bioassays were run for 24 hours under white light supplemented with 3 μmol m^{-2} s^{-1} broadband UV-B radiation. N=5. Significance of the +UV-B treatment against the –UV-B treatment was calculated using ANOVA and Tukey's Honest Significant Difference (HSD) post-hoc test $p = 0.126$.

These results do not clearly indicate whether or not invertebrates are capable of detecting UV radiation or not, as it is possible that the *Plutella* larvae, which show no preference for one side of the cage over the other in either bioassay (Figure 3-9), may detect components of UV radiation, but their feeding habits are not affected by them. What is clear is that, regardless of their ability to detect UV or not, *Plutella* larvae feeding behaviour is unaffected by the presence of UV-A and UV-B, while slugs consume slightly higher levels of *B. napus* tissue when it is positioned under +UV-B conditions.

3.7 Discussion

Components of solar radiation are known to modify the attractiveness of many plant species to several invertebrate pests, with low red:far-red ratios increasing plant vulnerability to invertebrate consumption and *Botrytis cinerea* infection (Izaguirre et al., 2006, Cerrudo et al., 2012), and UV-B radiation reducing plant attractiveness to pests (Izaguirre et al., 2003, Caputo et al., 2006, Demkura and Ballaré, 2012). UV-B's ability to promote plant defence has been documented in many studies examining different plant and

invertebrate species, such as Arabidopsis and *Plutella xylostella* (Caputo et al., 2006) broccoli and Thripidae (Kuhlmann and Muller, 2009a) and Nicotiana and *Manduca sexta* (Izaguirre et al., 2003). While members of the Brassica family have been employed as model organisms for many of these studies, UV-B-mediated defence in *B. napus* has not been investigated before. The range of invertebrate pests focused upon in previous studies is also quite narrow, with one of the main destructive herbivores in British agriculture, the greyfield slug (*Deroceras reticulatum*) receiving little to no attention. This chapter therefore aimed to investigate whether or not UV-B radiation is capable of reducing *B. napus* susceptibility to herbivory from juvenile slugs and *Plutella xylostella* larvae. The effects of another component of solar radiation on invertebrate feeding preferences, UV-A, was also briefly examined, as to the best of our knowledge, no studies have been conducted to investigate any influence UV-A radiation may have on plant-invertebrate interactions.

3.7.1 UV-B reduces *B. napus* susceptibility to *Plutella* and slug herbivores

UV-B was found to reduce the average area of leaf tissue consumed by both 2nd instar *Plutella* larvae and juvenile slugs on *B. napus* (Figure 3-1 and Figure 3-2, respectively). *Plutella* larvae's preference for consuming –UV-B-treated Brassica plants was as expected, based on previous findings indicating a clear aversion of larvae from +UV-B Arabidopsis Col-0 (Caputo et al., 2006). As the effect of UV radiation on slug feeding preferences is novel, the results obtained could not have been predicted. A previous study examined slug feeding habits with leaf tissue obtained from six species of a fen ecosystem in Argentina exposed to –UV-B and +UV-B conditions (Zaller et al., 2003). The authors reported that out of the 6 species, only one of them, *Nothofagus antarctica* (a beech tree species), displayed a UV-B-induced reduction in susceptibility to slugs, as up to two-thirds more tissue was consumed from specimens maintained under reduced UV-B conditions. However, as slugs were presented with detached leaf material from all 6 species at once, the results generated could also indicate a feeding preference for one plant species over another, regardless of the light treatment they received. The experimental set up in this study was also significantly different to the methods used here, including the use of detached leaf material, as opposed to intact plants. Intact and physically undamaged plants were favoured for the experiments presented in this chapter, as it was feared that stimulating a wound response in the tissue could mask UV-B-induced defence responses.

Therefore, the results presented by Zaller et al. were unable to help predict slug feeding preferences in this study.

When the area of –UV-B and +UV-B *B. napus* leaf tissue consumed by invertebrates was examined for each individual replicate (Figures 3-1C and 3-2C), variation across the bioassays became evident. As all replicates were carried out in the same manner, using plants of the same age, larvae at the same development stage, and bioassays conducted for the same length of time following a uniform period of larval starvation, experimental technical set-up was not thought to be the primary source of this variation. Unforeseen and uncontrollable differences in plant illumination conditions between replicates conducted on separate occasions must be acknowledged as a potential cause for variation, although it cannot be ascertained if it was the cause. As some replicates that were illuminated with white light or UV-B radiation at the same time and underwent invertebrate bioassays together displayed variation in the area of leaf tissue consumed, it is unlikely that fluctuations in light emissions or growth room conditions was the reason for the mixed results.

It was asked if the variation could be attributed to the starting leaf area of *B. napus* presented to the larvae serving as a limiting factor, as complete consumption of tissue from one plant could force the invertebrates to consume more on the less favourable plant. However as there was always ample leaf tissue remaining at the end of the bioassays to facilitate leaf area measurements, it seemed unlikely that the initial leaf area was responsible for such variation. ANOVA was employed to determine if the starting leaf area for both –UV-B- and +UV-B-treated *B. napus* significantly influenced the areas consumed, and for both invertebrates, it was found not to. As leaves on the +UV-B plants were typically smaller than those on the –UV-B plants, the quantity of leaf tissue remaining at the end of the bioassay along with the statistics also suggests that the smaller area of +UV-B plants was not a limiting factor affecting the results. Other logical explanations for variation in the area consumed by the pests include mistakes when isolating invertebrates of a specific developmental stage for bioassays, or irreversibly damaging invertebrates (especially delicate larval mouthpieces) while handling them, and reducing the number of active feeding pests in each replicate. Both of these errors could affect the total area of leaf tissue consumed in each replicate, while allowing any trends in feeding preference of one light-treated plant over another to be retained across replicates. The possible explanations of this variation are many, but it is important to remember that biology is a non-linear subject, and the task of working with invertebrate organisms brings with it a certain risk of variation, which must be accepted and handled. There is therefore

a need to carry out a large number of biological replicates when evaluating invertebrate feeding preferences, as it will allow a more accurate understanding on the statistical significance of UV radiation on invertebrate feeding preferences. This was made evident when comparing the results obtained for *Plutella* larvae and slugs, as while both invertebrates showed a level of variation in the areas of -/+UV-B leaf tissue consumed across the biological replicates, (Figure 3-1C and Figure 3-2C, respectively), yet still displayed general preferences in consuming –UV-B-treated plants over +UV-B-treated plants, the statistical significance of this was only detected for *Plutella* larvae, which possessed the largest number of replicates (24, compared to 10 for slugs). It could be that with a greater sample size, the effects of UV-B on slug feeding preferences would be more statistically significant. This statement is not an attempt to rule out the possibility that UV-B elicits greater plant deterrents against *Plutella* larvae than slugs, but simply states that more replicates are required to improve our appreciation of the effects of UV-B radiation in promoting plant defence against slugs.

While all results presented in this chapter have been labelled with statistical values, the *p*-values have on several occasions been acknowledged but not used to draw conclusions from the results. In these cases, the areas of tissue consumed for each replicate or the spread of area consumed has been referred to, helping identify general trends across the data. Where invertebrate preference for one plant treatment over another is obvious when presented as such, regardless of the *p*-value obtained from the average of the replicates, then it is concluded that that particular light source influences levels of invertebrate herbivory. Although dismissal of the statistics may not be advisable, more informative results appear to be obtained when biological replicates are presented next to one another. As such, it is evident that UV-B radiation can reduce *B. napus* susceptibility to *Plutella* larvae and juvenile slug herbivore pests.

3.7.2 UV-A reduces *B. napus* susceptibility to *Plutella* and slug herbivores

The effects of UV-A radiation in modifying plant-invertebrate interactions have not, to our knowledge, been directly investigated. However, results obtained from previous studies where UV-A was retained in the light spectrum of –UV-B-treated plants implies that if UV-A is capable of promoting plant defence against invertebrate pests, the mechanisms activated are not as effective as those initiated by UV-B (Ballaré et al., 1996, Izaguirre et al., 2003, Izaguirre et al., 2007). The bioassays presented in this chapter show that UV-A is capable of inducing invertebrate deterrents in *B. napus,* with slug responses to +UV-A-

treated plants more obvious than those of the *Plutella* larvae (Figure 3-4 and Figure 3-3, respectively). UV-A-treated *B. napus* is considerably less susceptible to slug herbivory than –UV-A plants, a statistically significant finding that was unexpected, considering the results obtained with UV-B-treated *B. napus* (Figure 3-2). UV-B was not found to significantly deter slug herbivores, despite the presence of a trend in slug feeding preferences for -UV-B-treated *B. napus* across individual replicates, indicating UV-B-induced *B. napus* defence against these pests (Figure 3-2C). With only 6 replicates in the UV-A bioassays with slugs, the reliability of this result could be queried. As these 6 replicates were carried out in two batches of three on 2 separate occasions, all plants were grown at different times, irradiated with UV-A at different times, and bioassays were conducted with slugs from a different batch of eggs. Therefore, the results are not considered to be influenced by random, uncontrollable factors that may have materialised over the duration of a single 48-hour bioassay. The effects of UV-A- on *B. napus* susceptibility to *Plutella* are not as evident (Figure 3-3). While the average area of tissue consumed is statistically less for +UV-A-treated *B. napus*, examination of each individual replicate shows a mixture in larval feeding preferences across the bioassays (Figure 3-3C). The majority of replicates display higher levels of consumption on –UV-A-treated *B. napus*, but three replicates, which were not all conducted on the same day, showed little to no difference in areas consumed across the two light-treated plants. From the results presented, it is concluded that UV-A can induce deterrents against both slugs and larvae in *B. napus*, however to provide more clear cut results, further replicates must be conducted with *Plutella* larvae.

3.7.3 UV-B-mediated defence is still apparent in *uvr8-1* null mutants, while UVR8 over-expression does not heighten this defence mechanism

UV-B-treated *B. napus* are less susceptible to slug and *Plutella* larvae consumption. It remains elusive, however, whether or not UV-B-enhanced defence is dependent upon the UV-B photoreceptor, UVR8. To investigate the importance of UVR8, bioassays were conducted using two Arabidopsis lines, the null *uvr8-1* mutant and the *35S*pro:GFP-UVR8 over-expressing line. Differences in tissue area consumed between either line exposed to –UV-B or +UV-B conditions were compared to results obtained for the Arabidopsis progenitor line, L*er*. The absence of functional UVR8 in the *uvr8-1* mutant does not appear to affect slug or *Plutella* feeding patterns when compared to the wild type bioassays (Figure 3-6 and Figure 3-7), as, for both L*er* and *uvr8-1*, the –UV-B-treated plants lose a

larger area of leaf tissue to both invertebrates than the +UV-B WT or mutant lines. This result, however, may not necessarily mean that UVR8 is not involved in UV-B-induced plant defence. While the *uvr8-1* plants used in these bioassays were grown for 4 days under 1.5 μmol m^{-2} s^{-1} UV-B and appeared healthier than those previously grown for 7 days under 3 μmol m^{-2} s^{-1} (but not used in bioassays on account of their appearance), they still possessed some physical signs indicative of stress, such as minor browning of older leaves around the tips (figure not shown). It is therefore possible that UV-B-treated *uvr8-1* mutants appeared physically less attractive to *Plutella* and slugs, with the reduction in leaf tissue area consumed due to the overall appearance of the plants, and not a result of UV-B-induced defences. As further bioassay studies with *uvr8-1* would be unable to confirm or dismiss this hypothesis, slug and *Plutella* feeding preferences of –UV-B- and +UV-B-treated *35S*pro:GFP-UVR8 over-expressing lines were examined in a second attempt to investigate whether or not UVR8 regulates UV-B-induced defence. In these lines, UVR8 protein levels are estimated to be 20% higher than that in L*er* (Figure 3-5). UV-B-treatment of *35S*pro:GFP-UVR8 plants reduces their susceptibility to herbivore attack (Figure 3-6C and Figure 3-7C), although the difference in area consumed between the two light treatments is not regarded as being statistically significant. The spread of data obtained in bioassays for each invertebrate was visualised in boxplots (Figure3-6C and Figure3-7C), and the positions of the median values were noted. The highest areas consumed by larvae and slugs on the +UV-B-treated *35S*pro:GFP-UVR8 were 0.9 and 1.4 cm^2, respectively, while the highest areas consumed on the respective –UV-B plants were 3.5 and 2.4 cm^2. The median value for the –UV-B plants also exceeds the highest area consumed by both invertebrates on the +UV-B plants (1.8 cm^2), which indicates that over 50% of replicates sustain higher levels of tissue loss in the –UV-B-treated *35S*pro:GFP-UVR8 plants by both *Plutella* and slugs. So despite the average area of leaf tissue consumed by both invertebrates not being statistically significant, UV-B radiation does appear to elicit a reduction in *35S*pro:GFP-UVR8 susceptibility to *Plutella* larvae and slugs. However, it remains unclear if UV-B-induced defence is more effective in *35S*pro:GFP-UVR8 plants than L*er*. Unfortunately, no bioassays were conducted to examine invertebrate feeding preferences between the three lines, therefore any differences in attractiveness of the two vegetative sources presented to the pests cannot be concluded, only hypothesised. Calculating the percentage average area of leaf tissue consumed by *Plutella* and slugs on *uvr8-1* and *35S*pro:GFP-UVR8 plants in relation to L*er* indicated that the over-expressing lines lost higher areas of tissue to both invertebrates than the other two

lines (Table 3-1 and Table 3-2 for *Plutella* and slug, respectively). It would be beneficial to conduct bioassays in the future to investigate invertebrate feeding preferences between the different lines.

3.7.4 UV-B radiation cannot promote defence in Arabidopsis mutants impaired in JA-signalling

UV-B was found to be incapable of promoting defence within an Arabidopsis JA-insensitive mutant, *jar1-1*, suggesting that JA-amino acid conjugates, such as the bioactive JA-Ile, is essential for regulating UV-B-induced response. This also leads us to believe that UV-B probably promotes plant defence via the JA-pathway, a finding that has been confirmed in *N. attenuata as-lox3* mutants impaired in JA-biosynthesis (Demkura et al., 2010). In these mutants, anti-sense silencing of a JA-biosynthetic gene, *LOX3*, reduces JA biosynthesis, and they sustain higher levels of tissue consumption by thrips compared to wild type plants. UV-B is also unable to promote defence in these mutants, despite successfully deterring thrip herbivores in wild type *N. attenuata*. These results suggest that UV-B induces plant defence via the JA pathway, presumably down stream of JA biosynthesis.

3.7.5 UV radiation does not influence *Plutella* herbivory patterns, but does influence slug location for feeding

As all bioassays up until now were conducted under –UV conditions, the data represents the effects of UV-induced defences in *B. napus* and Arabidopsis on invertebrate feeding preferences, and not the direct effects of UV perceived by invertebrates. Several invertebrate species are known to detect and respond to various components of solar radiation, including wavelengths in the UV spectrum (Raviv and Antignus, 2004, U, 1935, Mazza et al., 2002). UV radiation serves as an important environmental signal to invertebrates, assisting with orientation, navigation, feeding and mating patterns. Experiments conducted with the thrip species *Caliothrips phaseoli* under controlled conditions found that they can detect the presence of UV-B radiation and actively migrate away from the source, an avoidance act that is not seen under UV-A conditions, where invertebrates are instead attracted to areas of high UV-A intensity (Mazza et al., 2002). However, the direct effects of UV radiation on *Plutella* larvae and slug activity have not, to our knowledge, been investigated before. Bioassays were therefore conducted over 24

hours to gain insight into the direct effects of UV-A and UV-B radiation on invertebrate feeding behaviour, with the area of –UV-treated *B. napus* tissue consumed over this period measured to assess the preferred location of invertebrates.

Plutella larvae feeding preferences were not found to be influenced by either UV-A or UV-B radiation (Figure 3-9), suggesting that larvae are neither deterred nor attracted by these two components of solar radiation. These results do not necessarily mean that *Plutella* larvae are incapable of detecting UV radiation, as it is possible that they can detect wavelengths between 280-380 nm, but their feeding behaviour is not affected by them. It is interesting to note higher rates of *B. napus* tissue consumption in the *Plutella* UV-A bioassays (Figure 3-8A) compared to the UV-B bioassays (Figure 3-8A), an observation which may be coincidental, or an implication that UV-A positively affects invertebrate behaviour by encouraging them to eat. UV-A has previously been documented to serve as an attractive wavelength for invertebrates (Mazza et al., 2002), therefore it is not improbable that the same effect is seen in these bioassays. The similar levels of tissue consumed in *B. napus* plants positioned under the –UV-A and +UV-A sections of the cages do not readily support this hypothesis, however, as it would be expected that if UV-A enhanced larval feeding activity, then a higher rate of tissue consumption would be seen on the plant positioned under UV-A conditions. A UV meter did not detect any UV-A in the section of the cages covered by the UV-A cut-off filter, so it is clear that UV-A did not reach this side of the cage. As no analysis was done on the physical light detecting mechanisms of the invertebrates, it is possible that the results seen in Figure 3-8B are caused by UV-detection by *Plutella* larvae. By being positioned in the centre of the chamber at the start of the bioassay, it is highly probable that all larvae were exposed to UV-A at some point over the 24-hour bioassay. Brief detection of UV-A may have triggered a behavioural response in the larvae, a response that may have been masked or repressed in the UV-B bioassays (Figure 3-8A). As the UV-B source used for these bioassays also emits part of the UV-A spectrum, it is interesting to note that a smaller area of leaf tissue is consumed in these bioassays. However, it cannot be confirmed that this observation is due to attraction and repression properties of UV-A and UV-B, respectively, or is simply coincidental. Further studies into genetic and metabolic differences induced by both UV sources in *B. napus*, along with studies into any responses select compounds may have on invertebrate behaviour, could help improve our understanding on the effects of UV radiation on plant susceptibility to invertebrate pests.

UV-B radiation did not significantly affect slug feeding preferences, however despite this lack in statistical significance, there does seem to be a higher level of tissue consumption

on the *B. napus* plant positioned directly underneath the UV-B source (Figure 3-9). The distribution of tissue areas consumed by slugs on plants positioned under –UV-B and +UV-B conditions is relatively narrow. At least 50% of replicates are spread within a 1 cm^2 or 2.5 cm^2 range for –UV-B and +UV-B *B. napus,* respectively (Figure 3-9B), which highlights how favourable the *B. napus* plants positioned under UV-B are for slugs.

This finding is highly surprising, as slugs are notorious nocturnal creatures, therefore it would be expected that they would take evasive action from UV-B radiation. During the bioassay, regular checks were made to note the position of the slugs on plants. They were found predominantly underneath the leaves on both plants in the cages, a highly unsurprising find. Plant leaves are very effective UV-B filters and would have sheltered the slugs from the radiation. However, this still doesn't explain why slugs spent more time consuming plant material positioned under the UV-B source. Perhaps, additional environmental factors also contribute towards slug feeding patterns and behaviour during the hours of daylight, such as temperature and humidity. The humidity in the treatment rooms could not be measured, however a layer of freshly dampened soil lined the bottom of the cages. For reasons unknown, the nocturnal feeder preferred to consume tissue from *B. napus* plants positioned under UV-B radiation, whilst remaining on the underside of the leaves. Due to the previous results in this chapter demonstrating that slugs consume higher levels of tissue from plants maintained under -UV-B conditions (Figure 3-2 and Figure 3-6), it is difficult to believe how reliable the results in Figure 3-9 are. It might be, that by positioning themselves under the low-lying *B. napus* leaves, slugs are perfectly sheltered from UV-B radiation, and are able to consume palatable –UV-B-treated plants. If the bioassay was allowed to progress for an extra 24 hours or more, the accumulation of UV-B-induced defences in *B. napus* may have deterred the slugs and promoted their movement to the other side of the cage. It would have been interesting to conduct such a bioassay, however time constraints and a lack of juvenile slugs over the course of the project prevented extended bioassays and UV-A bioassays to be conducted with slugs. What can be concluded from the results obtained, is that *Plutella* larvae consumption of –UV-treated *B. napus* is not directly affected by either UV-A or UV-B radiation, while slugs appear to consume higher areas of –UV-B-treated *B. napus* positioned under UV-B conditions over a 24-hour period.

3.7.6 Conclusions and outlook

All experiments presented in this chapter aimed to better understand if UV components of solar radiation influence plant–invertebrate interactions, a naturally occurring process that is seen on a daily basis in the field. As with any experiment conducted under controlled conditions to mimic in-field scenarios, various issues need addressing. The first is the light qualities and quantities used. The fluence rate of white light used was approximately 70 μmol m^{-2} s^{-1}, a small fraction of what can typically be seen outside. Similarly, the UV-B fluence rates used (1.5-3 μmol m^{-2} s^{-1}), do not reflect the appropriate levels of UV-B seen alongside the stated levels of white light in terrestrial ecosystems. By using an ecologically irrelevant UV-B : PAR ratio, it is difficult to state that what is presented in this chapter reflects what happens in the field. Conducting bioassays under controlled conditions theoretically allowed the effects of UV radiation alone on feeding preferences to be evaluated, however, these test conditions do not represent what would happen in the field, and therefore it is possible that key factors that could influence plant-invertebrate interactions have been over-looked. As a result, the next step for these bioassays is to progress into the field, where UV filters can be utilised to provide the desired spectrum across various plots of *B. napus*. By monitoring invertebrate species located within these plots and assessing plant damage, it will be possible to conduct ecologically relevant in-field research that will generate more informative results on UV-induced plant defence.

UV-B and UV-A radiation were found to reduce *B. napus* and wild type Arabidopsis susceptibility to second instar larvae of *Plutella xylostella,* and juvenile slugs. It is unclear whether or not the UV-B photoreceptor, UVR8, is required for UV-B-induced defence, however UV-B's inability to increase resistance in an Arabidopsis mutant impaired in JA-signalling suggests that these responses function downstream of JA-biosynthesis. To better understand the molecular mechanisms of UV-B-mediated herbivore defence in *B. napus*, a transcriptomic and global metabolomics approach was employed using RNASeq and reverse-phased chromatography, respectively. The results obtained from these two omics-based approaches are discussed over the next 2 chapters, with chapter 4 focused upon the transcriptomic overlaps between UV-B- and herbivory-induced responses.

Chapter 4: Transcriptional Overlaps Between UV-B and Wound Response Pathways in *Brassica napus*

4.1 Introduction

Transcriptomic studies have the ability to reveal genetic reprogramming events in organisms in response to different treatments. The information collected from such studies is extensive, and can provide insight into the genetic overlaps between different biotic and/or abiotic stimuli. On account of the wealth of information that can be obtained from transcriptomics, RNA-seq was employed to identify *B. napus* transcripts similarly regulated by UV-B radiation, slug herbivory, *Plutella* herbivory, or exogenous MeJA treatment, in an attempt to better understand the molecular basis of UV-B-mediated resistance in *B. napus*. As the *B. napus* genome was not yet sequenced at the start of this project when RNA-seq was first performed, the Brassica 95K Unigene was used as a reference 'genome' for read alignment. Reads were later realigned to the *B. napus* genome following its publication (Chalhoub et al., 2014), with the Arabidopsis genome used to provide putative functions to the identified transcripts in both alignments. The results from these alignments were slightly different to on another, however it was possible to gain better insight into the genetic overlaps between UV-B- and herbivore-induced signalling pathways in *B. napus* via the identification of putative early-induced transcriptional regulators and additional transcripts that were similarly up-regulated by UV-B and invertebrate treatments (section 4.5). In addition, several transcripts were selected from these findings for over-expression in Arabidopsis, with the aim of investigating any roles their encoded products may have in mediating UV-B-enhanced resistance (section 4.4; the findings from the over-expressing lines are detailed in Chapter 6).

4.2 Optimising UV-B, herbivory and MeJA treatment conditions for generating samples for RNA-seq

The aim of carrying out transcriptomic analysis was to identify early-induced transcription factors and/or regulators that would enable pathways thought to be involved in UV-B-mediated defence to be acknowledged. Given the dynamics of an organism's transcriptome over a period of time, it would have been beneficial to carry out RNA-seq analysis on samples collected over a 24-hour time period. Initial planning limited the

investigation to three replicates of a single time point for each treatment, however, as we hoped to conduct further genetic analysis on additional plant material at a later date. It was therefore important to ensure plants received an adequate treatment over an appropriate length of time, to generate a genetic response that would reveal information about UV-B-mediated *B. napus* defence. To achieve this, a series of optimisation experiments were conducted over 24-hour time courses, where 3-week old *B. napus* plants were treated with different concentrations of MeJA, various fluence rates of UV-B radiation, or an hour herbivory with juvenile slugs or second instar *Plutella* larvae. True leaf samples were harvested at 1, 4, 8, 16 and 24 hours after the start of MeJA or UV-B treatment, and 1, 2, 5, 17 and 25 hours after the start of invertebrate herbivory. Three independent experiments were conducted on separate occasions, with three 'technical' replicate plants harvested in each experiment. Therefore, after finishing the 3 independent replicates, a total of 9 samples from separate plants were collected for each time point of a given treatment. Control plants were those that were maintained under white light-only conditions for the duration of the treatments, in an invertebrate-free growth chamber. After RNA extraction, cDNA was synthesised for use in qPCR with primers designed to amplify known UV-B- or wound-response genes (Table 4-1).

UV-B-Response Marker Genes	Wound-Response Marker Genes
CHALCONE SYNTHASE (*CHS*)	*JASMONATE INSENSITIVE 1* (*JIN1* / *MYC2*)
FLAVONOL SYNTHASE (*FLS*)	*LIPOXYGENASE 2* (*LOX2*)

Table 4-1. Four UV-B- and wound-response marker genes selected for expression analysis in *B. napus*.

On account of the *B. napus* genome not being sequenced at this stage in the project, the Brassica 95K Unigene, and sequenced genome of a *B. napus* progenitor species, *B. rapa*, were used as platforms for primer design. By studying changes in gene expression over a 24-hour time course and noting where peaks in expression occurred, a suitable time point considered to show optimum levels of UV-B- and wound-response gene expression could be estimated, and appropriate samples sent for RNA-sequencing.

4.2.1 UV-B Optimisation

When selecting the optimum UV-B radiation conditions for treatment of *B. napus*, several requirements had to be met. First, the fluence rate of UV-B had to be comparable to what would typically be recorded in terrestrial ecosystems, so as not to bombard plants with

unnaturally high levels of UV-B photons. Second, it was considered advantageous to use a fluence rate similar to that previously used for the invertebrate bioassays, allowing the observed UV-B-enhanced defence mechanisms discussed in Chapter 3 to be related to transcriptomic modifications within the plant when irradiated with a specific range of fluence rates. Finally, the source of UV-B radiation and the associated light spectrum emitted had to be carefully selected. Two radiation sources were available for use, a narrowband tube, Philips TL20W/01RS, which as the name suggests emits a small range of the UV-B spectrum, and a broadband source, UV-B-313 (Q panel), which emits a longer range of UV-B. A spectrum of the wavelengths emitted by each of these tubes can be found in Figure 2-2 (section 2.5.1 of Materials and Methods). The maximum emissions for these tubes are at 311 nm and 313 nm, respectively, and in addition to UV-B radiation, both sources emit small quantities of UV-A and blue light. While the shortest wavelength that reaches the Earth's surface is approximately 295 nm, it is the longer wavelengths of UV-B (i.e. as emitted by narrowband sources) that are considered to activate UVR8-specific responses, while broadband UV-B is thought to activate both UVR8-dependent and -independent pathways. As it was unknown whether or not UVR8 was involved in UV-B-enhanced defence in *B. napus*, it was considered logical to use the broadband UV-B source for plant treatment, to allow the effects of both UVR8-dependent and –independent pathways to be examined.

To identify a suitable UV-B fluence rate that would permit expression of known UV-B-response genes, the expression of putative *B. napus* orthologues of two UV-B-inducible genes, *CHS* and *FLS*, was monitored across a 24-hour time course where 3-week old *B. napus* plants were irradiated with three fluence rates of broadband UV-B: 0.5, 1.5 and 3 μmol m^{-2} s^{-1} (Figure 4-1). These two genes encode enzymes involved in the flavonoid biosynthesis pathway, with CHS catalysing the first committed step of this pathway (Figure 4-1C). They are therefore not transcriptional regulators, the main targets of the RNA-seq analysis. Two UV-B-regulated transcription factors that activate downstream responses, such as transcription of *CHS*, are HY5 and HYH. Previous microarray analysis reported over a 2-fold increase in *HY5* and *HYH* expression following a 15 minute exposure to 7 W/m^2 UV-B radiation followed by 1 hour under –UV-B conditions before harvesting (Ulm et al., 2004), highlighting how responsive these two genes are to UV-B radiation. Attempts were made at the start of this project to examine *HY5* expression in UV-B-treated *B. napus*, with primers designed to amplify putative *B. napus* homologues. However, amplification of a *B. napus* PCR product with the various primer combinations failed, hence the reason results from two HY5-regulated genes are shown here.

CHS expression follows a general trend across a 24-hour time course in response to the three different fluence rates (Figure 4-1A), with expression increasing up to and peaking at 8 hours into the illumination period. Here, transcript levels are more than 50% higher compared to levels seen at any other time point in response to 1.5 and 3 μmol m^{-2} s^{-1} UV-B, with these two fluence rates evidently enforcing a greater effect on *CHS* transcript levels than 0.5 μmol m^{-2} s^{-1}. Such a peak in expression of *CHS* this far into an illumination period has previously been reported with Arabidopsis cell cultures (Christie and Jenkins, 1996a). Analysis of Variance (ANOVA) and the Tukey's Honest Significant Difference (HSD) post-hoc test was used to evaluate the statistical difference:

- Across all time points within each fluence rate,
- For all fluence rates within each time point.

Statistically, the peak in *CHS* expression at T=8 was found to be significant for all fluence rates, however no statistically significant difference was observed between 1.5 and 3 μmol m^{-2} s^{-1} at this time point. A statistically significant difference between the two highest fluence rates and 0.5 μmol m^{-2} s^{-1} was also observed at T=1 and T=8. While transcript abundance of *CHS* follows a similar pattern in response to all three UV-B fluence rates, *FLS* does not appear to be similarly regulated (Figure 4-1B). The relative fold change in expression of *FLS* exceeds that of *CHS*, in some instances by at least 2-fold. A low fluence rate of 0.5 μmol m^{-2} s^{-1} induces a peak in expression at T=8, before transcript abundance decreases by approximately 50% by T=16. Optimum *FLS* fold changes in expression in the presence of 1.5 or 3 μmol m^{-2} s^{-1} UV-B occur at 4 and 16 hours into the illumination period, respectively, suggesting that an intermediate fluence rate of 1.5 μmol m^{-2} s^{-1} induces a more rapid response of *FLS* transcription. Within each time point, the statistical difference between the fluence rates varies. At T=4, the difference between each fluence rate is $p \leq 0.01$, while T=8 and T=16 display a significant difference between 1.5 or 3 μmol m^{-2} s^{-1}, but not between 0.5 and 1.5 μmol m^{-2} s^{-1}. The different patterns in the regulation of *CHS* and *FLS* expression were not expected, as both genes are involved in the flavonoid biosynthesis pathway, and operate within close proximity to each other in this pathway, so were thought to respond to UV-B in a similar manner. The results in Figure 4-1 make it difficult to select a particular time point for RNA-seq analysis, on account of the different peaks in expression across the time course. Optimum levels of *CHS* expression at T=8, along with high relative fold changes in expression of *FLS* at the same time point for all fluence rates (fold change ~400-500), resulted in this sample being considered the one

displaying optimum expression of the two target genes. However, it was thought that this sample may not identify UV-B-induced transcriptional regulators in RNA-seq, as peaks in their transcription would occur before peaks in the transcription of their target genes. A time point before T=8 was therefore considered suitable for RNA-seq analysis, and to that end, the sample considered appropriate for RNA-seq analysis was 'T=4, 3 μmol m^{-2} s^{-1}.

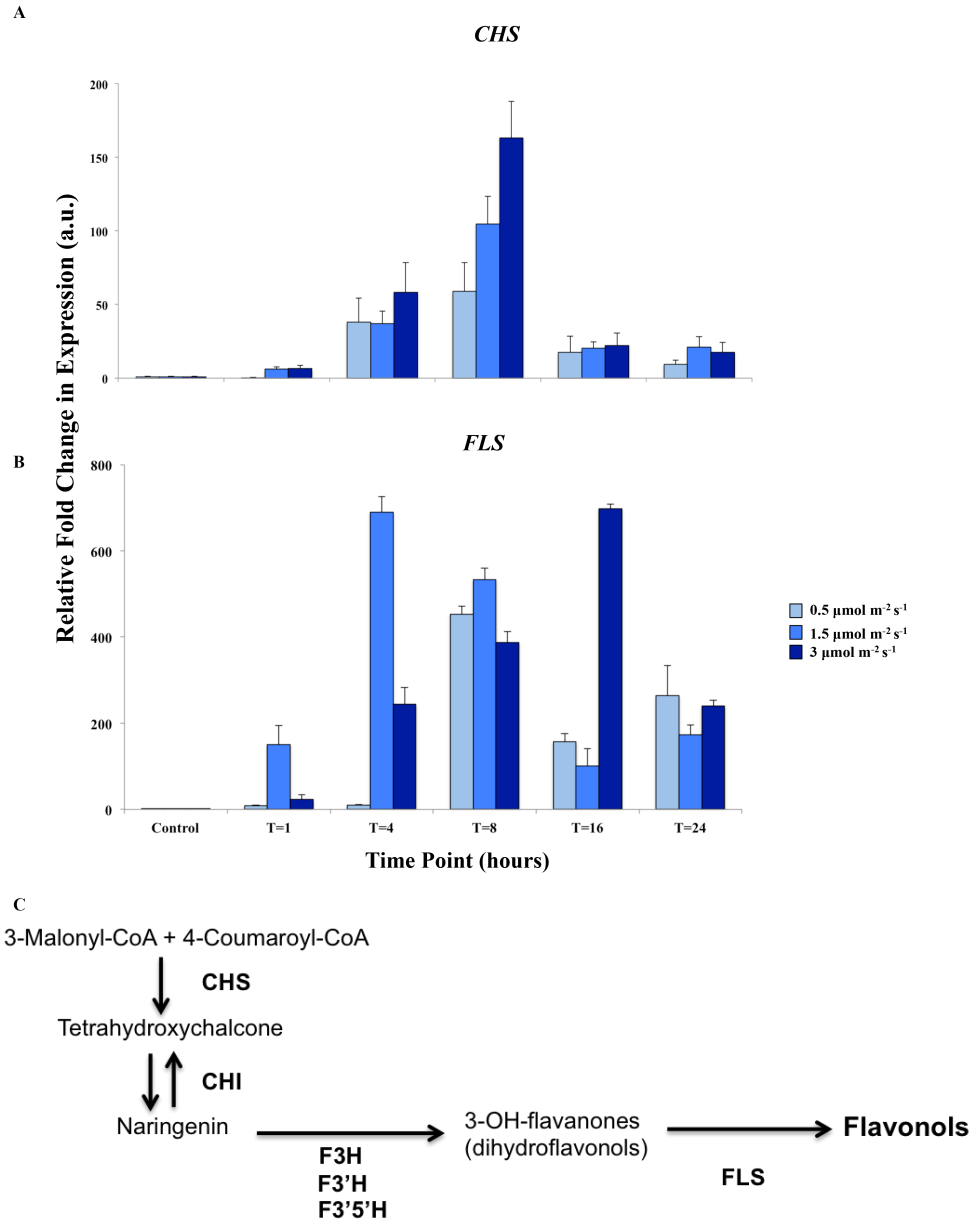

Figure 4-1. Relative fold change in expression of *B. napus CHS* and *FLS* in response to UV-B radiation over a 24-hour period. Expression of **A,** *CHS* and **B**, *FLS* in *B. napus* over a 24-hour time course in response to 0.5 μmol m^{-2} s^{-1} (light blue bars) 1.5 μmol m^{-2} s^{-1} (darker blue bars) or 3 μmol m^{-2} s^{-1} (navy blue bars) broadband UV-B. The location of CHS and FLS in the flavonoid biosynthesis pathway, **C**, derived from (Winkel-Shirley, 2002). Results are presented as relative transcript level normalised against the reference gene, *EF1a*, and the –UV-B control using the comparative Ct method (Schmittgen and Livak, 2008). Error bars represent SD from three independent replicates, each containing three technical replicates.

4.2.2 MeJA Optimisation

Three concentrations of MeJA were tested on *B. napus*, 10 μM, 100 μM and 1mM. The MeJA stock required a preliminary dilution in ethanol, and in the preparation of working MeJA solutions, a wetting agent was included to facilitate penetration through the waxy epidermal surface of the *B. napus* leaves. The final concentration of ethanol and wetting agent, Surfac UN65 (Surfachem), in working solutions was always 0.01%. To rule out any effects of 0.01% ethanol and 0.01% UN65 on genetic changes in *B. napus*, a control solution was tested alongside the MeJA treatment, by diluting ethanol and UN65 in sterile dH_20 (v/v) to obtain a final 0.01% concentration of each solute. Plants were sprayed with approximately 5 ml of solution, until the surface of all leaves was saturated with solution. The three MeJA treatments and EtOH/UN65 control were run alongside an untreated control, where plants received no spraying treatment of any kind, and were maintained under white light-only conditions. Tissue was harvested over a 24 hour time course, with T=X representing the number of hours following the application of a working solution. The expression of two MeJA-responsive genes, *MYC2* and *LOX2*, was assayed over the 24-hour time course, to determine where peaks in their expression occurred (Figure 4-2). *MYC2* encodes a bHLH transcription factor, involved in the JA-Ile-dependent regulation of defence responses (Lorenzo. et al., 2004). *LOX2* is a downstream target of MYC2 (Hou et al., 2010), and is a component of the JA-biosynthesis pathway (Bell et al., 1995).

The effect of 0.01% EtOH/UN65 on *MYC2* expression is minimal in relation to the effects elicited by the MeJA treatments, as only a small and fairly consistent fold change in expression of *MYC2* is observed in response to this treatment (Figure 4-2A). Following exposure to 10 μM MeJA, expression of *MYC2* steadily increases up to 227-fold at T=8, before transcript abundance starts to decline (Figure 4-2 A). The peak in expression at T=8 was found to be statistically significant in contrast to the other time points. 1 mM MeJA induced a slight peak in expression shortly after treatment at T=1, but levels become exceedingly low thereafter, implying that high concentrations of MeJA can suppress expression of *MYC2*. 100 μM of MeJA, on the other hand, generated a rapid increase in *MYC2* transcript abundance, which was maintained throughout the time course. As a result, no visual or statistically significant peaks were identified.

Relative fold change in *LOX2* expression is not as high as that of *MYC2* over a 24-hour period (Figure 4-2 B), with the highest peak of 73-fold occurring 16 hours after treatment with 10 μM MeJA. The control spray treatment of 0.01% EtOH/UN65 appears to increase *LOX2* expression at this time point, too, with the relative fold change in expression similar

to that seen following 1 mM MeJA, and higher that that induced by 100 µM MeJA. A steady increase in expression can be seen in response to both 10 µM and 100 µM of MeJA, with peaks in response to the latter concentration occurring at T=8. 1 mM, again, does not stimulate such a response in *LOX2* levels as the other two concentrations, reminiscent of what was observed for *MYC2*.

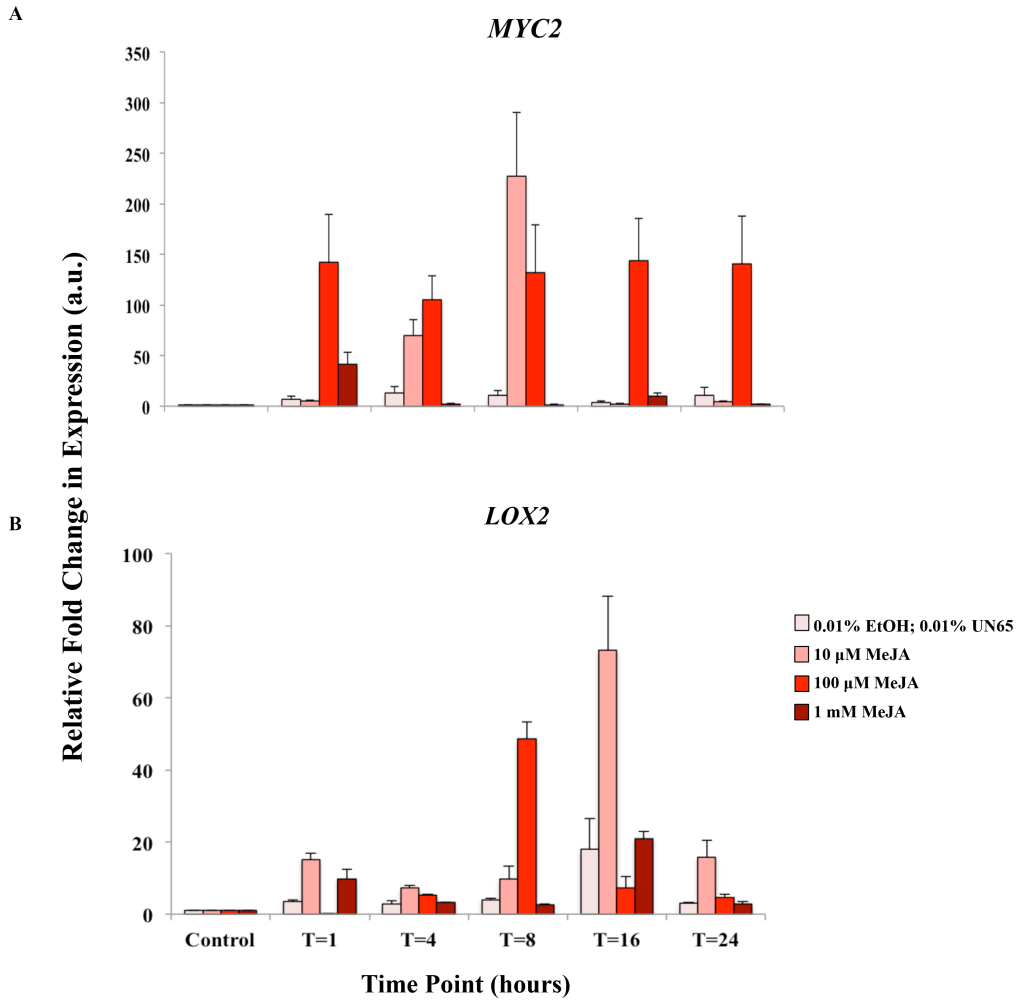

Figure 4-2. Relative fold change in expression of *B. napus MYC2* and *LOX2* over a 24-hour period in response to exogenous application of MeJA. Expression of **A,** *MYC2* and **B,** *LOX2* in *B. napus* over a 24-hour time course in response to exogenous application of 10 µM, 100 µM or 1 mM MeJA. MeJA solutions contained 0.01% ethanol (EtOH) and 0.01% Surfac UN65. Effects of a 0.01% EtOH; 0.01% UN65 application on gene expression was tested (light pink bars) alongside working solutions of MeJA (light red-dark red bars). Results are presented as relative transcript level normalised against the reference gene, *EF1a*, and the –UV-B control using the comparative Ct method (Schmittgen and Livak, 2008). Error bars represent SD from three independent replicates, each containing three technical replicates.

On account of the constant expression of *MYC2* across the 24-hour period in response to 100 μM MeJA, samples treated with this concentration were considered appropriate for RNA-seq analysis. As no statistically significant difference existed between the 5 time points, 'T=4, 100 μM' was selected for analysis. By analysing T=4 for UV-B (Figure 4-1) and MeJA, it was thought that a better comparison could be made between the responses provoked by each stimulus.

4.2.3 Herbivory Optimisation

Initial herbivory assays were conducted at the John Innes Centre's Entomology department, where staff provided both invertebrates and guidance on experimental design that enabled repetition of these experiments at the University of Glasgow at later dates. To ensure that enough tissue was available for harvesting at the end of the invertebrate feeding period, a 1-hour grazing time was enforced on all experiments, with tissue from individual plants collected at set time points thereafter. Invertebrates were subjected to a period of starvation before grazing commenced (16 hours for slugs, 1-2 hours for *Plutella* larvae), to guarantee that they were hungry at the start of the experiments. Further details of the experimental setup can be found in section 2.5.3.3 of the Materials and Methods chapter. Tissue was harvested from individual plants at slightly different time points to those used previously (Figure 4-3A). T=1 represents the time at which the invertebrates were removed from the plants after a 1-hour feeding period, and T=2 stands for 1 hour herbivory plus 1 hour after the removal of invertebrates (in other words, 'T=' refers to the time elapsed since the start of herbivory). Expression of *LOX2* was studied over the 25-hour period for both invertebrates (Figure 4-3A).

The relative fold change in *LOX2* expression across the time course is not very high (maximum increase is 5.6 seventeen hours into the slug herbivory treatment). Despite this, evident maximum fold changes in expression of *LOX2* can be seen at T=5/17 for *Plutella*, and T=17 for slug herbivory, although the difference in *LOX2* expression following *Plutella* herbivory across the time points is not statistically significant. The peak in slug-induced *LOX2* expression at T=17 was found to be significantly different to T=1 ($p \leq 0.05$), but not to any other time point.

Due to some inconvenient restraints at this point of the project, qPCR analysis of *MYC2* could not be assessed in these samples. Therefore, to allow progression of the RNA-seq analysis, semi-quantitative PCR (sqPCR) was conducted with *MYC2* primers (Figure 4-3B).

As an early time point for RNA-seq analysis was desired, and peaks in *LOX2* expression take place up to T=17, the T=25 sample was omitted from these sqPCR events. *MYC2* expression peaks at T=2, in a semi-quantitative manner. This prompted the 'T=2' samples from each invertebrate experiment to be submitted for RNA-seq analysis, along with the designated samples from UV-B treatment (section 4.2.1) and MeJA treatment (section 4.2.2).

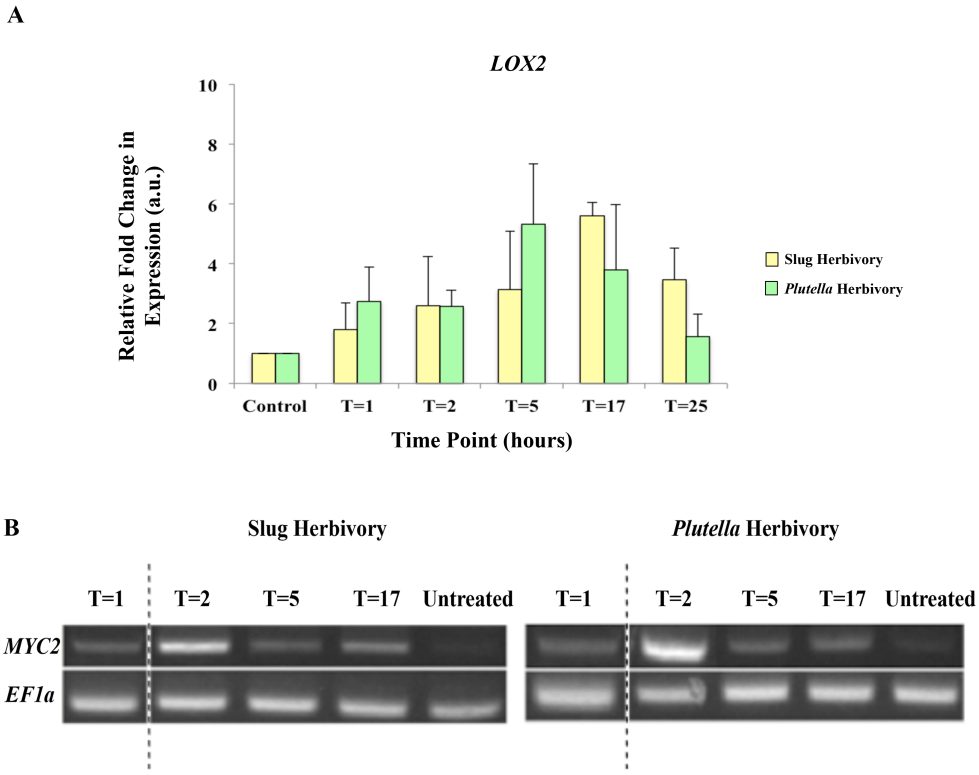

Figure 4-3. Relative change in expression of *B. napus LOX2* and *MYC2* over a 24-hour time course following one hour exposure to slug or *Plutella* larvae herbivory. Expression of **A,** *LOX2* with qPCR in *B. napus* over a 25-hour time course in response to 1-hour herbivory by juvenile slugs (yellow bars) or second instar *Plutella* larvae (green bars). **B,** *MYC2* expression was determined by sqPCR. Results in **A** are presented as relative transcript level normalised against the reference gene, *EF1a*, and the –UV-B control using the comparative Ct method (Schmittgen and Livak, 2008). Error bars represent SD from three technical replicates from one biological experiment. **B** is representative of 2 technical replicates, with dotted lines representing the separation of agarose gels.

4.3 RNA-seq was used to identify early-induced transcriptional regulators commonly expressed in response to UV-B, MeJA and invertebrate herbivory

During this project, two RNA-seq events took place at the Glasgow Polyomics Facility using a NextSeq™ 500 desktop platform (Illumina). The initial analysis in 2012 utilised the Brassica 95K Unigene (Trick et al., 2009) as a reference 'genome' for gene alignment,

while the latter event in 2014 aligned reads to the newly sequenced *B. napus* genome (Chalhoub et al., 2014). The Brassica 95K Unigene comprises of 94,558 sequences assembled from approximately 800,000 expressed sequence tags (ESTs), derived predominantly from three Brassica species: *B. napus* and its two progenitor lines, *B. rapa* and *B. oleracea.*

In 2012, a single biological replicate from each of the four treatments underwent RNA-seq analysis and alignment to the Unigene. Details of these samples and associated untreated controls can be found in Table 4-2. Two additional independent replicates of these treatments took place at a later date, and subsequently underwent RNA-seq in 2014 (samples detailed in Table 4-3). The reads obtained from this event were aligned to the *B. napus* genome alongside the initial reads from 2012, resulting in a total of three independent replicates being analysed against the *B. napus* genome for the majority of samples. The exclusion of an additional control for the MeJA treatments, 0.01% EtOH/0.0% UN65 (described in section 4.2.2) in the initial RNA-seq event in 2012 led to only two replicates undergoing RNA-seq analysis.

The four treatments presented in Table 4-2 were conducted on different days and at two different locations. The UV-B and MeJA treatments took place at the University of Glasgow, while slug and *Plutella* herbivory treatments were carried out at the John Innes Centre's Entomology department. Separate untreated controls were harvested alongside the UV-B and MeJA samples, while the two invertebrates shared the same untreated controls, on account of these assays being conducted on the same day. As a result, three separate untreated controls underwent RNA-seq with their respective treated samples. For the latter two replicates from 2014, as all treatments in each replicate were conducted at the same time, only one untreated control for each replicate underwent RNA-seq analysis.

The annotated Arabidopsis genome was used to assign gene functions to putative *B. napus* homologues, which facilitated analysis of the RNA-seq data. In both cases, reads were aligned to either the Unigene or the *B. napus* genome using TopHat v 2.0.12 and differential expression analysis was achieved with Cufflinks software, v 2.2.1 (Trapnell et al., 2012).

Treatment	Details of Treatment	Time Point for RNA-seq	No. of Replicates
UV-B Radiation	Continuous irradiation with 3 μmol m^{-2} s^{-1} broadband UV-B	T=4	1
Slug Herbivory	1-hour herbivory period.	T=2	1
***Plutella* Herbivory**	1-hour herbivory period.	T=2	1
MeJA	Exogenous application of 100 μM MeJA (0.01% EtOH/UN65) on whole plant with spray bottle (~ 5mL/plant).	T=4	1
Untreated Control	Continuous irradiation with white light (-UV-B, -MeJA, - invertebrate herbivory)	T=4 (Individual control for UV-B) T=2 (Shared control for slug and *Plutella* herbivory) T=4 (Individual control for MeJA)	1 replicate of each of the three untreated controls

Table 4-2. Details of the samples, treatment conditions and replicates sent for RNA-seq in 2012 and aligned to the Brassica 95K Unigene. Treatments described lasted for 24 hours, with leaf tissue samples from individual plants harvested at regular time points. The time point selected for RNA-seq analysis is indicated, and the use of three individual untreated controls for given samples is indicated. No. of replicates refers to the number of biological replicates subjected to RNA-seq analysis.

As already mentioned in this chapter, the main aim of the transcriptomic analysis was to identify early-induced transcription factors commonly up-regulated by at least 2-fold in any of the treatments, one of them preferably being UV-B radiation, the other(s) being invertebrate herbivores. It was hypothesised that identification of these transcription factors would reveal biological pathways potentially important in mediating UV-B-induced defence in *B. napus*.

The forthcoming section of this chapter briefly discusses the findings from the initial RNA-seq analysis, along with the identification of several *B. napus* genes thought to encode proteins involved in mediating UV-B-induced defence. Section 4.5 focuses on the second read alignment against the *B. napus* genome, with more detailed analysis on the commonalities between the various treatments provided. Similarities and differences in the results obtained from each alignment are discussed thereafter.

Treatment	Details of Treatment	RNA-seq Time Point	No. of Replicates
UV-B Radiation	Continuous irradiation with 3 μmol m^{-2} s^{-1} broadband UV-B	T=4	2
Slug Herbivory	1-hour herbivory period.	T=2	2
***Plutella* Herbivory**	1-hour herbivory period.	T=2	2
MeJA	Exogenous application of 100 μM MeJA (0.01% EtOH/UN65) on whole plant with spray bottle (~ 5mL/plant).	T=4	2
0.01% EtOH / UN65	Exogenous application of 0.01% EtOH/UN65 on whole plant with spray bottle (~ 5mL/plant).	T=4	2
Untreated Control	Continuous irradiation with white light (-UV-B, -MeJA, - invertebrate herbivory)	T=4	2

Table 4-3. Details of the samples, treatment conditions and replicates sent for RNA-seq in 2014 and aligned to the *B. napus* genome. Treatments described lasted for 24 hours, with leaf tissue samples from individual plants harvested at regular time points. The time point selected for RNA-seq analysis is indicated, and the use of three individual untreated controls for given samples is indicated. No. of replicates refers to the number of biological replicates subjected to RNA-seq analysis.

4.4 Initial alignments with the Brassica 95K Unigene

4.4.1 Setting appropriate cut-offs in the dataset

To allow easier interpretation of the results obtained from the RNA-seq event, cut-off parameters were implemented on the datasets to eliminate transcripts that do not appear responsive to the treatments. This was achieved by targeting two aspects of the data:

- The RPKM (Reads Per Kilobase per Million) values
- The fold change (FC) in transcript expression

The RPKM values are commonly used in RNA-seq to normalise data, which is of course an approximate number or 'count' of the abundance of target transcripts in the samples. RPKM removes technical biases that are common in sequencing on account of the varying lengths of transcripts and the depth of sequencing across different runs. For instance, longer transcripts are likely to have more sequences mapped to them, and therefore a higher 'count' than smaller transcripts. By taking into account the length of the transcripts,

the RPKM effectively provides a more accurate indication of the abundance of transcripts in each sample. In addition to the RPKM, a minimum FC in expression of the transcripts was imposed, to aid in identifying those that were either up-regulated or down-regulated in response to the treatments. To establish suitable numerical cut-off points for each of the filters, several datasets were generated, each containing lists of genes meeting various RPKM and FC criteria. The importance of selecting suitable cut-off points was to ensure that a reasonable number of genes meeting the criteria could progress for further analysis: applying too stringent a cut-off would reduce the number of genes available for further investigation, while establishing overly lenient filters would lead to a large list of genes that may not actually be important in UV-B-mediated defence pathways. Three minimum RPKM values were chosen for this purpose, 3, 4 and 5, while two minimum FC values were selected, 1.5 and 2. The number of Unigenes that met the imposed criteria in each treatment are listed in Table 4-4. Transcripts possessing an RPKM and FC value that met the stated criteria in at least one sample were retained for further study. Those found to be similarly regulated by 2 or more treatments (either up- or down-regulated) were identified as being commonly regulated transcripts, while those that met the imposed criteria in a single sample were classed as being differentially regulated by one stimulus.

	RPKM ≥ 3 1.5 FC	RPKM ≥ 3 2 FC	RPKM ≥ 4 1.5 FC	RPKM ≥ 4 2 FC	RPKM ≥ 5 1.5 FC	RPKM ≥ 5 2 FC
UV-B	9011	4612	4862	2055	4109	1770
Slug	9833	5613	4876	2346	4173	1987
Plutella	9432	5261	4632	2100	3925	1768
MeJA	8644	4488	5595	2465	4888	2125

Table 4-4: Number of transcripts differentially regulated by each treatment meeting the stated RPKM and FC cut-off criteria. All transcripts found to increase or decrease in expression in response to each treatment within the imposed RPKM and FC filters are listed. RPKM: Reads per Kilobase per Million, FC: Fold Change.

Understandably, the number of Unigenes differentially regulated by each treatment decreases as the stringency in the cut-off filters are increased (Table 4-4). To select the suitable cut-off parameters for the dataset, the extent of overlap between the Unigenes differentially up-regulated (Figure 4-4) and down-regulated (Figure 4-5) by the four treatments was examined using Venn diagrams. For simplicity, the overlap in Unigenes with an RPKM ≥ 4 has been omitted from this report, and only those with a minimum RPKM of 3 or 5 are discussed.

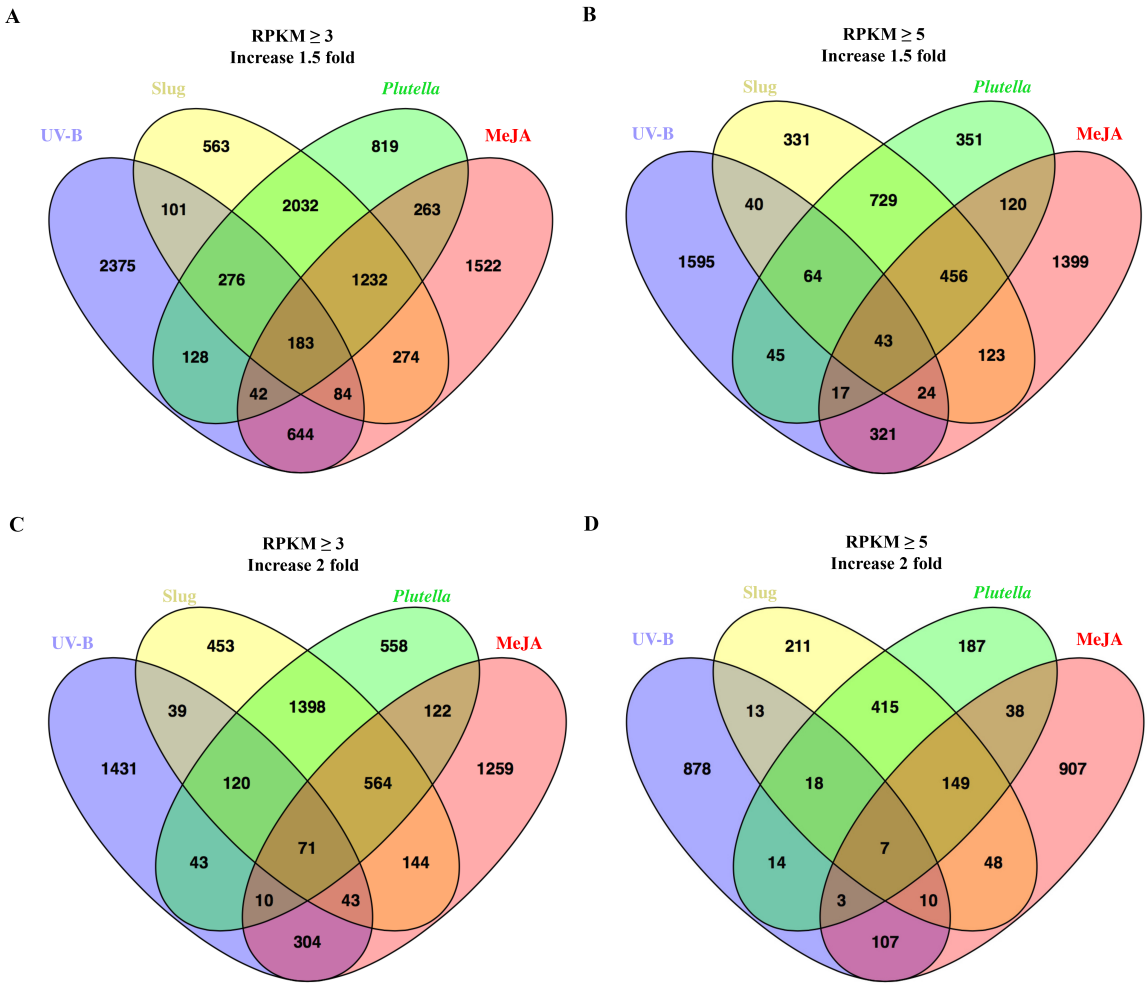

Figure 4-4: The number of Unigenes differentially up-regulated by four treatments with varying minimum RPKM and FC cut-off points. The degree of overlap between Unigenes that are up-regulated by **A** and **B,** 1.5 fold or **C** and **D,** 2 fold, with RPKM values of **A** and **C,** ≥ 3 or **B** and **D**, ≥ 5 following exposure to UV-B radiation, slug herbivory, *Plutella* herbivory or exogenous MeJA application. RPKM: Reads per Kilobase per Million, FC: Fold Change.

As expected, there is a considerable fluctuation in the number of transcripts commonly regulated by several stimuli when different cut-off criteria are imposed on the data. A total of 10,538 Unigenes with an RPKM ≥ 3 and a FC of at least 1.5 are identified in Figure 4-4A, while 5,658 Unigenes are isolated when the RPKM value is increased to ≥ 5 (Figure 4-4B), a 46.3% reduction in the number of Unigenes in Figure 4-4A. Increasing the FC cut-off inevitably decreases the number of identifiable Unigenes further, with 6,559 found in Figure 4-4C, and 3,005 when an RPKM minimum value of 5 is applied (Figure 4-4D).

To further assess the suitability of each cut-off, the number of Unigenes commonly regulated by 2 or more treatments was taken into consideration. 5,259 Unigenes with an RPKM ≥ 3 and a FC ≥1.5 were identified as being similarly responsive to several stimuli (Figure 4-4A), while a lower number of 1,982 were present when the RPKM is increased

to a minimum of 5 (Figure 4-4B). 2,858 Unigenes increased in expression in response to two or more stimuli with an RPKM ≥ 3 and a FC of ≥ 2 (Figure 4-4C), but this number was reduced to 822 when the RPKM was raised to ≥ 5 (Figure 4-4D).

The extent of overlap in transcripts that decreased in expression across treatments was investigated (Figure 4-5), however as the overall aim of this transcriptomic study was to identify genes commonly up-regulated by UV-B, herbivory and MeJA, those that are down-regulated will only be touched upon briefly. A total of 11,866 Unigenes with an RPKM ≥ 3 and an FC ≥ 1.5 are identified as decreasing in expression (Figure 4-5A), with 5,259 of these being commonly regulated by at least 2 of the administered treatments. A relatively substantial number of these Unigenes are commonly regulated by all four treatments (212), which is slightly more than the number commonly up-regulated by all treatments in Figure 4-4A. Adjustment of the minimum RPKM value reduces the number of differentially expressed Unigenes by approximately 50%, and the number of commonly regulated transcripts by ~56% to 5,259 and 2, 286, respectively (Figure 4-5B). As seen in Figure 4-4, increasing the stringency of the minimum FC value also decreases the number of transcripts identified as differentially regulated, with 6,623 and 2,535 present in Figures 4-5C and D, respectively. For both Unigene lists with a FC ≥ 2 and a minimum RPKM of 3 or 5, the number of Unigenes commonly down-regulated by at least 2 stimuli is approximately 36.6% of the total number of differentially regulated genes (2,425 and 929, respectively).

Based on the reasonable number of Unigenes meeting the imposed criteria, the two cut-offs implementing a FC ≥ 2 were considered appropriate for this dataset, with the minimum RPKM value of 3 later selected as the final filtering parameter to prevent exclusion of potentially interesting genes that are not identified with the more stringent RPKM cut-off.

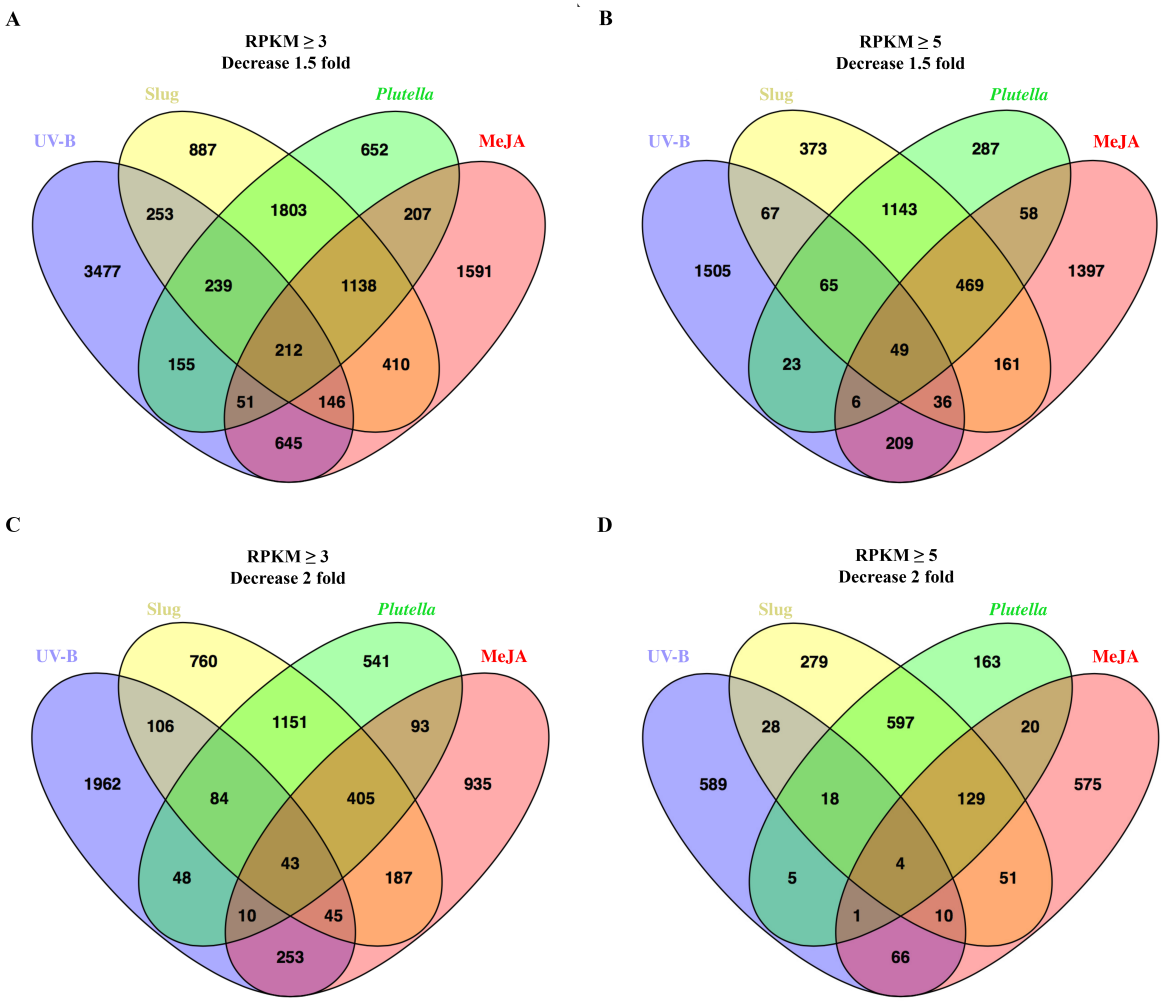

Figure 4-5: The number of Unigenes differentially down-regulated by four treatments with varying minimum RPKM and FC cut-off points. The degree of overlap between Unigenes that are down-regulated by **A** and **B,** 1.5 fold or **C** and **D**, 2 fold with RPKM values of **A** and **C**, ≥ 3 or **B** and **D**, ≥ 5 following exposure to UV-B radiation, slug herbivory, *Plutella* herbivory or exogenous MeJA application. RPKM: Reads per Kilobase per Million, FC: Fold Change.

4.4.2 Unigenes commonly up-regulated by UV-B, MeJA or invertebrate herbivory

Functional analysis of the transcripts possessing a minimum RPKM of 3 and FC of 2 in at least 2 of the treatments was investigated using the online bioinformatics resource, DAVID (Huang et al., 2009), where annotation clusters detailing enriched gene ontology (GO) terms was obtained. As DAVID was unable to compute the Brassica Unigene IDs, those of the putative Arabidopsis homologues were used instead. While this was effective at providing basic insight into the potential gene clusters differentially regulated by several treatments in *B. napus*, it failed to analyse those genes that do not possess an Arabidopsis homologue. Therefore, it should be brought to the readers' attention that Unigenes not

found to have an Arabidopsis homologue or are perhaps unique to other members of the Brassicaceae family have been overlooked in this analysis.

Approximately 47% of the 2,858 Unigenes possess a putative Arabidopsis homologue. These genes were grouped into GO terms based on their known functions in Arabidopsis, and each GO term was grouped into annotation clusters. On account of the redundant nature of the majority of encoded gene products, many genes are found in more than one GO term, as they may have multiple roles in the plant. Enrichment scores were allocated to each annotation cluster to highlight the extent of regulation of a set of genes following exposure to the various treatments, by relating the number of genes within this functional annotation cluster to their abundance in the Arabidopsis genome. The accuracy of this calculation for each GO term in DAVID is indicated by *p*-values.

A total of 45 annotation clusters possessing GO terms with $p \leq 0.05$ were identified (Appendix 1), of which the top 10 enriched annotation clusters are presented in Table 4-5. The most enriched annotation cluster contains GO terms and genes associated with the cell wall, such as xylem cysteine peptidase, tubulin beta chain 3 and several beta galactosidase. Other GO terms represented in Table 4-5 include those associated with defence responses (annotation cluster 5), hormone biosynthesis (annotation cluster 6) and abiotic stress (annotation cluster 8).

Examination of the remaining 35 annotation clusters in Appendix 1 identified enriched GO terms related to the biosynthesis and metabolism of glucosinolates and indole derivatives (cluster 25), oxylipins and JA (annotation cluster 15), and L-ascorbic acid (cluster 36). No GO terms linked to transcriptional regulation were identified in these annotation clusters, despite the presence of approximately 76 transcription factor-encoding genes in this list.

From the list of Unigenes with a minimum FC of 2 and RPKM ≥ 3 across 2 or more treatments, two were identified as interesting candidates for over-expression in Arabidopsis (chapter 6). These Unigenes, or to be more precise, their putative Arabidopsis orthologues, were selected based on their responsiveness to UV-B, MeJA or invertebrate herbivory, along with previous studies acknowledging the biological pathways that the encoded gene products or close family members are typically found in as potentially intrinsic to plant defence against invertebrate pests.

Annotation Cluster 1	Enrichment Score: 8.82	Count	PValue	FDR
GOTERM_CC_FAT	GO:0005618~cell wall	77	5.62E-11	7.20E-08
GOTERM_CC_FAT	GO:0030312~external encapsulating structure	77	1.14E-10	1.46E-07
GOTERM_CC_FAT	GO:0009505~plant-type cell wall	38	5.33E-07	6.83E-04
Annotation Cluster 2	**Enrichment Score: 5.32**	**Count**	**PValue**	**FDR**
GOTERM_BP_FAT	GO:0009628~response to abiotic stimulus	113	5.15E-08	8.46E-05
GOTERM_BP_FAT	GO:0006970~response to osmotic stress	45	1.66E-05	2.73E-02
GOTERM_BP_FAT	GO:0009651~response to salt stress	40	1.25E-04	2.05E-01
Annotation Cluster 3	**Enrichment Score: 4.80**	**Count**	**PValue**	**FDR**
GOTERM_BP_FAT	GO:0016053~organic acid biosynthetic process	53	2.99E-08	4.92E-05
GOTERM_BP_FAT	GO:0046394~carboxylic acid biosynthetic process	53	2.99E-08	4.92E-05
GOTERM_BP_FAT	GO:0006633~fatty acid biosynthetic process	23	8.90E-05	1.46E-01
GOTERM_BP_FAT	GO:0006631~fatty acid metabolic process	25	1.06E-03	1.73E+00
GOTERM_BP_FAT	GO:0008610~lipid biosynthetic process	36	1.19E-02	1.78E+01
Annotation Cluster 4	**Enrichment Score: 4.68**	**Count**	**PValue**	**FDR**
GOTERM_MF_FAT	GO:0004674~protein serine/threonine kinase activity	95	2.53E-07	3.83E-04
GOTERM_BP_FAT	GO:0006468~protein amino acid phosphorylation	99	8.40E-07	1.38E-03
GOTERM_BP_FAT	GO:0006796~phosphate metabolic process	112	2.04E-06	3.35E-03
GOTERM_BP_FAT	GO:0006793~phosphorus metabolic process	112	2.14E-06	3.52E-03
GOTERM_MF_FAT	GO:0004672~protein kinase activity	99	7.19E-06	1.09E-02
GOTERM_BP_FAT	GO:0016310~phosphorylation	103	7.56E-06	1.24E-02
GOTERM_MF_FAT	GO:0032559~adenyl ribonucleotide binding	181	1.49E-05	2.25E-02
GOTERM_MF_FAT	GO:0005524~ATP binding	177	3.54E-05	5.35E-02
GOTERM_MF_FAT	GO:0001882~nucleoside binding	188	6.11E-05	9.25E-02
GOTERM_MF_FAT	GO:0032555~purine ribonucleotide binding	193	6.93E-05	1.05E-01
GOTERM_MF_FAT	GO:0032553~ribonucleotide binding	193	6.93E-05	1.05E-01
GOTERM_MF_FAT	GO:0030554~adenyl nucleotide binding	187	7.12E-05	1.08E-01
GOTERM_MF_FAT	GO:0001883~purine nucleoside binding	187	7.12E-05	1.08E-01
GOTERM_MF_FAT	GO:0017076~purine nucleotide binding	199	2.87E-04	4.34E-01
GOTERM_MF_FAT	GO:0000166~nucleotide binding	221	6.28E-03	9.10E+00
Annotation Cluster 5	**Enrichment Score: 4.61**	**Count**	**PValue**	**FDR**
GOTERM_BP_FAT	GO:0009617~response to bacterium	37	1.15E-07	1.89E-04

GOTERM_BP_FAT	GO:0042742~defense response to bacterium	29	1.57E-06	2.58E-03
GOTERM_BP_FAT	GO:0006952~defense response	70	7.94E-02	7.43E+01
Annotation Cluster 6	**Enrichment Score: 4.36**	**Count**	**PValue**	**FDR**
GOTERM_BP_FAT	GO:0010033~response to organic substance	120	1.60E-10	2.62E-07
GOTERM_BP_FAT	GO:0009719~response to endogenous stimulus	102	1.37E-09	2.25E-06
GOTERM_BP_FAT	GO:0009725~response to hormone stimulus	82	2.62E-05	4.31E-02
GOTERM_BP_FAT	GO:0007242~intracellular signalling cascade	69	3.32E-04	5.43E-01
GOTERM_BP_FAT	GO:0009755~hormone-mediated signalling	43	4.33E-04	7.09E-01
GOTERM_BP_FAT	GO:0032870~cellular response to hormone stimulus	43	4.33E-04	7.09E-01
GOTERM_BP_FAT	GO:0009873~ethylene mediated signalling pathway	19	7.71E-03	1.19E+01
GOTERM_BP_FAT	GO:0000160~two-component signal transduction system (phosphorelay)	22	1.20E-02	1.80E+01
GOTERM_BP_FAT	GO:0009723~response to ethylene stimulus	24	1.92E-02	2.73E+01
Annotation Cluster 7	**Enrichment Score: 3.50**	**Count**	**PValue**	**FDR**
GOTERM_BP_FAT	GO:0018130~heterocycle biosynthetic process	20	1.56E-04	2.56E-01
GOTERM_BP_FAT	GO:0044271~nitrogen compound biosynthetic process	50	1.60E-04	2.62E-01
GOTERM_BP_FAT	GO:0009309~amine biosynthetic process	25	5.36E-04	8.76E-01
GOTERM_BP_FAT	GO:0008652~cellular amino acid biosynthetic process	23	7.22E-04	1.18E+00
Annotation Cluster 8	**Enrichment Score: 3.24**	**Count**	**PValue**	**FDR**
GOTERM_BP_FAT	GO:0009266~response to temperature stimulus	40	5.09E-05	8.35E-02
GOTERM_BP_FAT	GO:0009409~response to cold	29	1.33E-04	2.19E-01
GOTERM_BP_FAT	GO:0009408~response to heat	14	2.75E-02	3.68E+01
Annotation Cluster 9	**Enrichment Score: 3.11**	**Count**	**PValue**	**FDR**
GOTERM_MF_FAT	GO:0005529~sugar binding	19	2.25E-04	3.40E-01
GOTERM_MF_FAT	GO:0030246~carbohydrate binding	24	2.69E-03	4.00E+00
Annotation Cluster 10	**Enrichment Score: 2.88**	**Count**	**PValue**	**FDR**
GOTERM_CC_FAT	GO:0048046~apoplast	45	5.74E-06	7.35E-03

Table 4-5: Top 10 enriched annotation clusters of the putative Arabidopsis homologues of the Brassica Unigenes commonly up-regulated by at least two treatments with FC ≥ 2 and RPKM ≥ 3. 'Count' column refers to the number of Arabidopsis genes that are in each GO term. FDR = False Discovery Rate**.**

The first of the two genes is thought to encode *ELICITOR-ACTIVATED GENE 3/CINNAMYL-ALCOHOL DEHYDROGENASE 8* (*ELI3-2/CAD8*), an aromatic alcohol dehydrogenase present in the phenylpropanoid pathway (Figure 4-6) and thought to be involved in plant defence against hemi-biotrophic pathogens (Somssich et al., 1996) (Schmelzer et al., 1989). In the functional analysis, this gene was clustered under GO terms related to plant defence (such as "GO:0006952~defense response" and "GO:0006955~immune response" in annotation clusters 5 and 39, respectively) and secondary metabolite and aromatic compound biosynthesis (annotation cluster 27, Appendix 1). The second gene encodes a putative GDP-L-galactose phosphorylase, *VITAMIN C DEFECTIVE 2* (*VTC2*), that converts GDP-L-galactose to L-galactose-1-P, and catalyzes the first committed step in the biosynthesis of L-ascorbate (Urzica et al., 2012). Functional analysis of *VTC2* located the gene under GO terms associated with abiotic stress ("GO:0009266~response to temperature stimulus"), plant defence ("GO:0042742~defense response to bacterium" and "GO:0052482~cell wall thickening during defense response"), and, of course in the two GO terms indicative of L-ascorbic acid biosynthesis (annotation cluster 36, Appendix 1).

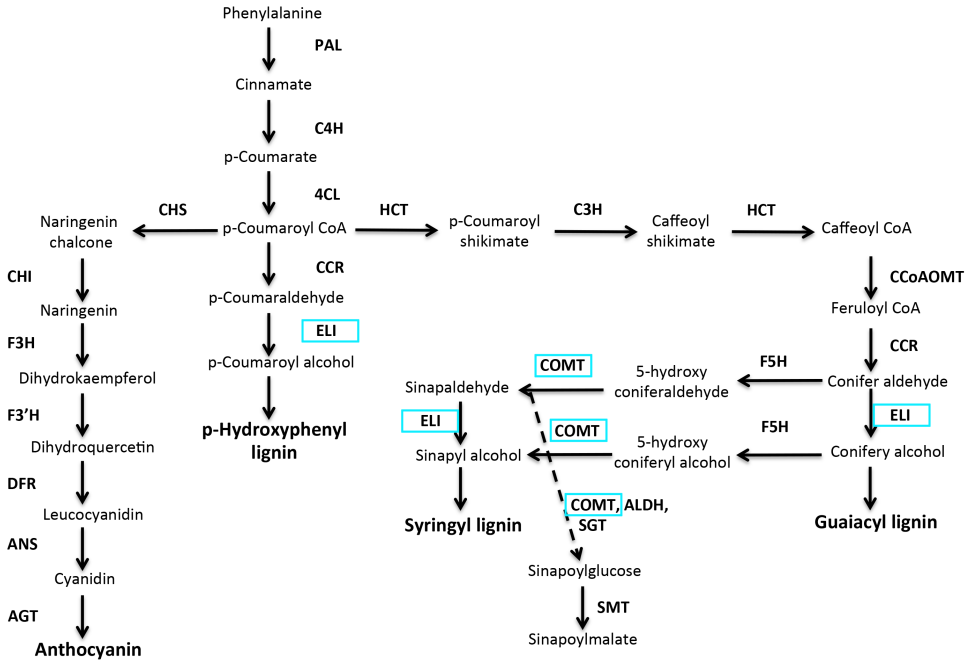

Figure 4-6: Schematic representation of the main steps, enzymes and compounds found in the phenylpropanoid pathway. The enzymes encoded by *ELI3-2, COMT1* or their related family members are highlighted in light blue boxes. Diagram adapted from (Peng et al., 2008) and (Demkura and Ballaré, 2012).

The log_2 fold change expression profiles of the Brassica Unigenes thought to encode *ELI3-2* or *VTC2* are shown in Figure 4-7. Inclusion of a light grey dotted line across the charts at '1' and '-1' indicates the minimum log_2 fold change cut-off that was imposed on the dataset. Three Unigenes putatively encode *ELI3-2*, however only one of them, EV141577, increases in expression by at least 2-fold (Figure 4-7A). This Unigene so happens to be similarly responsive to all four treatments examined. *VTC2* is thought to have 4 Brassica Unigene homologues, neither of which are regulated by the 4 treatments in a similar manner to EV141577 (Figure 4-7B). *Plutella* herbivory induces a decrease in expression of 50% of the Unigenes, while the other 2 are not significantly regulated by this invertebrate, at least not in relation to the cut-off parameters. MeJA is also found to induce an increase and a decrease in expression of some of these Unigenes, while UV-B and slug stimulate a significant increase and decrease in expression of EV165278, respectively. Despite the fluctuating expression profiles of these 4 Unigenes in response to the various treatments, *VTC2* was still selected for over-expression. This decision was based partly on previous studies indicating a possible influence of ascorbic acid on plant defence against pests, and also on sequence alignment analysis suggesting that the Unigene EX043301 shares more sequence similarity to the Arabidopsis *VTC2* gene. Expression of this particular Unigene increases in response to UV-B, slugs and *Plutella,* however only the two former treatments induce a significant increase in expression that is over 2-fold.

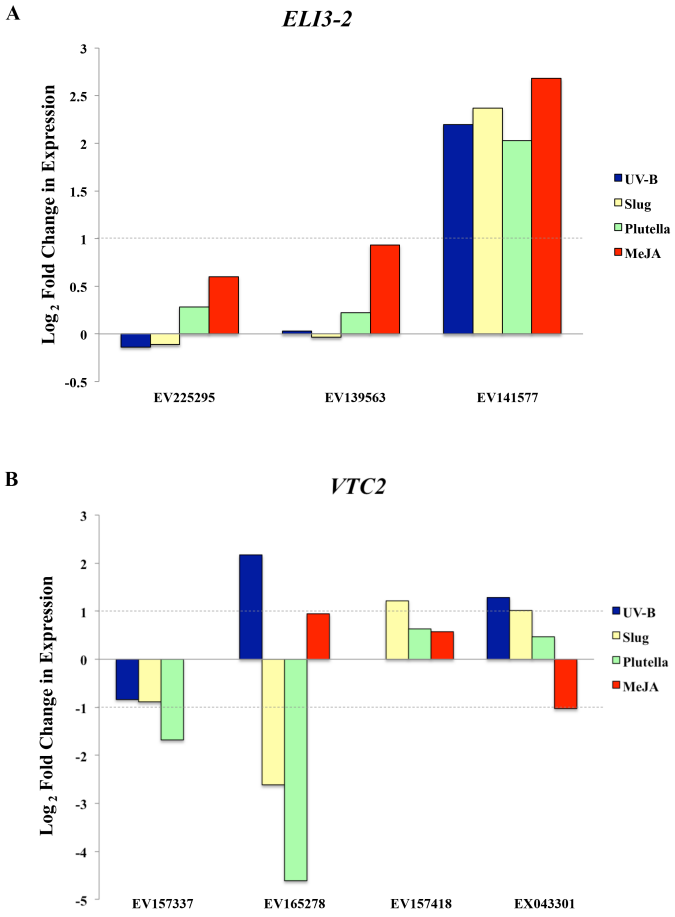

Figure 4-7: Log_2 fold change expression profiles of the putative Brassica Unigene homologues of *ELI3-2* and *VTC2*. A, expression profiles (log_2 FC) of the three Brassica Unigenes thought to be homologues of the Arabidopsis gene, *ELI3-2*, and **B** the 4 putative Unigene homologues of *VTC2*. The log_2FC has been displayed on the y-axis to allow for easy interpretation of the direction of gene regulation. Faint grey dotted lines at '1' and '-1' mark the minimum log_2FC cut-off values required to class a Unigene as differentially regulated by any of the treatments. As only one biological repeat is presented here, no error bars are shown.

In addition to these two genes, a third was also selected for over-expression in Arabidopsis, despite not being differentially expressed by any of the treatments in the RNA-seq analysis. *CAFFEATE O-METHYLTRANSFERASE 1* (*COMT1*) is a flavonol 3-methyltransferase also found in the phenylpropanoid pathway (Figure 4-6). Selection of this gene for over-expression in Arabidopsis was due to a recent study examining the extent of *B. cinerea* lesion area on an Arabidopsis mutant lacking functional F5H protein, which is active in the same branch of the phenylpropanoid pathway as COMT. This mutant was reported to be more susceptible to the necrotrophic fungus than WT Arabidopsis, both in the presence and absence of UV-B radiation (Demkura and Ballaré, 2012). Based on these results, *COMT1* was selected for over-expression *in planta*, to determine whether or not hyperactivation of this can enhance UV-B-mediated plant defence.

Over-expression of the *B. napus* homologues of these selected genes in Arabidopsis, along with genetic analysis of these lines and invertebrate bioassay results, will be discussed in chapter 6.

4.5 The second alignment with the *B. napus* genome

4.5.1 Applying appropriate cut-off parameters to the dataset

A second RNA-seq event took place in 2014, where the obtained reads were aligned against the recently sequenced *B. napus* genome (Chalhoub et al., 2014) along with the previous reads that were aligned to the Unigene. The results from this alignment also underwent a filtration process, where transcripts considered unresponsive or insufficiently responsive to all treatments were removed from the dataset. To achieve this, a series of numerical cut-offs were imposed on the datasets, targeting the FC in expression of each transcript, along with statistical *p*-values and false discovery rates (FDRs), the latter of which assesses the probability of the data generated for each gene being a false positive.

For the purposes of this study, a minimum RPKM value of 3 was required in at least one sample for a transcript to be retained for further investigation, regardless of the sample being a treated or untreated sample. This initial filtering event reduced the dataset substantially from 101,040 transcripts down to 37,401. Additional filters were subsequently enforced to help identify transcripts that are differentially expressed across the treatments. These filters included the application of a minimum FC, along with a maximum *p*-value and a maximum FDR. Two minimum FC values of 1.5 and 2 were imposed, alongside two *p*-values of 0.01 and 0.05. Three FDR values were also applied to the dataset, 0.1, 0.05 and a more stringent 0.01 (Table 4-6).

The difference in the number of genes differentially regulated when a fold change cut-off of 1.5 or 2 is applied is relatively small, with the most noticeable alteration in gene number occurring in the UV-B gene list, where an approximate 7% increase in the number of genes possessing a minimum fold change of 1.5 and an FDR of 0.1 is seen. As there is no large difference between the number of genes with at least a 1.5 or 2 fold change in expression across each treatment (when the same *p*- and FDR value conditions are examined), a 1.5 fold change was selected as a minimum cut-off.

	FC ≥ 1.5 $p \leq 0.05$ FDR ≤ 0.01	FC ≥ 1.5 $p \leq 0.05$ FDR ≤ 0.05	FC ≥ 1.5 $p \leq 0.05$ FDR ≤ 0.1	FC ≥ 2 $p \leq 0.05$ FDR ≤ 0.01	FC ≥ 2 $p \leq 0.05$ FDR ≤ 0.05	FC ≥ 2 $p \leq 0.05$ FDR ≤ 0.1
UV-B	**606**	**1556**	**2407**	**593**	**1497**	**2244**
Slug	**0**	**48**	**74**	**0**	**43**	**67**
Plutella	**0**	**0**	**26**	**0**	**0**	**26**
MeJA	**431**	**755**	**975**	**427**	**738**	**940**

Table 4-6: Number of genes differentially regulated by each treatment meeting the stated cut-off criteria. FC: Fold Change, p: P-value, FDR: False Discovery Rate. The gene lists comprise both up- and down-regulated genes.

Only one *p*-value cut-off (≤ 0.05) is presented in Table 4-6, as no difference in the number of genes differentially regulated with a $p \leq 0.01$ or ≤ 0.05 was seen (when compared to the same fold change and FDR criteria). As no difference in gene number was discovered, the higher *p*-value was mentioned as opposed to the more stringent value, to inform the reader that some genes with a *p*-value ≥ 0.01 (but ≤ 0.05) are included in the lists.

A relatively large difference in the number of transcripts possessing different FDR cut-offs is seen, especially for the slug and *Plutella* samples. Interestingly, no transcripts have an FDR of ≤ 0.01 following slug herbivory, or an FDR of ≤ 0.05 in response to *Plutella* herbivory. This suggests that variation may be present in the replicates for each of these treatments, subsequently increasing the chances of obtaining higher false positives compared to the UV-B and MeJA treatments. The reason for this finding is highly likely due to 'natural' variation obtained across replicates, where differences in invertebrate spatiotemporal feeding patterns over the 1-hour grazing window may have provoked dissimilar transcriptional responses in *B. napus* at the point of harvesting. As no transcripts with an FDR ≥ 0.01 were identified as being differentially expressed following slug or *Plutella* herbivory, this stringent FDR cut-off was not used to generate a transcript list for further analysis. Likewise, the next FDR filter of ≥ 0.05 was also dismissed, as no transcripts were found to be differentially regulated by *Plutella* when this cut-off was applied, and only a small number of transcripts were responsive to slug herbivory. Applying a minimum FDR cut-off of 1 still revealed a small number of differentially regulated transcripts in response to slug or *Plutella* herbivory (under 100 transcripts), therefore it was investigated if removal of an FDR cut-off would increase the number of transcripts meeting the remaining criteria. To this end, two lists were generated comprising transcripts differentially up-regulated or down-regulated by at least 1.5 fold with a *p*-value ≤ 0.05, and either an FDR value of ≤ 0.1 or no FDR limit (Table 4-7). As expected, a considerably higher number of transcripts across all treatments meet the

criteria when no FDR cut-off was applied, however as the main aim of the transcriptomics was to identify transcripts commonly regulated by UV-B and herbivory/MeJA treatment, it was important to determine the extent of overlap between the four treatments to conclude whether or not removal of an FDR cut-off facilitated data interpretation. Venn diagrams were therefore generated to visualise the overlap in commonly up-regulated or down-regulated transcripts across the treatments (Figure 4-8).

	FC ≥ 1.5; $p \leq 0.05$ FDR ≤ 0.1 Up-regulated	**FC ≥ 1.5; $p \leq 0.05$ FDR ≤ 0.1 Down-regulated**	**FC ≥ 1.5; $p \leq 0.05$ Up-regulated**	**FC ≥ 1.5; $p \leq 0.05$ Down-regulated**
UV-B	**1822**	**585**	**3651**	**1904**
Slug	**28**	**46**	**736**	**1301**
Plutella	**14**	**12**	**496**	**928**
MeJA	**905**	**70**	**2054**	**574**

Table 4-7: Number of genes differentially up-regulated or down-regulated by each treatment meeting the stated cut-off criteria. FC: Fold Change, p: P-value, FDR: False Discovery Rate.

Few transcripts were commonly regulated across multiple genes when an FDR cut-off of ≤ 0.1 was applied, and in many instances no commonalities occurred across treatments (Figure 4-8A and B). For the purposes of this study, five categories were of particular interest for studying transcriptomic overlaps between treatments:

- UV-B, slug, *Plutella* and MeJA
- UV-B, slug and *Plutella*
- UV-B and slug
- UV-B and *Plutella*
- Slug and *Plutella*.

Unfortunately, only three of these categories possessed common up-regulated or down-regulate transcripts, with the number of these transcripts being very low. When the FDR filter was removed, however, a higher number of transcripts were found to be similarly regulated by multiple treatments, particularly between UV-B and slug, UV-B and *Plutella*, slug and *Plutella*, and UV-B, slug and *Plutella* (Figure 4-8C and D). While these numbers are still relatively low (i.e. only 8 *B. napus* transcripts are commonly up-regulated by all four treatments), they are still higher than the number of transcripts available for analysis when an FDR cut-off was enforced. Transcripts identified in these lists include those encoding transcription factors and various known defence proteins, suggesting that

removal of the ≤ 0.1 FDR cut-off allows transcripts relevant to the study to be accessible for interpretation. It was therefore considered appropriate to remove the FDR cut-off, resulting in a final set of filtering measures comprising of a minimum fold change in expression of 1.5 and a maximum *p*-value of 0.05.

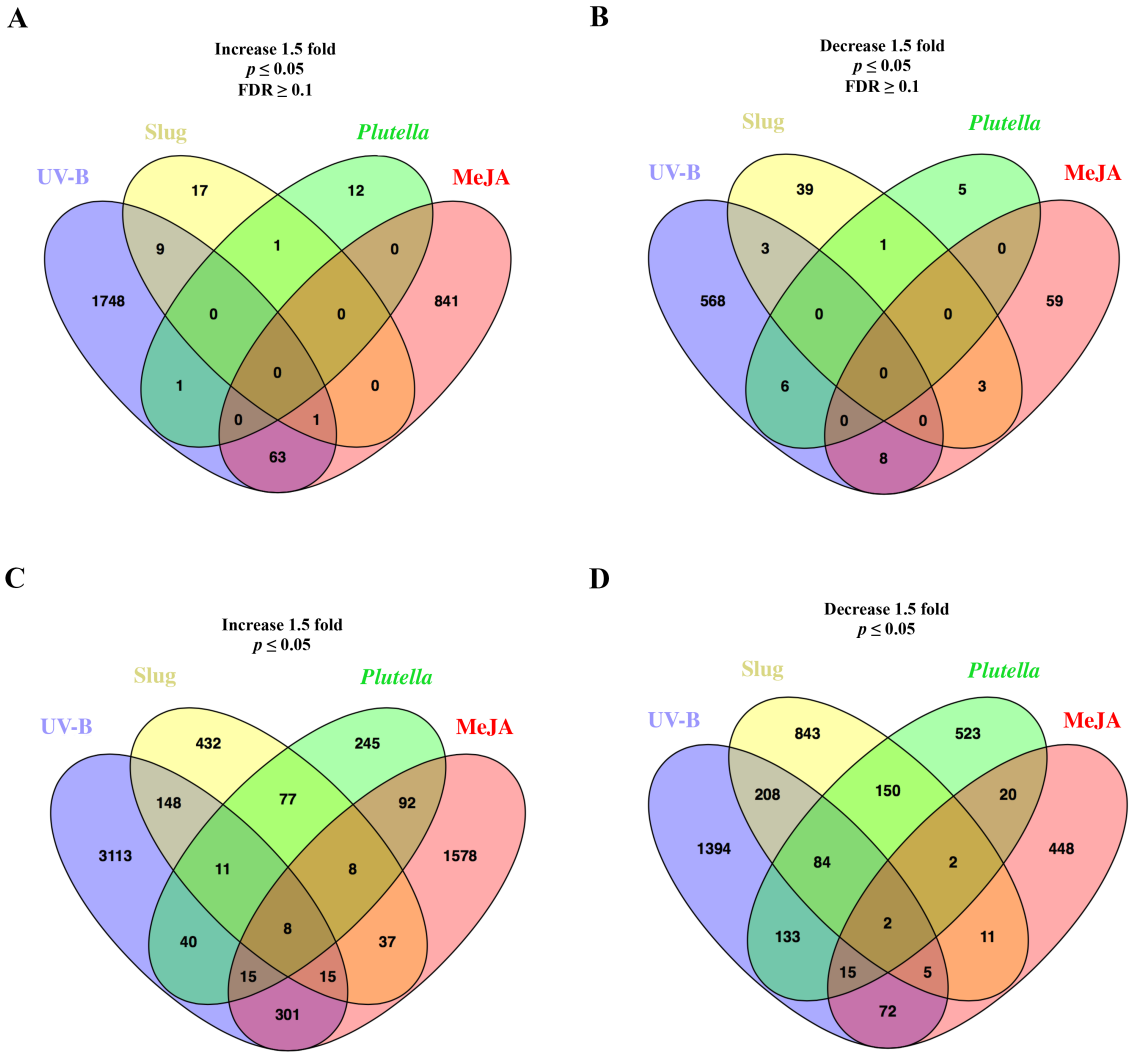

Figure 4-8. The number of *B. napus* genes differentially regulated by four individual treatments using two cut-off criterias. The degree of overlap between genes that are up-regulated, **A** and **C**, or down-regulated, **B** and **D**, by at least 1.5 fold with a *p*-value of up to 0.05 following exposure to UV-B radiation, slug herbivory, *Plutella* herbivory or exogenous MeJA application. An additional FDR cut-off of ≤ 0.1 is applied for **A** and **B,** but absent for **C** and **D**.

4.5.2 Genes up-regulated over multiple treatments

The wealth of information derived from transcriptomic analysis of any organism following exposure to stimuli is outstanding, and it is easy for the researcher to become so engrossed in the data that the overall aim of the project is forgotten. In this project, the effects of four individual treatments on the *B. napus* transcriptome were studied, however the main

objective was to identify the mechanisms behind UV-B-enhanced defence against *Plutella* and slugs. As a result, the primary focus was to identify the genetic overlaps between the following 5 treatment combinations:

1. UV-B, slug, *Plutella* and MeJA
2. UV-B, slug and *Plutella*
3. UV-B and slug
4. UV-B and *Plutella*
5. Slug and *Plutella*.

The fifth category on this list, 'slug and *Plutella*,' allowed the differences and similarities elicited in *B. napus* by these two invertebrates to be examined. As this is the first time, to our knowledge, that the effects of slug herbivory on a plant transcriptome has been studied, and also because the two pests appear to share a relatively small number of commonly regulated genes (Figure 4-8C and D), the extent of genetic overlap between the two pests in *B. napus* was studied in more detail.

As in the first alignment in section 4.4, functional analysis of the genes was achieved using DAVID (Huang et al., 2009) and the TAIR ID's of the putative Arabidopsis gene annotations of the *B. napus* genes.

4.5.3 Transcripts differentially regulated by UV-B, slug, *Plutella* and MeJA

The number of *B. napus* transcripts commonly regulated by all four treatments is relatively small (10 in total; 8 increasing in expression, 2 decreasing in expression; Figure 4-8C and D), and the roles the encoded gene products play in the plant, based on their putative Arabidopsis annotations, is diverse (Table 4-8). Functional analysis of the two lists using DAVID failed due to the small number of genes present (DAVID requires a minimum gene list of 10 units for performing functional annotation analysis)(Huang et al., 2009), and the presence of one *B. napus* transcript not possessing a putative Arabidopsis homologue prevented the input of 10 genes into the software, to gain at least some insight into the categories of genes differentially expressed by all treatments. Therefore, the transcripts differentially regulated by all 4 treatments will briefly be discussed here.

B. napus Gene ID	Putative Arabidopsis Gene ID	Arabidopsis Gene Name / Function	UV-B FC	Slug FC	*Plut.* FC	MeJA FC
BnaC09g51700D	AT1G43710 *EMB1075*	Pyridoxal phosphate (PLP)-dependent transferases superfamily protein	2.87	4.35	3.45	9.42
BnaA07g21340D	AT1G76520	Auxin efflux carrier family protein	2.52	1.87	2.69	2.80
BnaA07g38390D	AT1G78820	D-mannose binding lectin protein with Apple-like carbohydrate-binding domain	4.64	3.21	2.47	2.66
BnaAnng07910D	AT3G30775 *ERD5, PRODH, AT-POX*	Methylenetetrahydrofolate reductase family protein (proline dehydrogenase)	7.51	5.55	2.42	6.33
BnaA06g39660D	AT3G30775 *ERD5, PRODH, AT-POX*	Methylenetetrahydrofolate reductase family protein (proline dehydrogenase)	9.29	5.63	3.77	4.91
BnaC07g26120D	AT3G30775 *ERD5, PRODH, AT-POX*	Methylenetetrahydrofolate reductase family protein (proline dehydrogenase)	14.20	5.90	3.27	4.55
BnaA02g01840D	AT5G13740 *ZIF1*	zinc induced facilitator 1	2.73	1.94	2.15	2.89
BnaC03g15270D	AT5G53050	alpha/beta-Hydrolases superfamily protein	7.75	2.70	2.51	1.95
BnaC01g41460D	AT4G11650 *OSM34*	osmotin 34	0.06	0.27	0.06	0.31
BnaC03g33270D	Unknown	Unknown	0.02	0.16	0.19	0.25

Table 4-8. *B. napus* genes differentially regulated by UV-B, slug herbivory, *Plutella* herbivory and MeJA. The first 8 genes listed are up-regulated in response to all 4 treatments, while the latter two are down-regulated. FC (fold change) ≥ 1.5, $p \leq 0.05$.

Out of the 8 *B. napus* transcripts found to increase in expression, three potentially encode the same or similar gene products to the Arabidopsis proline dehydrogenase, *EARLY RESPONSE TO DEHYDRATION 5* (*ERD5*), an osmotic stress-responsive gene involved in the conversion of proline to glutamic acid via Δ^1-pyrroline-5-carboxylate (P5C)(Kiyosue et al., 1996). These three transcripts undoubtedly undergo the highest fold change in expression out of all 8 listed in response to UV-B radiation or slug herbivory, and, with the exception of BnaC09g51700D, in response to MeJA. Additional transcripts found in Table 4-8 include *EMBRYO DEFECTIVE 1075* (*EMB1075*), which encodes a serine carboxylase implicated in growth and development (Tzafrir et al., 2004) and the zinc inducer facilitator,

ZIF1, a member of the major facilitator superfamily (MFS) of membrane proteins. The auxin efflux carrier and the alpha/beta-hydrolase have previously been reported as JA-responsive genes (Dombrecht et al., 2007, Hasegawa et al., 2011). Of the two transcripts that are down-regulated by all four treatments, only one of them has an Arabidopsis homologue (AT4G11650, *OSM34*). This gene encodes an osmotin-like protein that is responsive to many developmental, environmental hormonal and microbial cues.

4.5.4 UV-B, slug and *Plutella*

Eleven *B. napus* transcripts were found to be up-regulated by UV-B radiation, slug or *Plutella* herbivory (Figure 4-8C). While this is again a small number of transcripts, functional analysis on DAVID was achievable, on account of $n \geq 10$ (n representing the number of transcripts). The *B. napus* transcripts, and their putative Arabidopsis homologues with associated gene functions, are listed in Table 4-9.

B. napus ID	Arabidopsis ID	Gene Name	Gene Function
BnaA01g15350D	AT4G26150	*CGA1, GATA22, GNL*	cytokinin-responsive gata factor 1
BnaA09g26310D	AT1G30250		Unknown protein
BnaA10g25850D	AT5G04340	*C2H2, CZF2, ZAT6*	zinc finger of Arabidopsis thaliana 6
BnaC02g38230D	AT3G30775	*ERD5, PRODH, AT-POX*	Methylenetetrahydrofolate reductase family protein
BnaC03g50570D	AT5G63790	*ANAC102, NAC102*	NAC domain containing protein 102
BnaC04g24950D	AT3G56360		Unknown protein
BnaC04g56750D	AT2G40000	*HSPRO2, ATHSPRO2*	ortholog of sugar beet HS1 PRO-1 2
BnaC06g40170D	AT1G80840	*WRKY40*	WRKY DNA-binding protein 40
BnaC07g16750D	AT5G66470		RNA binding;GTP binding
BnaC07g28950D	AT5G25930		Protein kinase family protein with leucine-rich repeat domain
BnaC07g30000D	AT5G24420	*PGL5*	6-phosphogluconolactonase 5

Table 4-9: The 11 *B. napus* genes and putative Arabidopsis homologues up-regulated by UV-B radiation, slug herbivory or *Plutella* herbivory. FC ≥ 1.5, $p \leq 0.05$.

Functional annotation clustering in DAVID identified a single cluster with five GO terms, 2 of which possess a *p*-value of 0.05 or below (Table 4-10). On account of only 1 annotation cluster being identified in this analysis, and all GO terms being functionally related to one another, all GO terms have been retained on this occasion, regardless of their *p*-value.

The five GO clusters all appear to be involved in transcriptional processes, and analysis of the genes included in each GO term revealed that only 4 of the 11 Arabidopsis genes in Table 4-9 were successfully clustered into functional categories on DAVID (Table 4-10).

***B. napus* ID**	**Arabidopsis ID**	**Gene Function**	**GO:0003700~transcription factor activity**	**GO:0030528~transcription regulator activity**	**GO:0003677~DNA binding**	**GO:0006350~transcription**	**GO:0045449~regulation of transcription**
BnaC06g40170D	**AT1G80840** *WRKY40*	WRKY DNA-binding protein 40					
BnaA01g15350D	**AT4G26150** *CGA1, GATA22, GNL*	cytokinin-responsive gata factor 1					
BnaC03g50570D	**AT5G63790** *ANAC102, NAC102*	NAC domain containing protein 102					
BnaA10g25850D	**AT5G04340** *C2H2, CZF2, ZAT6*	zinc finger of Arabidopsis thaliana 6					

Table 4-10: GO categories enriched in the list of Arabidopsis ID's with sequence similarity to the *B. napus* transcripts up-regulated by UV-B, slug and *Plutella*. The Arabidopsis gene name and function is provided, and the GO categories that each gene is present in is highlight with a blue box.

4.5.4.1 Four putative transcription factors are up-regulated in response to UV-B radiation, slug herbivory or *Plutella* herbivory

As the aim of the project was to identify early-induced transcription factors that are responsive to both UV-B and herbivory, and as no enriched GO terms related to such transcription factors were identified in the first alignment, the presence of 4 transcription factors out of 11 transcripts in this instance was promising. These transcription factors include the pathogen-induced *WRKY40, CGA1,* which encodes a GATA transcription factor, a zinc finger protein transcription factor, *ZAT6*, and a NAC-encoding gene, *ANAC102.*

4.5.5 UV-B and slug herbivory

UV-B radiation and slug herbivory commonly up-regulate 148 *B. napus* transcripts (Figure 4-8C), one of which has no Arabidopsis annotations. The 147 transcripts that do possess Arabidopsis annotations show sequence similarity to 109 Arabidopsis genes. After conducting GO analysis on the gene list, and isolating only those terms with $p \leq 0.05$, a total of 6 annotation clusters and 16 GO terms were uncovered (Table 4-11).

Annotation cluster 4 possesses two GO terms related to transcriptional regulators ("GO:0006355 ~ regulation of transcription, DNA-dependent" and "GO:0051252 ~ regulation of RNA metabolic"), with the same genes found in both functional groups (Table 4-12).

4.5.5.1 Transcription factors up-regulated by UV-B and slug herbivory

Out of the 147 *B. napus* transcripts with known sequence similarity to Arabidopsis genes, 6.8% encode transcription factors. The transcript proposed to encode the cytokinin-responsive GATA transcription factor, CGA1 (section 4.5.4.1), appears in this list again, suggesting that homologues of this protein are responsive to UV-B and herbivory. In addition, two BTB and TAZ domain-encoding genes, *BT1* and *BT5*, are identified as being responsive to these treatments, along with the JA/ET-responsive gene, *ETHYLENE RESPONSE FACTOR 104* (*ERF104*), which encodes a member of the AP2/ERF transcription factor family (Lorenzo et al., 2004).

Annotation Cluster 1	Enrichment Score: 1.79	%	PValue	FDR
GOTERM_MF_FAT	GO:0031406~carboxylic acid binding	3.67	0.01	12.61
GOTERM_MF_FAT	GO:0016597~amino acid binding	2.75	0.02	20.54
GOTERM_MF_FAT	GO:0043176~amine binding	2.75	0.02	21.35
Annotation Cluster 2	Enrichment Score: 1.66	%	PValue	FDR
GOTERM_BP_FAT	GO:0010200~response to chitin	3.67	0.01	15.03
GOTERM_BP_FAT	GO:0009743~response to carbohydrate stimulus	3.67	0.04	41.17
Annotation Cluster 3	Enrichment Score: 1.39			
GOTERM_CC_FAT	GO:0009507~chloroplast	18.35	0.04	32.52
GOTERM_CC_FAT	GO:0009536~plastid	18.35	0.04	38.04
Annotation Cluster 4	Enrichment Score: 1.32	%	PValue	FDR
GOTERM_BP_FAT	GO:0010033~response to organic substance	12.84	0.00	0.45
GOTERM_BP_FAT	GO:0009719~response to endogenous stimulus	10.09	0.00	4.15
GOTERM_BP_FAT	GO:0006355~regulation of transcription, DNA-dependent	9.17	0.02	23.38
GOTERM_BP_FAT	GO:0009725~response to hormone stimulus	8.26	0.02	23.53
GOTERM_BP_FAT	GO:0051252~regulation of RNA metabolic process	9.17	0.02	24.05
GOTERM_MF_FAT	GO:0046983~protein dimerization activity	4.59	0.04	35.38
Annotation Cluster 5	Enrichment Score: 1.18	%	PValue	FDR
GOTERM_MF_FAT	GO:0008270~zinc ion binding	14.68	0.01	15.35
Annotation Cluster 6	Enrichment Score: 0.82	%	PValue	FDR
GOTERM_MF_FAT	GO:0030246~carbohydrate binding	4.59	0.02	23.02
GOTERM_MF_FAT	GO:0005529~sugar binding	3.67	0.02	24.63

Table 4-11: Annotation clusters and grouped GO categories enriched in the list of Arabidopsis ID's with sequence similarity to the *B. napus* transcripts up-regulated by UV-B and slug.

Arabidopsis ID	*B. napus* ID	Gene Name	Gene Function
AT1G25560	BnaC05g20560D	TEM1, EDF1	AP2/B3 transcription factor family protein
AT4G01120	BnaA09g00170D	GBF2, ATBZIP54	G-box binding factor 2
AT4G14540	BnaA03g33970D	NF-YB3	nuclear factor Y, subunit B3
AT4G26150	BnaC01g18190D	CGA1, GATA22,	cytokinin-responsive gata factor 1
AT4G37610	BnaC07g46630D	BT5	BTB and TAZ domain protein 5
AT5G28770	BnaC07g27440D	BZO2H3	bZIP transcription factor family protein
AT5G49450	BnaA06g29500D	AtbZIP1, bZIP1	basic leucine-zipper 1
AT5G51190	BnaC09g27360D		Integrase-type DNA-binding family protein
AT5G61600	BnaC07g31350D	ERF104	ethylene response factor 104
AT5G63160	BnaA06g22570D	BT1	BTB and TAZ domain protein 1

Table 4-12: The ten genes commonly up-regulated by UV-B and slug herbivory that fall into the GO term, "GO:0006355~regulation of transcription, DNA-dependent," in annotation cluster 4 of Table 4-11.

4.5.6 UV-B and *Plutella* herbivory

A total of 40 *B. napus* transcripts appear to be UV-B- and *Plutella*-responsive, all of which have assigned Arabidopsis annotations (Table 4-13). Within this list are putative transcription factors and genes known to be wound-responsive (e.g. *VSP2*). Seven annotation clusters possessing GO terms with $p \leq 0.05$ are presented in Table 4-14. Annotation cluster 1 contains eight GO terms related to transcriptional processes with an enrichment score of 3.88. Fourteen Arabidopsis genes are found in these GO terms, some of which belong to transcription factor families already identified in the analysis (i.e. *NAC, ERF* and *WRKY*). Interestingly, some of these transcription factors have been shown to be responsive to *B.cinerea* and aphid herbivory, such as *WRKY33* (Zheng et al., 2006) and *ZAT10* (Kuśnierczyk et al., 2011).

B. napus ID	Arabidopsis ID	Gene Name	Gene Function
BnaC05g00910D	AT1G01010	ANAC001	NAC domain containing protein 1
BnaA08g18790D	AT1G27730	STZ, ZAT10	salt tolerance zinc finger
BnaA08g18380D BnaCnng63180D	AT1G28370	ERF11	ERF domain protein 11
BnaC08g02910D	AT1G49450		Transducin/WD40 repeat-like superfamily protein
BnaC06g05920D BnaC06g05910D	AT1G52890	ANAC019	NAC domain containing protein 19
BnaC09g14610D	AT1G60590		Pectin lyase-like superfamily protein
BnaC01g29930D BnaA01g36280D	AT1G61800	GPT2	glucose-6-phosphate/phosphate translocator 2
BnaC06g23560D	AT1G73480		alpha/beta-Hydrolases superfamily protein
BnaAnng23990D BnaC02g26030D	AT1G80840	WRKY40	WRKY DNA-binding protein 40
BnaCnng32820D	AT2G29090	CYP707A2	cytochrome P450/family 707/subfamily A/polypeptide 2
BnaA04g22040D BnaCnng66020D	AT2G38470	WRKY33	WRKY DNA-binding protein 33
BnaA04g22700D	AT2G39980		HXXXD-type acyl-transferase family protein
BnaA03g56550D	AT2G40000	HSPRO2	ortholog of sugar beet HS1 PRO-1 2
BnaC04g02730D	AT2G43120		RmlC-like cupins superfamily protein
BnaA03g56880D	AT2G45660	AGL20, SOC1	AGAMOUS-like 20
BnaCnng05480D	AT3G02060		DEAD/DEAH box helicase, putative
BnaCnng18320D	AT3G03090	VGT1	vacuolar glucose transporter 1
BnaC01g40360D	AT3G03950	ECT1	evolutionarily conserved C-terminal region 1
BnaC05g41640D	AT3G11580		AP2/B3-like transcriptional factor family protein
BnaC05g34990D	AT3G18290	EMB2454, BTS	zinc finger protein-related
BnaA06g32440D BnaC07g48980D	AT3G27060	TSO2, ATTSO2	Ferritin/ribonucleotide reductase-like family protein
BnaA06g38950D	AT3G44260		Polynucleotidyl transferase, ribonuclease H-like superfamily protein
BnaC08g21640D	AT3G50260	ERF011	cooperatively regulated by ethylene and jasmonate 1
BnaA04g02530D	AT3G56360		Unknown protein
BnaA03g47030D	AT4G24960	HVA22D	HVA22 homologue D
BnaA01g15250D	AT4G26080	ABII	Protein phosphatase 2C family protein
BnaA03g48570D	AT4G27410	RD26, ANAC072	NAC (No Apical Meristem) domain transcriptional regulator superfamily protein
BnaC09g49020D	AT5G06530		ABC-2 type transporter family protein
BnaC02g04980D	AT5G13740	ZIF1	zinc induced facilitator 1
BnaA02g32350D	AT5G24770	VSP2	vegetative storage protein 2
BnaCnng60520D	AT5G47220	ERF2	ethylene responsive element binding factor 2
BnaA03g39820D	AT5G60910	AGL8, FUL	AGAMOUS-like 8
BnaC09g06860D	AT5G65300		Unknown protein
BnaC09g07320D	AT5G67370		Protein of unknown function (DUF1230)

Table 4-13: The 40 *B. napus* genes commonly up-regulated by UV-B and *Plutella* herbivory and their putative Arabidopsis homologues. FC ≥1.5, $p \leq 0.05$.

Annotation Cluster 1	Enrichment Score: 3.88	%	PValue	FDR
GOTERM_MF_FAT	GO:0003700~transcription factor activity	38.24	0.00	0.01
GOTERM_BP_FAT	GO:0006350~transcription	35.29	0.00	0.01
GOTERM_MF_FAT	GO:0030528~transcription regulator activity	38.24	0.00	0.02
GOTERM_BP_FAT	GO:0045449~regulation of transcription	38.24	0.00	0.08
GOTERM_MF_FAT	GO:0003677~DNA binding	38.24	0.00	0.26
GOTERM_BP_FAT	GO:0006355~regulation of transcription, DNA-dependent	26.47	0.00	0.53
GOTERM_BP_FAT	GO:0051252~regulation of RNA metabolic process	26.47	0.00	0.55
GOTERM_MF_FAT	GO:0043565~sequence-specific DNA binding	11.76	0.05	39.80
Annotation Cluster 2	Enrichment Score: 2.84	%	PValue	FDR
GOTERM_BP_FAT	GO:0009743~response to carbohydrate stimulus	17.65	0.00	0.03
GOTERM_BP_FAT	GO:0010200~response to chitin	14.71	0.00	0.09
GOTERM_BP_FAT	GO:0042742~defense response to bacterium	11.76	0.00	5.02
GOTERM_BP_FAT	GO:0009617~response to bacterium	11.76	0.01	10.66
Annotation Cluster 3	Enrichment Score: 2.59	%	PValue	FDR
GOTERM_BP_FAT	GO:0009414~response to water deprivation	14.71	0.00	0.31
GOTERM_BP_FAT	GO:0009415~response to water	14.71	0.00	0.37
GOTERM_BP_FAT	GO:0009409~response to cold	14.71	0.00	0.89
GOTERM_BP_FAT	GO:0009628~response to abiotic stimulus	26.47	0.00	0.99
GOTERM_BP_FAT	GO:0009266~response to temperature stimulus	14.71	0.00	4.06
GOTERM_BP_FAT	GO:0009737~response to abscisic acid stimulus	11.76	0.01	15.79
GOTERM_BP_FAT	GO:0009651~response to salt stress	11.76	0.03	28.91
GOTERM_BP_FAT	GO:0006970~response to osmotic stress	11.76	0.03	34.17
Annotation Cluster 4	Enrichment Score: 2.24	%	PValue	FDR
GOTERM_BP_FAT	GO:0009911~positive regulation of flower development	8.82	0.00	1.59
GOTERM_BP_FAT	GO:0048582~positive regulation of post-embryonic development	8.82	0.00	2.40
GOTERM_BP_FAT	GO:0051094~positive regulation of developmental process	8.82	0.00	3.22
GOTERM_BP_FAT	GO:0009909~regulation of flower development	8.82	0.01	14.26
GOTERM_BP_FAT	GO:0009791~post-embryonic development	17.65	0.02	17.85
GOTERM_BP_FAT	GO:0048580~regulation of post-embryonic development	8.82	0.03	28.74
Annotation Cluster 5	Enrichment Score: 2.09	%	PValue	FDR
GOTERM_BP_FAT	GO:0010033~response to organic substance	35.29	0.00	0.00
GOTERM_BP_FAT	GO:0009719~response to endogenous stimulus	23.53	0.00	1.51
GOTERM_BP_FAT	GO:0009725~response to hormone stimulus	20.59	0.00	5.42
GOTERM_BP_FAT	GO:0009873~ethylene mediated signaling pathway	8.82	0.04	36.99
GOTERM_BP_FAT	GO:0009755~hormone-mediated signalling	11.76	0.04	40.12
GOTERM_BP_FAT	GO:0032870~cellular response to hormone stimulus	11.76	0.04	40.12
GOTERM_BP_FAT	GO:0007242~intracellular signalling cascade	14.71	0.05	46.65
GOTERM_BP_FAT	GO:0000160~two-component signal transduction system (phosphorelay)	8.82	0.06	51.81

GOTERM_BP_FAT	GO:0009723~response to ethylene stimulus	8.82	0.08	62.35
Annotation Cluster 6	Enrichment Score: 1.90	%	PValue	FDR
GOTERM_BP_FAT	GO:0009624~response to nematode	8.82	0.00	5.92
GOTERM_CC_FAT	GO:0016021~integral to membrane	17.65	0.01	9.13
GOTERM_MF_FAT	GO:0051119~sugar transmembrane transporter activity	8.82	0.01	14.32
GOTERM_CC_FAT	GO:0031224~intrinsic to membrane	17.65	0.03	19.35
Annotation Cluster 7	Enrichment Score: 1.28	%	PValue	FDR
GOTERM_BP_FAT	GO:0009791~post-embryonic development	17.65	0.02	17.85
GOTERM_BP_FAT	GO:0048608~reproductive structure development	14.71	0.04	38.82
GOTERM_BP_FAT	GO:0003006~reproductive developmental process	14.71	0.05	48.91
GOTERM_BP_FAT	GO:0009908~flower development	8.82	0.06	55.85

Table 4-14: Annotation clusters and grouped GO categories enriched in the list of Arabidopsis ID's with sequence similarity to the *B. napus* transcripts up-regulated by UV-B and *Plutella*.

4.5.7 *Plutella* and slug herbivory

4.5.7.1 *B. napus* genes commonly regulated by slug herbivory and *Plutella* herbivory

For this section of the chapter, a direct comparison was made between all *B. napus* transcripts commonly regulated by slug and *Plutella* herbivory at least 1.5 fold with $p \leq 0.05$. The regulatory effects of UV-B and MeJA on the *B. napus* genome have been omitted from this comparison, resulting in a higher number of transcripts being identified as commonly regulated between the two invertebrates compared to the numbers presented in Figures 4-8C and D. Venn diagrams were generated to illustrate the extent of genetic overlap between the two invertebrate treatments (Figure 4-9), and out of the 3,106 transcripts found to be differentially regulated by either pest, 11% are differentially regulated by both invertebrate treatments (4-9A). To identify the transcripts commonly up-regulated or down-regulated by slugs and *Plutella*, two additional Venn diagrams were generated (Figure 4-9B and C, respectively). Nine percent of 1,128 transcripts are commonly up-regulated by both herbivores, while a slightly higher 12% are commonly down-regulated.

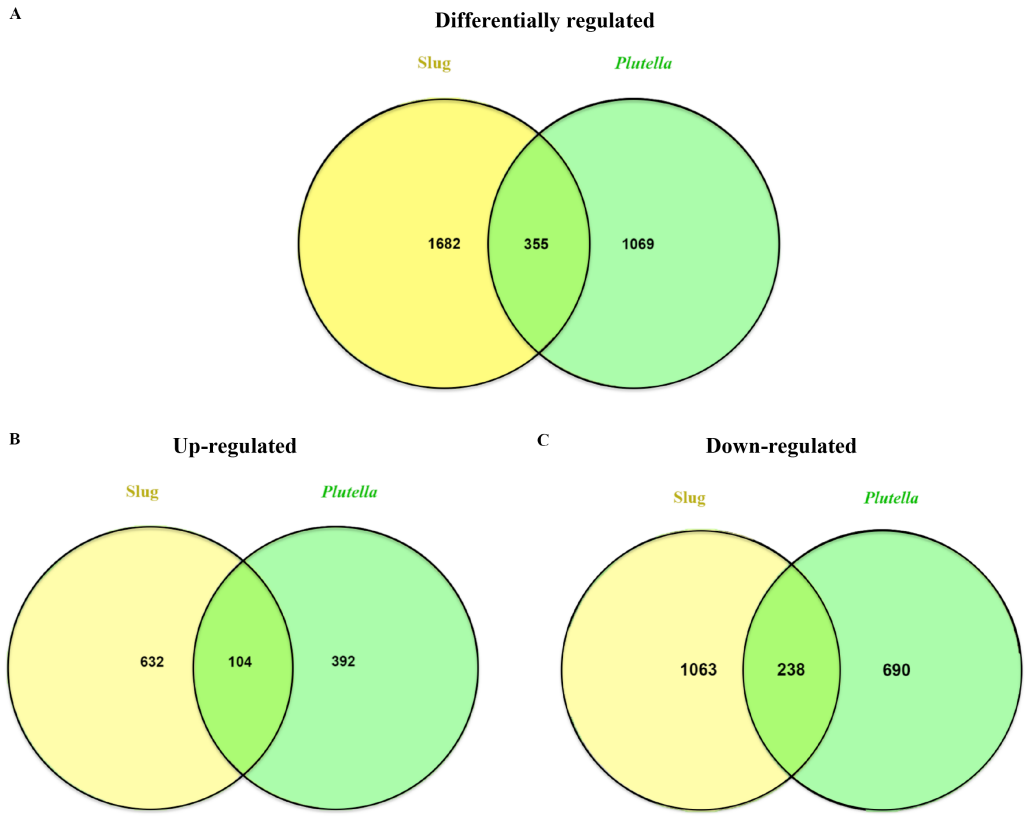

Figure 4-9. *B. napus* transcripts differentially regulated by slug herbivory and *Plutella* herbivory. A, *B. napus* transcripts differentially regulated with a FC ≥ 1.5 and $p \leq 0.05$ by slug and *Plutella* herbivory. Separation of these transcripts into **B** 'up-regulated,' and **C** 'down-regulated' Venn diagrams.

Functional annotation analysis of the Arabidopsis genes sharing sequence similarity to the *B. napus* transcripts up-regulated by slug and *Plutella* herbivory identified several annotation clusters and 25 GO terms with $p \leq 0.05$ (Table 4-15). The annotation cluster possessing the largest enrichment score of 4.03 is made up of 17 Arabidopsis genes distributed into 5 GO categories related to processes occurring at the cell-wall, such as "GO:0005576~extracellular region," "GO:0030312~external encapsulating structure" and "GO:0009505~plant-type cell wall."

Annotation Cluster 1	Enrichment Score: 4.03	%	PValue	FDR
GOTERM_CC_FAT	GO:0005576~extracellular region	17.72	2.49E-05	0.02
GOTERM_CC_FAT	GO:0005618~cell wall	12.66	4.97E-05	0.05
GOTERM_CC_FAT	GO:0030312~external encapsulating structure	12.66	5.57E-05	0.05
GOTERM_CC_FAT	GO:0048046~apoplast	10.13	1.01E-04	0.10
GOTERM_CC_FAT	GO:0009505~plant-type cell wall	7.59	1.05E-03	1.00
Annotation Cluster 2	Enrichment Score: 1.75	%	PValue	FDR
GOTERM_BP_FAT	GO:0010033~response to organic substance	17.72	1.45E-04	0.19
GOTERM_BP_FAT	GO:0009725~response to hormone stimulus	12.66	3.86E-03	4.96
GOTERM_BP_FAT	GO:0009743~response to carbohydrate stimulus	6.33	5.10E-03	6.50
GOTERM_BP_FAT	GO:0009719~response to endogenous stimulus	12.66	6.10E-03	7.74
GOTERM_BP_FAT	GO:0000160~two-component signal transduction system (phosphorelay)	6.33	7.01E-03	8.85
GOTERM_BP_FAT	GO:0010200~response to chitin	5.06	9.92E-03	12.29
GOTERM_MF_FAT	GO:0030528~transcription regulator activity	17.72	1.31E-02	13.76
GOTERM_BP_FAT	GO:0032870~ response to hormone stimulus	7.59	1.71E-02	20.33
GOTERM_BP_FAT	GO:0009755~hormone-mediated signalling	7.59	1.71E-02	20.33
GOTERM_MF_FAT	GO:0003700~transcription factor activity	15.19	2.91E-02	28.18
GOTERM_BP_FAT	GO:0006355~regulation of transcription, DNA-dependent	11.39	3.40E-02	36.56
GOTERM_BP_FAT	GO:0051252~regulation of RNA metabolic process	11.39	3.50E-02	37.40
GOTERM_BP_FAT	GO:0006350~transcription	12.66	3.62E-02	38.42
GOTERM_BP_FAT	GO:0045449~regulation of transcription	16.46	4.30E-02	43.92
Annotation Cluster 3	Enrichment Score: 1.71	%	PValue	FDR
GOTERM_BP_FAT	GO:0009063~cellular amino acid catabolic process	3.80	1.03E-02	12.79
GOTERM_BP_FAT	GO:0009310~amine catabolic process	3.80	1.17E-02	14.39
GOTERM_BP_FAT	GO:0016054~organic acid catabolic process	3.80	3.41E-02	36.69
GOTERM_BP_FAT	GO:0046395~carboxylic acid catabolic process	3.80	3.41E-02	36.69
Annotation Cluster 4	Enrichment Score: 1.41	%	PValue	FDR
GOTERM_CC_FAT	GO:0048046~apoplast	10.13	1.01E-04	0.10
GOTERM_MF_FAT	GO:0016762~xyloglucan:xyloglucosyl transferase activity	3.80	5.96E-03	6.49

Table 4-15. Annotation clusters and grouped GO categories enriched in the list of Arabidopsis ID's with sequence similarity to the *B. napus* transcripts up-regulated by slug and *Plutella* herbivory.

Annotation cluster 2 holds the largest grouping of GO terms, 7 of which are associated with transcriptional regulation (**"**GO:0030528~transcription regulator activity," "GO:0003700~transcription factor activity," "GO:0006355~regulation of transcription, DNA-dependent," "GO:0051252~regulation of RNA metabolic process,"

"GO:0006350~transcription" and "GO:0045449~regulation of transcription"). The 16 Arabidopsis genes in each GO term are listed in Table 4-16.

Arabidopsis ID	GO Term						
	GO:0030528~transcription regulator activity	GO:0003700~transcription factor activity	GO:0006355~regulation of transcription, DNA-dependent	GO:0051252~regulation of RNA metabolic process	GO:0006350~transcription	GO:0045449~regulation of transcription	GO:0003677~DNA binding
AT1G01030 (NGA3)	■	■	■	■	■	■	■
AT1G09750 (AED3)							■
AT1G19050 (ARR7)	■		■	■	■	■	
AT1G64380	■	■	■	■	■	■	■
AT1G80840 (WRKY40)	■	■	■	■	■	■	■
AT2G02450 (ANAC034)	■	■				■	■
AT2G20880	■	■	■	■	■	■	■
AT3G57040 (ARR9)	■		■	■	■	■	
AT4G26150 (CGA1)	■	■	■	■	■	■	■
AT4G28140	■	■	■	■	■	■	■
AT4G28610 (PHR1)	■	■				■	■
AT5G04150 (BHLB101)	■	■			■	■	■
AT5G04340 (ZAT6)	■	■					■
AT5G15230 (GASA4)	■	■					
AT5G15310 (MYB16)			■	■		■	■
AT5G63790 (ANAC102)	■	■			■	■	■

Table 4-16. The 7 GO terms in annotation cluster 2 of Table 4-15, and the 16 Arabidopsis genes grouped into each term. The known Arabidopsis gene names are provided, and the GO categories that each gene is present in is highlight with a blue box.

Some of these Arabidopsis genes have previously been identified as commonly regulated by one or both invertebrate treatments and UV-B radiation (e.g. *WRKY40, CGA1* and *ANAC102* in sections 4.5.4 to 4.5.6), while others that have not yet been highlighted in this chapter have implicated roles in regulating plant defence (e.g. ARR-encoding genes)(Argueso, et al., 2012). Of the 238 transcripts commonly down-regulated by both invertebrate treatments, 227 were assigned putative gene functions based on their sequence similarity to 181 Arabidopsis genes. Functional analysis of these genes revealed that the

most enriched GO terms in annotation cluster 1 were associated with responses to abiotic stress, and at least 3 clusters contained GO terms related to plant response to bacterial stress (Table 4-17). Several genes in the latter GO categories encode pathogen-related genes, such as *PATHOGENESIS-RELATED GENE 1* (*PR-1*) and *PR-4,* a cytochrome P450 involved in tryptophan metabolism (*CYP79B2*) and an ELICITOR-ACTIVATED GENE, *ELI3-1*.

Annotation Cluster 1	Enrichment Score: 6.69	Count	PValue	FDR
GOTERM_BP_FAT	GO:0009266~response to temperature stimulus	17	5.69E-08	8.19E-05
GOTERM_BP_FAT	GO:0009628~response to abiotic stimulus	30	2.08E-07	2.99E-04
GOTERM_BP_FAT	GO:0009409~response to cold	13	7.37E-07	1.06E-03
Annotation Cluster 2	Enrichment Score: 2.78	Count	PValue	FDR
GOTERM_BP_FAT	GO:0009814~defense response, incompatible interaction	7	1.73E-04	2.49E-01
GOTERM_BP_FAT	GO:0045087~innate immune response	9	2.53E-03	3.58E+00
GOTERM_BP_FAT	GO:0009627~systemic acquired resistance	4	2.54E-03	3.60E+00
GOTERM_BP_FAT	GO:0006952~defense response	19	2.91E-03	4.11E+00
GOTERM_BP_FAT	GO:0006955~immune response	9	3.72E-03	5.23E+00
Annotation Cluster 3	Enrichment Score: 2.74	Count	PValue	FDR
GOTERM_BP_FAT	GO:0019438~aromatic compound biosynthetic process	9	5.24E-04	7.52E-01
GOTERM_BP_FAT	GO:0009698~phenylpropanoid metabolic process	8	5.63E-04	8.08E-01
GOTERM_BP_FAT	GO:0006575~cellular amino acid derivative metabolic process	10	6.80E-04	9.75E-01
GOTERM_BP_FAT	GO:0009699~phenylpropanoid biosynthetic process	7	8.11E-04	1.16E+00
GOTERM_BP_FAT	GO:0019748~secondary metabolic process	12	1.02E-03	1.46E+00
GOTERM_BP_FAT	GO:0042398~cellular amino acid derivative biosynthetic process	7	6.50E-03	8.96E+00
GOTERM_BP_FAT	GO:0009809~lignin biosynthetic process	4	6.71E-03	9.24E+00
GOTERM_BP_FAT	GO:0009808~lignin metabolic process	4	1.83E-02	2.33E+01
Annotation Cluster 4	Enrichment Score: 2.30	Count	PValue	FDR
GOTERM_BP_FAT	GO:0009617~response to bacterium	9	1.19E-03	1.71E+00
GOTERM_BP_FAT	GO:0042742~defense response to bacterium	6	2.11E-02	2.64E+01
Annotation Cluster 5	Enrichment Score: 2.18	Count	PValue	FDR
GOTERM_BP_FAT	GO:0010035~response to inorganic substance	13	2.30E-03	3.26E+00

GOTERM_BP_FAT	GO:0010038~response to metal ion	10	5.77E-03	8.00E+00
GOTERM_BP_FAT	GO:0046686~response to cadmium ion	8	2.25E-02	2.79E+01
Annotation Cluster 6	Enrichment Score: 2.08	Count	PValue	FDR
GOTERM_CC_FAT	GO:0005618~cell wall	15	1.01E-03	1.12E+00
GOTERM_CC_FAT	GO:0030312~external encapsulating structure	15	1.16E-03	1.28E+00
Annotation Cluster 7	Enrichment Score: 1.95	Count	PValue	FDR
GOTERM_BP_FAT	GO:0000272~polysaccharide catabolic process	6	4.28E-04	6.15E-01
GOTERM_BP_FAT	GO:0005976~polysaccharide metabolic process	9	5.92E-04	8.49E-01
GOTERM_MF_FAT	GO:0030247~polysaccharide binding	4	6.03E-04	7.90E-01
GOTERM_MF_FAT	GO:0001871~pattern binding	4	6.03E-04	7.90E-01
GOTERM_MF_FAT	GO:0008061~chitin binding	3	3.04E-03	3.93E+00
GOTERM_BP_FAT	GO:0006026~aminoglycan catabolic process	3	1.92E-02	2.44E+01
GOTERM_BP_FAT	GO:0006030~chitin metabolic process	3	1.92E-02	2.44E+01
GOTERM_BP_FAT	GO:0006032~chitin catabolic process	3	1.92E-02	2.44E+01
GOTERM_MF_FAT	GO:0004568~chitinase activity	3	2.01E-02	2.35E+01
GOTERM_BP_FAT	GO:0006022~aminoglycan metabolic process	3	2.38E-02	2.93E+01
GOTERM_BP_FAT	GO:0016998~cell wall macromolecule catabolic process	3	3.06E-02	3.61E+01
GOTERM_BP_FAT	GO:0016052~carbohydrate catabolic process	6	3.11E-02	3.65E+01
GOTERM_BP_FAT	GO:0009251~glucan catabolic process	3	4.40E-02	4.77E+01
Annotation Cluster 8	Enrichment Score: 1.95	Count	PValue	FDR
GOTERM_BP_FAT	GO:0005976~polysaccharide metabolic process	9	5.92E-04	8.49E-01
GOTERM_BP_FAT	GO:0044042~glucan metabolic process	6	9.66E-03	1.31E+01
GOTERM_BP_FAT	GO:0006073~cellular glucan metabolic process	5	2.19E-02	2.74E+01
GOTERM_BP_FAT	GO:0005982~starch metabolic process	3	3.42E-02	3.94E+01
GOTERM_BP_FAT	GO:0044264~cellular polysaccharide metabolic process	5	4.34E-02	4.73E+01
Annotation Cluster 9	Enrichment Score: 1.77	Count	PValue	FDR
GOTERM_BP_FAT	GO:0006970~response to osmotic stress	10	7.35E-03	1.01E+01
GOTERM_BP_FAT	GO:0009651~response to salt stress	8	3.95E-02	4.41E+01
Annotation Cluster 10	Enrichment Score: 1.67	Count	PValue	FDR
GOTERM_CC_FAT	GO:0044434~chloroplast part	19	1.80E-03	1.99E+00
GOTERM_CC_FAT	GO:0044435~plastid part	19	2.53E-03	2.78E+00
GOTERM_CC_FAT	GO:0009570~chloroplast stroma	10	1.23E-02	1.29E+01

GOTERM_CC_FAT	GO:0009532~plastid stroma	10	1.67E-02	1.70E+01
GOTERM_CC_FAT	GO:0009536~plastid	39	3.50E-02	3.27E+01
GOTERM_CC_FAT	GO:0009941~chloroplast envelope	9	4.17E-02	3.77E+01

Table 4-17: Top ten annotation clusters and grouped GO categories enriched in the list of Arabidopsis ID's with sequence similarity to the *B. napus* transcripts down-regulated by slug and *Plutella* herbivory.

Despite over 100 transcripts being commonly up- or down-regulated by slug and *Plutella* herbivory, a large number of transcripts appear to be specifically regulated by or the other invertebrate (Figure 4-9B and C). To further examine similarities and differences elicited by slug and *Plutella* herbivory on the *B. napus* genome, the degree of overlap between transcripts up-regulated by one invertebrate and down-regulated by the other were examined (Figure 4-10). A small number of transcripts were found to be up-regulated one by one herbivore and down-regulated by the other, with some known defence-induced genes, such as *LOX2*, being down-regulated by slug herbivory but increasing in response to *Plutella* herbivory (Table 4-18). However, the small number of genes regulated by both invertebrates in opposing directions implies that slug and *Plutella* herbivory elicit more similar responses on the genome of *B. napus,* when specific cut-off parameters are applied to the transcript lists.

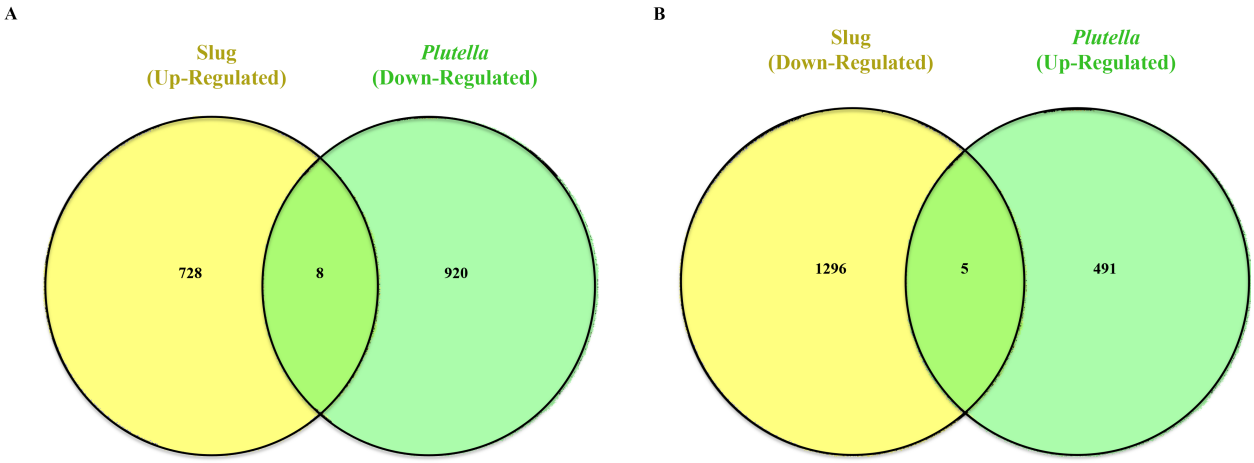

Figure 4-10: Overlap in transcripts oppositely regulated by herbivory from either invertebrate pest. A, the degree of overlap between transcripts with FC ≥ 1.5 $p \leq 0.05$ that are up-regulated by slug and down-regulated by *Plutella* herbivory, and **B,** those that are down-regulated by slug and up-regulated by *Plutella* herbivory.

UR Slug vs. DR *Plutella*					
***B. napus* Gene ID**	**Arabidopsis Gene ID**	**Gene Name**	**Gene Function**	**Slug FC**	***Plutella* FC**
BnaA07g35640D	AT1G80440		Galactose oxidase/kelch repeat superfamily protein	3.26	0.32
BnaC08g25210D	AT3G54420	CHIV, EP3	homolog of carrot EP3-3 chitinase	2.48	0.35
BnaAnng26280D	AT3G15630		Unknown protein	2.95	0.38
BnaC09g22280D	AT4G05070		Wound-responsive family protein	2.68	0.39
BnaC09g38470D	AT5G19120		Eukaryotic aspartyl protease family protein	3.53	0.40
BnaA08g09100D	AT4G19160		Unknown protein	3.65	0.45
BnaA02g05360D	AT5G21940		Unknown protein	2.15	0.54
BnaA08g09510D	AT4G20830		FAD-binding Berberine family protein	2.67	0.59

DR Slug vs. UR *Plutella*					
***B. napus* Gene ID**	**Arabidopsis Gene ID**	**Gene Name**	**Gene Function**	**Slug FC**	***Plutella* FC**
BnaA05g05760D	AT2G39800	P5CS1	delta1-pyrroline-5-carboxylate synthase 1	0.36	2.57
BnaA07g30760D	AT1G73260	KTI1	kunitz trypsin inhibitor 1	0.27	2.75
BnaA07g24880D	AT3G45140	LOX2	lipoxygenase 2	0.31	2.81
BnaA07g24870D	AT3G45140	LOX2	lipoxygenase 2	0.51	3.57
BnaA02g04750D	AT5G20190		Tetratricopeptide repeat (TPR)-like superfamily protein	0.23	4.18

Table 4-18: The 13 transcripts regulated by slug and *Plutella* herbivory in opposing directions. FC ≥ 1.5, $p \leq 0.05$. UR, Up-Regulated transcripts; DR, Down-Regulated transcripts; FC, Fold Change in expression**.**

4.6 Comparisons of the results obtained from the two alignments in 2012 and 2014

4.6.1 Differences exist in the number of transcripts differentially regulated in each alignment

Following the second read alignment in 2014, a comparison was carried out to assess the similarities and differences in the transcripts considered as differentially regulated by any of the 4 treatments. On account of the 2 alignments having two different cut-off parameters applied to them (RPKM ≥ 3 and FC ≥ 2 for the initial alignment, RPKM ≥ 3, FC ≥ 1.5 and $p \leq 0.05$ for the second), and both reference sequences used for the alignments possessing a different number of Unigenes or genes (~95,000 for the Brassica Unigene and ~101,000 for the *B. napus* genome), differences between the number of transcripts identified as differentially regulated from both alignments was, to some extent, expected. Initial analysis of the transcripts from both alignments identified as differentially regulated by at least one treatment was achieved with a Venn diagram (Figure 4-11). Due to the gene ID's assigned to the reads being different for the Brassica Unigene and *B. napus* genome alignment, it was impossible to use these identifiers as a means of matching similarly regulated transcripts between the two alignments with a Venn diagram. Instead, the Arabidopsis gene ID's that were appointed to transcripts (based on their sequence similarities to the Arabidopsis genome) were utilised to compare genes differentially up- and down-regulated from each alignment. It is important to note, however, that the use of the Arabidopsis gene ID's limited the number of transcripts from each alignment for comparison, as the expression of transcripts lacking a putative Arabidopsis homologue could not be compared between alignments. Of the 4,692 and 4,212 transcripts assigned an Arabidopsis gene annotation in the first and second alignment, respectively, approximately 40% were found to overlap with one another, while the other ~60% remain uniquely expressed in their respective alignments.

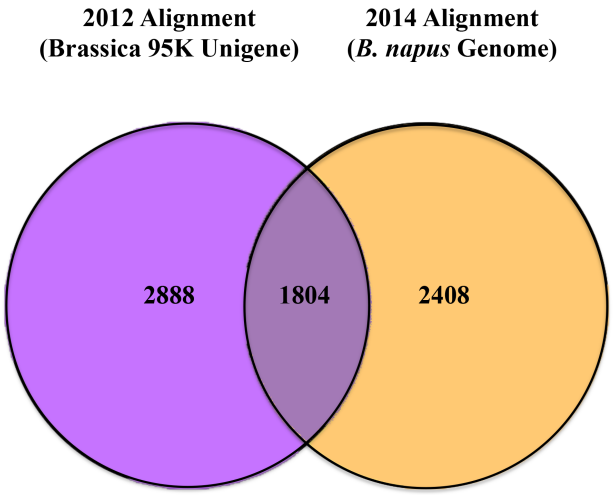

Figure 4-11: The overlap in the Arabidopsis gene ID's assigned to differentially expressed transcripts between the two read alignments in 2012 and 2014. Transcripts that were designated a putative Arabidopsis gene function, based on their sequence similarity to the Arabidopsis genome, and considered as differentially regulated in each alignment (both up- and down-regulated) were compared to one another.

Of the transcripts that were identified as being commonly regulated when aligned to both the Unigene and *B. napus* genome, those associated with light-induced responses were the most enriched (e.g. GO:0009416~response to light stimulus, GO:0009314~response to radiation and GO:0009639~response to red or far red light). These transcripts were proposed to encode *B. napus* orthologues of Arabidopsis *CHALCONE FLAVONONE ISOMERASE 1*, *HY5, MYB4, CYP83B1, CYP83A1* (glucosinolate biosynthesis-related), as well as *PHOT2, PHYA* and *PHYB*, with many additional red-light/phytochrome-associated genes also being found in this list (e.g. *PROTEIN SUPPRESSOR OF PHYA-105* and *PHYTOCHROME A-ASSOCIATED F-BOX PROTEIN*). The majority of these transcripts, including those associated with phytochrome/red-light signalling, *PHOT2* and *HY5* and *MYB4,* were positively responsive to only UV-B radiation in both alignments, however *PHYA* increased in response to slug and *Plutella* herbivory in the *B. napus* and Unigene alignment, respectively. Additional transcripts significantly regulated by at least one treatment from each alignment included those associated with osmotic stress, response to metal ions and response to abiotic stress, with approximately 119 transcripts described as being responsive to hormonal stimulus based on their putative gene annotations (GO:0009725~response to hormone stimulus, enrichment score 4.98). These transcripts include multiple auxin-responsive elements (e.g. *IAA16* to *IAA19*), approximately 11 ethylene-responsive transcription factors such as *ERF034* and *ERF106,* along with *MYC2*,

which is proposed to possess multiple orthologues in *B. napus* that accumulate in response to *Plutella* herbivory and/or MeJA treatment.

Approximately 16 and 116 transcripts documented as being significantly regulated by at least one treatment in the 2012 alignment only were categorised in the GO groups associated with hormone-signalling pathways or plant defence-responses, respectively (GO:0010817~ regulation of hormone levels and GO:0006952~defense response, enrichment score 0.4 and 3.8 respectively). Transcripts associated with hormone response include those putatively encoding CYTOCHROME P450 proteins, while those implicated in plant defence putatively encode AOS, several myrosinase-binding proteins, pathogenesis-related protein 5 and multiple TGA transcription factors (e.g. TGA1-4) which are proposed to regulate expression of *PR* genes (Kesarwani et al., 2007).

Of the transcripts found as being differentially regulated by at least one treatment in the 2014 alignment, those associated with plant response to metal ions and inorganic substances were the most enriched (enrichment score 9.1), while a large number of ethylene-responsive transcription factors (approximately 26) were shown as being differentially regulated by one or more treatments in this alignment only (e.g. *ERF1* in response to UV-B radiation, MeJA treatment or *Plutella* herbivory). It is apparent that differences exist in the results obtained from each alignment, however the identification of light- and hormone-associated elements considered as being significantly regulated in both the 2012 and 2014 data indicates that some commonalities do exist between them.

4.6.2 Putative *ELI3-2, VTC2* and *COMT1* transcripts from both alignments display different patterns in expression across the four treatments

To further evaluate similarities and differences between the two alignments, the expression changes of the transcripts putatively assigned the Arabidopsis gene names that were selected for over-expression (section 4.4.2) were compared from each alignment. All transcripts, regardless of being classed as differentially regulated or not when the specific cut-off parameters were enforced on the dataset, were identified (Table 4-19). As a result, some transcripts originating from the initial and second alignment possessing a FC ≥ 2 or 1.5, respectively, but an RPKM and/or *p*-value below the minimum cut-off point, will not be classed as being differentially regulated.

Differences in the number of transcripts putatively encoding VTC2 or COMT1 proteins are seen between the two alignments, with 4 Unigenes and 6 *B. napus* genes possessing sequence similarity to Arabidopsis *VTC2*, and 2 Unigenes and 4 *B. napus* transcripts

reported as putative *COMT1* genes. *ELI3-2,* on the other hand, has three putative orthologues in the Brassica Unigene and the *B. napus* genome, however expression patterns of these transcripts are not similar in response to the majority of treatments. The Unigene, EV141577, which is proposed to share sequence similarity to *ELI3-2*, was identified as being positively responsive to all 4 treatments with a minimum FC in expression of 4.07 for *Plutella* herbivory. The three *B. napus* transcripts, however, all decrease in expression following *Plutella* or slug herbivory. Expression of the three *B. napus* transcripts increases in response to MeJA treatment, with the intensity of the FC ranging from 2.36 to 9.90, which averages close to the FC of 6.41 seen for EV141577. Likewise, UV-B radiation increases expression of the majority of *B. napus* transcripts by approximately 2-fold, which, while being approximately 50% less than the FC of EV141577 in response to UV-B, is still indicative of a positive regulatory effect of this light treatment on the expression of putative *ELI3-2* genes in *B. napus*.

The two Brassica Unigenes sharing sequence similarity to Arabidopsis *COMT1,* EV218973 and EV120446, did not possess the required minimum FC or RPKM values of 2 and 3, respectively, to be classed as differentially regulated transcripts. As a result, these transcripts were omitted from analysed dataset acquired from the first alignment. All four *B. napus* transcripts with sequence similarity to *COMT1,* however, did meet all imposed cut-off criteria in at least one treatment, and the majority were found to increase in expression following UV-B or MeJA treatment, as was reported with EV218973. Slug and *Plutella* herbivory, on the other hand, caused all 4 transcripts to decrease in expression, results that are again reminiscent of what is seen in EV218973.

Gene Name (Arabidopsis ID)	Brassica Unigene or *B. napus* Gene ID	UVB		SLUG		PLUTELLA		MeJA	
		EC	FC	EC	FC	EC	FC	EC	FC
ELI3-2 (AT4G37990)	EV139563	-	1.02	-	0.98	-	1.17	-	1.52
	EV141577	↑	4.59	↑	5.17	↑	4.07	↑	6.41
	EV225295	-	0.91	-	0.92	-	1.21	-	1.52
	BnaC03g61130D	-	0.83	↓	0.44	-	0.71	↑	2.36
	BnaA08g15930D	↑	2.12	↓	0.48	-	0.52	↑	3.65
	BnaC03g61120D	↑	2.70	-	0.57	-	0.51	↑	9.90
VTC2 (AT4G26850)	EV157337	-	0.56	-	0.54	↓	0.31	-	1.00
	EV165278	-	4.49	↓	0.16	↓	0.04	-	1.92
	EV157418	-	1.00	-	2.33	-	1.55	-	1.48
	EX043301	↑	2.44	↑	2.03	-	1.38	↓	0.49
	BnaC01g19060D	↑	3.30	↓	0.24	↓	0.33	↓	0.39
	BnaA01g15950D	-	1.36	↓	0.42	↓	0.35	-	1.78
	BnaA08g14270D	-	1.00	-	0.56	-	0.81	-	0.87
	BnaC08g12340D	-	1.23	-	0.67	-	0.78	↓	0.50
	BnaA03g48310D	-	0.51	-	1.11	-	1.30	-	1.71
	BnaC07g40500D	-	1.00	↑	2.02	-	1.20	-	1.00
COMT1 (AT5G54160)	EV120446	-	0	-	0	-	0	-	0
	EV218973	-	4.02	-	0.35	-	0.36	-	4.73
	BnaC09g30560D	-	1.20	↓	0.26	↓	0.33	-	0.90
	BnaA10g07270D	-	0.98	↓	0.36	↓	0.45	-	1.28
	BnaC03g14720D	↑	2.15	-	0.60	-	0.83	-	1.57
	BnaA03g11990D	-	1.87	-	0.61	-	0.51	↑	4.43

Table 4-19. Differences in regulation of three genes selected for over-expression in Arabidopsis when aligned to the Brassica 95K Unigene or *B. napus* genome. Expression changes of transcripts from the second alignment proposed to encode *ELI3-2, VTC2* and *COMT1* were compared to those of the transcripts from the initial alignment. Brassica Unigenes possess an 8-digit ID beginning with either 'EV' or 'EX,' while *B. napus* gene ID's have 13 digits and start with the letters 'Bna.' The fold change (FC) of the Unigenes or *B. napus* genes proposed to be orthologues of the three Arabidopsis genes is listed next to arrows illustrating the direction of their changes in expression (EC). An upwards arrow, '**é**' indicates an increase in expression, '**ê**' a decrease in expression, and '-' signifies no significant change in expression following treatment, or that the (Uni)gene failed to meet all cut-off parameters imposed on the dataset. Arrows and lines assigned to each transcript based on the cut-off parameters applied to each dataset (initial alignment, RPKM ≥ 3, FC ≥ 2; second alignment, RPKM ≥ 3, FC ≥ 1.5, $p \leq 0.05$).

The putative *VTC2* Unigene transcript that encouraged selection of this gene for further study and over-expression, EX043301, increased by approximately 2-fold in response to UV-B radiation or slug herbivory. *Plutella* herbivory also induced an increase in expression of this transcript, however not by the minimum 2-fold requirement imposed on the dataset. Interestingly, 50% of the putative *VTC2* Unigenes were up-regulated by invertebrate herbivory, while the other 50% were down regulated. The level of expression of these two transcripts two hours after the start of invertebrate herbivory was higher in the samples subjected to slug grazing than *Plutella* grazing. Examination of the 6 putative *B. napus* orthologues of Arabidopsis *VTC2* found that expression of two thirds of these transcripts was down-regulated by herbivory from invertebrates, with the other 2 transcripts displayed between a approximate 1 to 2-fold change in expression in response to herbivory. With the exception of one transcript, BnaA03g48310D, UV-B radiation increased expression of putative *VTC2* transcripts, although only BnaC01g19060D met the minimum FC requirements of 1.5. MeJA induced a 1-1.78-fold increase in expression of 3 transcripts, while the remaining 50% were down-regulated. No *B. napus* transcript displayed a similar pattern in expression to the Unigene, EX043301, in response to any of the 4 treatments. Every *B. napus* transcript that increased in expression following UV-B radiation is down-regulated by slug herbivory, and vice-versa. However, the previously mentioned BnaC01g19060D and BnaC07g40500D *B. napus* transcripts were up-regulated in expression by UV-B and slug herbivory, respectively, with the FC in expression being very similar to that observed in EX043301. Additionally, BnaC01g19060D was down-regulated by MeJA in a similar manner to that documented in EX043301, and the slug-responsive BnaC07g40500D was positively regulated by *Plutella* herbivory to a near-identical FC in expression as the Unigene. The degree of similarity between the two *B. napus* transcripts and the Unigene prompted further investigation into the sequence similarity between the three transcripts. ClustalW was used to align the sequences of these three transcripts to one another as well as to the sequence of the Arabidopsis *VTC2* gene (AT4G26850). An approximate 400-base pair region of this alignment shows high similarity between these sequences (Figure 4-12), with the majority of sequence differences between the transcripts and the *VTC2* gene being C-T or A-G substitutions. Indeed, the high degree of sequence similarity between the three transcripts may account for any overlap in expression found between EX043301, BnaC01g19060D and BnaC07g40500D in response to the 4 treatments, as it is possible that *B. napus* transcripts assigned the Unigene ID EX043301 during the 2012 RNA-seq experiment were derived from the *B. napus* genes now known as BnaC01g19060D and BnaC07g40500D. As a

result, differences observed in the transcriptomic data obtained in 2012 and 2014 could be attributed to overlaps in sequence similarity between one Unigene ID and multiple transcripts that originate from similar, yet separate, *B. napus* genes.

```
VTC2 (AT4G26850)   AGGATAGGTTCCAAAGAGGACTTTTTCGCTATGATGTCACTGCCTGCGAAACCAAAGTTA 798
BnaC01g19060D      AGGATAGGTTCCAAAGAGGACTCTTCCGCTACGATGTGACAGCCTGCGAGACCAAAGTGA 728
BnaC07g40500D      AGGATAGGTACCAAAGAGGACTCTTTCGCTACGATCTCACTGCCTGCGTAACCAAAGTCA 653
EX043301           ----------------------TTTT----------------------------AGGTCA 101
                                          **                              * ** *
VTC2 (AT4G26850)   TCCCGGGGAAGTATGGTTTCGTTGCTCAGCTTAACGAGGGTCGTCACTTGAAGAAGAGGC 858
BnaC01g19060D      TCCCGGGGAAGTACGGTTTCGTTGCTCAGCTAAACGAGGGTCGTCACCTGAAGAAGAGAC 788
BnaC07g40500D      TCCCGGGGAAGTATGGCTTTATTGCTCAGCTTAACGAGGGTCGTCACCTAAAGAGG---C 710
EX043301           TCCCGGGGAAGTATGGCTTTATTGCTCAGCTTAACGAGGGCCGTCACCTAAAGA---GGC 158
                   ************* ** **  ********** ******** ****** * ****     *
VTC2 (AT4G26850)   CAACTGAGTTCCGTGTAGATAAGGTGTTGCAGTCTTTTGATGGCAGCAAATTCAACTTCA 918
BnaC01g19060D      CCACCGAGTTTCGTGTAGATAAGGTTTTGCAGTCTTTTGATGGCAACAAGTTCAACTTCA 848
BnaC07g40500D      CAACGGAGTTTCGTGTAGATAAGGTTTTGCAGTCTTTCGATGGCAGCAAGTTCAACTTCA 770
EX043301           CAACCGAGTTCCGTGTAGATAAGGTTTTGCAGTCTTTCGATGGCAACAAATTCAACTTCA 218
                   * ** ***** ************** ************ ******* *** **********
VTC2 (AT4G26850)   CTAAAGTTGGCCAAGAAGAGTTGCTCTTCCAGTTTGAAGCTGGTGAAGATGCCCAAGTTC 978
BnaC01g19060D      CTAAAGTTGGCCAGGAAGAGCTGCTCTTCCAGTTTGAAGCTGGTGAAGATAGTGAAGTTC 908
BnaC07g40500D      CTAAAGTTAGCCAGGAAGAGCTGCTCTTCCAGTTTGAAGCTGGTGAAGATAGCGAAGCTC 830
EX043301           CTAAAGTTAGCCAAGAAGAATTGCTCTTTCAGTTCGAAGCTGGTGAATATGAAGAAGCTC 278
                   ******** **** *****  ******* ***** ************ **    *** **
VTC2 (AT4G26850)   AGTTCTTCCCTTGCATGCCTATTGACCCTGAGAATTCTCCCAGTGTTGTTGCCATCAATG 1038
BnaC01g19060D      AGTTCTTCCCGTGCATGCCTCTTGACGCTGAGAATTCTCCCAGTGTTGTTGCCATCAATG 968
BnaC07g40500D      GGTTCTTCCCCTGCATGCCTCTTGTCGCTGAGAATTCTCCCAGTGTTGTTGCCATCAATG 890
EX043301           AGGTCTTACCCTGCATGCCTCTTCTCGCTGAGAATTCTCCCAGTGTTGTTGCCATCAATG 338
                    * **** ** ********* **  * ********************************
VTC2 (AT4G26850)   TTAGTCCGATAGAGTATGGCCATGTGCTGCTGATTCCTCGTGTTCTTGACTGCTTGCCTC 1098
BnaC01g19060D      TTAGTCCAATTGAGTATGGCCACGTGCTGCTGATTCCTCGTGTTCTTGACTGCTTGCCTC 1028
BnaC07g40500D      TTAGTCCGATCGAGTATGGCCATGTGCTGCTGATTCCTCGTGTTCTTGACTGCTTGCCTC 950
EX043301           TTAGTCCCATCGAGTATGGGCATGTGCTGCTGATTCCTCGTGTTCTCGACTGCTTGCCTC 398
                   ******* ** ******** ** ********************** *************
VTC2 (AT4G26850)   AAAGGATCGATCACAAAAGCCTTTTGCTTGCAGTTCACATGGCTGCTGAGGCTGCTAATC 1158
BnaC01g19060D      AGAGGATCGACCACAAAAGCCTTTTGCTTGCGCTTCACATGGCTGCTGAAGCTGCTAATC 1088
BnaC07g40500D      AGAGGATGGATCACAAAAGCATGTTGCTTGCACTCCACATGGCTTCCGAGTCTAAGAATC 1010
EX043301           AGAGGATGGATCACAAAAGCATGTTGCTAGCACTTCACATGGCTTCCGAGGCTAAGAATC 458
                   * ***** ** ********* * ***** **  * ********* * **  **   ****
VTC2 (AT4G26850)   CATACTTCAGACTCGGTTACAACAGCTTGGGTGCTTTTGCCACTATCAATCATCTCCACT 1218
BnaC01g19060D      CTTACTTTAGACTCGGTTACAACAGCTTGGGTGCTTTTGCCACTATCAACCATCTTCACT 1148
BnaC07g40500D      CTTACTTCAGAGTTGGTTACAACAGCCTTGGTGCTTTCGCCACTATCAACCATCTTCACT 1070
EX043301           CTTACTTCAGAGTTGGTTACAACAGCCTTGGTGCTTTTG--------------------- 497
                   * ***** *** * ************ * ******** *
```

Figure 4-12: Sequence similarity between part of the Arabidopsis *VTC2* gene, AT4G26850, and three putative homologues identified from the RNA-seq analysis. Matching nucleotides in the four sequences are highlighted with an asterisk.

4.7 Discussion

Transcriptomic studies have the ability to reveal genetic reprogramming events in organisms in response to different treatments. The information collected from such studies is extensive, and can provide insight into the genetic overlaps between different biotic and/or abiotic stimuli. On account of the wealth of information that can be obtained from transcriptomics, RNA-seq was employed to identify *B. napus* transcripts similarly regulated by UV-B radiation, slug herbivory, *Plutella* herbivory, or exogenous MeJA treatment, in an attempt to better understand the molecular basis of UV-B-mediated resistance in *B. napus*. As the *B. napus* genome was not yet sequenced at the start of this project when RNA-seq was first performed, the Brassica 95K Unigene was used as a reference 'genome' for read alignment. Reads were later realigned to the *B. napus* genome following its publication (Chalhoub et al., 2014), with the Arabidopsis genome used to provide putative functions to the identified transcripts in both alignments. The results from these alignments were slightly different to on another, however it was possible to gain better insight into the genetic overlaps between UV-B- and herbivore-induced signalling pathways in *B. napus* via the identification of putative early-induced transcriptional regulators and additional transcripts that were similarly up-regulated by UV-B and invertebrate treatments (section 4.5). In addition, several transcripts were selected from these findings for over-expression in Arabidopsis, to investigate any roles their encoded products may have in mediating UV-B-enhanced resistance (section 4.4; the findings from the over-expressing lines are detailed in Chapter 6).

4.7.1 Genes selected for over-expression in Arabidopsis

Three genes were selected for over-expression in Arabidopsis, two of which were differentially regulated by at least two treatments (one being UV-B, the other herbivory from one invertebrate) in the initial RNA-seq analysis (section 4.4.2). The third gene was not differentially expressed in this alignment, but was selected due to the presence of its encoded gene product in a biological pathway previously implicated in promoting UV-B-enhanced plant defence (Demkura and Ballaré, 2012). Details of the genes are provided below.

4.7.1.1 *ELICITOR-ACTIVATED GENE 3* (*ELI3-2*)

The first gene selected for over-expression is an aromatic alcohol dehydrogenase, *ELICITOR-ACTIVATED GENE 3/CINNAMYL-ALCOHOL DEHYDROGENASE 8* (*ELI3-2/CAD8*)(Somssich et al., 1996). Three Brassica Unigenes, EV225295, EV139563 and EV141577, were found to share sequence similarity to Arabidopsis *ELI3-2*, although only one of these transcripts was identified as being differentially regulated by at least one treatment with a minimum RPKM value of 3 and a FC ≥ 2. The Unigene in question, EV141577, was found to increase in expression 4.07 to 6.40-fold in response to all four treatments. This finding highlighted *ELI3-2* as a possible candidate for over-expression in Arabidopsis, and previous reports identifying this gene as being responsive to pathogen infection secured *ELI3*-2's selection for further study.

There are nine members of the ELI/CAD protein family in Arabidopsis (Kim et al., 2007a), the majority of which catalyse the final step in the biosynthesis of lignin precursors in the phenylpropanoid pathway (Figure 4-6). ELI3-2, however, is not as well characterised as some other family members, and despite being localised alongside CAD proteins in the vascular apparatus, it displays weak expression in stem cross-sections, where lignin biosynthesis and deposition is at its highest (Kim et al., 2007a). The second most abundant biopolymer on earth, lignin is a complex aromatic polymer that both waterproofs and provides structural support to specific cell walls in plants. It is composed of phenylpropanoid units originating from monolignol cinnamyl alcohols, with the three major monolignols being *p*-coumaryl, coniferyl and sinapyl alcohols. Lignin polymers are generated by the formation of ether and carbon-carbon linkages between monomers, which, along with their ability to from cross-linkages with components of the cell wall, makes them very resistant to degradation (Halpin et al., 1994), and, putatively, an effective structural defence mechanism against pests.

ELI3-2 has previously proposed to be involved in plant defence against hemi-biotrophic pathogens (Schmelzer et al., 1989), as mRNA levels of this transcript accumulates in seedlings of parsley (*Petroselinum crispum*) inoculated with *Phytophthora megasperma* f. sp. *glycinea* (Schmelzer et al., 1989) and in Arabidopsis tissue infected with *P. syringae* (Kiedrowski et al., 1992) or *Verticillium longisporum* (Konig et al., 2014). However, changes in expression of this gene in response to invertebrate pests have not been reported, and putative roles ELI3-2 may have in promoting plant defence remain elusive.

4.7.1.2 *VITAMIN C DEFECTIVE 2* (*VTC2*)

The second gene selected from the RNA-seq data encodes a mannose-1-phosphate guanlylytransferase involved in ascorbate biosynthesis, *VITAMIN C DEFECTIVE 2* (*VTC2*)(Linster, et al., 2007). Four Brassica Unigenes were assigned the gene name of *VTC2*, based on sequence similarity to the Arabidopsis gene. Two of these Unigenes increase in response to UV-B radiation by 2.43 and 4.49-fold, which is consistent with what has previously been reported in Arabidopsis microarrays, as *VTC2* has been found to increase 2.24-fold following 4 hours of 3 μmol m^{-2} s^{-1} broadband UV-B (Brown et al., 2005), and 2.2 to 1.2-fold following 1 and 6 hours of narrowband UV-B treatment, respectively (Favory et al., 2009). Selection of this gene for over-expression in Arabidopsis was based on the responsiveness of Unigene EX043301 to UV-B radiation and slug herbivory, and also due to *VTC2* being a JA-responsive gene that has previously been found to increase in expression following *Brevicoryne brassicae* herbivory in Arabidopsis (Broekgaarden et al., 2011).

VTC2 encodes a GDP-L-galactose phosphorylase, which converts GDP-L-galactose to L-galactose-1-P in the first committed step of the L-ascorbic acid biosynthesis pathway, also known as the Smirnoff-Wheeler pathway (Linster et al., 2007). Ascorbic acid (AsA) is an antioxidant and cellular reductant, as well as an important enzyme cofactor and precursor for oxalate synthesis (Smirnoff and Wheeler, 2000). X-ray crystallography revealed that AsA strongly activates myrosinase activity by serving as a catalytic base, promoting the hydrolysis, and therefore activation, of glucosinolate defence compounds (Burmeister et al., 2000). Mutants deficient in AsA, such as *vtc1-1*, possess less myrosinase activity and appear more susceptible to *S. littoralis* herbivory than WT Arabidopsis plants (Schlaeppi et al., 2008). Supplementation of the *vtc1-1* mutant with AsA, however, restored myrosinase activity, suggesting that the biosynthesis of L-ascorbic acid is important in promoting plant defence against invertebrate herbivores.

4.7.1.3 *COMT1*

A third gene selected for over-expression in Arabidopsis was not shown as being assigned to any of the differentially regulated transcripts in the initial RNA-seq data. *CAFFEATE O-METHYLTRANSFERASE 1* (*COMT1*) encodes a flavonol 3-methyltransferase active in the phenylpropanoid pathway (Figure 4-6), with high substrate specificity towards myricetin and quercetin for the biosynthesis of sinapate and lignin, particularly syringyl (S)

lignin (Fellenberg et al., 2012). Selection of *COMT1* for over-expression in Arabidopsis was based on a recent study implicating the lignin/sinapate biosynthesis branch of the phenylpropanoid pathway, of which COMT1 is active in, as being involved in UV-B-mediated plant defence against *B. cinerea* (Demkura and Ballaré, 2012). In this investigation, the susceptibility of a UV-B-treated Arabidopsis mutant lacking functional copies of a protein located upstream of COMT1, FERULIC ACID 5-HYDROXYLASE (F5H), to *B. cinerea* infection was assessed. UV-B-treated WT Arabidopsis plants were more resistant to *B.cinerea* and possessed smaller lesion areas compared to –UV-B-treated WT plants, while the F5H mutant (*fah1-7*) developed similar lesion areas on both UV-B and non-UV-B-treated plants, with the lesions on the UV-B-treated *fah1-7* line being significantly higher than that of UV-B-treated WT plants. The authors hypothesized that this branch of the phenylpropanoid pathway was important in regulating UV-B-mediated plant defence against necrotrophic pests, although no studies have been conducted to assess whether or not this is also true for invertebrate pests. It was therefore decided to investigate any effects components of this pathway have in mediating plant defence against invertebrate pests. Instead of continuing work from Demkura and co-workers (2012) with F5H, COMT1 was selected for further study as it is a vital component of the sinapate and lignin biosynthesis pathway located downstream of F5H, and to date no report has been published describing the influence of COMT activity in promoting plant defence against microbial or invertebrate pests, making any discovery on transgenic Arabidopsis lines over-expressing *COMT1* novel.

4.7.2 Few transcripts are commonly regulated by all four treatments

The number of transcripts differentially regulated by all 4 treatments was relatively low (8 and 2 were up- and down-regulated, respectively), however the putative gene functions of these transcripts proved interesting. BnaA06g39660D is proposed to encode the proline dehydrogenase, *EARLY RESPONSE TO DEHYDRATION 5* (*ERD5*), an osmotic stress-responsive gene involved in the conversion of proline to glutamic acid via Δ^1-pyrroline-5-carboxylate (P5C)(Kiyosue, 1996 #90). ERD5, often referred to as *ProDH*, is localised in the mitochondria, and is one of the first enzymes involved in the conversion of proline to glutamic acid. Proline is an osmolyte that accumulates in plant cells upon exposure to drought or salinity stress, with transgenic lines over accumulating proline or mannitol displaying a higher tolerance to salt stress (Kavi-Kishor et al., 2005). Previous studies have reported the presence of ERD5 and additional components of the proline

biosynthesis/metabolism pathway in response to pathogens and pests in plants, with proline itself found to accumulate in response to incompatible plant-pathogen interactions. Indeed, higher levels of this osmolyte were observed around hypersensitive response (HR) lesions in Arabidopsis leaf tissue inoculated with *P. syringae* (Fabro et al., 2004), suggesting that proline perhaps serves as a signalling molecule to aid in the defence response against pests. An increase in proline levels stimulates an increase in expression of *ERD5*, which serves to limit the quantity of the osmolyte in cells. Silencing of *ERD5* has been reported to delay the occurrence of the HR and reduce levels of ROS in Arabidopsis and *N. benth*, leading to decreased resistance against the non-host *P. syringae* pathogen, and its subsequent growth and establishment on plant tissue (Cecchini et al., 2011, Senthil-Kumar and Mysore, 2012). It was therefore hypothesized that the conversion of proline to P5C via ERD5 generates the accumulation of ROS, which lessens the extent of oxidative damage on surrounding photosynthetic tissue, and implicates ERD5 as an important component of plant defence via the HR (Cecchini et al., 2011). *ERD5* has also been found to increase following wounding in WT and *coi1-1* Arabidopsis plants, with *P. rapae* herbivory on WT Arabidopsis sparking a lesser response (Reymond et al., 2000), perhaps by inducing an increase in ROS levels around wound sites.

In addition to *ERD5*, a transcript putatively encoding a zinc-induced facilitator was identified as increasing in expression following all 4 treatments. ZIF1 is involved in Zn homeostasis and sequestration, and tends to be localized in the vacuolar membrane to promote basal Zn tolerance. Metals are known to promote plant defence against pests, and various studies have reported increased resistance of plants to invertebrates and pathogens in the presence of metals. For instance, iron chelators, such as ferritin, serve as a form of basal defence against pathogens, while selenium is lethal to *P. rapae* in *B. juncea*, and toxic to two fungi, *Fusarium* (sp.) and *A. brassicicila.* Interestingly, zinc has previously been documented at effectively deterring *P. brassicae* caterpillars along with *Deroceras carvanae* (Poschenrieder et al., 2006), a member of the *Deroceras* taxonomic genus and Agriolimacidae family of slugs, to which *D. reticulatum* also belongs.

Two additional transcripts in Table 4-8 have previously been reported as JA-responsive genes, and that is the auxin efflux carrier and the alpha/beta-hydrolase (Dombrecht et al., 2007, Hasegawa et al., 2011), however the D-mannose binding lectin, AT1G78820, may be an interesting member of this list, on account of the lectin carbohydrate-binding proteins considered to be defence-related proteins due to their ability to interact with pathogen- and insect-derived carbohydrates (Vandenborre et al., 2011). Addition of lectins into invertebrate artificial diets or their ectopic expression in crops has uncovered their

toxic effect on many members of the Lepidoptera, Coleoptera, Diptera and Hemiptera orders, presumably due to the timely release of lectins upon ingestion by the invertebrate, and their subsequent interaction with carbohydrate structures in the digestive tract of the pest (Vandenborre et al., 2011).

4.7.3 Transcription factors commonly regulated by UV-B radiation and invertebrate herbivory

In this part of the discussion, transcription factors identified as being differentially regulated by UV-B radiation and herbivory from at least one invertebrate will be examined. The decision to merge the results obtained from sections 4.5.4 to 4.5.6 was based on the fact that several transcripts from each section were assigned the same Arabidopsis gene name, based on their sequence similarity. The allocation of the same Arabidopsis gene name to multiple *B. napus* transcripts is not surprising, as the nature of the allopolyploid *B. napus* genome means that a single-copy Arabidopsis gene can potentially have three orthologues in the *B. napus* genome. However, to prevent repetition of the known functions of these genes and enable a more fluid interpretation of the results from the RNA-seq, key transcription factors from the three sections have been discussed at once.

Functional analysis and GO clustering of the Arabidopsis gene ID's assigned to the transcripts commonly up-regulated by UV-B, slug herbivory and *Plutella* herbivory (section 4.5.4), UV-B and slug herbivory (section 4.5.5) or UV-B and *Plutella* herbivory (section 4.5.6) identified 28 transcripts sharing sequence similarity to known Arabidopsis transcription factors in enriched GO categories. It is worth noting at this point that more than 28 transcripts sharing sequence similarity to Arabidopsis transcription factors were identified overall in this study, however, for simplicity reasons, only those that were grouped into enriched annotation clusters were discussed in this chapter. Four of the 28 transcripts are commonly regulated by UV-B, slug herbivory and *Plutella* herbivory, 10 by UV-B and slug, while the remaining 14 were identified as being differentially regulated by UV-B and *Plutella* herbivory in section 4.5.6.

Some of the Arabidopsis genes assigned to these transcripts have previously been implicated in promoting plant defence against invertebrates and/or pathogens. For instance, *WRKY40,* which has been assigned to two transcripts, one commonly regulated by UV-B, slug and *Plutella* herbivory, the other by UV-B and *Plutella* herbivory, encodes a pathogen-induced transcription factor, which, along with *WRKY18*, regulates JA-induced plant defences. Transcriptomic-based studies on WT Arabidopsis and a mutant of

WRKY18/40 infected with the powdery mildew virus, *Golovinomyces orontii*, found that WRKY18 and WRKY40 function in a feedback loop to repress basal defences, with the mutant displaying elevated pathogen-dependent defence responses (Pandey et al., 2010). Further ChIP analysis found that WRKY40 interacts directly with W-box elements in the promoters of regulatory genes, such as *JAZ8,* a repressor of JA-responses. This interaction was found to directly supress *JAZ* transcript accumulation in Arabidopsis, as WT plants possessed substantial increases in the expression of two JA-responsive genes, *LOX2* and *AOS,* following infection with the powdery mildew virus, while the *wrky18/wrky40* mutant did not show any increase in expression of either gene across a 48-hour time course. However, the mutant did display elevated *JAZ* transcript levels, while the WT plants contained a very low abundance of the same transcripts. It was therefore suggested that WRKY40 positively regulates JA-responses by directly controlling the expression of a subset of JA-repressors (Pandey et al., 2010). In addition to *WRKY40,* another WRKY transcription factor thought to be encoded by a *B. napus* transcript commonly up-regulated by UV-B and *Plutella* herbivory was identified. This gene, *WRKY33*, was previously reported to increase in expression, along with *WRKY40*, in Arabidopsis plants infested with aphids (Barah et al., 2013). Over-expression of *WRKY33* has been found to suppress expression of the pathogen-induced *PR-1* gene in Arabidopsis, resulting in plants being more susceptible to *P. syringae*. The *wrky33* mutant is also more susceptible to *B. cinerea* than WT Arabidopsis (Koornneef and Pieterse, 2008), implying that this gene may be involved in promoting plant defence to necrotrophic pathogens. Unfortunately, it is unknown whether or not this gene mediates plant defence against invertebrate pests, and the unfortunate absence of both *WRKY* genes from the initial RNA-seq analysis in 2012 prevented either of them from being selected for further study in Arabidopsis.

Several transcripts share sequence similarity to Arabidopsis genes encoding C_2H_2 zinc finger transcription factors, primarily *ZAT6* (UV-B, slug and *Plutella*) and *ZAT10* (UV-B and *Plutella*). ZAT6 is known to repress primary root growth and regulate phosphate homeostasis by controlling root architecture (Shi et al., 2014), while ZAT10 enhances plant tolerance to salinity, heat and osmotic stress (Mittlera et al., 2006). Expression of *ZAT6* increases in response to SA and pathogenesis (Shi et al., 2014), while *ZAT10* expression was recently reported as increasing in response to wounding or *Spodoptera exigua* herbivory in Arabidopsis, but not in response to *P. rapae* (Rehrig et al., 2014). Possible roles for ZAT6 and ZAT10 in promoting plant defence against invertebrate pests, however, have not to my knowledge been reported, although increased expression of genes encoding C_2H_2 transcription factors in potato plants following invertebrate grazing has

been previously described (Lawrence et al., 2014). Four hours grazing of the generalist *M. sexta* or specialist Colorado potato beetle *Leptinotarsa decemileata* on potato plants led to the expression of *ZFP1* and *ZFP2* increasing by approximately 20 to 80-fold (Lawrence et al., 2014)). Interestingly, application of SA, ABA or JA to potato plants significantly repressed expression of *ZFP2,* while *ZTF1* was not significantly regulated by SA or JA, but was significantly down-regulated by ABA over a 24-hour time course (Lawrence et al., 2014). The responsiveness of these two C_2H_2 zinc finger transcription factors to invertebrate herbivory in potatoes, and the increased expression of *B. napus* transcripts putatively encoding ZAT6 and ZAT10 (sections 4.5.4 and 4.5.6), does not necessarily imply that these transcription factors are involved in promoting plant defence. However, it would have been interesting to study the effects of UV-B radiation on enhancing the defence mechanisms in *ZAT6* and/or *ZAT10* mutants and over-expressing lines against slug and *Plutella* herbivores.

Transcripts assigned the names of several Arabidopsis genes encoding NAC proteins and ethylene-responsive factors were also identified in this study, with three putative *ANAC* transcription factors commonly regulated by UV-B and *Plutella* herbivory (*ANAC001, ANAC019* and *ANAC072*), and one commonly regulated by UV-B and both invertebrate herbivore treatments (*ANAC102*). The NAC proteins are a large family of plant-specific transcriptional regulators that are involved in regulating various plant development processes, such as boundary cell formation in shoot apical meristems, secondary cell wall development and lateral root development, as well as moderating many stress responses (Christianson et al., 2010). *ANAC102* is responsive to cold, drought, salinity and low-oxygen conditions (Christianson et al., 2010), while *ANAC019* and *ANAC072* are drought-, high salinity- and abscisic acid (ABA)-induced transcription factors (Li et al., 2014). Expression of *ANAC072* was previously found to rapidly increase in Arabidopsis following inoculation with the Gram-negative bacteria *Burkholderia cepacia* and the bacteria's associated microbe-associated molecular patterns (MAMPs), but was relatively unaffected by treatment with ET, SA and MeJA (Huang et al., 2012). ANAC102 is a member of the stress-induced ATAF subgroup of NAC domain transcription factors, and is closely related to two genes, *ATAF1* and *ATAF2*, that increase in expression following JA treatment in rice (Ohnishi et al., 2005) and MeJA in Arabidopsis (Delessert et al., 2005). In the latter study, *ATAF2* expression was found to peak rapidly after wounding, and was induced by SA and pathogenesis. Over expression of *ATAF2* in Arabidopsis led to repression of several pathogenesis-related genes such as *PDF1.2, PR1* and *PR4*, implying that this transcription factor represses pathogen-induced defence responses in plants (Delessert et

al., 2005). While ANAC102 has not been identified as wound-responsive in rice and Arabidopsis, it is possible that the identified *B. napus* transcript in section 4.5.4 shares more functional similarity to ATAF1 or ATAF2 than ANAC102. While the three *ANAC* genes described this far do not have evident roles in promoting plant defence against invertebrate pests, *ANAC019* has previously been proposed to work alongside *ANAC055* to regulate JA-responses downstream of MYC2 in Arabidopsis (Bu et al., 2008). Expression levels of *ANAC019* increase in Arabidopsis following treatment with MeJA, a response that was shown to be dependent on both COI1 and MYC2, and the encoded *ANAC019* protein binds directly to the promoter region of the JA-responsive gene, *VSP1*, indicating a putative role of ANAC019 in regulating JA-response pathways in Arabidopsis. The expression of select JA-responsive genes was reduced in Arabidopsis *anac019 anac055* double mutants compared to the WT plants, whereas over-expression of *ANAC019* enhanced expression of these genes.

The transcriptomic analysis of *B. napus* revealed several interesting early-induced transcription factors that may promote the convergence of UV-B- and herbivore-induced pathways, perhaps with the aim of heightening plant defence mechanisms against invading pests. Unfortunately, the absence of these transcripts in the original RNA-seq experiment in 2012 prevented any of these genes from being over-expressed in Arabidopsis, however some of these genes, particularly the *WRKYs* and the proline dehydrogenase-encoding *ERD5* would have been selected for over-expression if they were identified in 2012, based on the information obtained about these proteins in plants from publications.

4.7.4 Transcripts commonly regulated by slug and *Plutella*

In addition to identifying early-induced transcriptional regulators common between UV-B, slug herbivory and *Plutella* herbivory, the genetic overlaps elicited by the two herbivore pests were also examined in *B. napus.* Several studies have previously investigated the transcriptomic overlaps inflicted by herbivory of two invertebrate species on plants, usually examining differences and similarities between a generalist and a specialist feeder (Reymond et al., 2004, Voelckel and I.T., 2004) or a phloem feeder and a leaf-chewing invertebrate (Kempema et al., 2007). No studies, to the best of my knowledge, have investigated the effects of slug herbivory on the transcriptome of a plant. Therefore, some of the data obtained from this study is novel.

A relatively small overlap exists between the transcripts commonly regulated by both invertebrate herbivores in the second alignment (Figure 4-9A). Separation of these

transcripts into up-regulated and down-regulated lists (Figures 4-9B and C) facilitated functional of the putative Arabidopsis gene annotations assigned to the transcripts. Annotation clustering identified 16 transcripts that putatively encode transcriptional regulators (Table 4-16). As the comparison between transcripts commonly regulated by slug or *Plutella* herbivory in this section omits any regulatory effects of UV-B or MeJA on the transcripts from the dataset, transcripts previously identified as being commonly regulated by invertebrate herbivory and UV-B radiation are found in this section of the chapter, and as such the assigned gene function of some of the transcripts have already been discussed (e.g. *WRKY40, ANAC102* and *ZAT6*). Some of the genes that have not yet been identified or discussed in this chapter include *ANAC034*, *CGA1* and the two *ARR* genes.

ARABIDOPSIS RESPONSE REGULATOR (ARR) proteins, are known to negatively regulate SA-induced plant defence, and can be separated into two groups: Type-A ARRs and Type-B ARRs which differ by the length of their C-terminal regions (Type-A's have shorter C-terminal regions, and act as negative regulators of cytokinin signaling, while Type-B have elongated C-terminal regions with a DNA binding domain to directly mediate transcription of cytokinin-responsive genes). Increased resistance to many pathogens, such as *P. syringae* pv. *tomato* DC3000, is facilitated in Arabidopsis by type-B ARRs and SA. Type-A ARRs on the other hand, of which there are 10 family members in Arabidopsis, negatively regulate cytokinin signaling and plant defence against bacterial pathogens that activate the SA pathway. ARR7 and ARR9 are both type-A ARRs, while ARR1 is a type-B, indicating that both invertebrates activate a series of defence regulators that, in all effectiveness, work antagonistically to one another. As these proteins appear to positively and negatively regulate plant defence against microbial pests that activate the SA pathway, it may be possible that they then, in turn, negatively and positively regulate JA-responsive signaling events. While it is therefore highly unlikely that over-expression of type-B ARRs would heighten plant defence against invertebrate and necrotrophic pests in a UV-B-dependent manner, it would be interesting to note any change in levels of JA and expression of associated marker genes in transgenic lines affected in the expression of type-A and type-B ARRs, to evaluate any roles they could have in regulating plant defence against *Plutella* and/or slug herbivores.

An additional gene associated with cytokinins was also shown as being differentially regulated by slug and *Plutella* herbivory, *CGA1*. This gene is a GATA transcription factor known to be involved in regulating the development, growth and division of chloroplasts in plants (Chiang et al., 2012), its expression found to increase in response to the

phytohormone, cytokinin, along with white and red light in a phyA- and phyB-dependent manner (Argueso et al., 2010).

Chloroplasts are the site of biosynthesis of JA and SA, and therefore serve as an important organelle in plant defence (Nomura et al., 2012). It was recently discovered that detection of PAMPs induces transient Ca^{2+} signalling events in chloroplasts via a calcium-sensing receptor (CAS), which then promotes transcriptional reprogramming to promote basal resistance and the HR (Nomura et al., 2012). However, a direct role of CGA1 in this defence is unknown. Cytokinins, on the other hand, have been suggested to positively regulate JA/ET signalling events by effectively suppressing PAMP-induced responses in chloroplasts (Robert-Seilaniantz et al., 2007). Putative models displaying the interplay of hormones in plant defence have suggested that cytokinins and auxin function in a similar manner, and inhibit SA-regulated responses (such as the HR) to promote plant resistance against necrotrophic pathogens, and presumably herbivore pests (Robert-Seilaniantz et al., 2007). Although strictly hypothetical, the presence of putative *CGA1* transcripts in this study could be indicative of an increase in the levels of cytokinins, although whether or not this is true, and more importantly, if its presence promotes JA/ET-regulated defence responses, is unknown.

The up-regulation of several genes by slug and *Plutella* herbivory known to be associated with cytokinin responses suggests that these herbivores not only target JA-signalling pathways, but also those affected by this phytohormone. Cytokinin has been implicated in priming plant defence against invertebrate herbivory, with one study in particular observing an increase in levels of JA and linolenic acid in response to exogenous application of cytokinin on Poplar, along with increased accumulation of wound-responsive transcripts, such as *AOS,* PI- and chitinase-encoding genes (Dervinis et al., 2010). The weight of gypsy moth (*Lymantria dispar*) caterpillars was also shown to decrease after feeding upon Poplar treated with cytokinin, suggesting that cytokinin-signalling can negatively impact invertebrate herbivore fitness (Dervinis et al., 2010).

4.7.5 Differences between the two alignments

To assess how similar the results from the two RNA-seq read alignments in 2012 and 2014 were, in relation to the number of transcripts found to be significantly regulated by the treatments and the putative annotations of these transcripts, a Venn diagram was generated using the Arabidopsis gene ID's assigned to transcripts identified as being differentially regulated by at least one treatment from each alignment (Figure 4-11). Use of the

Arabidopsis gene IDs over the transcript IDs derived from the Brassica Unigene and *B. napus* reference genomes had to be employed for this comparison, as the Arabidopsis IDs were the only terms common to both datasets, allowing the comparison to be made between the two alignments. It is therefore important to note that only those transcripts assigned a putative Arabidopsis gene annotation are found in Figure 4-11. It should also be remembered that the use of different cut-off parameters in each dataset, and the different number of Unigene and *B. napus* gene IDs in the reference 'genomes,' affected the degree of overlap between the two datasets.

Approximately 40% of differentially regulated transcripts from each alignment (38% and 43%, respectively) overlapped with one another (Figure 4-11), suggesting that many effects of each treatment on the genetic reprogramming of the *B. napus* genome was not detected in each alignment. Out of the transcripts classed as being significantly regulated by one or more treatments in 2012 and 2014, a large number were associated with light- and hormone-responses, including *HY5* and *MYC2*. What's more, the regulation of these transcripts appeared relatively similar in each alignment, although the presence of multiple putative *B. napus* orthologues of each Arabidopsis gene made it difficult to assess any differences in expression of specific *B. napus* genes in response to a given treatment from 2012 and 2014.

What was of particular interest was the recorded trend in expression of certain transcripts in each alignment. The 22 transcripts sharing sequence similarity to the three genes selected for over-expression in section 4.4.2 were examined for this purpose (Table 4-19). Different numbers of Unigene and *B. napus* gene identifiers sharing sequence similarity to Arabidopsis *COMT1* and *VTC2* were found in this study, while *ELI3-2* was assigned to three Unigenes and *B. napus* IDs. The expression profiles for all Unigene and *B. napus* identifiers for each Arabidopsis gene varied slightly in response to the 4 treatments, a result that may be due to different efficiencies in sequence alignment of the reads to the identifiers and subsequent transcript annotation, or due to overlapping sequences of multiple *B. napus* genes to one Brassica Unigene. As the Brassica 95K Unigene is composed of assembled ESTs and singletons that may not span the whole sequence of a *B. napus* gene, it is possible that multiple reads obtained from an RNA-seq run that originate from different loci in *B. napus* (and may be not be similarly regulated by a given treatment) share conserved nucleotide sequences which align to one particular Unigene. The combination of the varied expression profiles of these reads may affect interpretation of how this particular Unigene (and putative Arabidopsis orthologue) responds to a treatment, and it is possible that the expression profile of a single Unigene represents that

of two or more *B. napus* genome identifiers, as is hypothesised to have taken place with the putative *VTC2* orthologues in *B. napus*: EX043301, BnaC01g19060D and BnaC07g40500D (section 4.6.2). The expression of EX043301 was shown to significantly increase in response to UV-B and slug treatment and decrease following *Plutella* herbivory (Table 4-19), while BnaC01g19060D and BnaC07g40500D exhibited differential responses to the 4 treatments that partially overlapped with those seen for EX043301. EX043301, BnaC01g19060D and BnaC07g40500D were shown to possess sequence similarity over an approximate 400bp region (Figure 4-12), suggesting that reads obtained from the two *B. napus* genes now referred to as BnaC01g19060D and BnaC07g40500D may have exhibited a suitable level of identity to the sequence of EX043301, therefore accounting for the partial similarities in the expression profiles of the Unigene and *B. napus* identifiers.

As alignment of reads obtained from RNA-seq to the sequenced *B. napus* genome may arguably provide more accurate findings than alignment to the Brassica 95K Unigene, access to this resource facilitated progression of this study before publication of the *B. napus* genome, and as such was an invaluable resource despite generating different results from those seen in 2014.

4.7.6 Conclusions and outlook

The findings in this chapter have provided insight into the genetic overlap of UV-B- and herbivory-responses in *B. napus*. Several early-induced transcription factors, such as *WRKY40, ZAT10* and *CGA1*, were identified, with some genes previously reported as being responsive to at least one of the treatment studied in this investigation. To further assess the potential role of select genes in mediating UV-B-enhanced resistance, three were chosen for over-expression in Arabidopsis and subjected to bioassay experiments following treatment with or without UV-B radiation. However, before the results from these experiments are touched upon (Chapter 6), the findings from an additional "omics"-based study on overlaps in UV-B- and wound-induced pathways in *B. napus* will be presented.

Chapter 5: Investigating Metabolic Overlaps Between UV-B and Wound Response Pathways in *Brassica napus*

5.1 Introduction

The transcriptomic analysis in chapter 4 provided some insight into the putative transcription factors that are regulated commonly by UV-B radiation and invertebrate herbivory. To expand upon this information and identify components of biological pathways that accumulate in response to these treatments, a metabolomic approach was employed using reversed-phase HPLC.

Targeted and global metabolite approaches have previously been conducted to investigate the effects of UV-B radiation, invertebrate herbivory and MeJA treatment on the metabolite profile of numerous plants species. Studies on UV-B-irradiated Arabidopsis (Stracke et al., 2010b, Kusano et al., 2011, Demkura and Ballaré, 2012), *Populus trichocarpa* (Warren et al., 2003), European silver birch (*Betula pendula*)(Lavola et al., 1998)(Morales et al., 2010), maize (Casati et al., 2011) and broccoli plants (Mewis et al., 2012) revealed an increase in the abundance of many phenolic compounds, particularly flavonoids such as quercetin glucosides (Stracke et al., 2010b). The effects of herbivory and JA treatment on the plant metabolome have also been documented, with both MeJA and *Plutella* herbivory found to increase the abundance of malate-conjugated hydroxycinnamates, especially caffeoyl, coumaroyl, feruloyl, and sinapoyl malates, along with indole glucosinolates and indole-3-acetic acid in *B. rapa* (Liang et al., 2006a, Widarto et al., 2006). Few studies have compared responses elicited by UV-B radiation or herbivory on plant metabolic responses, however Izaguirre and co-workers revealed that separate treatments of UV-B radiation and simulated herbivory induced similar levels of chlorogenic acid (CGA) in *N. longiflora* but not in *N. attenuata* (Izaguirre et al., 2007), indicating that variable responses to these stimuli may exist between closely related plant species. Recent work investigating the combined effects of UV-B radiation and invertebrate herbivory on glucosinolate levels in broccoli sprouts reported a depletion in the quantity of aliphatic and indole glucosinolates in these plants compared to levels induced by UV-B or herbivory alone (Mewis et al., 2012). This result indicates that combining the two stimuli does not have an additive effect but rather an overall negative effect on glucosinolate accumulation in broccoli sprouts, although the ability of UV-B to reduce plant susceptibility to herbivory suggests that lower levels of select glucosinolates

in such situations do not impair plant defence.

It is known that reprogramming events at the genetic level do not always have repercussions at the metabolite level, and as such transcriptomic studies alone may not provide accurate insight into various biological pathways in plants, such as plant defence (Mewis et al., 2006). It was therefore deemed appropriate to carry out a metabolomic study on *B. napus* plants treated with UV-B radiation, invertebrate herbivory or MeJA to complement the results presented in chapter 4 from the RNA-seq. As many studies tend to focus on the levels of specific plant compounds in response to these treatments, an untargeted, global metabolomics approach was adopted to provide greater insight into changes in *B. napus* following treatment with the aforementioned stimuli, by studying adjustments in the abundance of numerous compounds at the one time, to hopefully identify signalling components not previously reported. While global metabolomics is able to provide the researcher with a broader view of plant responses to a given treatment in comparison to targeted metabolomics, one of the downsides associated with this approach is that a large amount of time is required to analyse and identify peaks (Van der Hooft et al., 2013). As this study was conducted relatively late on in the project, time restraints unfortunately prevented in depth data analysis, and as such only a small number of compounds are described. This chapter presents a brief description of the methods used to examine metabolic changes in *B. napus,* and details some of the results obtained.

5.2 Metabolite analysis of *B. napus* plants

To obtain an overview of the metabolomic responses to UV-B radiation, MeJA treatment, slug or *Plutella* herbivory, a global metabolite profile of 3-week old *B. napus* plants exposed to separate treatments was obtained in triplicate using reverse-phased chromatography at the Glasgow Polyomics Facility. Plants were grown under 70 μmol m^{-2} s^{-1} white light for approximately three weeks before being treated with 4 different stimuli for 24 hours (Table 5-1). All samples were harvested at the end of this 24-hour period, and compounds were extracted using an acidified methanol protocol outlined by De Vos and co-workers (De Vos et al., 2007).

Reversed-phase HPLC was carried out on all samples using an Orbitrap™ Elite (Thermo Scientific) mass spectrometer with a C18 column in negative ionisation mode. Samples were injected into a nonpolar stationary phase (i.e. C18 column) and eluted with a biphasic linear gradient of 5% to 50% acetonitrile, 0.1% formic acid and water. The length of time taken for different components of the test samples to pass through the column is classed as

the retention time (RT) of the compound, and is influenced by the chemical nature of the compound and its interaction with both the eluent and the stationary phase of the sorbent. In this case, less polar compounds possessed a longer RT, while polar molecules were eluted more rapidly (and had a shorter retention time). The RT is therefore indicative of the nature of each compound, and shall be referred to throughout this chapter, particularly when drawing the reader's attention to peak location on chromatograms.

Table 5-1: Description of *B. napus* treatments used for reversed-phase chromatography

Treatment	Description of treatment
3 µmol m^{-2} s^{-1} UV-B	Plants irradiated under UV-B only conditions.
100 µM MeJA (0.01% EtOH / UN65)	Exogenous application of MeJA (0.01% EtOH / UN65) to whole plant (~5 mL/plant).
Slug herbivory	Continuous single slug grazing on one true leaf for 24 hours.
***Plutella* herbivory**	Continuous grazing by three 2nd instar *Plutella* larvae on one true leaf for 24 hours.
0.01% EtOH / UN65	Exogenous application of 0.01% EtOH / UN65 to whole plant (~5 mL/plant).
Untreated control	Plants maintained under white light conditions with no exposure to UV-B, invertebrates of MeJA.

The obtained full-scan mass (or mass over charge, i.e. *m/z*) of compounds and masses of their fragmentation data were analysed using Xcalibur™ v2.2 software (Thermo Scientific) and processed with an in-house Glasgow Polyomics R-based pipeline to align all LC-MS peaks based on their mass and RT. Comparisons were made between treatments and controls to identify potentially interesting metabolites that displayed at least a ≥ 1.5-fold increase in abundance. Masses were initially annotated with candidates from the KEGG compound database. Manual examinations of full scan and fragmentation spectral data facilitated the assignment of the most likely elemental formulae to masses with differential abundances, and subsequent annotations were assigned by referring to publications and additional online resources such as MassBank and ChemSpider for chemical structure clarification.

As HPLC LC-MS was conducted in the negative-ionisation mode ($[M-H]^-$), the *m/z* and putative elemental formulae of these compounds are presented in the $[M-H]^-$ format (e.g. C_2H_6 would be presented as C_2H_5 due to the absence of a proton, and the *m/z* would be 29 as opposed to 30) unless stated otherwise.

5.3 Initial analysis reveals overlaps and differences in the metabolic profile of *B. napus* regulated by different treatments

A total of 2,215 compounds were detected in this study, 1,600 of which were assigned putative annotations and chemical formulas using the KEGG compound database. A principle component analysis (PCA) chart was generated using the obtained profiles of all compounds, allowing the spread of variability between the three replicates of each treatment to be visualised, along with any overlapping effects of the 6 separate treatments (Figure 5-1). The three untreated samples, represented by yellow circles, are clustered relatively close to one another and also to two of the EtOH/UN65 replicates that are depicted as red circles. The relatively close clustering of the untreated and EtOH/UN65 replicates, along with the considerable distance between EtOH/UN65 replicates and MeJA replicates (blue circles), indicates that applying a solution of 0.01% EtOH/UN65 to *B. napus* plants does not have a major effect on the plant's metabolome, and that any changes observed in plants treated with 100 μM MeJA (0.1% EtOH/UN65) is highly likely to be down to the presence of the JA derivative in the exogenous solution. The slug herbivory and *Plutella* herbivory replicates (purple and green circles, respectively) are clustered relatively close to one another, however there is a noticeable spread in the *Plutella* herbivory replicates, with one in particular located next to two MeJA replicates. The spread of *Plutella* herbivory replicates is not necessarily a surprising find, as variability across replicates is almost unavoidable when working with live, mobile organisms such as invertebrates. The spread in UV-B replicates is surprising; such a variation was not expected between biological replicates exposed to the same static treatment on the same day. Despite this variation, the UV-B-treated samples elicit very different responses in *B. napus* as compared to the MeJA-treated samples, while the slug-treated samples and majority of *Plutella*-treated replicates appear to cluster closer to the UV-B replicates than the MeJA replicates.

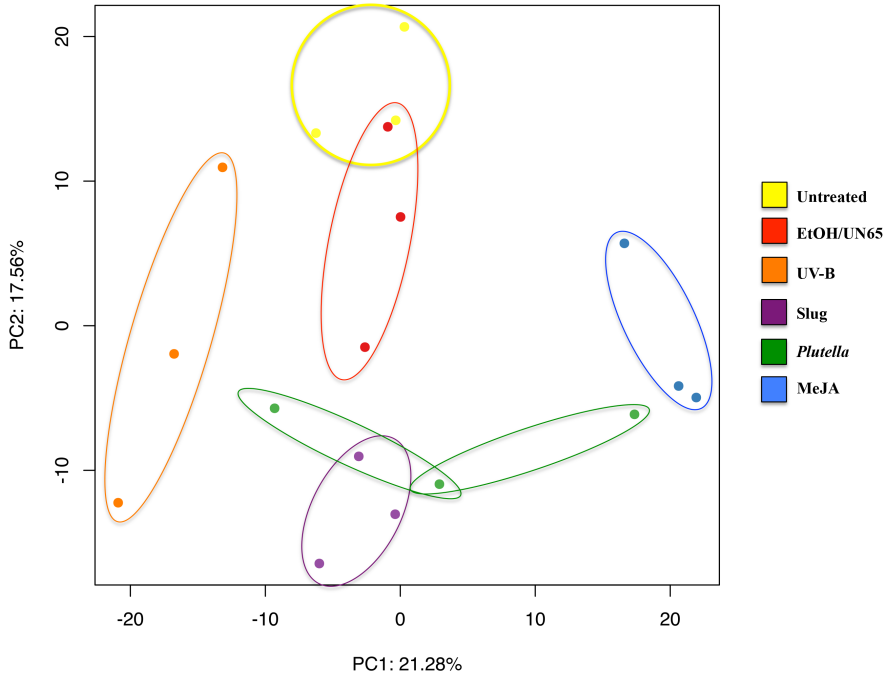

Figure 5-1: PCA chart displaying the spread of variability across the three *B. napus* replicates for each of the 6 treatments.

Following on from the PCA, compounds were selected for further analysis based on their minimum fold change in peak intensity (≥ 1.5) and adjusted *p*-value (≤ 0.05) that corrects for any false positives obtained from the multiple t-tests used to calculate the *p*-value. The compounds possessing these criteria were depicted in a Venn diagram (Figure 5-2A), and those that increased in abundance in response to two or more of treatments were listed alongside their mass, RT and fold change in peak intensity for each treatment (Figure 5-2B). For convenience, a compound number (CN) has been assigned to each metabolite, to enable easier identification of these compounds later in the chapter. Putative elemental formulas derived from KEGG and by manual investigation have also been listed where possible. Additional information on putative characteristics of selected compounds listed in Figure 5-2B along with those that are specifically regulated by only one treatment (Table 5-2), can be found in Appendix 2. The peak IDs associated with each compound can also be found here.

A total of 93 compounds are present in the Venn diagram in Figure 5-2, twenty-six of which accumulate in response to 2 or more of the studied stimuli. Structural examination of these peaks and their fragmentation data allowed putative annotations to be assigned to a selection of compounds. Some compounds are known UV-B-responsive metabolites and many have not, to my knowledge, been previously described.

A

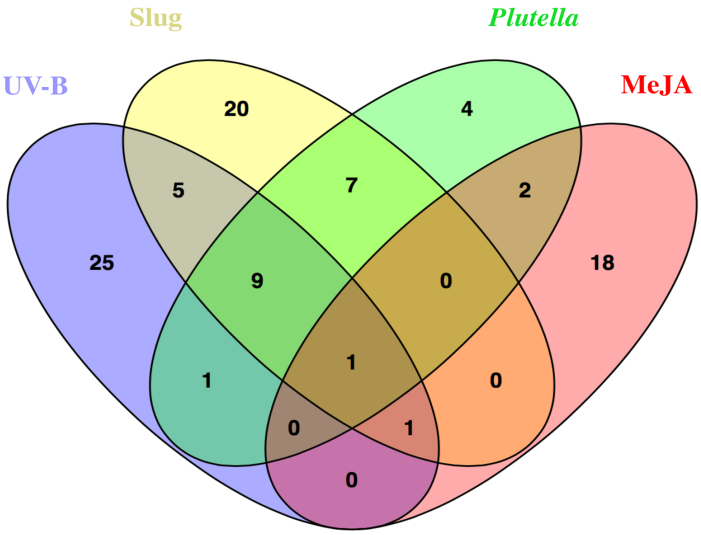

B

CN	Proposed KEGG EF ([M-H]⁻)	Putative EF ([M-H]⁻)	RT (s)	Mass	Fold Change in Peak Intensity			
					3 µmol m⁻² s⁻¹ UV-B	Slug Herbivory	*Plutella* Herbivory	100 µM MeJA
1	N/A	N/A	2407.95	104.9539	2.15	2.03	2.18	2.18
2	N/A	C14H29O7Cl	1024.01	343.1524	2.20	5.53	3.63	1.10
3	N/A	N/A	164.75	158.9786	2.34	2.54	1.83	1.31
4	C15H22O9	C15H22O9	953.61	345.1186	3.13	12.78	5.34	1.57
5	N/A	C14H14O9	887.54	325.1500	3.25	9.14	5.39	1.53
6	N/A	N/A	1812.90	436.1794	3.46	3.23	3.90	0.74
7	C6H8O7	N/A	218.69	191.0197	3.49	2.77	2.68	0.57
8	C6H8O7	N/A	143.72	191.0197	6.67	4.46	5.04	0.50
9	N/A	N/A	145.98	171.9739	11.57	11.71	9.15	0.45
10	C17H20O9	C17H20O9	981.45	367.1029	49.70	48.88	24.43	1.14
11	C23H31ClO6	N/A	1815.53	437.1731	3.21	3.03	1.82	2.20
12	N/A	N/A	1137.34	393.0928	4.28	3.12	2.26	1.40
13	C16H14F3N5O	C17H19NO7	1050.33	348.1084	8.04	2.95	1.36	1.19
14	C23H29NO12	N/A	995.96	510.1608	8.97	8.78	2.70	1.74
15	N/A	C14H24O12S	1011.41	415.0908	10.90	4.79	2.89	1.34
16	N/A	N/A	2046.91	328.7560	1.97	1.48	1.86	0.88
17	N/A	N/A	1827.82	435.1760	1.27	1.51	1.53	1.18
18	N/A	C20H36O9	1828.59	419.2280	1.40	3.22	2.08	1.38
19	N/A	C20H36O9	1856.51	419.2280	1.41	3.35	2.03	1.40
20	N/A	N/A	869.11	367.1604	2.02	4.71	3.91	0.96
21	N/A	C14H27O8Cl	891.64	357.1317	1.31	5.10	3.98	1.44
22	N/A	C18H35O8Cl	1723.78	413.1940	1.52	5.54	2.92	1.02
23	N/A	N/A	1089.14	353.1812	1.85	8.03	5.03	1.44
24	N/A	N/A	2102.88	483.2720	1.54	3.66	40.33	29.00
25	N/A	C18H20N4OS3	820.46	403.0729	0.85	1.56	148.99	8.89
26	C5H4O3	N/A	157.44	111.0089	4.54	3.34	0.27	24.33

Figure 5-2: *B. napus* compounds increasing in abundance following UV-B radiation, MeJA treatment or invertebrate herbivory. **A**, Venn diagram of compounds with an adjusted *p*-value ≤ 0.05 and fold change in peak intensity ≥ 1.5 in response to at least one treatment, and the degree of metabolic overlap induced by these stimuli. **B**, table listing the putative elemental formulas (EFs; $[M-H]^-$) and fold change in peak intensity of compounds that accumulate in response to at least two treatments by ≥ 1.5-fold with adjusted *p*-value ≤ 0.05 (highlighted in blue). EFs calculated by KEGG and manually. RT, retention time (seconds); *m/z*, molecular mass ($[M-H]^-$); CN, compound number.

5.4 Phenylpropanoid-derived metabolites are responsive to both UV-B radiation and invertebrate herbivory

A selection of compounds identified in this study, the majority of which increased in abundance following exposure to UV-B radiation or subjection to invertebrate herbivory, were thought to be products of the phenylpropanoid pathway. Most of these compounds, including sinapoyl glycoside derivatives, feruloylquinic acids and CGAs, have previously been found to increase in abundance following treatment with UV-B radiation or wounding (Lavola, 1998, Demkura et al., 2010), providing some confidence in the results obtained from this study. Chromatogram and fragmentation analysis of these compounds is presented below.

5.4.1 Feruloylquinic acid derivatives increase in response to herbivory and UV-B radiation

Two compounds, numbers 10 and 20 listed in Figure 5-2B, were found to possess parental ion masses of 367.1029 and 367.1604 ($[M-H]^-$), respectively, indicating that they may be feruloylquinic acids or isoferuloyl quinic acid derivatives (Kuhnert et al., 2010)(Figure 5-3A and C). Their identity was confirmed upon examination of fragmentation data, as the characteristic fragment ions of feruloylquinic acids at *m/z* 191, 173 and 175 ($[M-H]^-$) were present (Figure 5-3B and D). Compound number 10 (thought to possess the elemental formula $C_{17}H_{20}O_9$, $[M-H]^-$) exhibits an approximate 50-fold increase in peak intensity in response to UV-B radiation and slug herbivory, and a slightly less but still significant ~ 25-fold increase following *Plutella* herbivory. The double peaks shown in the chromatogram for this compound (Figure 5-3C) are a result of the incomplete separation of isoferulic and ferulic acid isomers, which typically present identical MS spectra in the negative ion mode with molecular ions peaking at *m/z* 193 (Kuhnert et al., 2010). The second compound, number 20 (Figure 5-3B), has a slightly shorter RT than compound number 10 (approximately 2 minutes shorter), and a different ratio between the *m/z* peaks 173.0456/191.056 ($[M-H]^-$) to compound number 10 (Figure 5-3D). This compound is thought to represent two isomers of the feruloylquinic acid, namely 3-O-feruoyl/isoferuoylquinic acid.

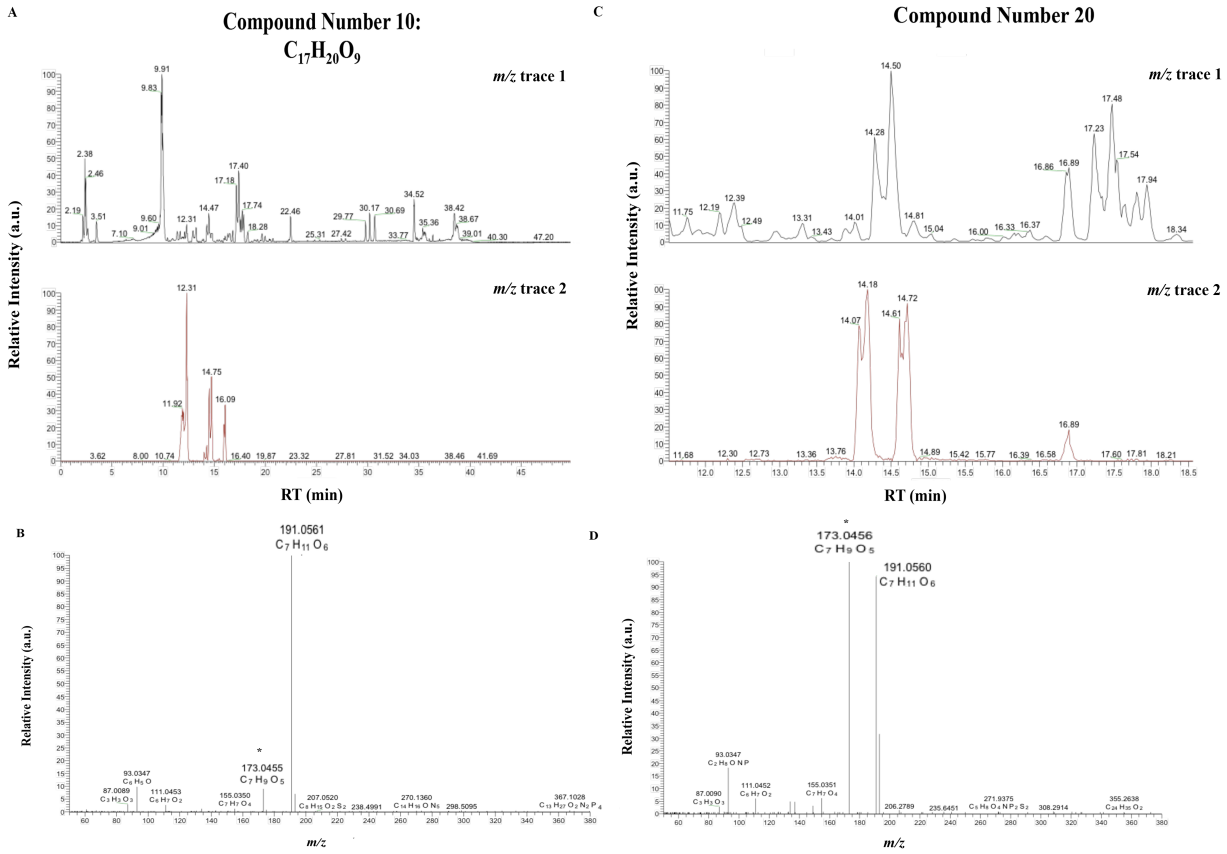

Figure 5-3: Chromatogram and fragmentation data of compound numbers 10 and 20, putative feruloylquinic acid derivatives. A, the base peak chromatograms (RT window 0-50 mins) of compound number 10 assigned the putative elemental formula $C_{17}H_{20}O_9$ ($[M-H]^-$) which possesses an RT of approximately 16.35 mins in MS^2 and undergoes incomplete separation of isomers in *m/z* trace 2 and **B**, fragmentation of this compound. **C**, the base peak chromatograms (RT window 11.5-18.5 mins) of compound number 20 which peaks at an RT of 14.5 mins in MS^2 and undergoes incomplete separation of isomers in *m/z* trace 2 and **D**, fragmentation data of this compound. Relative peak intensity is provided in arbitrary units. * indicates the difference in peak intensity of *m/z* 173 between the two compounds in **B** and **D**.

An additional compound believed to be 5-hydroxyferulic acid was found to be responsive to both UV-B radiation and invertebrate herbivory. However, as the adjusted *p*-value for this compound exceeded 0.05 for both herbivores, it was not classed as being differentially regulated by 2 or more treatments, and is therefore absent from Figure 5-2B and listed in Table 5-2 (compound number UV6). This compound possesses a mass of 209.0454 and elemental formula of $C_{10}H_9O_5$, which matches that of 5-hydroxyferulic acid (Fiehn et al., 2000).

Chromatograms reveal how this compound, with an RT of approximately 14.2 min, is located next to poorly separated isomers (Figure 5-4A), making its analysis challenging. Its fragmentation data is indicative of hydroxyferulic acid methyl ester (Figure 5-4B), however it cannot be concluded whether or not it is 5-hydroxyferulic acid, and not perhaps

3-hydroxyferulic acid. This compound is thought to be a fragment of a larger compound with a mass of 383 ($[M-H]^-$) and elemental formula $C_{17}H_{19}O_{10}$ (Figure 5-4C). This putative parental ion may possess a structure similar to what is depicted in Figure 5-4C, however better separation of the isomer peaks and clearer fragmentation data is required to gain more insight into the nature of this compound.

Compound Number	Putative EF ($[M-H]^-$)	RT (s)	Mass (*m/z*)	Fold Change in Peak Intensity			
				3 µmol m^{-2} s^{-1} UV-B	**Slug Herbivory**	***Plutella* Herbivory**	**100 µM MeJA**
UV5	**$C_{15}H_{26}O_{12}S$**	1213.64	429.1065	**3.13**	1.73	1.12	0.88
UV6	**$C_{10}H_{10}O_5$**	854.84	209.0454	**3.25**	2.63	1.78	0.91
UV7	**$C_{17}H_{22}O_{10}$**	850.66	385.1134	**4.61**	2.04	1.81	1.78
UV20	**$C_{21}H2_6O_{11}NCl$**	1164.06	502.1120	**23.85**	1.15	0.77	0.98
UV22	**$C_{16}H_{19}NO_7Cl$**	1246.59	372.0849	**58.20**	1.23	0.76	1.47
S13	**$C_{16}H_{29}O_8$**	1240.60	349.1862	1.30	**3.94**	2.18	2.15
S18	**$C_{20}H_{35}O_9$**	1914.86	419.2279	1.38	**5.83**	2.55	2.74
S19	N/A	1875.43	465.2333	1.68	**7.27**	3.44	2.64

Table 5-2: Selection of *B. napus* compounds examined that increase by ≥ 1.5-fold (adjusted *p*-value ≤ 0.05) in response to either UV-B or slug treatment. Fold change in peak intensity is provided for each compound in response to the 4 treatments, and the peaks classed as significantly regulated (≥ 1.5-fold, adjusted *p*-value ≤ 0.05) are highlighted in bold underneath the appropriate treatment (UV-B or slug herbivory). Putative elemental formulas (EFs; $[M-H]^-$) were assigned to compounds via manual investigations, while the compound without an EF was unable to be fully annotated. RT, retention time (seconds); *m/z*, mass of compound ($[M-H]^-$).

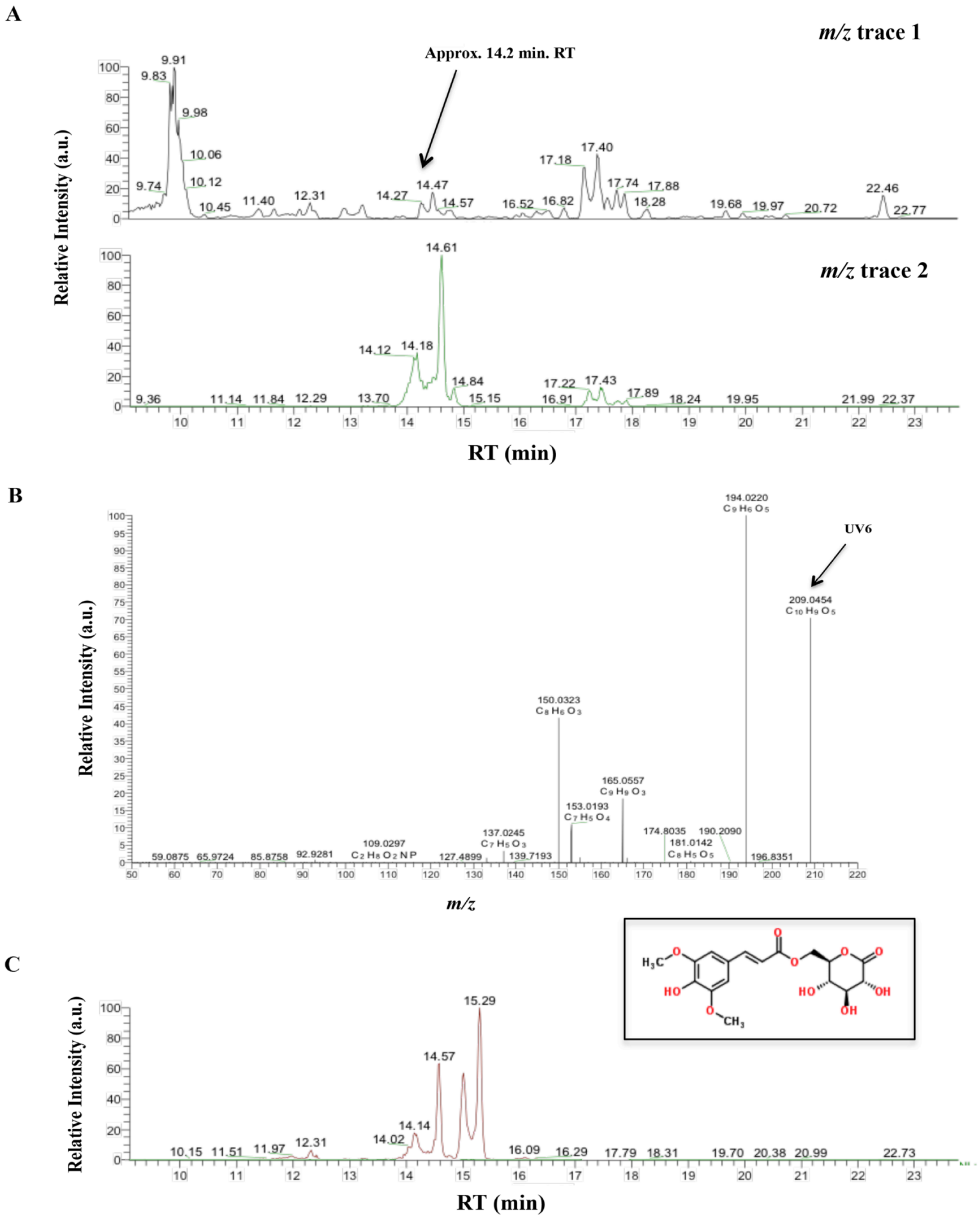

Figure 5-4: Chromatogram and fragmentation data of compound number UV6, a putative hydroxyferulic acid. **A**, location of compound number UV6 possessing an RT of approximately 14.2 min and mass of 209 in base peak chromatogram *m/z* trace 1 (mass range 115-1000; RT window 9-23.5 min) and its enhancement in *m/z* trace 2 (mass range 209.0442-209.0462; RT window 9-23.5 min). **B**, fragmentation analysis reveals the elemental formula of this compound as being $C_{10}H_9O_5$ ($[M\text{-}H]^-$), and **C**, the larger parental compound with mass 383 and elemental formula of $C_{17}H_{19}O_{10}$ ($[M\text{-}H]^-$), along with putative schematic of this compound's chemical structure. Relative peak intensity is provided in arbitrary units.

5.4.2 A sinapoyl glycoside compound accumulates in response to UV-B radiation

An additional compound proposed to originate from the phenylpropanoid pathway as a sinapoyl glycoside was shown to accumulate in response to all treatments, exhibiting a ≥ 1.5-fold increase in peak intensity following UV-B radiation (Figure 5-5A). This

compound, listed in Table 5-2 with the compound number UV7, was identified from a chromatogram displaying several compounds with double peaks that are indicative of phenolic acid glycoside-like compounds (Figure 5-5B). The compound in question that was identified as being sensitive to UV-B radiation has an RT of approximately 850 seconds (14.1 mins), and is located in the middle of the larger peaks shown in Figure 5-5B. Fragmentation data revealed the elemental formula of this compound as being $C_{17}H_{21}O_{10}$ (Figure 5-5C), while analysis of the larger peaks seen in Figure 5-5B identified a sinapoyl peak ($C_{11}H_9O_4$) at *m/z* 205.0505 in negative ionisation mode (Figure 5-5D), suggesting the presence of sinapoyl glycoside compounds.

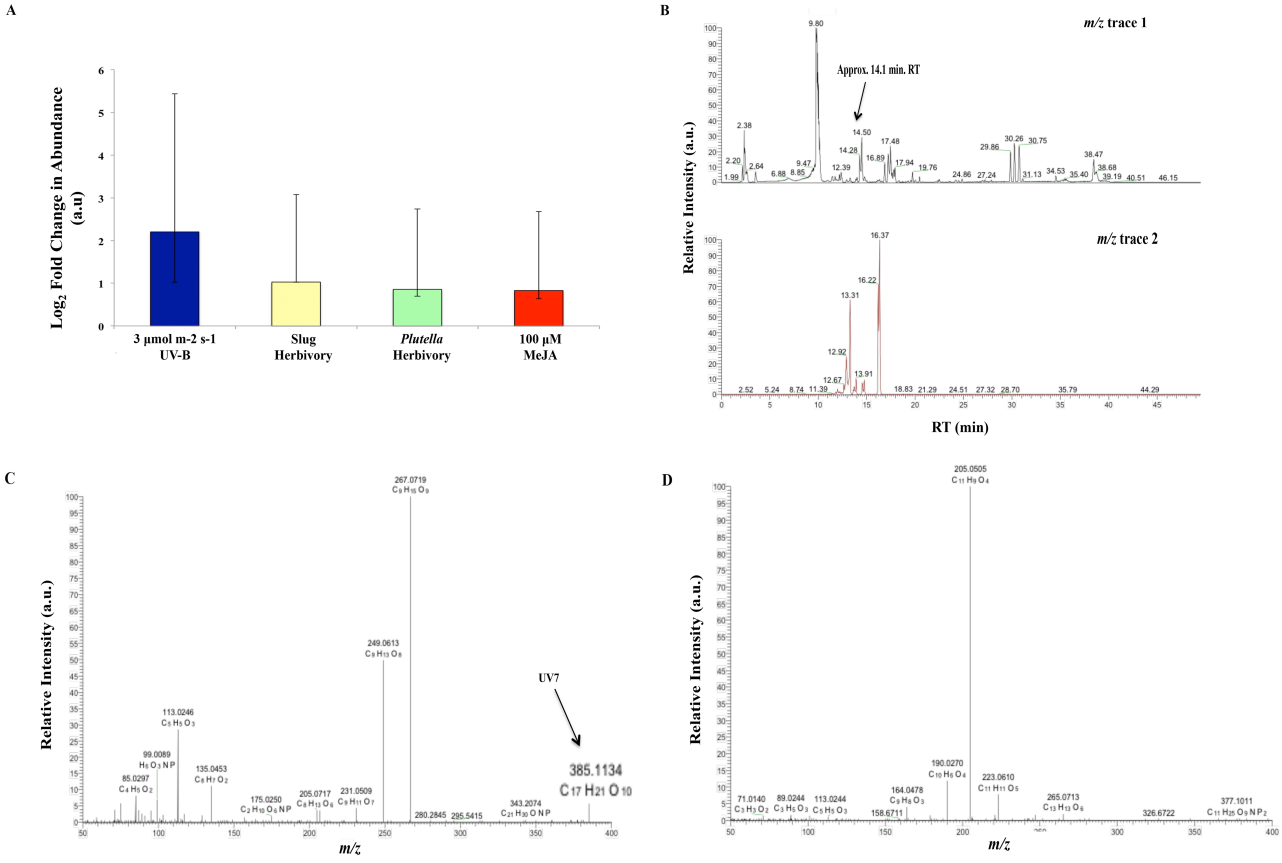

Figure 5-5: Peak intensity, chromatogram and fragmentation analysis of compound number UV7, a putative sinapoyl-glycoside. **A**, the $\log_2$ fold change in peak intensity of compound UV7 across the 4 treatments, and **B**, location of this compound possessing an RT of approximately 14.1 min and mass of 385 in base peak chromatogram *m/z* window 1 (mass range 115-1000; RT window 0-50 min) and its enhancement in *m/z* window 2 (mass range 385.111-385.115; RT window 0-50 min). **C**, fragmentation analysis reveals the elemental formula of this compound as being $C_{17}H_{21}O_{10}$ ($[M\text{-}H]^-$), and **D**, fragmentation of the more abundant isomers reveals the presence of a sinapoyl peak ($C_{11}H_9O_4$) at *m/z* 205.0505. Relative peak intensity is provided in arbitrary units. Error bars represent the 95% confidence interval across three biological replicates.

5.4.3 Chlorogenic acid-related compounds are UV-B-responsive

One compound (S16) was found to increase ≥ 1.5-fold in response to slug herbivory (and slightly following MeJA treatment) but decrease in samples subjected to either UV-B radiation or *Plutella* herbivory (Figure 5-6A). Fragmentation analysis of this compound revealed the presence of a caffeic acid moiety at 179.0350 *m/z* (Quirantes-Piné et al., 2009) along with fragments containing phosphorous in their elemental formulas (Figure 5-6B), indicating that this compound could be caffeic acid-related and conjugated to a phosphor sugar group.

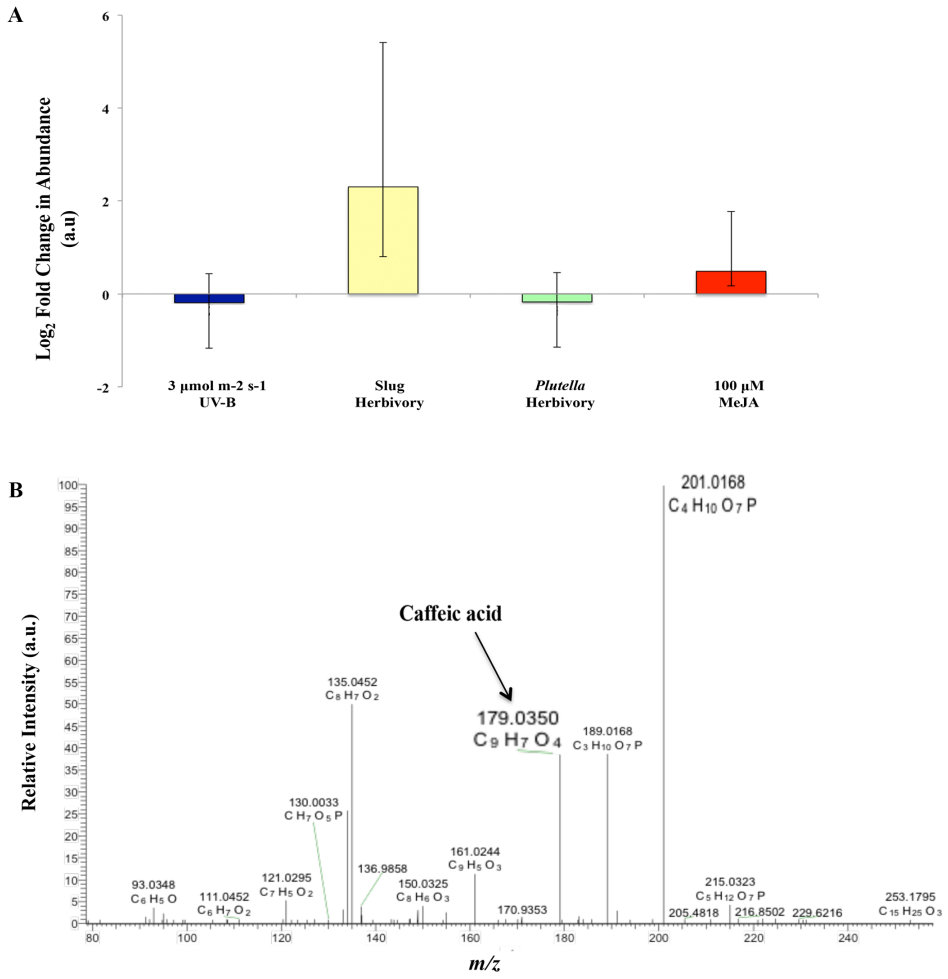

Figure 5-6: Peak intensity, chromatogram and fragmentation analysis of compound number S16, a potential chlorogenic acid-related compound. **A**, the $\log_2$ fold change in peak intensity of compound S16 across the 4 treatments, and **B**, fragmentation analysis reveals the presence of caffeic acid moiety with an *m/z* of 179.0350 along with phosphorous-containing compounds. Relative peak intensity is provided in arbitrary units. Error bars represent the 95% confidence interval across three biological replicates.

The accumulation of putative feruloylquinic acid derivatives and sinapoyl-glycosides in response to UV-B radiation and invertebrate herbivory highlights the sensitivity of the phenylpropanoid pathway in response to these environmental stimuli, and could be indicative of a possible convergence point between these two pathways in plant signaling.

5.5 Numerous chlorine-containing compounds are responsive to UV-B radiation and/or invertebrate herbivory

Several high intensity peaks were found to contain chlorine, a slightly unexpected find due to the lack of studies reporting the presence of chlorine-containing compounds in response to UV-B radiation or invertebrate herbivory. Some of these compounds, which were more significantly regulated by UV-B radiation than any other treatment, possessed indole subunits, while those that were particularly responsive to invertebrate herbivory did not possess the indole group. Those that lacked the indole groups and accumulated in response to slug and *Plutella* herbivory shall be outlined first, and the UV-B-sensitive molecules, which also appeared to possess ascorbic acid upon fragmentation analysis, shall be described afterwards.

5.5.1 Chlorine-containing compounds increase in abundance following slug and *Plutella* grazing

Two compounds in Figure 5-2B (numbers 21 and 22) significantly increased in abundance following slug and *Plutella* herbivory, and were both found to possess at least three isomers from fragmentation analysis (Figure 5-7). The different masses of each compound (357.1317 and 413.1940, respectively) confirmed that these are two different molecules, and were assigned the elemental formulae ($[M-H]^-$) $C_{14}H_{26}O_8Cl$ and $C_{18}H_{34}O_8Cl$, respectively. If these formulae are correct, then a difference of C_4H_8 exists between them, perhaps suggesting that they are somewhat closely related to one another. Unfortunately, further identification of these compounds was unsuccessful, and any role they may have in plant biological systems remains elusive.

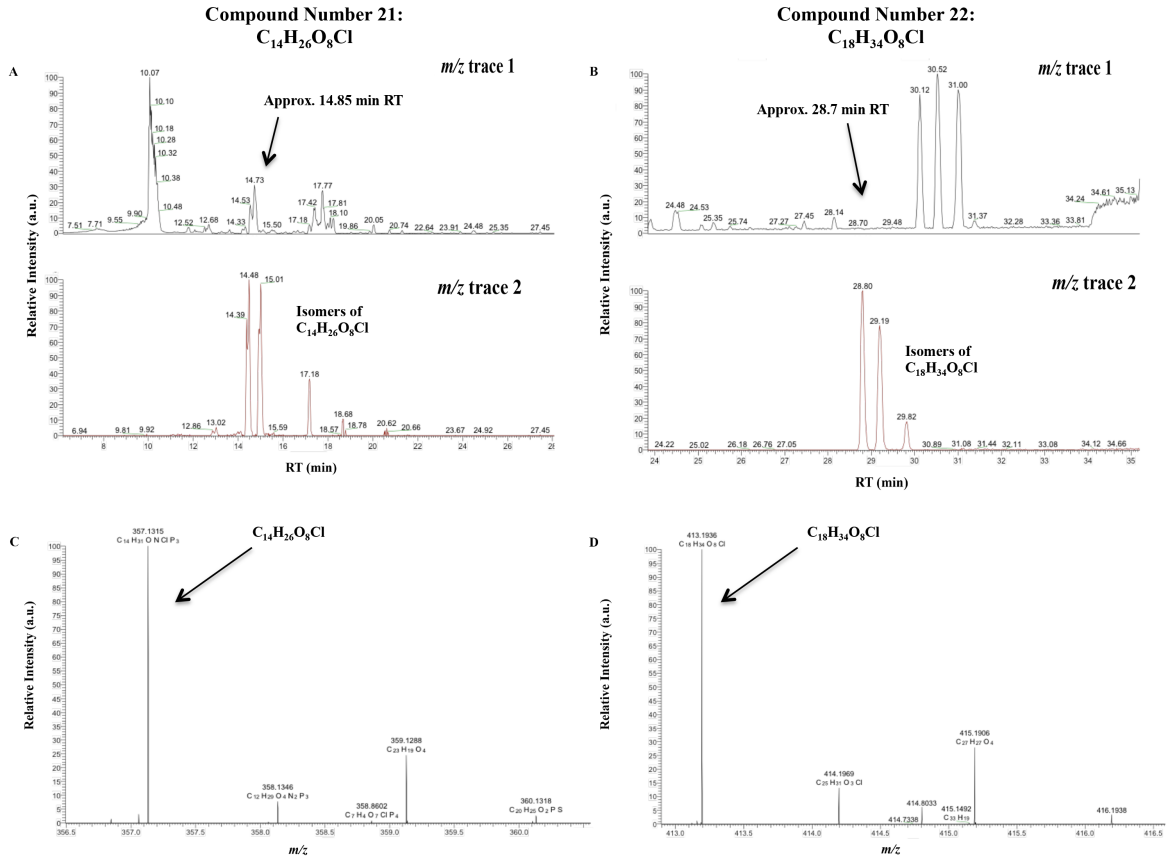

Figure 5-7: Chromatogram and fragmentation data of compound numbers 21 and 22, putative chlorine-containing compounds. Chromatogram and fragmentation data of CN21 (putative elemental formula $C_{14}H_{26}O_8Cl$) in **A** and **C**, and CN22 (putative elemental formula $C_{18}H_{34}O_8Cl$) in **B** and **D**. **A**, the position of CN21 with RT of ~ 14.85 min and mass of 357.1317 in chromatogram *m/z* window 1 (mass range 115-1000; RT window 6-28 min) and its enhancement in *m/z* window 2 (mass range 357.1299-357.1335; RT window 6-28 min) identifying at least three isomers of the compound. **C**, fragmentation analysis reveals the putative elemental formula of this compound as being $C_{14}H_{31}ONClP_3$, but further studies reveal it to be $C_{18}H_{34}O_8Cl$ ($[M-H]^-$). **B**, location of CN22 possessing an RT of approximately 28.7 min and mass of 413.1940 in chromatogram *m/z* window 1 (mass range 115-1000; RT window 24-35 min) and its enhancement in *m/z* window 2 (mass range 413.1919-413.1961; RT window 24-35 min) identifying three isomers of the compound. **D,** fragmentation analysis reveals the elemental formula of this compound as being $C_{18}H_{34}O_8Cl$ ($[M-H]^-$). Relative peak intensity is provided in arbitrary units.

5.5.2 UV-B increases levels of a proposed chlorinated ascorbic acid-containing molecule

One compound that was of particular interest in this study (UV22; Table 5-2) was shown to increase by approximately 58-fold in *B. napus* plants exposed to UV-B radiation, while remaining relatively unchanged in response to the other treatments investigated (Figure 5-8A). Further analysis of this compound, which possesses an RT of 20.77 min and *m/z*

372.0849, found it to possess the putative elemental formula $C_{16}H_{19}NO_7Cl$ in negative ionisation mode ($[M-H]^-$).

Fragmentation of this peak (Figures 5-8B and C) revealed several fragments containing a chloride group, along with an indole core (C_8H_6N) at *m/z* 116.0510 and ascorbic acid (AsA) fragments at *m/z* 115 and 175 ($C_4H_3O_4$ and $C_6H_7O_6$, respectively). An additional fragment was identified in Figure 5-8C possessing a putative elemental formula of $C_6H_8O_6Cl$. This elemental formula implies that the compound could be a chlorinated ascorbic acid (ascorbic acid EF: $C_NH_{N+1}O_N$), although to the best of my knowledge, such a compound has not yet been described in plants. However, that is not to say that compounds of this calibre do not exist, and it would be interesting to further investigate the identity of this compound in *B. napus*, along with its kinetics over an elongated time course while exposed to UV-B radiation or invertebrate herbivory.

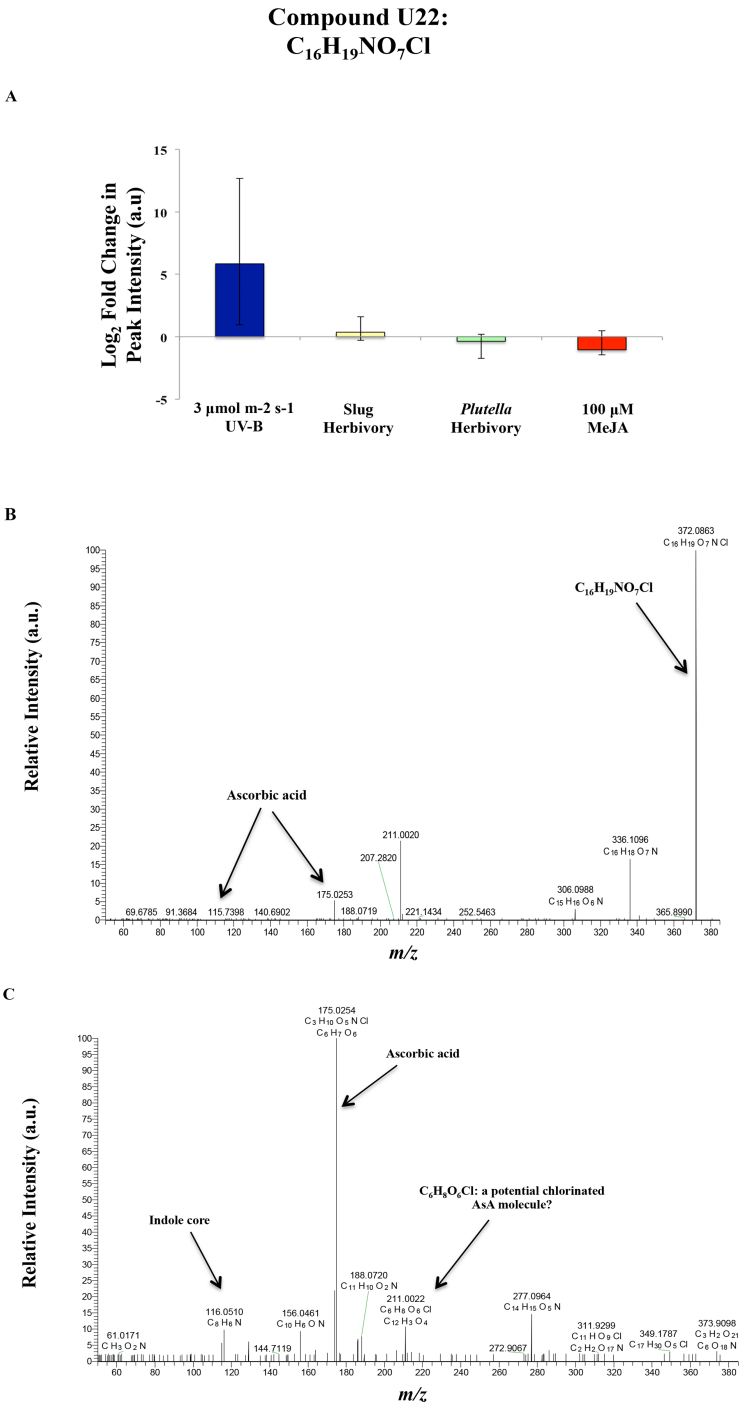

Figure 5-8: Fold change in peak intensity and fragmentation data of compound number UV22, a putative chlorine-containing compound. **A**, the $\log_2$ fold change in peak intensity of compound UV22 across the 4 treatments. **B,** fragmentation reveals the putative elemental formula as being $C_{16}H_{19}NO_7Cl$ ($[M\text{-}H]^-$) and the presence of two ascorbic acid fragments at *m/z* 115.7398 ($C_4H_3O_4$) and 175.0253 ($C_6H_7O_6$), while **C**, fragmentation analysis identifies an indole core at *m/z* 116.0510 (C_8H_6N), an ascorbic acid at 175.0254 ($C_6H_7O_6$) and a putative chlorinated ascorbic acid compound at *m/z* 211.0022 ($C_6H_8O_6Cl$). Relative peak intensity is provided in arbitrary units. Error bars represent the 95% confidence interval across three biological replicates.

5.6 Several putative lipid compounds accumulate in response to invertebrate herbivory and MeJA treatment

Several compounds found to accumulate in response to herbivory and MeJA treatment (but not UV-B radiation) are thought to be lipid-based on account of their elemental formulas and subsequent potential chemical structures. Two compounds in particular, S18 and S19, were found to have the same elution profile based on their *m/z* (S18 *m/z* = 419.2279, S19 *m/z* = 465.2333), and also possess very similar RTs, at 1914.86s (31.91 min) and 1875.43s (31.25 min), respectively. The larger mass (S19) is thought to be a formic acid (CH_2O_2) adduct of S18, which has a putative elemental formula $C_{20}H_{35}O_9$. Fragmentation analysis of this compound revealed a single fragment, $C_4H_7O_2$, which did not aid in the identification of this compound. The elemental formula of this compound matches that of the fatty acid, butyric acid, which is present in plants and forms part of a well-known compound, indole-3-butyric acid ($C_{12}H_{13}NO_2$). It is therefore plausible that this could be a butyric acid fragment from a plant-based molecule, however it has not yet been confirmed. Based on the putative elemental formula of S18/S19, two chemical structures were proposed to represent the metabolite (Figure 5-9), one of them being a lipid possessing a polar and apolar region (Figure 5-9B). The $(CH_2)_{12}$-COOH group in Figure 5-9B could perhaps have contributed towards the formation of the $C_4H_7O_2$ fragment, with the fragmentation of a $(CH_2)_3$-COOH group and its association with a proton producing $C_4H_8O_2$ ($C_4H_7O_2$ $[M\text{-}H]^-$). Again, this can only be speculated as not enough information is available on the nature of this compound.

A second putative lipid-based molecule shown to increase in response to both herbivory and MeJA treatment (but not UV-B radiation) was assigned the elemental formula, $C_{16}H_{29}O_8$ based on its *m/z* (349.1862) and isotopic pattern. Two possible molecular structures of this compound (compound number S13) were identified (Figures 5-9C and D), the first being a lipid-like molecule (methyl 9-(β-D-galactopyranosyloxy)nonanoate; ChemSpider ID no. 4484248) and the second has been implicated in human anti-inflammatory responses. Fragmentation analysis could not provide further insight into the nature of this compound, and as no study has reported the existence of such a structure in plants, its exact identity remains elusive.

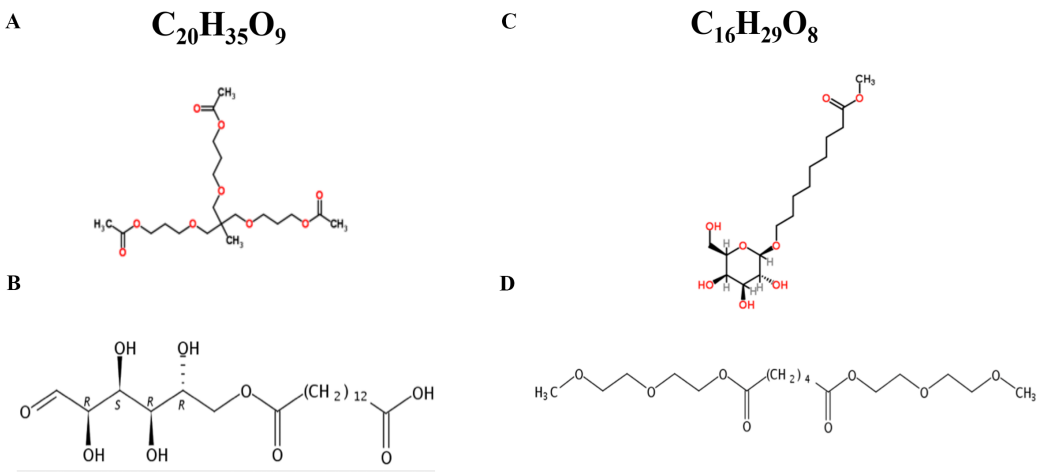

Figure 5-9: The putative chemical structures of potential lipid-containing compounds. **A** and **B,** putative chemical structures of compound number S18 (elemental formula $C_{20}H_{35}O_9$, *m/z* 419.2279 and RT 1914.86s/31.91 min), and **C** and **D**, the putative structures of S13 (elemental formula $C_{16}H_{29}O_8$, *m/z* 349.1862 and RT 1240.6s/20.67min). **A** and **C** were identified from online resource ChemSpider (ID no. 8773594 and 4484248, respectively), **B** and **C** are lipid-like structures.

5.7 Discussion

Plant responses to environmental stresses require input from genetic, proteomic and metabolic reprogramming events. While transcriptomic approaches are considered easier to execute and analyse than proteomics or metabolomics, some genetic modifications are not always observed at the protein or metabolome level. As a result, it is sometimes beneficial to incorporate multiple "omics" experiments into the one study, to allow the researcher to link changes at the genetic level to changes further on in the signalling event, and also prevent vital metabolite components involved in a particular pathway from being missed due to insignificant modifications of encoding transcripts. A global metabolic study was therefore incorporated into this project to study *B. napus* responses to UV-B radiation, slug herbivory, *Plutella* herbivory or MeJA treatment and to compliment the results obtained from the transcriptomic data. Such a comparison has not been conducted in this model crop before, and to date only one study has investigated the effects of slug herbivory on targeted plant metabolites (Falk et al., 2014). While time restrains and technical issues with the sample concentrations prevented extensive analysis of the data obtained from this study, some interesting compounds were identified that have not been previously described in plants.

5.7.1 Initial impressions suggest that *B. napus* responses to invertebrate herbivory are very different to those induced by MeJA

One of the first impressions of the results obtained in this study came from the PCA chart, where the evident separation between the MeJA and invertebrate treatments was observed (Figure 5-1). As the two herbivores were thought to regulate many of the same pathways that are sensitive to MeJA, close clustering of these treatments was expected. Instead, the chart suggests that the invertebrate herbivory treatments have slightly more in common with the UV-B treatment than they do with the MeJA treatment. It is possible that the signalling pathways elicited by MeJA are slightly different to those induced by invertebrate pests, as the latter response is highly dependent on the presence of JA-Ile, while MeJA-induced responses are not. Another possible explanation is that a time gap exists between the responses induced by MeJA and those elicited by the two herbivores, with some biological pathways perhaps being activated more quickly upon application of MeJA than by invertebrate herbivory, and vice versa. If this is true, then the differences seen in the metabolite profile of *B. napus* plants subjected to herbivory or MeJA treatment may reflect the kinetics of the defence response pathway. To confirm whether or not this is true, and to enhance the knowledge gained from the metabolomics, inclusion of more time points over a set treatment period (e.g. of 48 hours) would have been beneficial.

The lack of similarity between MeJA-elicited responses and those induced by the other treatments is reiterated throughout the analysis, with only four out of 26 of the masses listed in Figure 5-2B that increase by at least 1.5-fold in peak intensity (adj. $p \leq 0.05$) in response to two or more treatments being stimulated by MeJA. Again, this could be attributed to the kinetics of these compounds in *B. napus* or variation between the three biological replicates for each treatment, and as such repetition of this experiment with at least one, preferably 2, additional time points will better clarify the differences elicited by the treatments on *B. napus* at the metabolic level.

5.7.2 Several phenylpropanoid-derived compounds accumulated in response to UV-B radiation and invertebrate herbivory

The increased abundance of select phenylpropanoid compounds provided some confidence in the results obtained from this study as their accumulation in response to UV-B radiation or wounding and importance in these signalling pathways have previously been reported (Koeppe et al., 1969, Landry et al., 1995, Lavola et al., 1997). The majority of the

phenolics identified and discussed in this chapter are involved in the biosynthesis of sinapates as opposed to the production of flavonoids, a finding that is surprising due to the known influence of UV-B on the accumulation of these compounds (Stracke et al., 2010b, Mewis et al., 2012). Despite this, the presence of several ferulic acid derivatives and putative sinapate glycosides is a very interesting finding for this particular project, especially as a recent report revealed that UV-B-mediated Arabidopsis defence against *B. cinerea* is more dependent on the sinapate branch of the phenylpropanoid pathway than the flavonoid biosynthetic branch (Demkura et al., 2010). The use of mutants in this study devoid of the enzyme ferulic acid-5-hydroxylase (F5H), which converts ferulate into 5-hydroxyferulic acid (UV6), increased susceptibility of Arabidopsis to infection from *B. cinerea* and facilitated its spread on leaf tissue in the presence of UV-B, while *chs* mutants impaired in the flavonoid biosynthetic pathway were still able to protect themselves against the nectrotrophic pest. Therefore, this branch of the phenylpropanoid pathway may provide important regulators of UV-B-mediated plant defence, a hypothesis that deserves further investigation based on the approximate 25 to 50-fold increase in peak intensity of this compound in response to UV-B and invertebrate herbivory (Figure 5-2B). CGA is also considered to be one of many phenolics involved in conferring basic resistance to plants, with a previous study investigating the defence potential of phenolic compounds containing orthohydroxyl groups, such as catechol, quercetin and CGA, observing their toxic effects on the greenbug *Schizaphis graminum* when presented as part of an artificial diet (Levin, 1976). While this study did not investigate the effects of these defence mechanisms in a plant model organism, the potential role of CGA derivatives in the promotion of plant defence, particularly in the formation of lignin as a structural defence, has been documented (Saxena and Stotzky, 2001). CGA can also confer potato tuber resistance against numerous microbial pathogens, including *Streptomyces scabies, Verticillium alboatrum* and the blight-inducing *Phytophthora infestans* (Johnson and Schaal, 1952, Lattanzio and Cardinali, 2006). Studies with 4 species of leaf beetles presented with leaf tissue from willow plants (all of which possessed different quantities of CGA) revealed that the deterring effects of CGA were not uniform across all beetle species. *Lochmaea capreae* L. preferred consuming willow tissue possessing low doses of CGA over tissue with high doses, while feeding preferences of *Galerucella lineola* F. and *Plagiodera versicolora* Laich was not affected by the presence of CGA on leaf tissue, not even when applied in unnaturally high doses (Ikonen et al., 2001). These findings highlight the complexity of plant-pest interactions, indicating that while these phenolic compounds may be effective at providing protection against a selection of invertebrate pests, other

closely related species may not be so easily deterred. Despite this, components of the phenolic pathway may be important mediators of UV-B-enhanced defence, and therefore warrant further attention. To further evaluate the influence and downstream molecular effects of phenolic compounds in plant defence, a comparison of targeted metabolomics with UV-B- and/or herbivore-treated WT Arabidopsis plants and mutants impaired in the sinapate/lignin biosynthetic branch of the phenylpropanoid pathway (e.g. *fah1-7*) will be beneficial.

5.7.3 Chlorine-containing compounds were induced by UV-B radiation and invertebrate herbivory

The identification of putative chlorine-containing compounds was both surprising and interesting, mainly because few (if any) studies have reported the presence of such compounds accumulating in response to these treatments in plants, and in general there are a sparse number of publications detailing chlorine-containing compounds as a whole (Engvild, 1986, Gribble, 1998, Monde et al., 1998). Chlorine-containing compounds have previously been implicated in plant defence responses against invertebrate and pathogen pests, and can include a variety of terpenoids, alkaloids and phenolics (Engvild, 1985, Gribble, 1998, Gribble, 1999). Studies in the edible lily *Lilium maximowiczii* identified several chlorine-containing orcinol derivatives in bulbs irradiated by UV or subjected to the pathogenic fungus, *Fusarium oxysporum* (Monde et al., 1998), with the authors concluding that chlorination of ornicol with chloroperoxidase and hydrogen peroxide resulted in the accumulation of these chlorine-containing defence compounds. With the exception of this study, however, no other report has identified plant-based chlorine-containing compounds accumulating in response to UV-B radiation.

The peak intensity of two chlorine-containing compounds (numbers 21 and 22 in Figure 5-7) were found to increase by 3 to 8-fold in response to invertebrate herbivory, but were unaffected by UV-B or MeJA treatment (Figure 5-2B). The presence of at least three isomers in the fragmentation data of each compound, their similarity in elemental formulas (a C_4H_8 group difference between them) and near identical regulation by the two invertebrates suggests that these compounds could be related to one another and may play a role in plant defence. Sadly, further details on these compounds could not be obtained from the fragmentation data, and no reports were found to credit the existence of these compounds in plants, let alone any putative function they may have in defence responses.

The presence of a UV-B-responsive putative chlorinated-AsA compound was fascinating, as to the best of my knowledge such a compound has never been described in plants. It is of course possible that the identified compound has been incorrectly annotated, however the existence of such a molecule in plants is not beyond the realms of possibility.

AsA is a known, effective ROS scavenging compound (Smirnoff and Wheeler, 2000, Conklin and Barth, 2004), and has previously been shown to increase in abundance following UV-B radiation (Nunes-Nesi et al., 2005, Kusano et al., 2011) as well as to facilitate plant defence against invertebrate pests. X-ray crystallography has revealed the importance of this compound in accelerating the hydrolysis of glucosinolate compounds via its interaction with myrosinase (Burmeister et al., 2000), and mutants deficient in AsA (e.g. the *vtc1-1* Arabidopsis mutant) are more susceptible to *S. littoralis* herbivory than WT Arabidopsis plants (Schlaeppi et al., 2008).

Several studies in mammalian systems have demonstrated that AsA stimulates leukocyte functioning in host defence against microorganism invaders, by accelerating the chlorinating activity of a key defence-promoting enzyme, myeloperoxidase, to produce the oxidising agent, hypochlorous acid (HOCl) in the presence of its substrate hydrogen peroxide (Marquez et al., 1989). AsA and HOCl react with one another to yield dehydroascorbate and chloride via an oxidation reaction (Chesney et al., 1991). Interestingly, application of porcine myeloperoxidase and H_2O_2 to pathovars of plant pathogens from the genera *Erwinia, Pseudomonas* and *Xanthomonas* was effective at inhibiting their growth and fitness at low enzyme concentrations, and was even more effective when applied directly to young rice plants infected with the blast pathogen *Magnaporthe grisea* (Yang and Anderson, 1999). A plant-based compound sharing chemical and activity similarities to the heme-containing glycoprotein that is myeloperoxidase has not been documented to my understanding, however it is possible that a similar defence system operates in plants where the interaction of AsA and chlorine-containing compounds generates strong Cl-based oxidising agents to support plant resistance against attacking organisms. The potential for such a defence mechanism in plants is purely hypothetical, however if this or related compounds are found in future metabolic studies, then they deserve more investigation to elucidate their role in promoting plant defence.

5.7.4 Putative lipid-based molecules

The presence of lipid-like compounds in this study is not overly surprising, as the wound-response pathway is known to be regulated primarily by constituents derived from the octadecanoid pathway (Farmer and Ryan, 1992). It is therefore possible that the compounds described in section 5.6 represent candidates from this biological pathway, which could explain why their abundance increases in response to herbivory and MeJA application, but not in response to UV-B radiation.

Compound numbers S18 and S19 were shown to share similar elution profiles to one another, however fragmentation analysis did not deduce the exact annotation of this compound. Their putative chemical structures imply the option of this compound being lipid-based, perhaps with a formic acid adduct provided by S19. The identification of a sole fragment ($C_4H_7O_2$) for this compound (data not shown) did not offer any aid in annotating this compound, however while not confirmed, it is possible that this fragment is butyric acid, a fatty acid present in various chemical structures in plants, including a plant growth regulator indole-3-butyric acid (Figure 5-10A), and intermediates of JA biosynthesis (Schaller, 2001)(Figure 5-10B). The putative chemical structure of S18/S19 in Figure 5-9B possesses an $(CH_2)_{12}$-COOH group, which could generate a $C_4H_7O_2$ fragment upon fragmentation via the association of a proton with $(CH_2)_3$-COOH, producing $C_4H_8O_2$ ($C_4H_7O_2$ $[M-H]^-$). This interpretation is merely speculative, however, and requires further investigation to confirm the true identity of these compounds. Another three or four isomers of S18/S19 were identified in this study, all of which were responsive to slug herbivory and, to a lesser extent, *Plutella* herbivory and MeJA treatment, supporting the hypothesis that these putative-lipids could be defence-related.

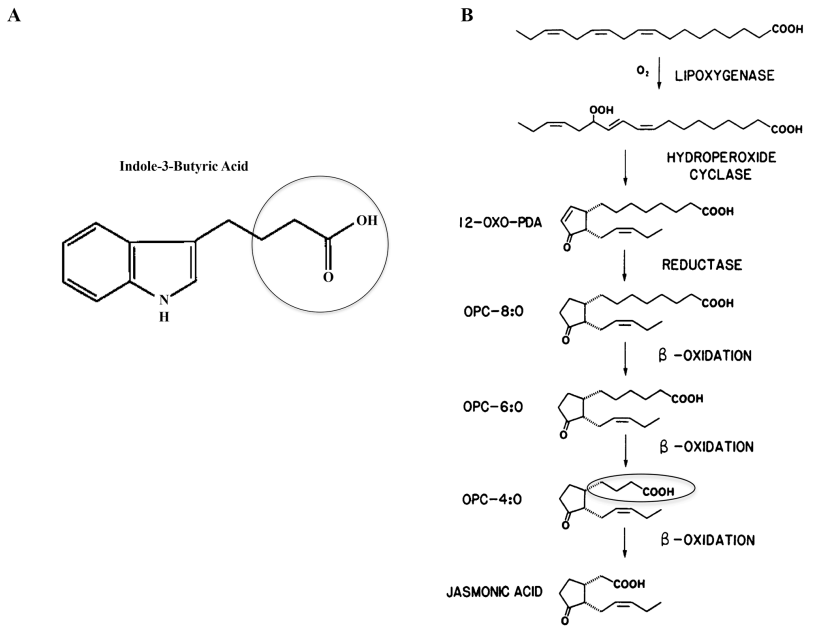

Figure 5-10: Butyric acid-containing compounds involved in various biological processes in plants. A, indole-3-butryic acid, a growth regulator in plants, possesses a butyric group (circled) similar to that possessed in the lipid structure shown in Figure 5-9B. **B**, components of the octadecanoid pathway, several of which contain butyric acid, including JA intermediate OPC-4:0 (circled). **A** was modified from (Zolman et al., 2000), **B** from (Vick and Zimmerman, 1984).

A second putative lipid-based molecule, compound number S13, was again poorly annotated based on the lack of useful fragmentation data. Potential chemical structures of this compound, assigned the elemental formula $C_{16}H_{29}O_8$, include a lipid-like molecule (methyl 9-(β-D-galactopyranosyloxy)nonanoate; Figure 5-9C) and a compound implicated in human anti-inflammatory responses (Figure 5-9D). Initial attempts to find publications reporting a peak at *m/z* 349.19 led to a series of articles detailing a barbituric acid, 5,12,18 *R*-trihydroxy-EPE, a by-product of Aspirin metabolism *in vivo* (Serhan et al., 2004). Fragmentation analysis could not provide further insight into the nature of this compound, and as no study has reported the existence of such a structure in plants, its exact identity remains elusive. If this compound does indeed transpire to be an anti-inflammatory-like compound, then it is may be a derivative of the SA-signalling pathway due to its association with anti-inflammatory responses (Vane, 2000), indicating a potential convergence of signalling molecules in response to invertebrate herbivory and MeJA treatment.

If these putative lipid-based compounds are related to defence signalling molecules, then that might explain why levels of these compounds accumulate in response to herbivore and MeJA, but not UV-B radiation. The reported effects of UV-B radiation on levels of JA or

related compounds have not been described in *B. napus*, however for other plant species the findings have been variable. The phytohormone was found to accumulate in Arabidopsis plants (A-H-Mackerness et al., 1999) but remain unaffected in tomato and Nicotiana while enhancing sensitivity of plants to JA-signalling by heightening accumulation of various wound-response transcripts and metabolites (Stratmann et al., 2000, Izaguirre et al., 2007). To enable better conclusive data to be drawn from these putative lipid molecules, repetition of this experiment, perhaps in a more sensitive positive ionisation mode with more concentrated samples, is required.

5.7.5 Global metabolomics identified some *B. napus* compounds that are sensitive to slug herbivory

To date, very little has been published describing the effects of slug herbivory on the metabolic profile of a plant. However, recent reports have detailed the effects of slug locomotive mucus on levels of phytohormones in various plants, with work published by Falk and co-workers (2014) demonstrating that mucus from the Spanish slug, *Arion lusitanicus*, increases levels of jasmonates in Arabidopsis plants (Falk et al., 2014), while a similar study identified the presence of SA in the locomotive mucus of the grey field slug (*D. reticulatum*), and found that application of this mucus to wounded Arabidopsis leaf tissue activated SA-induced signalling pathways (Kästner et al., 2014). This latter finding was particularly interesting, as it is possible that the presence of SA, a known suppressor of many wound-induced responses, in the mucus of these slugs serves to regulate plant defence pathways to facilitate slug grazing. If this is true, then it demonstrates the ability of a generalist herbivore to elegantly overcome plant-induced defence mechanisms by repressing many responses that would otherwise deter or destroy the slug. As the levels of phytohormones were not investigated in this particular study, it is unknown if the grey field slug induced the accumulation of SA-responsive molecules in *B. napus*. Falk and co-workers (2014) found that levels of glucosinolates in WT Arabidopsis were not modified by herbivory from the Spanish slug, a result which the authors hypothesise could be due to the suppressive nature of other slug-induced responses, and likewise, the grey field slug was not found to significantly increase levels of glucosinolates in this study. However, as few glucosinolates were identified during this project, repetition or this experiment or utilisation of a targeted approach may reveal an accumulation of certain glucosinolates in response to this species of slug. An increased abundance of several phenylpropanoid compounds in response to slug herbivory, such as feruloylquinic derivatives and sinapoyl

glycosides, was revealed in this study, and provides novel findings on the effects of grey field slug herbivory on *B. napus.*

5.7.6 Conclusions and outlooks

Based on results from previous metabolic studies on UV-B- or invertebrate/MeJA-treated plants, the detection of a variety of flavonoid and glucosinolate compounds, such as kaempferol and quercetin derivatives and indole glucosinolate compounds was expected in this member of the Brassicacea family (Mewis et al., 2012). The surprising absence of these compounds from the analysis could be due to technical error with sample extraction or dilution of the compounds, as the relatively low peak intensities of some detected metabolites suggests that the overall concentrations of the samples were quite low. Indeed, as plant leaves are composed primarily of water, dilution of metabolites can be easily achieved. However, the absence of these compounds from this particular experiment does not necessarily mean that they are not responsive to the given treatments, and repetition of this experiment with more concentrated samples will be beneficial in re-examining levels of various compounds, while also confirming or dismissing the findings discussed in this chapter. Further metabolic studies should be conducted in the future to repeat this experiment, with samples run in both positive and negative ionisation mode accompanied with fragmentation analysis to facilitate their annotation. In addition, a more targeted metabolite approach should then be utilised to examine some of the chloro-indole compounds identified in this study in more depth, along with other interesting compounds detected at a later date.

This chapter attempted to identify metabolites commonly regulated by UV-B radiation and invertebrate herbivory utilising a global metabolic approach with reversed-phase HPLC. In doing so, several components of the phenylpropanoid pathway were identified, including a putative sinapoyl-glycoside, several feruloylquinic/isoferuloyl quinic acid derivatives, a possible CGA and a few chloride-containing metabolites. Further examination of these compounds and additional repeats of this experiment will help reinforce the results obtained in this study and facilitate the discovery of the convergence points between UV-B- and wound-induced signalling in *B. napus.*

The next and final results chapter of this study details the over-expression of three *B. napus* genes in Arabidopsis, and presents data obtained from invertebrate bioassays with these plants to elucidate their potential role in mediating UV-B-enhanced pest defence.

Chapter 6: Enhancing *Arabidopsis thaliana* resistance to invertebrate pests in a UV-B-dependent manner

6.1 Introduction

In an attempt to investigate similarities and differences elicited by UV-B radiation, MeJA treatment, slug herbivory or *Plutella* herbivory in *B. napus*, an "omics"-based approach was utilised which revealed commonly regulated early-induced transcription factors and metabolites putatively indicating areas of convergence between UV-B- and herbivore-induced-responsive pathways. Data acquired from the initial RNA-seq alignment against the Brassica 95K Unigene (Chapter 4) enabled several transcripts to be selected for further study to elucidate any possible roles their encoded products may have in mediating UV-B-enhanced plant defence. These genes were selected on account of their increased levels of expression in response to two or more treatments, one treatment preferably being UV-B radiation, the other(s) invertebrate herbivory. The two transcripts selected from the RNA-seq data for further analysis were assigned the Arabidopsis gene annotations *ELI3-2* and *VTC2*, with the former encoding a cinnamyl-alcohol dehydrogenase involved in the biosynthesis of lignin precursors in the phenylpropanoid pathway (Figure 6-1A and section 4.7.1.1 of Chapter 4**)**, and *VTC2* encoding a mannose-1-phosphate guanylyltransferase involved in ascorbate biosynthesis (Figure 6-1B and section 4.7.1.2 of Chapter 4). Four Brassica Unigenes were found to putatively encode VTC2, with one in particular, EX043301, increasing in expression by at least 2-fold in response to UV-B and slug treatment, while one out of three Unigenes possessing sequence similarity to Arabidopsis *ELI3-2* (EV141577) was shown to increase 4 to 6.4-fold in response to all 4 treatments (Table 4.19, Chapter 4). In addition to these two genes, a third, *COMT1,* was also selected for further investigation despite the initial RNA-seq analysis identifying no *B. napus* orthologues of this gene being significantly regulated by any of the treatments. Selection of this gene (which encodes a flavonol 3-methyltransferase; Figure 6-1A and section 4.7.1.3 of Chapter 4) for further analysis was based on recent research implicating the lignin/sinapate biosynthesis branch of the phenylpropanoid pathway, which COMT1 is active in, in UV-B-mediated plant defence against *B. cinerea* (Demkura and Ballaré, 2012). In this study, the authors found that one mutant lacking functional FERULIC ACID 5-HYDROXYLASE (F5H), an enzyme located upstream of COMT1, was shown to lack UV-B-enhanced defence against *B. cinerea* infestation and remained equally susceptible to

fungal infection as the non-UV-B-treated mutants. Wild-type (WT) plants, on the other hand, displayed smaller lesion areas following exposure to UV-B, indicating that the production of sinapates, lignin or associated precursors aided plant defence against *B. cinerea* in a UV-B-dependent manner. On account of this report, it was decided to investigate any role this branch of the phenylpropanoid pathway may have in conferring UV-B-mediated defence against invertebrate pests. Instead of focusing upon F5H, however, *COMT1* was selected for investigation, on account of no previous study (to the best of my knowledge) documenting any role of COMT1 in UV-B-mediated plant defence, therefore any results obtained with *COMT1* were likely to be novel.

The potential for COMT1, ELI3-2 or VTC2 to mediate UV-B-enhanced plant defence against slug and *Plutella* herbivory was investigated via a series of invertebrate bioassays with Arabidopsis lines affected in the expression of the corresponding genes. These lines were either SALK T-DNA-insertion mutants or transgenic lines expressing putative *B. napus* orthologues of the three genes fused to a *35S* promoter from Cauliflower mosaic Virus (CaMV) and either a GFP or 3xHA-tag. The area of leaf tissue consumed by slug and *Plutella* herbivores on -/+UV-B-treated mutant and transgenic lines was measured and compared to that on WT Col-0 plants, and to further assess any impact on plant defence caused by the modified levels of either gene, bioassays were set up to directly compare the average area of leaf tissue consumed on WT and mutant lines or WT and transgenic lines following exposure to plus or minus UV-B conditions.

This final chapter presents the results obtained from invertebrate bioassays with SALK T-DNA-insertion mutants affected in the expression of *COMT1, ELI3-2* and *VTC2*, and details the generation of transgenic Arabidopsis lines over-expressing putative *B. napus* orthologues of the aforementioned Arabidopsis genes. The chapter concludes by comparing the levels of susceptibility of Col-0 and one of the over-expressing lines, *35S*pro:3xHA-COMT1 9.5, to *Plutella* herbivores in choice chamber bioassays, to investigate if hyper-accumulation of this component of the phenylpropanoid pathway can enhance plant resistance to invertebrate herbivory in a UV-B-dependent manner.

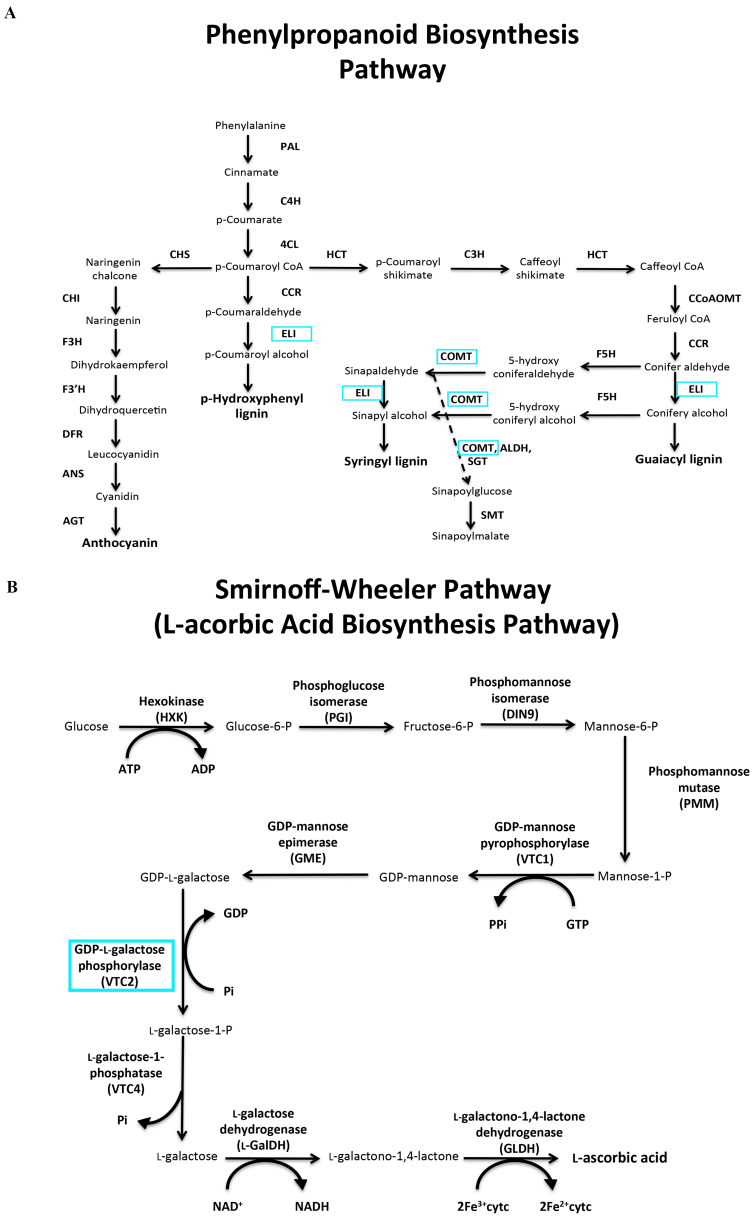

Figure 6-1: Schematic representation of where the encoded products of three genes selected for over-expression in Arabidopsis are found in the phenylpropanoid and Smirnoff-Wheeler pathways. **A**, The location of ELI and COMT (or related family members) in the phenylpropanoid pathway, and **B** of VTC2 in the Smironoff-Wheeler L-ascorbic acid biosynthesis pathway are indicated with light blue boxes. **A** adapted from (Peng et al., 2008) and (Demkura and Ballaré, 2012), **B** from (Linster et al., 2007).

6.2 Identification of putative Brassica orthologues of *COMT1*, *ELI3-2* and *VTC2*

Following the identification of *B. napus* transcripts putatively encoding *ELI3-2* and *VTC2* in the RNA-seq analysis (Chapter 4, section 4.4.2), and their subsequent selection for over-expression in Arabidopsis along with *COMT1*, the first port of call was to compare the sequence similarity of the selected Unigenes to the corresponding Arabidopsis gene and to

genes of the *B. napus* progenitor species, *B. rapa* and *B. oleracea* (genomes of which were used for primer design before publication of the sequenced *B. napus* genome). Use of the *B. rapa* and *B. oleracea* genomes for primer design as opposed to the Arabidopsis genome was due to anticipated higher degrees of sequence similarity between *B. napus* and the two former plant species than Arabidopsis, an assumption based on the knowledge that the *B. napus* genome was formed by several independent fusions between those belonging to ancestors of today's *B. rapa* and *B. oleracea* plants, and that no homologous recombination has since occurred between these two donor genomes (AA and CC, respectively).

Sequence similarity between the Unigenes, Arabidopsis and Brassica genes was assessed by using the BLAST resource with the Unigene sequence against the Arabidopsis genome (TAIR database) and both the Unigene and Arabidopsis sequences against the *B. rapa* and *B. oleracea* genomes in the Brassica database (Vick and Zimmerman). The Brassica gene(s) possessing the highest degree of nucleotide similarity to both the Unigene and Arabidopsis gene sequences were selected as appropriate platforms for primer design. For illustrative purposes, alignment of the Arabidopsis, Unigene and *B. rapa*/*B. oleracea* nucleotide sequences of each gene was conducted using ClustalW (EMBL-EBI). As no differentially regulated Unigenes assigned the putative gene annotation *COMT1* were identified, only the Arabidopsis and *B. rapa* genes (AT5G54160 and Bra029041, respectively) were aligned to one another; both nucleotide sequences are approximately 90% identical to one another, with Bra029041 encoding only one extra codon than AT5G54160. Likewise, the Arabidopsis *ELI3-2* gene, AT4G37990, was shown to possess approximately 86% nucleotide sequence identity to the *B. oleracea* gene Bol032749 (Table 6-1), although sequence homology between these two genes and the Unigene identified in Chapter 4, EV141577, was relatively poor, with only ~57-60% identity between the Unigene and AT4G37990 and Bol032749, respectively. Closer inspection of the sequence alignments revealed that, despite possessing a relatively long sequence (805bp), approximately 30% of EV141577 did not align to AT4G37990 or Bol032749, but instead extended beyond the stop codon of these two genes for an extra ~225 bp. However, as this Unigene was putatively annotated as *COMT1* in both the RNA-seq data in Chapter 4 and Brassica 95K Unigene set (Brassica Genome Gateway, http://brassica.nbi.ac.uk), and proposed to have a higher sequence similarity to *COMT1* in both Arabidopsis and *B. oleracea*, this Unigene was considered as representing Brassica *COMT1*.

	AT4G37990	EV141577	Bol032749
AT4G37990	100%	56.39%	86.62%
EV141577	56.39%	100%	59.19%
Bol032749	86.62%	59.19 %	100%

Table 6-1: Percentage nucleotide sequence identity between the Arabidopsis, Unigene and *B. oleracea* genes of *ELI3-2*.

The sequence alignment of *VTC2* revealed relatively high homology between the Arabidopsis gene, AT4G26850, the Brassica Unigene, EX043301, and a *B. oleracea* gene Bol006503, with the Unigene possessing approximately 78% sequence identity to both AT4G26850 and Bol006503 (particularly over a ~ 400bp region) and AT4G26850 and Bol006503 sharing approximately 89% sequence identity (Table 6-2).

	AT4G26850	EX043301	Bol006503
AT4G26850	100%	78.07%	88.94%
EX043301	78.07%	100%	77.87%
Bol006503	88.94%	77.87%	100%

Table 6-2: Percentage nucleotide sequence identity between the Arabidopsis, Unigene and *B. oleracea* genes of *VTC2*.

From the alignments with confirmed and putative gene sequences of *COMT1, ELI3-2* and *VTC2*, three *B. rapa* and *B. oleracea* genes were selected to serve as platforms for primer design to facilitate amplification of full-length gene sequences of putative *B. napus* orthologues of the genes of interest (Table 6-3). Amplification of *B. napus* gene products with these primers was successful, and the PCR products were found to be of similar size to the *B. rapa* or *B. oleracea* genes to which the primers were designed to (Figure 6-2).

Arabidopsis Gene Annotation	Brassica Gene Selected for use in Primer Design	CDS Gene Length (Arabidopsis/Brassica)
COMT1	Bra029041	1082/1085
ELI3-2	Bol032749	1080/792
VTC2	Bol006503	1389/1326

Table 6-3: The *B. rapa* and *B. oleracea* genes used for putative *B. napus COMT1*, *ELI3-2* and *VTC2* gene amplification, and the lengths of the coding sequences (CDS) for both Arabidopsis and Brassica copies of each gene.

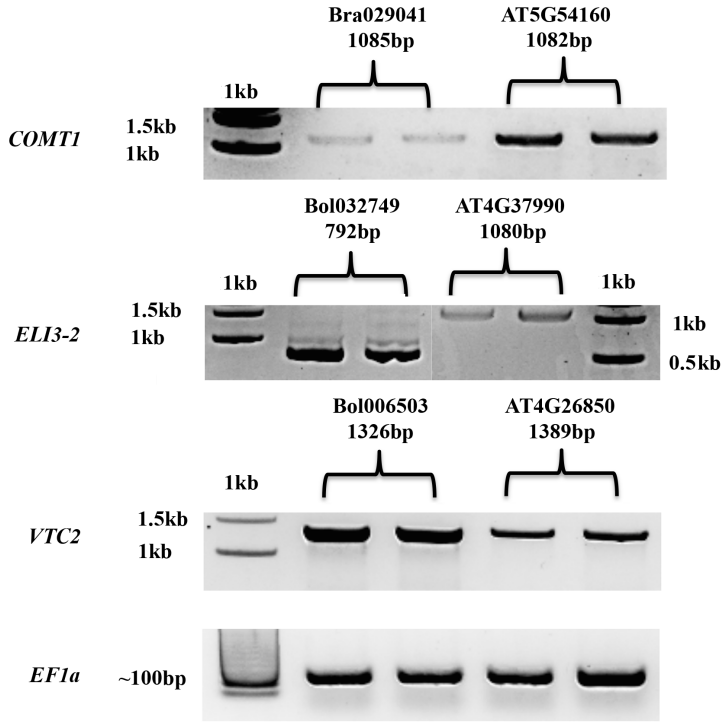

Figure 6-2: Primers designed to putative *B. rapa* and *B. oleracea COMT1, ELI3-2* and *VTC2* gene sequences successfully amplify *B. napus* genes. Gene primers designed to amplify the full-length coding sequence of putative *COMT1, ELI3-2* and *VTC2* genes from Bra029041, Bol032749 and Bol006503 nucleotide sequences, respectively, successfully amplified *B. napus* gene products corresponding to the known *B. rapa* and *B. oleracea* gene lengths. Gene-specific primers for Arabidopsis *COMT1, ELI3-2* and *VTC2* were also used to amplify whole-gene products (latter two lanes for each panel), and the *EF1a* reference gene was amplified using primers specific for *B. napus* (first two lanes) and Arabidopsis (last two lanes). The name of the *B. rapa, B. oleracea* or Arabidopsis gene to which the primers were designed is indicated above each gel, along with the approximate PCR product size expected. 1kb DNA ladder from New England Biolabs®.

Amplified products were cloned into the TA cloning vector pCR™2.1 (Life Technologies) and constructs were sequenced. The nucleotide sequences for each gene were subsequently aligned to those of the corresponding Unigene and Brassica genes used for primer design, to both check that the amplified products possessed some sequence similarity to the selected Unigenes, and also to compare the *B. napus* sequence to that of the *B. rapa* or *B. oleracea* gene used for primer design. Constructs found to possess *B. napus* genes with sequence identity to the appropriate genes were retained for use as standards in qRT-PCR, and also used for generating transgenic Arabidopsis lines.

6.3 Generating transgenic Arabidopsis lines over-expressing *B. napus* genes

Generation of transgenic Arabidopsis plants over-expressing the putative *B. napus COMT1*, *ELI3-2* and *VTC2* genes was achieved by sub-cloning the pCR™2.1 gene constructs described in section 6.2 into Gateway destination vectors possessing the constitutive *35S* promoter and either a GFP or 3xHA tag, and utilising a floral dip approach with transformed *Agrobacterium tumefaciens* expressing these constructs. Three destination vectors were employed for this purpose; the first pGWB15, contained a 3xHA tag at the N-terminus (Nakagawa et al., 2007), while the remaining two, pEZRLC and pEZRLN, contained a GFP tag at the N-terminus and C-terminus, respectively (note, the "C" and "N" of pEZRLC and pEZRLN indicate the position of the gene of interest in relation to the GFP tag). Initially, all genes were destined to be sub-cloned into pGWB15, however unexplainable complications arose during sub-cloning, and as such only one gene (*COMT1*) was successfully cloned into pGWB15, while the other two genes consistently failed to ligate with the vector. *VTC2* and *ELI3-2* were instead later sub-cloned into the two pEZRL vectors possessing a GFP tag, and as such a time gap exists between transformation of Arabidopsis plants with *35S*pro:3xHA-COMT1 constructs and transformation with *35S*pro:GFP-ELI3-2 and *35S*pro:GFP-VTC2.

To the best of my knowledge, *COMT1* and *ELI3-2* have not been previously over-expressed in Arabidopsis or alternative plant species, therefore little is known about any effects an N- or C-terminal tag could have on the activity of the translated protein, and the project was unable to benefit from the use of pre-existing transgenic Arabidopsis lines to additionally assess the effects of over-expressing native *COMT1* on UV-B-mediated plant defence. Several attempts to find reports of *VTC2* over-expressing lines failed, and as such it was believed that no transgenic line existed. However, one report was recently discovered describing an over-expressing *VTC2* Arabidopsis line driven by the *35S* promoter and tagged to YFP at the C-terminus (Muller-Moule, 2008), although the late identification of this report in this project prevented obtaining this line from the authors and its subsequent use in invertebrate bioassays, although it would be beneficial to access seeds of this line for future comparisons with the project's own *35S*pro:GFP-VTC2 line.

Successful transformation of WT (Col-0) Arabidopsis plants with the different constructs was confirmed by screening seeds on ½ MS agar or silicon dioxide plates containing the appropriate antibiotics for the specific vectors (section 2.9.3 Materials and Methods), as well as analysing protein levels of WT and transgenic plants by Western blots using antibodies specific for the GFP and HA tags and amplifying Arabidopsis gene products

using a forward primer specific to the *35S* promoter and a reverse primer specific to the particular *B. napus* gene in question. Homozygous *35S*pro:3xHA-COMT1 lines were identified in this project, however plants over-expressing *ELI3-2* and *VTC2* were still segregating during the writing of this thesis, and as such these two lines will not be discussed in the results section of this chapter, as further laboratory work is required to assess the levels of over-expression in T3 lines, as well as their susceptibility to invertebrate herbivory. The results obtained from studies with *35S*pro:3xHA-COMT1 will be described however, starting with identification of homozygous Arabidopsis lines displaying heightened levels of putative *B. napus COMT1*.

6.3.1 Transgenic Arabidopsis *35S*pro:3xHA-COMT1 lines

Two Arabidopsis *35S*pro:3xHA-COMT1 lines, referred to as 9.3 and 9.5, were found to possess 100% resistance to kanamycin and gentamycin antibiotics when grown on silicon dioxide plates (Figure 6-4A), and were additionally confirmed to possess the desired construct upon gene expression analysis with one *35S*-specific primer and one *B. napus COMT1*-specific primer (Figure 6-3B), as well as with Western blot analysis using the anti-HA antibody (Figure 6-3C). The presence of a protein possessing a molecular weight of approximately 44 kDa in Figure 6-3C was indicative of 3xHA-tagged COMT1, as it was predicted that the encoded product of the putative *B. napus COMT1* would be approximately 40 kDa based on knowledge of Arabidopsis COMT1 (Wirsing et al., 2011), with the 3xHA tag itself being 3-4 kDa in size. The absence of an antibody-bound product in the WT Col-0 sample and successful identification of 3xHA-PHOT1 in a transgenic Arabidopsis line (kindly provided by a fellow lab member) further indicated that the band present in the transgenic samples represents HA-tagged *B. napus* COMT1.

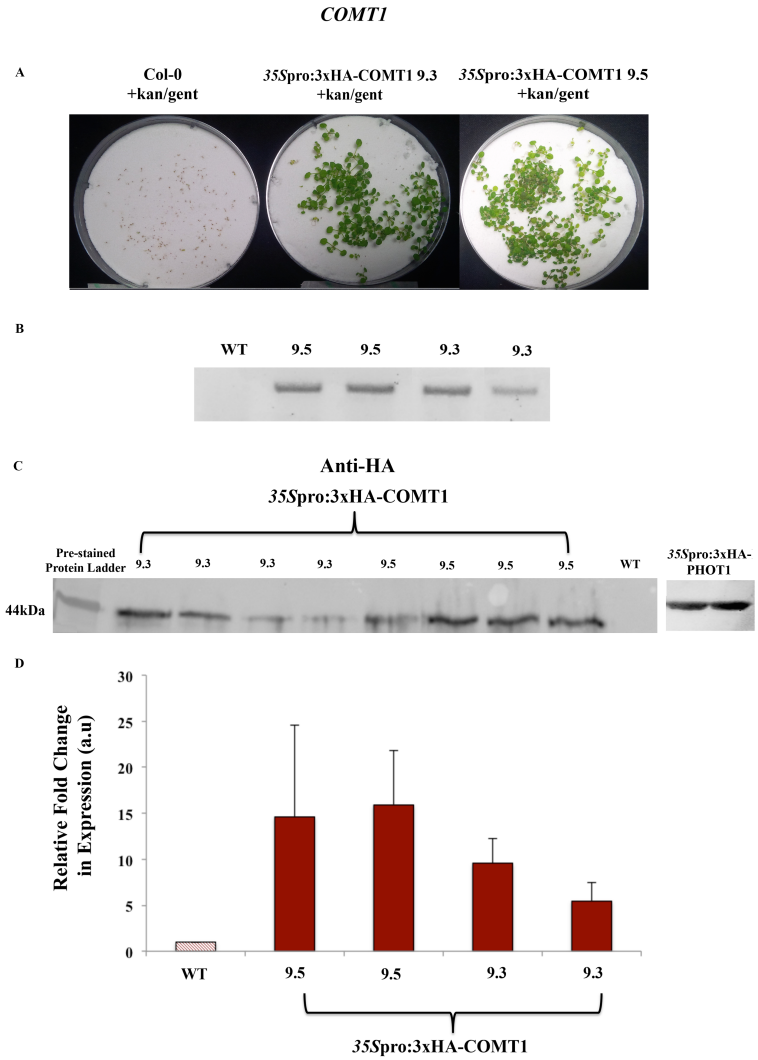

Figure 6-3: The generation of Arabidopsis *35S*pro:3xHA-COMT1 transgenic lines is confirmed via antibiotic resistance screens, genetic and protein analysis. **A**, antibiotic resistance screens revealed two T3 *35S*pro:3xHA-COMT1 lines, referred to as 9.3 and 9.5, that possess 100% resistance to kanamycin and gentamycin; **B**, semi-quantitative PCR with a *35S*-specific forward primer and a *B. napus COMT1*-specific reverse primer amplifies a PCR product in the transgenic lines, but not in WT Col-0, while **C**, Western blot analysis of several individuals from the two lines using the anti-HA antibody reveals a band at approximately 44 kDa, which matches the proposed size of the COMT1 protein (~40 kDa) plus the 3xHA tag (~3 to 4 kDa). The anti-HA antibody was unable to associate with any protein in WT plants, but interacted with HA-bound PHOT1 in an internal control sample from a 3xHA:PHOT1 line. **D**, the relative abundance of *COMT1* transcripts in white light-treated Arabidopsis transgenic and Col-0 lines in relation to the *EF1a* reference transcript. Error bars represent SD from 3 technical replicates. 3xHA:PHOT1 sample used in **C** was kindly provided by Dr. Jonathan Schnabel.

To assess the degree of over-expression of *COMT1* in these transgenic lines, qRT-PCR was conducted on white light-treated WT and *35S*pro:3xHA-COMT1 lines using internal primers that annealed to conserved regions between the Arabidopsis and *B. napus* sequence (Figure 6-3D). The two transgenic lines were found to possess an approximate 6

to 16-fold increase in levels of *COMT1* expression compared to WT plants, with two *35S*pro:3xHA-COMT1 9.5 samples displaying higher transcript levels than *35S*pro:3xHA-COMT1 9.3 samples.

It was therefore confirmed that transformation of Arabidopsis Col-0 with putative *B. napus COMT1* was successful in producing a small number of over-expressing lines, one of which was subsequently used in a series of invertebrate bioassays alongside Col-0 to investigate UV-B-mediated defence responses of this plant to invertebrate herbivores (section 6.5).

6.4 Arabidopsis *comt1*, *eli3-2* and *vtc2* SALK T-DNA-insertion lines

In addition to investigating the susceptibility of Arabidopsis lines over-expressing putative *B. napus* orthologues of *COMT1, ELI3-2* and *VTC2* to invertebrate herbivores, studies were conducted to assess if mutation of these genes or their encoded gene products also affected interaction with pests. To this end, Arabidopsis SALK T-DNA-insertion mutants of *COMT1, ELI3-2* and *VTC2* (SALK_135290C, SALK_206866C and SALK_146824C, respectively) were obtained from The European Arabidopsis Stock Centre (NASC), and subjected to a series of invertebrate bioassays following treatment with –UV-B or +UV-B radiation. Before bioassays were conducted with these lines, however, more in-depth analysis as to the nature of these mutations was carried out, by investigating the position of the SALK T-DNA insertion in each line by referring to the TAIR database, genotyping leaf samples using gene-specific and T-DNA-specific primers to check for homozygosity, and establishing if these lines were knock-down or knock-out mutants using primers designed to amplify the full-length coding sequence (Figure 6-4).

The positions of the T-DNA-inserts in the Arabidopsis *COMT1* and *VTC2* genes were easily located on the TAIR database, with the insert in the *COMT1* SALK_135290C line positioned towards the end of the second exon and spanning right through to the end of the third exon (Figure 6-4A), while that of *VTC2* (SALK_146824C) was found in the first exon (Figure 6-4B). Genotyping of both mutants revealed the absence of a gene product when two primers flanking the T-DNA insert were used (LP-RP), and the presence of an amplicon in WT samples indicated that this observation was not due to a fault in the primers. Amplification of a PCR product in the mutants with a left border T-DNA-specific primer and a right border gene-specific primer (BP-RP) confirmed the presence of the T-DNA insert in these lines, and the inability to produce a PCR product using primers for the

full coding sequence of *COMT1* and *VTC2* in cDNA of the mutants identified these lines as being loss-of-function mutants.

The position of the T-DNA insert in *ELI3-2* (SALK_206866C) has not yet been identified on TAIR, however it is hypothesised to be located near the start of the second exon, due to the fact that qRT-PCR primers previously designed in this project to amplify a small fragment of *ELI3-2* in the second exon were unable to produce a PCR product in *eli3-2* mutants (Figure 6-4C). When the reverse primer for *ELI3-2* was used in conjunction with the T-DNA-specific primer, a fragment was successfully amplified indicating the presence of the T-DNA insert in the suspected area of the *ELI3-2* SALK_206866C line, and the lack of PCR product in this mutant when gene-specific primers were used to amplify the full length coding sequence implies that *eli3-2* is also a null mutant.

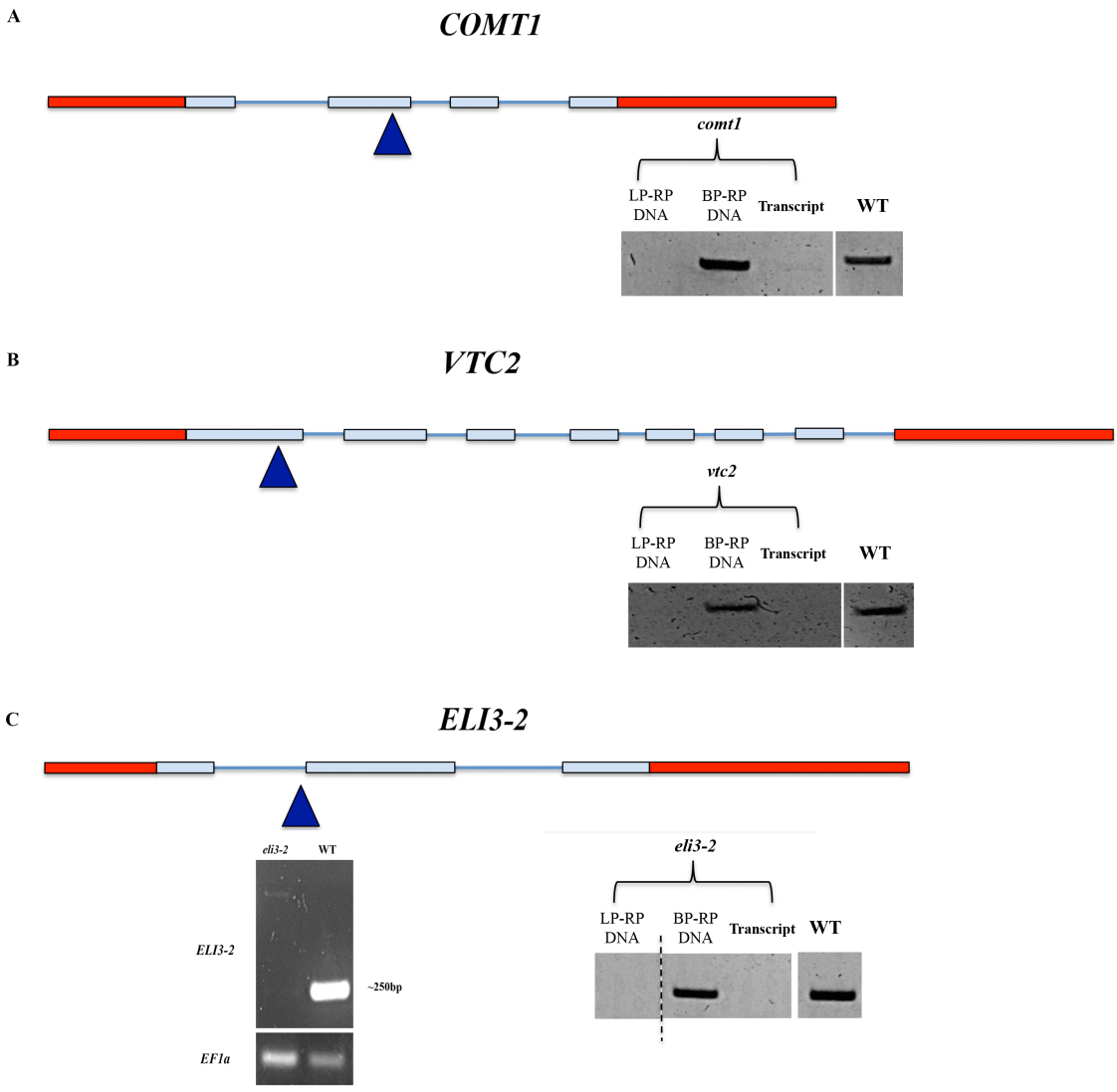

Figure 6-4: Identifying T-DNA-insertion mutant lines of *comt1*, *eli3-2* and *vtc2*. The location of the T-DNA inserts in **A**, *COMT1*, **B**, *ELI3-2* and **C**, *VTC2*, and genotyping results for each SALK T-DNA-insertion mutant line. Thick red bars represent untranslated regions on each gene, while the thick light blue bars indicate exons; thin blue lines represent introns and the dark blue triangles point to the approximate position of the T-DNA insert in each gene. For genotyping, the first lane of each gel reveals the PCR outcome when LP-RP primers flanking either side of the T-DNA insert were used on the mutants; the second lane reveals the PCR outcome when a Left Border T-DNA-specific primer and a gene-specific primer are used, with the presence of a band indicating the presence of a T-DNA insert. The third and fourth lanes show the results of RT-PCR in mutant and WT lines, respectively, using gene-specific primers designed to amplify the full-length coding sequence of each gene. An additional gel in **C** underneath the proposed position of the T-DNA insert on the second exon of *ELI3-2* shows how primers designed to amplify a ~250 bp fragment on exon 2 successfully produce a PCR product in WT plants but not in the *eli3-2* mutant. LP, Left Primer; RP, Right Primer; BP; T-DNA insert Border Primer.

6.4.1 UV-B-treated SALK T-DNA-insertion mutants of *COMT1, ELI3-2* and *VTC2* are not more susceptible to *Plutella* herbivory than UV-B-treated Col-0 plants

Following on from genotyping, invertebrate bioassays were conducted with 3-week old Col-0, *comt1, eli3-2* and *vtc2* lines previously subjected to either 4 days under UV-B-supplemented white light or white light-only conditions. Bioassays were conducted to compare the average area of leaf tissue consumed by *Plutella* herbivores between:

- -UV-B- and +UV-B-treated plants of the same genotype,
- -UV-B-treated mutant and Col-0 plants,
- +UV-B-treated mutant and Col-0 plants.

This was achieved by individual choice chamber cages containing one of the following genotype setups:

- One –UV-B- and one +UV-B-treated plant of the same genotype (Figures 6-5A-D),
- One -UV-B-treated mutant and one -UV-B-treated Col-0 plant (Figures 6-5E-G),
- One +UV-B-treated mutant and one +UV-B-treated Col-0 plant (Figures 6-5H-J).

By conducting the bioassays in this manner, a direct comparison of the areas consumed between mutant and WT plants in the same choice chamber could be made.

The ability of UV-B radiation to reduce susceptibility of Col-0 plants to *Plutella* herbivory is shown in Figure 6-5A, a finding that was also observed in the *comt1* and *eli3-2* phenylpropanoid pathway-mutants (Figures 6-5B and C), but absent in the *vtc2* mutant (Figure 6-5D). Bioassays directly comparing the average area of leaf tissue consumed by *Plutella* on Col-0 and *comt1* lines found no significant difference in susceptibility of either to *Plutella* herbivory when grown under white light-only (Figure 6-5E) or supplementary UV-B conditions (Figure 6-5H). The same observation is seen with Col-0 and *vtc2* mutants exposed to –UV-B (Figure 6-5G) or +UV-B conditions (Figure 6-5J), as no statistically significant difference in average leaf area consumed from either line is found, despite a slight suggestion that *vtc2* mutants sustain marginally more damage than Col-0 plants following –UV-B (Figure 6-5G) or +UV-B (Figure 6-5J) treatment. However, as only three biological replicates of these bioassays were conducted and *Plutella* only consumed small quantities of leaf tissue on both WT and *vtc2* lines following –UV-B or +UV-B treatment, this observation may be coincidental.

While *comt1* and *vtc2* lines sustained similar levels of *Plutella* herbivory as Col-0 (regardless of the light treatment), *eli3-2* mutants grown under –UV-B conditions sustained

significantly higher levels of consumption than Col-0 plants (Figure 6-4F), although this finding is absent when comparing the extent of *Plutella* herbivory on UV-B-treated Col-0 and *eli3-2* plants (Figure 6-4I).

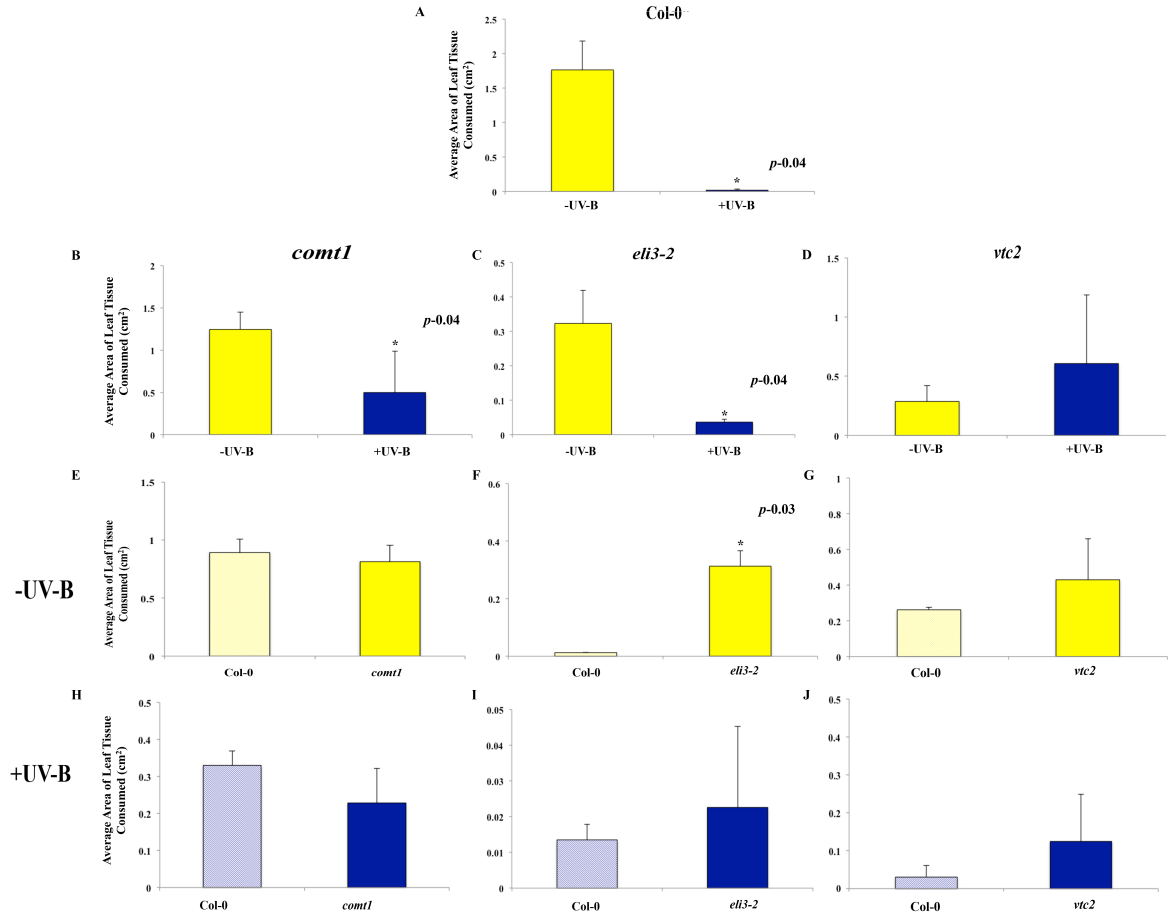

Figure 6-5: UV-B radiation has different effects on the susceptibility of three SALK T DNA-insertion lines to *Plutella* herbivory. The average area of leaf tissue consumed by *Plutella* on **A,** Col-0, **B**, **E and H,** *comt1,* **C, F, and I,** *eli3-2* and **D, G and J,** *vtc2*. Panels **A-D** display the results obtained from bioassays comparing -/+UV-B-treated plants of the same genotype; panels **E-G** present findings from bioassays comparing Col-0/mutants maintained under –UV-B conditions, and panels **H-J** display the results obtained from bioassays comparing Col-0/mutants grown under +UV-B conditions. Arabidopsis previously grown for 17 days under 70 µmol m^{-2} s^{-1} of continuous white light were either maintained under the same conditions or exposed to white light plus supplementary UV-B at 1.5 µmol m^{-2} s^{-1} (+UV-B) for 4 days before conducting bioassays with second instar *Plutella* larvae. Larvae were starved for 1 hour, and 5 were placed an equal distance between the two plants in each bioassay. Bioassays ran for 48 hours under a long day photoperiod (16h light:8h dark). Bars represent mean ± SEM of three biological replicates.

These results indicate that the two phenylpropanoid mutants, *comt1* and *eli3-2,* conserve UV-B-mediated defence responses against *Plutella* larvae, while *vtc2* mutants are incapable of enhancing their defence responses against *Plutella* in a UV-B dependent manner.

6.4.2 *fah1-7* mutants do not display UV-B-mediated defence against slug herbivory

Selection of *COMT1* for over-expression in Arabidopsis was accredited to a previous study which implicated one enzyme located upstream of COMT1 in the phenylpropanoid pathway, FERULIC ACID 5-HYDROXYLASE (F5H), as a potential component of UV-B-enhanced defence mechanisms in Arabidopsis against *B. cinerea* (Demkura and Ballaré, 2012). *F5H* encodes a cytochrome P450-dependent monooxygenase essential for the synthesis of both sinapate esters and syringyl lignin (Ruegger et al., 1999). Use of a mutant deficient in F5H, *fah1-7*, alongside its WT Col-0 progenitor demonstrated that loss of this enzyme from Arabidopsis prevented a UV-B-dependent reduction in susceptibility of this line to *B. cinerea*, as –UV-B- and +UV-B-treated *fah1-7* mutants sustained similar lesion areas following infection from this fungus (Demkura and Ballaré, 2012). To the best of my knowledge, no studies have been conducted to investigate invertebrate feeding preferences on -/+UV-B-treated *fah1-7* mutants, and as the results from work published by Demkura and co-workers (2012) fuelled selection of *COMT1* for further analysis, it was decided to investigate if *fah1-7* mutants retain a UV-B-induced reduction in susceptibility to slug herbivory (Figure 6-6). To this end, Col-0 and *fah1-7* plants were grown under –UV-B conditions for 17 days, and either maintained under these conditions or exposed to white light supplemented with 1.5 μmol m^{-2} s^{-1} broadband UV-B for 4 days before being presented to juvenile slugs.

UV-B-treated Col-0 plants appeared less susceptible to slug herbivory than –UV-B-treated plants (Figure 6-6A), although this finding was not deemed statistically significant on account of the variation in total leaf area consumed by invertebrates in different biological replicates (Figure 6-6B). The *fah1-7* mutant did not display any reduction in susceptibility to slug herbivory (Figure 6-6C), with the individual results from the 5 biological replicates (Figure 6-6D) indicating no conclusive feeding preference of slugs for one light-treated plant over another in the separate choice chambers.

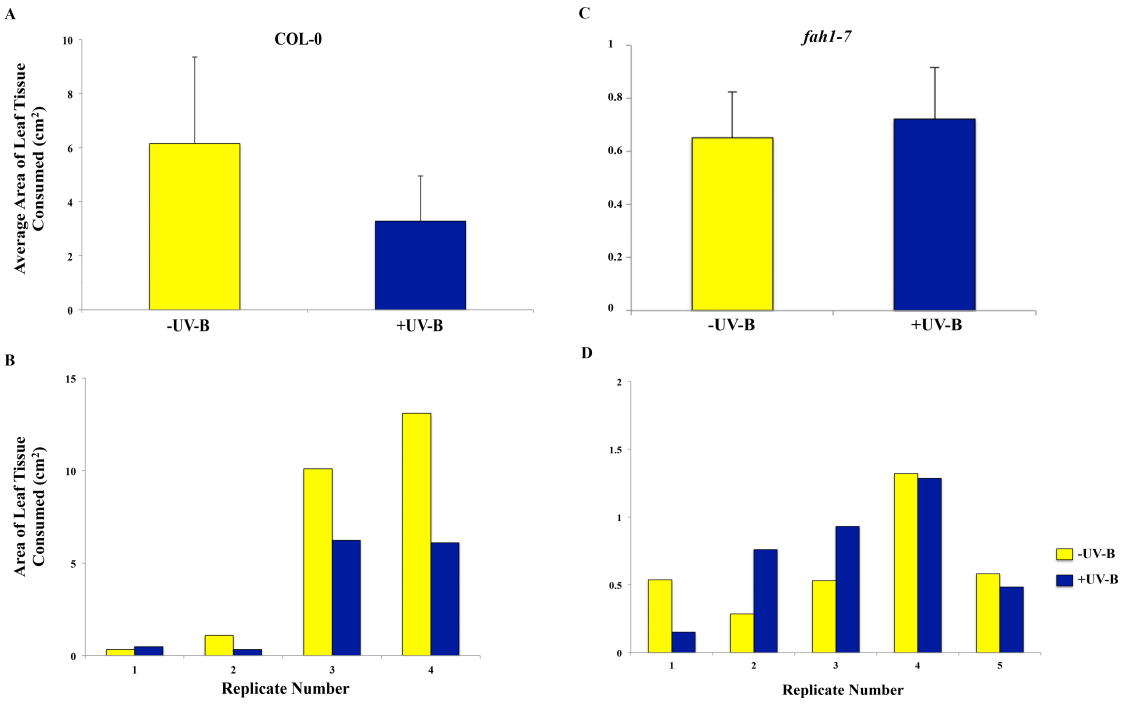

Figure 6-6: UV-B radiation does not reduce the susceptibility of *fah1-7* plants to slug herbivory. **A**, the average area of leaf tissue consumed by slugs in Col-0 plants, and **B**, the area of tissue consumed in four Col-0 biological replicates. **C**, the average area of leaf tissue consumed by slugs in *fah1-7* mutants, and **D**, the area of tissue consumed in five *fah1-7* biological replicates. Arabidopsis previously grown for 17 days under 70 µmol m^{-2} s^{-1} of continuous white light received 70 µmol m^{-2} s^{-1} of white light (-UV-B) or white light plus supplementary UV-B at 1.5 µmol m^{-2} s^{-1} (+UV-B) for 4 days before conducting bioassays with juvenile slugs. Slugs were starved for ~ 16 hours, and one was placed an equal distance between one –UV-B and one +UV-B plant in each bioassay. Bioassays ran for 48 hours under a long day photoperiod (16h light:8h dark). Bars for **A** represent mean ± SEM.

These findings indicate that *fah1-7* mutants lack UV-B-mediated defence against slug herbivores, which complements the results obtained by Demkura and co-workers on *B. cinerea.* While *fah1-7* is noticeably less capable of inducing UV-B-dependent defence mechanisms against slugs than *comt1* is against *Plutella* larvae (Figure 6-5B), the results from Figure 6-6 suggest that the particular branch of the phenylpropanoid pathway in which F5H (and COMT1) are active may be important in mediating UV-B-enhanced defence.

6.5 Over-expression of *B. napus COMT1* in Arabidopsis enhances plant defence against *Plutella* herbivory in a UV-B-dependent manner

To conclude upon the results obtained from this study, findings from invertebrate bioassays with the *35S*pro:3xHA-COMT1 lines detailed in section 6.3.1 are presented. Plant treatments and choice chamber setup was as described in section 6.4.1, with the *35S*pro:3xHA-COMT1 9.5 line used alongside the progenitor Col-0 ecotype. White light- and UV-B-treated *35S*pro:HA-COMT1 9.5 plants were presented to *Plutella* larvae in choice chambers, and the areas of leaf tissue consumed were measured after a 48-hour period. UV-B radiation was found to significantly reduce the attractiveness of *35S*pro:HA-COMT1 9.5 plants to *Plutella* larvae compared to –UV-B-treated transgenic plants, as the invertebrates consumed higher levels of plants maintained under white light for 3 weeks (Figure 6-7). This response was noticeable upon visual examination of the plants (Figure 6-7A) and by measuring the average area of leaf tissue consumed in 5 biological replicates, as larvae were found to consume ~90% more tissue on –UV-B-treated transgenic plants than +UV-B-treated plants (Figure 6-7B). Examination of each biological replicate highlighted the clear preference of *Plutella* for –UV-B-treated *35S*pro:HA-COMT1 9.5 plants over those exposed to UV-B radiation (Figure 6-7C). While the Col-0 progenitor line was likewise shown to be less susceptible to invertebrate herbivory following exposure to UV-B radiation (Figure 6-5A), the difference in the average area of leaf tissue consumed by *Plutella* in -/+UV-B-treated Col-0 plants was not found to be as statistically significant as that for *35S*pro:HA-COMT1 plants (p-0.04 for Col-0, p-0.0004 for *35S*pro:HA-COMT1 9.5).

To determine if any differences exist in the susceptibility of Col-0 and *35S*pro:3xHA-COMT1 9.5 lines to *Plutella* herbivory, bioassays were setup to directly compare the feeding preferences of *Plutella* presented with one Col-0 and one *35S*pro:HA-COMT1 plant previously grown under white light-only (-UV-B; Figure 6-8) or supplementary UV-B radiation (+UV-B; Figure 6-9).

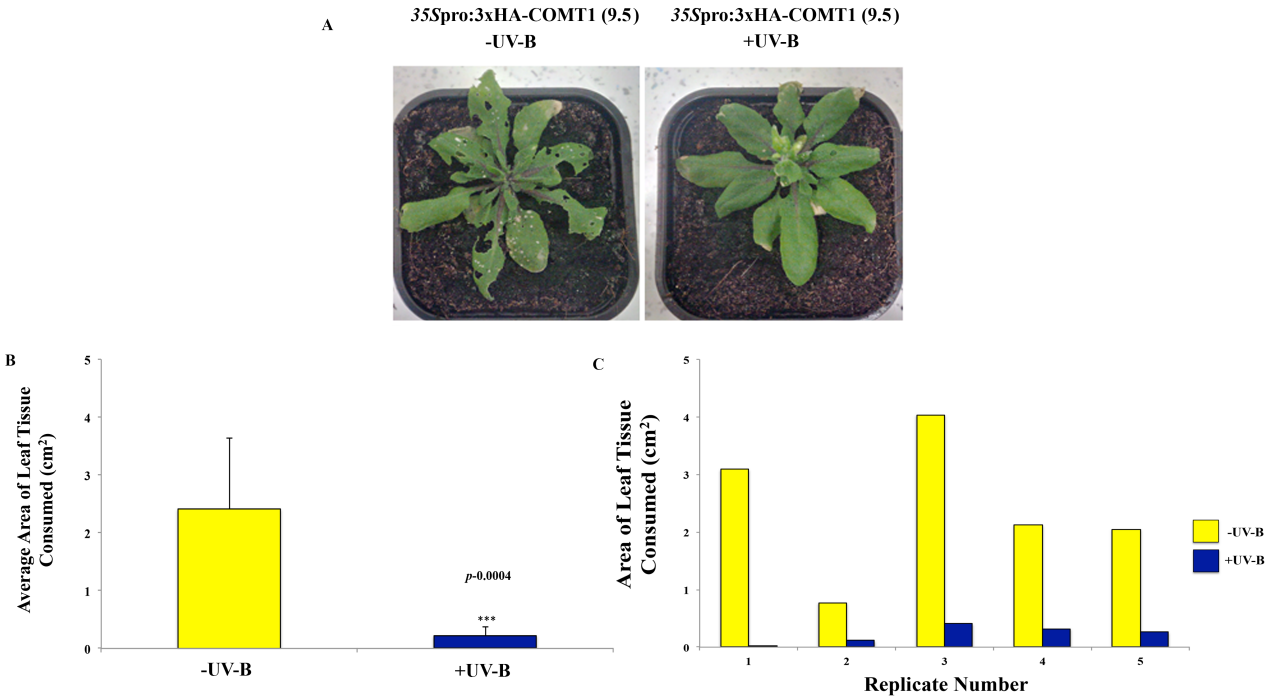

Figure 6-7. UV-B-treated Arabidopsis *35S*pro:HA-COMT1 95 over-expressing plants are less susceptible to *Plutella* herbivory than –UV-B-treated over-expressing lines. **A**, the visual difference in *Plutella* feeding between –UV-B- and +UV-B-treated *35S*pro:3xHA-COMT1 plants, **B**, the average area of leaf tissue consumed by larvae on -/+UV-B-treated plants, and **C**, the area of leaf tissue consumed by larvae in each biological replicate. Arabidopsis plants were grown under 70 μmol m^{-2} s^{-1} white light in the absence of UV-B for 17 days before being either transferred to +UV-B conditions (70 μmol m^{-2} s^{-1} white light + 1.5 μmol m^{-2} s^{-1} broadband UV-B), or maintained under –UV-B conditions for 4 days. Choice chambers contained one -UV-B and one +UV-B plant side by side. Ten 2nd instar larvae were transferred to the cage with a fine paintbrush following a 1-hour period of starvation, being deposited an equal distance between the two plants. Bioassays ran for 48 hours under a long day photoperiod (16h light:8h dark). N=5. Bars on **B** represent estimated mean ± SEM. Significance of the UV-B treatment against the –UV-B- treatment was calculated using ANOVA and Tukey's Honest Significant Difference (HSD) post-hoc test: $p \leq 0.001$ (0.0004).

Visual observations of white light-treated Col-0 and *35S*pro:3xHA-COMT1 9.5 plants along with comparison of the average area of leaf tissue consumed by *Plutella* larvae on each line shows no significant difference in the susceptibility of either ecotype to herbivory following exposure to –UV-B conditions (Figure 6-8A and B). The area of tissue consumed by larvae in each biological replicate identified a slight trend in *Plutella* preference for Col-0 over transgenic lines, with 80% of replicates sustaining higher levels of tissue consumption on –UV-B-treated WT plants (Figure 6-8C). The variation in quantity of tissue consumed in each replicate, however, may mask any statistical significance of this observation, and as such further replicates are required to continue investigating the effects of different light treatments on Col-0 and *35S*pro:3xHA-COMT1 9.5 susceptibility to *Plutella* herbivory.

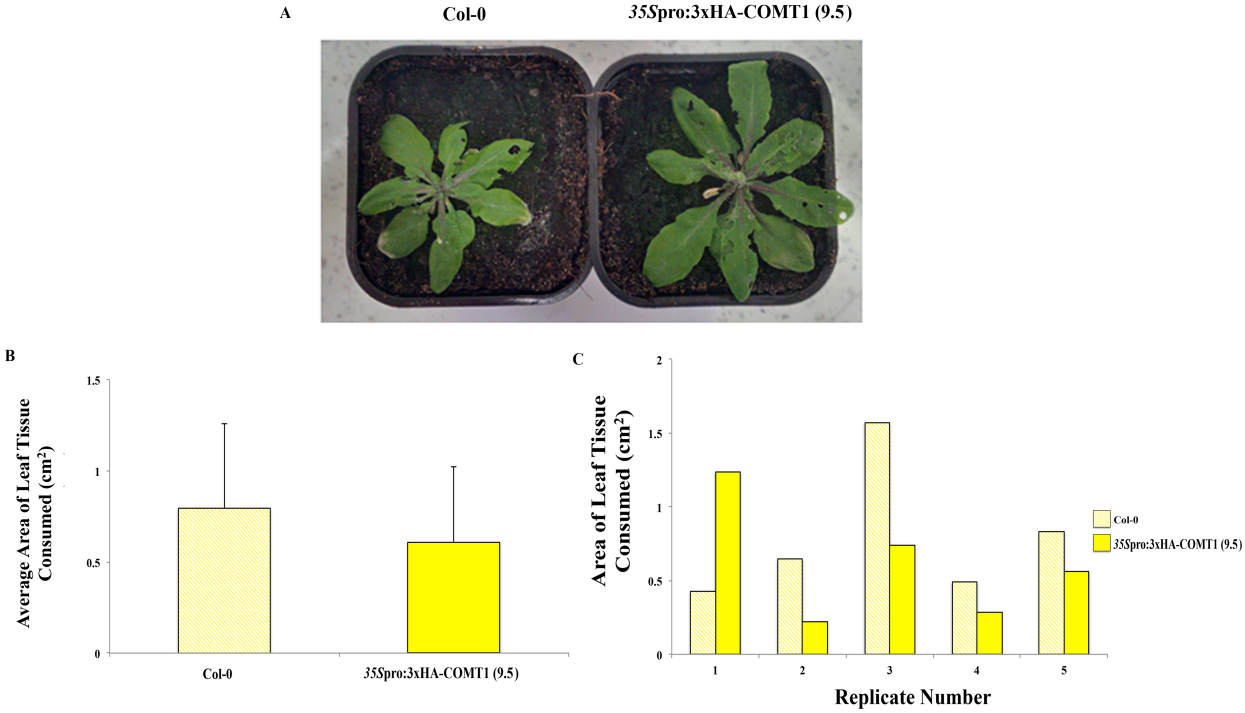

Figure 6-8. Col-0 and *35S*pro:HA-COMT1 plants are both susceptible to *Plutella* herbivory following –UV-B irradiation. **A**, the visual difference in *Plutella* feeding between Col-0 and *35S*pro:3xHA-COMT1 plants grown under white light-only conditions, **B**, the average area of leaf tissue consumed by larvae on each ecotype, and **C**, the area of leaf tissue consumed by larvae in each biological replicate. Arabidopsis plants were grown under 70 μmol m^{-2} s^{-1} white light in the absence of UV-B for 21 days. Choice chambers contained one Col-0 and one *35S*pro:3xHA-COMT1 plant, with ten 2nd instar larvae transferred to each cage with a fine paintbrush at an equal distance between the two plants following a 1-hour period of starvation. Bioassays ran for 48 hours under a long day photoperiod (16h light:8h dark). N=5. Bars on **B** represent estimated mean ± SEM. Significance of the UV-B treatment against the –UV-B-treatment was calculated using ANOVA and Tukey's Honest Significant Difference (HSD) post-hoc test: *p*-0.37.

UV-B-treated *35S*pro:HA-COMT1 9.5 and Col-0 lines were not found to be equally susceptible to *Plutella* larvae, as Col-0 plants sustained significantly higher levels of consumption from *Plutella* larvae than the transgenic line (Figures 6-9A and B). Examination of the results obtained from the 5 biological replicates again highlight a clear preference of *Plutella* for consuming Col-0 plants over *35S*pro:HA-COMT1 9.5 (Figure 6-9C). It is also interesting to note that while the area of tissue consumed on Col-0 plants fluctuates over the biological replicates, the quantity of *35S*pro:HA-COMT1 9.5 leaf tissue consumed remains fairly constant.

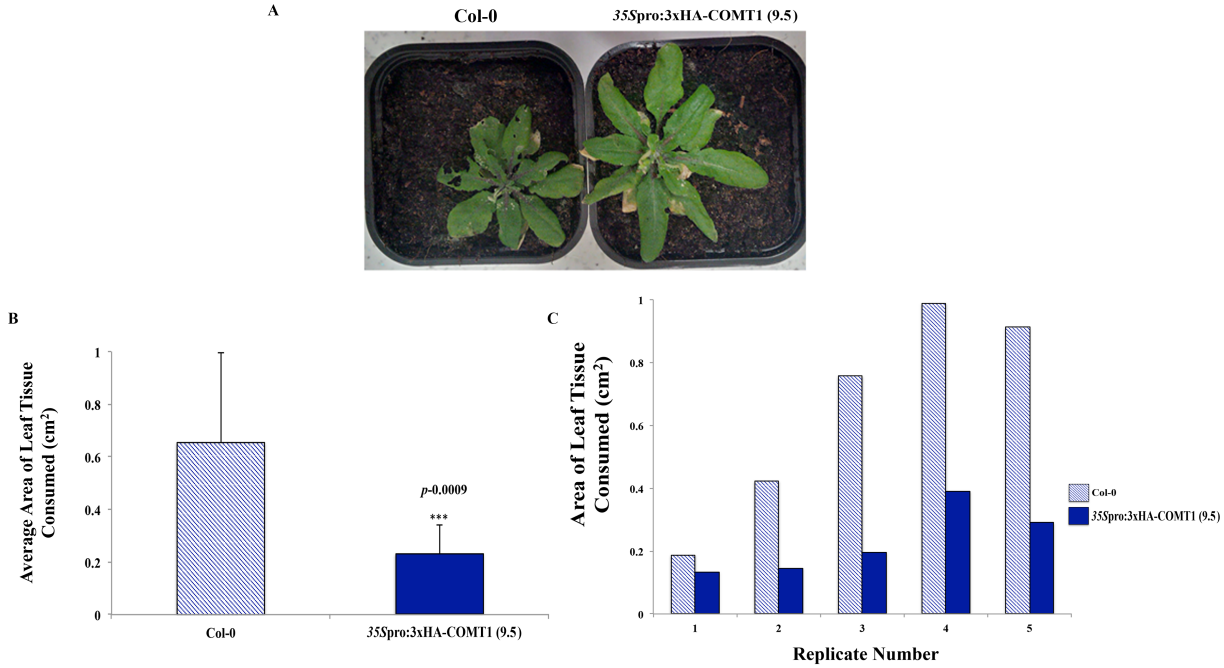

Figure 6-9. UV-B-treated Col-0 plants are more susceptible to *Plutella* herbivory than UV-B-treated *35S*pro:HA-COMT1 plants. **A**, the visual difference in *Plutella* feeding between +UV-B-treated Col-0 and *35S*pro:3xHA-COMT1 plants, **B**, the average area of leaf tissue consumed by larvae on each ecotype, and **C**, the area of leaf tissue consumed by larvae in each biological replicate. Arabidopsis plants were grown under 70 μmol m^{-2} s^{-1} white light in the absence of UV-B for 17 days before being either transferred to +UV-B conditions (70 μmol m^{-2} s^{-1} white light + 1.5 μmol m^{-2} s^{-1} broadband UV-B), or maintained under –UV-B conditions for 4 days. Choice chambers contained one Col-0 and one *35S*pro:HA-COMT1 plant side by side. Ten 2nd instar larvae were transferred to the cage with a fine paintbrush following a 1-hour period of starvation, being deposited an equal distance between the two plants. Bioassays ran for 48 hours under a long day photoperiod (16h light:8h dark). N=5. Bars on **B** represent estimated mean ± SEM. Significance of the UV-B treatment against the –UV-B-treatment was calculated using ANOVA and Tukey's Honest Significant Difference (HSD) post-hoc test: $p \leq 0.001$ (0.0009).

These results collectively indicate that over-expression of putative *B. napus COMT1* in Arabidopsis not only heightens UV-B-induced defence responses against *Plutella* larvae in comparison to –UV-B-treated plants of the same transgenic lines (Figure 6-7), but also in comparison to WT plants previously treated with UV-B radiation (Figure 6-9).

6.6 Discussion

The identification of *B. napus* transcripts commonly up-regulated in response to UV-B radiation, MeJA application, slug herbivory and/or *Plutella* herbivory using an RNA-seq approach (section 4.4, Chapter 4) facilitated the selection of several genes for over-expression in Arabidopsis to assess any roles they may have in promoting UV-B-enhanced plant defence. Annotation of these *B. napus* transcripts, based on their sequence similarity to the Arabidopsis genome, revealed that they putatively encode components of sinapate and lignin biosynthesis in the phenylpropanoid pathway (ELI3-2; Figure 6-1A) and ascorbic acid biosynthesis in the Smirnoff-Wheeler pathway (VTC2; Figure 6-1B). These genes were previously described as being UV-B- or wound-responsive (Brown et al., 2005, Favory et al., 2009, Suza et al., 2010), with their encoded products implicated in promoting plant protection or defence against UV radiation or invertebrate and microbial pests (Schmelzer et al., 1989, Kiedrowski et al., 1992, Burmeister et al., 2000, Schlaeppi et al., 2008, Konig et al., 2014). In addition to *ELI3-2* and *VTC2*, a third gene, *COMT1*, was selected for further analysis due to a recent study implicating the biological pathway in which COMT1 is active (sinapate and lignin biosynthesis in the phenylpropanoid pathway) in mediating Arabidopsis defence against the necrotrophic pathogen, *B. cinerea*, in a UV-B-dependent manner (Demkura and Ballaré, 2012). The effects of over-expressing putative *B. napus* orthologues of these genes in Arabidopsis was assessed by performing *Plutella* bioassays with transgenic and WT lines, with parallel assays using Arabidopsis loss-of-function mutants impaired in the expression of *COMT1, ELI3-2* and *VTC2* also conducted to assess if loss of Arabidopsis encoded products of these genes affects plant vulnerability to invertebrate consumption. The findings from these invertebrate bioassays with transgenic and mutant Arabidopsis lines shall be discussed in this final section of this chapter, along with suggestions of future work that needs to be conducted to support these findings and continue elucidation of the molecular mechanisms of UV-B-enhanced resistance in *B. napus*.

6.6.1 Arabidopsis loss-of-function mutants and their susceptibility to *Plutella* herbivory

While generating Arabidopsis transgenic lines over-expressing putative *B. napus* orthologues of *COMT1, ELI3-2* and *VTC2*, a series of SALK T-DNA-insertion mutants were obtained to assess if the absence of functional encoded products of these three genes affects plant susceptibility to invertebrate herbivory (section 6.4.1). After locating the position of the T-DNA insert in each gene, confirming their homozygosity and identifying them as loss-of–function mutants (Figure 6-4), a series of bioassays were conducted to compare the average area of leaf tissue consumed on -/+UV-B-treated mutants and Col-0 progenitor plants (Figures 6-5A-D). UV-B-treated Col-0 plants appeared less susceptible to *Plutella* herbivory than –UV-B-treated plants (Figure 6-5A), an observation that was also reported for the two phenylpropanoid mutants, *comt1* and *eli3-2,* as plants from both lines previously treated with UV-B radiation sustained a smaller average loss of tissue by *Plutella* herbivores than mutants maintained under –UV-B conditions (Figures 6-5B and C, B respectively). This finding indicated that loss of COMT1 or ELI3-2 from Arabidopsis did not affect UV-B-mediated plant defence against invertebrate pests, suggesting that either these components of the phenylpropanoid pathway are not implicated in this biological response, or that functional redundancy exists between multiple proteins in this branch of the phenylpropanoid pathway.

There is a strong case for functional redundancy influencing the results from these bioassays, with COMT1 reported to have similar substrates to the closely related caffeoyl coenzyme A dependent *O*-methyltransferase 1 (CCoAOMT1) for methylation in the biosynthesis of lignin monomers, coniferyl and sinapoylalcohol, and has additionally been proposed to overlap with CCoAOMT1 in the methylation of residual hydroxycinnamic acid amides during flower bud development (Fellenberg et al., 2012). While it is therefore possible that CCoAOMT1 can compensate for the absence of functional COMT1 in *comt1* mutants on account of their overlapping roles in plants, it is important to note that both enzymes still display preferences for select substrates over others, with COMT1 exhibiting methylation preferences for 5-hydroxyferuloyl CoA derivatives and certain flavonols such as quercetin, while CCoAOMT1 shows a strong preference for caffeoyl coenzyme A (Fellenberg et al., 2012). Therefore, CCoAOMT1 may only partially restore COMT1 processes in plants, if at all.

Functional redundancy may also exist in the *eli3-2* mutant, as this protein is one of at least 9 (possibly 17) members of the ELI/CAD family involved in the biosynthesis of

monolignol and lignin. A previous report investigating the structural profile of various *cad* mutants revealed little change in the overall lignin composition of these plants (Kim et al., 2007a), a finding which the authors concluded was a reflection of the degree of redundancy between these proteins, extending this statement to indicate that single ELI/CAD proteins were not rate-limiting in lignin biosynthesis. ELI/CAD family members possess varying roles in the biosynthesis of monolignol and lignin, with ELI3-2 (aka CAD8), CAD4, CAD5 and CAD7 believed to possess only minor roles in the formation of these biopolymers. It is therefore possible that a mutation in either of the genes encoding these 4 proteins will not significantly affect plant attractiveness to invertebrate pests, or that some degree of functional redundancy exists between these proteins. Regardless of the presence of any functional redundancy in these two phenylpropanoid mutants, it is clear that loss of functional COMT1 and ELI3-2 from Arabidopsis does not significantly affect their attractiveness to *Plutella* larvae following -/+UV-B exposure in comparison to WT plants. Over-expression of these genes may provide more insight into any affect these two proteins may have in UV-B-mediated plant defence.

In contrast to the phenylpropanoid mutants, the UV-B-treated *vtc2* mutant was as susceptible to *Plutella* grazing as –UV-B plants of the same genotype (Figure 6-5D), with statistical analysis finding no difference between the areas of leaf tissue consumed by larvae in three biological replicates with these mutants. Biosynthesis of ascorbic acid (AsA) may therefore be important in conferring plant defence against invertebrate pests in a UV-B-dependent manner, a perhaps unsurprising finding considering previous reports implicating this compound in promoting plant protection against UV-B radiation (Landry et al., 1995, Conklin et al., 1996, Gao and Zhang, 2008, Kusano et al., 2011) and herbivore or pathogen attack (Burmeister et al., 2000, Conklin and Barth, 2004) by serving as an effective ROS scavenging agent and enhancer of myrosinase activity in the hydrolysis of glucosinolates (Burmeister et al., 2000). Whether or not the lack of UV-B-mediated defence in *vtc2* mutants is attributed to modified ROS activity or slower accumulation of glucosinolates remains elusive, however metabolomic analysis of this mutant and the over-expressing line would be informative in revealing differences in the chemical profiles of these plants.

Additional bioassays with mutant and Col-0 lines attempted to directly compare *Plutella* feeding preferences when presented with –UV-B-treated mutant and Col-0 plants (Figure 6-5 E-G) or with +UV-B-treated mutant and Col-0 plants (Figure 6-5 H-J). These experiments found little difference in the susceptibility of Col-0 and *comt1* lines (Figures

6-5E and H) and Col-0 and *vtc2* lines (Figures 6-5G and J) to *Plutella* herbivory following either light treatment. However, -UV-B-treated *eli3-2* plants were significantly more attractive to *Plutella* larvae than WT plants (Figure 6-5F), an observation that was absent when both genotypes were grown under +UV-B conditions (Figure 6-5I) suggesting that loss of ELI3-2 could affect the overall attractiveness of Arabidopsis plants to *Plutella* while conserving UV-B-mediated defence responses that are indistinguishable between Col-0 and *eli3-2* lines. This heightened attraction of larvae to *eli3-2* mutants over WT lines could be a direct result of changes to the chemical composition of these mutants, as it has previously been documented that down-regulation of *ELI* in poplar results in incorporation of hydroxycinnamyl aldehyde monolignol precursors in lignin (Ralph et al., 2001). Whether or not the increased deposition of hydroxycinnamyl aldehyde monolignol precursors would affect plant susceptibility to herbivory is unknown. Examination of the lignin content of both the *eli3-2* mutant and transgenic lines would be beneficial in further elucidating if removal of ELI3-2 generally affects the attractiveness of plants to invertebrates.

6.6.1.2 *fah1-7* mutants lack UV-B-enhanced defences against slug herbivores

Work published by Demkura and co-workers (2012) implicating a cytochrome P450-dependent monooxygenase, FERULIC ACID 5-HYDROXYLASE (F5H), in promoting UV-B-enhanced defence against *B. cinerea* in Arabidopsis fuelled selection of *COMT1* for over-expression in this study, due to COMT1 being located downstream of F5H in the phenylpropanoid pathway and likewise serving as an important component in the biosynthesis of lignin and sinapates, and also on account of no previous report describing any role of COMT1 in UV-B-mediated plant defence, therefore making any result obtained from mutant and transgenic lines novel. The aforementioned study reported a loss of UV-B-mediated defence in the F5H mutant (*fah1-7*) to *B. cinerea*, made evident by –UV-B- and +UV-B-treated mutant plants possessing similar lesion areas resulting from *B. cinerea* infection. As the authors did not investigate the susceptibility of this line to invertebrate pests following treatment with or without UV-B radiation, and on account of selection of *COMT1* for over-expression being based on the results obtained with *fah1-7* and *B. cinerea*, it was deemed appropriate to investigate if Arabidopsis plants impaired in the expression of *F5H* were affected in their vulnerability to invertebrate consumption. To this end, *fah1-7* and Col-0 mutants were subjected to slug herbivory following a 4-day exposure to either white light or UV-B-supplemented white light (Figure 6-6). The *fah1-7* mutants appeared

equally as susceptible to slug herbivory following exposure to -/+UV-B radiation (Figure 6-6C), with the results of the individual replicates (Figure 6-6D) showing little pattern in feeding preference of slugs between -/+UV-B-treated mutants in the 5 choice chambers. However, the UV-B-induced reduction in Col-0 susceptibility to slug herbivory was not deemed statistically significant in Figure 6-6A, a surprising result likely attributed to the variation in total leaf area consumed by slugs in the 4 biological replicates, of which no logical explanation can be provided. As these replicates were conducted over the same 48-hour period, the extreme variation between the first two biological replicates presented in Figure 6-6B and replicates 3 and 4 cannot be attributed to variation in treatment conditions. However, it is clear from the individual replicates that larger areas of leaf tissue from – UV-B plants were consumed by slugs in the majority of choice chambers (Figure 6-6B), a result which is similar to previously observed feeding preferences of *Plutella* larvae on -/+UV-B-treated Col-0 plants (Figures 3-8 and 6-6 in Chapter 3 and 6, respectively). As such, it can provisionally be concluded that *fah1-7* mutants lack UV-B-enhanced defence responses against slug herbivores.

It is difficult to compare the results from the *fah1-7* bioassays (Figure 6-6) to those with *comt1* (Figure 6-5), as slug invertebrates were used for one study and *Plutella* for the other, respectively. The use of slugs as opposed to *Plutella* larvae in the *fah1-7* bioassays was due to resource limitations, as several invertebrate bioassays clashed with one another at the same time, and not enough slugs were available to repeat the bioassays from Figure 6-5 with the loss-of-function mutants. However, the results obtained from bioassays with *fah1-7* mutants and slugs complemented what has previously been described with -/+UV-B-treated mutants and *B. cinerea* (Demkura and Ballaré, 2012), therefore while some differences may exist in susceptibility of *fah1-7* and *comt1* mutants to invertebrate herbivory, it can be concluded that loss of functional F5H from Arabidopsis prevents activation of UV-B-enhanced defence mechanisms against *B. cinerea* (Demkura and Ballaré, 2012) and slug herbivory (Figure 6-6).

6.6.2 Over-expression of putative *B. napus COMT1* in Arabidopsis heightens plant defence against *Plutella* herbivores in a UV-B-dependent manner

To further establish any potential roles of the encoded *COMT1, ELI3-2* and *VTC2* products in mediating UV-B-induced plant defence against invertebrate pests, transgenic Arabidopsis lines over-expressing putative *B. napus* orthologues of these genes in the Col-0 background were generated using several vectors containing the constitutive *35S*

promoter and either a 3xHA or GFP tag. The unfortunate issues encountered in generating expression vectors containing putative *B. napus ELI3-2* and *VTC2* genes, and the late transformation of Arabidopsis plants with these constructs, prevented the production of homozygous T3 lines and subsequent analysis and experimental work with these lines from being conducted before the end of the experimental period in this project. However, experiments and invertebrate bioassays shall be conducted in the near future with lines that are currently segregating, which will allow the effects of over-expressing putative *B. napus ELI3-2* and *VTC2* genes in Arabidopsis on UV-B-mediated plant defence to be revealed.

In the meantime, results obtained from invertebrate bioassays with one T3 *35S*pro:3xHA-COMT1 line, referred to as 9.5, shall be discussed. Production of two homozygous T3 *35S*pro:3xHA-COMT1 lines (9.3 and 9.5) was achieved via antibiotic resistance screens, protein and gene expression analysis (Figure 6-3A and D), however no bioassay results from the *35S*pro:3xHA-COMT1 9.3 line were shown in this chapter, due to only a small number of replicate choice chambers being conducted to compare -/+UV-B-treated *35S*pro:3xHA-COMT1 9.3 susceptibility to *Plutella* herbivory. As such, further bioassays (incorporating –UV-B- and +UV-B-treated Col-0 lines) need to be carried out before conclusions can be made on the susceptibility of this line to invertebrate herbivores.

The results from bioassays with the *35S*pro:3xHA-COMT1 9.5 line, which exhibited a 16-fold increase in *COMT1* expression (Figure 6-7), showed that like the Col-0 progenitor, +UV-B-treated transgenic lines sustained less consumption from *Plutella* herbivores than –UV-B transgenic plants, indicating that over-expression of putative *B. napus COMT1* in Arabidopsis conserves UV-B-mediated plant defence responses. To assess any differences in susceptibility of the *35S*pro:3xHA-COMT1 9.5 transgene and Col-0 to *Plutella* herbivory, bioassays were conducted to study the average area of leaf tissue consumed on –UV-B-treated Col-0 and *35S*pro:3xHA-COMT1 9.5 (Figure 6-8) and +UV-B-treated Col-0 and *35S*pro:3xHA-COMT1 9.5 (Figure 6-9). The results from bioassays comparing –UV-B-treated Col-0 and *35S*pro:3xHA-COMT1 9.5 revealed no statistical difference in the average area of leaf tissue consumed (Figure 6-8B), although it would be beneficial to conduct several more repeats of these bioassays, as examination of the individual biological replicates suggests that *Plutella* larvae prefer consuming Col-0 plants over the *35S*pro:3xHA-COMT1 9.5 transgenic plants (Figure 6-8C). The lack of statistical significance in these bioassays may be attributed to the variable quantities of leaf tissue consumed over the 5 biological replicates, and further repeats may help clarify if a Col-0-preference does exist, or if –UV-B-treated Col-0 and *35S*pro:3xHA-COMT1 9.5 plants are equally as susceptible to *Plutella* herbivory. An evident preference of *Plutella* for +UV-B-

treated Col-0 plants over the *35S*pro:3xHA-COMT1 9.5 line is observed in Figure 6-9, with approximately 65% less leaf tissue area consumed on the transgenic line than the WT plants, an observation found to be statistically significant across the 5 biological replicates (*p*-0.0009; Figure 6-9B). Indeed, a *Plutella* preference for consuming Col-0 plants over the *35S*pro:3xHA-COMT1 9.5 line is observed across the replicates (Figure 6-9C), with ~30 to 75% less tissue being consumed on the transgenic line than the WT plants in each replicate, highlighting an enhanced ability of *35S*pro:3xHA-COMT1 9.5 to successfully deter *Plutella* larvae in a UV-B-dependent manner.

To reinforce the results obtained with *35S*pro:3xHA-COMT1 9.5, and to better assess if over-expression of putative *B. napus COMT1* in Arabidopsis can enhance UV-B-mediated defence responses, bioassays with additional lines must be conducted. Identification of additional lines over-expressing varying levels of *COMT1* would also be advantageous, not only to establish a minimum level of over-expression required for heightening UV-B-mediated plant defence to invertebrates, but also to assess any changes in the structural composition of these plants, in relation to lignin deposition, which could indicate the molecular mechanisms of this enhanced UV-B-mediated defence response. If bioassays with additional transgenic lines are successful in demonstrating that over-expression of *B. napus COMT1* in Arabidopsis can enhance UV-B-mediated resistance against invertebrate pests, then metabolomic analysis of these lines will also be invaluable in identifying key compounds and metabolites involved in this response. In addition to assessing the molecular basis of enhanced UV-B-mediated defences in *35S*pro:3xHA-COMT1, bioassays should also be conducted with slugs to determine if this herbivore responds to UV-B-treated *35S*pro:3xHA-COMT1 9.5 lines in a similar manner as *Plutella* larvae.

6.6.3 Conclusions and outlooks

The experiments presented in this chapter aimed to investigate if modification of the levels of *COMT1, ELI3-2* or *VTC2* in Arabidopsis affected plant susceptibility to invertebrate herbivory in bioassay experiments. The conserved UV-B-enhanced defence response of *comt1* and *eli3-2* mutants suggested either that these components of the phenylpropanoid pathway are not involved in conferring UV-B-mediated defence to plants, that functional redundancy between components of this biological pathway exists, or that input from multiple components and/or biological pathways is required to confer UV-B-mediated plant defence against invertebrate pests. Bioassays with transgenic Arabidopsis lines possessing elevated levels (~16-fold) of *COMT1* found that these lines not only exhibited

UV-B-mediated plant defence against *Plutella* larvae, but also appeared to possess enhanced levels of UV-B-dependent defence mechanisms, due to +UV-B *35S*pro:3xHA-COMT1 9.5 plants receiving less consumption from larvae than +UV-B Col-0 plants. While these bioassays need to be conducted on more *35S*pro:3xHA-COMT1 plants to support the findings from this particular transgenic line, the results suggest that the phenylpropanoid pathway is important in conferring UV-B-mediated defence against *Plutella* larvae. As no bioassays have yet been conducted on homozygous *35S*pro:GFP-ELI3-2 lines, it cannot be confirmed if additional components of this pathway are implicated in plant defence responses in the presence of UV-B. Likewise, the potential affects of over-expressing putative *B. napus VTC2* in Arabidopsis on UV-B-mediated defence are yet to be discovered, although it is hypothesised that enhancing levels of this gene in Arabidopsis could increase plant defence against *Plutella*, based on the findings from bioassays with *vtc2* mutants which showed that this line lacks UV-B-mediated defence responses against this particular herbivore. On-going research with segregating *35S*pro:GFP-ELI3-2 and *35S*pro:GFP-VTC2 lines will reveal their potential to influence UV-B-mediated defence responses in plants, however it can be concluded from the results presented in this chapter that the phenylpropanoid pathway is implicated in mediating plant defence against *Plutella* in a UV-B-dependent manner. Continuation of this research on Arabidopsis and generation of additional transgenic *B. napus* lines expressing these and other constructs will determine if it is possible to heighten the defence responses of this agriculturally important crop in a UV-B-dependent manner.

Chapter 7: Final Discussion

7.1 Introduction

UV-B radiation (280-315 nm) is a small yet potent component of sunlight that serves as an important environmental stimulus to plants, regulating various developmental and photomorphogenic processes while activating a series of UV-protective mechanisms (Flint et al., 2008, Jenkins, 2009, Tilbrook et al., 2013). Additionally, UV-B radiation has previously been shown to enhance plant resistance against a selection of invertebrate pests, with removal of UV-B from the growing environment of plants increasing their attractiveness and susceptibility to invertebrate herbivory and oviposition (Rousseaux et al., 1998, Izaguirre et al., 2003, Zaller et al., 2003, Rousseaux et al., 2004, Caputo et al., 2006, Foggo et al., 2007) as well as their vulnerability to necrotrophic pathogens such as *B. cinerea* (Demkura and Ballaré, 2012). The involvement of UV-B radiation in promoting plant resistance against herbivore pests has received much attention over the past several decades, however the exact molecular mechanisms underpinning the convergence between the UV-B- and herbivore-responsive signalling pathways remain elusive. This study sought to elucidate the molecular basis of UV-B-enhanced resistance in the commercially important crop, *Brassica napus* (oilseed rape), against larvae of the diamondback moth, *Plutella xylostella,* and the grey field slug, *Deroceras reticulatum,* using a transcriptomic and global metabolomics approach. The key findings from this study are discussed and reflected upon in this final chapter, and a model depicting the molecular mechanisms of UV-B-mediated *B. napus* resistance against pests as interpreted from these results is provided along with suggestions for future work.

7.2 UV-B and UV-A radiation reduces the susceptibility of *B. napus* and Arabidopsis to slug and *Plutella* grazing

The effects of UV-B radiation on plant susceptibility to invertebrates has been examined in numerous plant species, however relatively few studies have investigated UV-B-mediated resistance against pests in commercially important crops, such as *B. napus*. Based on findings from previous studies in two close relatives of *B. napus*, Arabidopsis and broccoli (*B. oleracea*)(Caputo et al., 2006, Kuhlmann and Muller, 2009a, Demkura and Ballaré, 2012), it was hypothesised that -UV-B *B. napus* plants would sustain greater levels of

consumption from invertebrate pests than UV-B-treated plants, a theory that was confirmed using choice chamber bioassays with *Plutella* larvae and juvenile slugs (Chapter 3). Both herbivores were repeatedly found to consume larger areas of leaf tissue on -UV-B *B. napus* plants than on +UV-B plants, indicating that UV-B radiation can induce modifications in *B. napus* that subsequently reduces its susceptibility to these pests. Similar results were obtained from bioassays with -/+UV-B-treated Arabidopsis L*er*, with +UV-B plants sustaining up to 74% less consumption from *Plutella* and slugs than -UV-B plants. Interestingly, the difference in susceptibility of -UV-B and UV-B-treated *B. napus* and Arabidopsis plants to *Plutella* larvae in these laboratory-based bioassays complements findings from previous studies conducted outdoors, where UV-B-treated Arabidopsis and *N. antarctica* were found to receive approximately 65% and 70% more damage respectively from various Lepidopteran species when grown under attenuated levels of UV-B (Rousseaux et al., 2001, Caputo et al., 2006). Little comparison can be made between the results obtained from slug bioassays in this project and those from previous investigations, however, as only one study has previously examined the indirect effects of UV-B radiation on the feeding preferences of slugs, employing very different experimental procedures to those used in this project while using detached leaf samples from plant species unrelated to *B. napus* (Zaller et al., 2003).

As all bioassays in this project were conducted under -UV-B conditions (with the exception of those described in section 3.6), it is clear that the reduced susceptibility of UV-B-treated plants is due to the direct effects of UV-B radiation on physical and/or biochemical characteristics of the plants, and not a result of any effects UV-B may have on invertebrate behaviour. This observation is in contrast to that from a previous study (Caputo et al., 2006), which, after repeating outdoor bioassays under -UV-B laboratory conditions, stated that invertebrate perception and avoidance of UV-B radiation caused reduced susceptibility of Arabidopsis plants to *Plutella* herbivory. The discrepancies between these two studies may be due to differences in experimental setup (Caputo and co-workers (2006) ran bioassays for only 3 hours using detached leaves rather than intact plants), however the conflicting results prompted investigation of whether or not components of the UV spectrum directly influence the feeding preferences of *Plutella* and slugs (Chapter 3). Slugs, for reasons unknown, were found to consume more tissue on -UV-B *B. napus* plants positioned under UV-B conditions than on -UV-B plants located underneath UV-B-excluding filters. This finding suggests that despite their notorious nocturnal activity, slugs may be inclined to move towards regions irradiated with UV-B, perhaps even using UV-B as a cue to locate food sources, although further research will be

required to confirm or dismiss this hypothesis. In contrast to this finding and those from Caputo and co-workers (2006), *Plutella* larvae feeding preferences were not found to be influenced by UV-B or UV-A radiation, as near equal quantities of leaf tissue were consumed on all *B. napus* plants positioned under UV-B and –UV-B conditions. While the findings from slug bioassays cannot be readily explained without conducting further studies, it is clear that the presence or absence of UV-B does not affect *Plutella* feeding habits, but rather the effects of UV-B on plant characteristics determines invertebrate feeding behaviour. This conclusion can also be extended to UV-A radiation, as invertebrate bioassays with -/+UV-A-treated *B. napus* revealed a significant reduction in the susceptibility of UV-A-treated plants to both *Plutella* and slugs, with -UV-A plants losing approximately 1 and 4 cm^2 more leaf tissue to these pests, respectively. To the best of my knowledge, no studies have previously sought to investigate any role of UV-A in conferring plant resistance to microbial or invertebrate pests, although it has been reported that removal of UV-B (but not UV-A) from terrestrial sunlight reaching outdoor-grown plants increases their susceptibility to pests, suggesting that UV-B may have a bigger influence in plant defence than UV-A (Ballaré et al., 1996, Izaguirre et al., 2003, Izaguirre et al., 2007). The results from these bioassays combined with the lack of knowledge on the effects of UV-A on plant-pest interactions should encourage future studies in this area of research, as it may be that both components of the UV spectrum are capable of heightening plant defence responses. Additional bioassays directly comparing the feeding habits of slugs and *Plutella* to +UV-A and +UV-B *B. napus* will also be useful in determining if one component of UV radiation has a greater influence on plant resistance than the other.

7.3 JA-signalling, but not UVR8, is required for promoting UV-B-mediated plant defence against slug and *Plutella* herbivores in Arabidopsis

After demonstrating that UV-B radiation reduces the susceptibility of *B. napus* and wild-type Arabidopsis to *Plutella* and slug herbivory, invertebrate bioassays were conducted with several Arabidopsis lines affected in UV-B- or JA-signalling, in an attempt to identify components of these pathways involved in promoting UV-B-mediated resistance against pests (Chapter 3). Bioassays with the JA-insensitive *jar1-1* mutant revealed an essential role of this JA-amino synthetase in UV-B-mediated resistance, as little difference was observed between the average areas of leaf tissue consumed by *Plutella* larvae on the -UV-B and +UV-B plants. It remains unclear, however, whether or not the UV-B-signalling pathway converges with the wound-response pathway at this direct site or if the overlap

occurs further upstream in the JA pathway, and as such further bioassays with additional JA-insensitive mutants will hopefully provide better insight into the exact location of cross-communication between these two pathways.

Unlike components of the JA-signalling pathway, the UV-B photoreceptor, UVR8, was not found to have a role in promoting UV-B mediated plant resistance. Bioassays with wild-type L*er* or *uvr8-1* null mutants found that both genotypes appeared similarly less susceptible to the two invertebrate species following a period of UV-B radiation, while UV-B-treated *35S*pro:GFP-UVR8 over-expressing plants displayed only modest levels of resistance against slugs and *Plutella* compared to -UV-B plants. Unfortunately, the setup of these bioassays prevented direct comparisons to be made between the susceptibility of L*er* and *35S*pro:GFP-UVR8 and L*er* and *uvr8-1* plants to invertebrate herbivory following exposure to a given light treatment (-UV-B or +UV-B), which would have helped to better assess any roles of UVR8 in mediating UV-B-dependent plant resistance. However, the results obtained from this project clearly indicate that UV-B radiation enhances Arabidopsis resistance against *Plutella* and slugs in an UVR8-independent manner via the JA-signalling pathway, with the site of UV-B integration into the wound-response pathway being located around or upstream from the site of JA-amino conjugate biosynthesis by the JAR1 protein. Interestingly, these findings contrast with those presented by a previous a study (Demkura and Ballaré 2012), which reported an essential role for UVR8 in the activation of UV-B-enhanced resistance against the necrotrophic pathogen *B. cinerea* in Arabidopsis, yet none for select components of the JA pathway. These different results could perhaps indicate that two separate mechanisms of UV-B-mediated resistance exist to defend plants against invertebrate pests or pathogens, however further research with mutants and/or transgenic lines affected in different branches of the plant defence pathways would be required to strengthen this hypothesis.

7.4 *B. napus* transcripts and metabolites commonly responsive to UV-B radiation and invertebrate herbivory

Findings from the RNA-seq analysis highlighted the degrees of overlap between UV-B radiation, MeJA application, *Plutella* herbivory or slug herbivory on the transcriptomic profile of *B. napus* (Chapter 4), with results from the second read alignment in 2014 identifying a total of 199 transcripts classed as being significantly up-regulated in expression by UV-B radiation and herbivory from one or both invertebrates. Within this transcript list were a variety of putative transcription factors, including several members of

the WRKY family (*WRKY18, WRKY33* and *WRKY40*) that have previously been implicated in promoting plant defence via activation of the JA pathway (Pandey et al., 2010), a series of ANAC transcription factors, such as *ANAC001, ANAC019* and *ANAC072,* that are responsive to various abiotic and biotic stresses including invertebrate/microbial pests (Delessert et al., 2005, Ohnishi et al., 2005, Bu et al., 2008, Christianson et al., 2010, Huang et al., 2012) and select ethylene response factors (*ERF104, ERF2* and *ERF11*). Unfortunately, any roles these putative transcription factors may have in regulating UV-B-mediated defence in *B. napus* remains unknown, as these transcripts were not found to be significantly expressed by multiple treatments in the first read alignment with the Brassica 95K Unigene in 2012, and as such were not selected for further study in this project. It would therefore be interesting to obtain and/or generate Arabidopsis mutant and transgenic lines affected in the expression of these genes to assess if they are involved in UV-B-dependent plant resistance against pests. Another observation from the RNA-seq data is that the two invertebrates elicit very different transcriptional responses in *B. napus* following herbivory, with only 104 transcripts out of 1,128 found to be commonly up-regulated by both pests. While some of these transcripts have previously been associated with mediating plant resistance against pests, such as the ARR protein-encoding genes (Argueso, et al., 2012), it was surprising to see such a small number of defence-related transcripts being commonly regulated by both slugs and *Plutella*. This finding suggests that despite both herbivores being leaf-chewing pests, they can elicit invertebrate-specific effects on plant transcriptional processes. Indeed, the different transcriptome profiles of these attacked plants may highlight the finely tuned defence responses employed by *B. napus* to specifically target offending pests, which may be governed by the detection of certain physical and/or chemical properties of invertebrates by host plants. Further studies will be required to investigate how these two pests induce different transcriptional responses in *B. napus*, focusing on any effects chemical elicitors in the invertebrate saliva or slug locomotive mucus may have on plant defence responses.

Analysis of the untargeted metabolomics data identified various compounds that increased in abundance following treatment with UV-B or invertebrate herbivory (Chapter 5), including those associated with the phenylpropanoid pathway, putative lipid-based metabolites and chlorine-containing compounds. As this study was conducted towards the end of this project, the labour-intensive task of assigning putative annotations to the peaks had to be performed in a relatively short period of time, meaning that the exact identity of many of these compounds, particularly the chlorine-containing and lipid-based compounds, remains elusive. Annotation of the phenylpropanoid compounds, however, was achieved

using information from the fragmentation data and knowledge from scientific literature. These compounds were identified as being sinapate esters, chlorogenic acid (CGA) and derivatives of feruloylquinic acid, the majority of which are associated with the biosynthesis of lignin and sinapate precursors in the phenylpropanoid pathway (Landry et al., 1995). While UV-B is known to increase levels of such phenylpropanoid compounds in plants (Kusano et al., 2011, Mewis et al., 2012), it was surprising that other members of this pathway, including the UV-B-responsive kaempferol and quercetin flavonoids (Stracke et al., 2010b, Mewis et al., 2012), were not detected in this analysis. Similarly, the absence of peaks representing glucosinolate defence compounds in MeJA- and herbivore-treated samples was also unexpected, as previous studies have reported heightened levels of these compounds following similar treatments (Huang and Renwick, 1994, Renwick and Lopez, 1999, Mewis et al., 2006, Mewis et al., 2012). While it cannot be fully explained why these compounds were not detected in this study, it is highly likely that the concentrations of samples were too low to enable their efficient identification, and as such repetition of the metabolomics with more concentrated samples will be essential for better identifying compounds similarly regulated by UV-B and invertebrate herbivory. However, it can be concluded from the findings from this study that both UV-B radiation and invertebrate herbivory can increase the abundance of various compounds in *B. napus*, including those associated with the biosynthesis of lignin and sinapate precursors in the phenylpropanoid pathway.

7.5 Involvement of the phenylpropanoid and ascorbic acid biosynthetic pathways in UV-B-mediated herbivore resistance

Analysis of the RNA-seq and metabolomics data revealed several transcripts and compounds associated with the phenylpropanoid pathway and ascorbic acid (AsA) biosynthetic pathway as being responsive to UV-B radiation and invertebrate herbivory, a finding that supported the selection of *COMT1, ELI3-2* and *VTC2* for over-expression in Arabidopsis and strengthened the hypothesis that these biological pathways may be involved in UV-B-mediated plant resistance against pests (Chapter 6). Findings from invertebrate bioassays with the Arabidopsis *vtc2* null mutant revealed that the AsA biosynthetic pathway is important in promoting UV-B-mediated resistance against *Plutella,* as UV-B-treated mutants appeared more susceptible to herbivory than –UV-B mutants, and both -/+UV-B *vtc2* plants sustained higher levels of consumption than -/+UV-B Col-0 plants when *Plutella* feeding preferences between the two genotypes were assessed

(Chapter 6). In contrast to this observation, invertebrate bioassays with *comt1* and *eli3-2* null mutants revealed that removal of these proteins from the phenylpropanoid pathway does not affect UV-B-mediated resistance against *Plutella* larvae, as UV-B-treated mutants were less susceptible to herbivory than –UV-B plants of the same genotype. In addition, *Plutella* larvae were found to consume similar levels of tissue from -/+UV-B Col-0 and mutant plants when in the same choice chamber, suggesting that the null mutants are equally as attractive to *Plutella* as Col-0 plants, regardless of the light conditions they were grown under. Interestingly, bioassays conducted with an additional phenylpropanoid mutant affected in FERULIC ACID 5-HYDROXYLASE (F5H) activity, *fah1-7*, found that both -UV-B and +UV-B mutants were equally susceptible to slug herbivory, suggesting that in contrast to the results from bioassays with *comt1* and *eli3-2* mutants, the phenylpropanoid pathway is involved in UV-B-mediated plant resistance against pests. It is unknown whether or not the different observations from slug-*fah1-7* bioassays and *Plutella-comt1/eli3-2* bioassays are attributed to the specific feeding preferences of the invertebrates themselves, or if functional redundancy in the ELI protein family (Kim et al., 2007a) and between COMT1 and the closely related CCoAOMT1 (Fellenberg et al., 2012) has resulted in these mutants retaining UV-B-mediated resistance against invertebrate pests. Either way, the findings from *Plutella* bioassays with an Arabidopsis line over-expressing a putative *B. napus* orthologue of *COMT1* provided strong evidence to support the hypothesis that the phenylpropanoid pathway is involved in promoting plant resistance against this pest (Chapter 6).

In accordance with what has been previously observed in bioassays with -/+UV-B wild-type Arabidopsis, UV-B-treated *35S*pro:3xHA-COMT1 plants were found to sustain significantly less consumption from *Plutella* than –UV-B plants. When the feeding preferences of *Plutella* were assessed between UV-B-treated *35S*pro:3xHA-COMT1 and Col-0 plants, the over-expressing line appeared significantly less susceptible to herbivory than the wild-type plants, indicating that hyper-activation of the particular branch of the phenylpropanoid pathway that COMT1 is active in enhances levels of UV-B-mediated resistance against *Plutella* larvae in Arabidopsis. It remains unclear, however, if this response is strictly UV-B-dependent, as bioassays investigating *Plutella* feeding preferences between –UV-B-treated Col-0 and *35S*pro:3xHA-COMT1 plants revealed little difference in the average areas of leaf tissue consumed by this pest on either genotype, although examination of the individual biological replicates found a clear feeding preference of *Plutella* for –UV-B-treated Col-0 plants over *35S*pro:3xHA-COMT1. While this observation suggests that –UV-B *35S*pro:3xHA-COMT1 plants are less susceptible to

invertebrate herbivory than wild-type Arabidopsis exposed to the same light treatment, it would be beneficial to repeat these bioassays to obtain more statistically significant results. It can be concluded from these invertebrate bioassays, however, that both the AsA and phenylpropanoid pathways are important in promoting UV-B-mediated resistance against *Plutella* and slug herbivores, and future research with additional *35S*pro:3xHA-COMT1 lines, along with the *35S*pro:GFP-ELI3-2 and *35S*pro:GFP-VTC2 transgenic lines, will hopefully provide greater insight into how these biological pathways improve plant tolerance to select herbivore pests.

7.6 The molecular mechanisms of UV-B-mediated herbivore resistance in *B. napus*

The main conclusions from this project can be summarised as follows:

1. Arabidopsis and *B. napus* grown under UV-B-supplemented light have reduced susceptibility to *Plutella* and slug herbivory.
2. UV-A-treated *B. napus* plants are also less attractive to *Plutella* and slugs.
3. UV-B responses integrate into the JA pathway either upstream of or directly at the site of JA-amino conjugate biosynthesis by the JAR1 protein to mediate UV-B-enhanced plant resistance against *Plutella* and slugs. This occurs independently of UVR8.
4. Invertebrate herbivory and UV-B radiation similarly increase the expression of various *B. napus* transcripts thought to encode putative transcription factors and genes previously associated with plant resistance against pests.
5. Few transcripts were identified as being commonly regulated by slug and *Plutella* herbivory, indicating that these two invertebrates can induce different transcriptomic responses in *B. napus*.
6. A small number of identifiable *B. napus* compounds increased in abundance following UV-B radiation and/or invertebrate herbivory, including phenylpropanoids, putative lipid-based metabolites, and chlorine-containing compounds, one of which is thought to contain an ascorbic acid group.
7. Three *B. napus* genes were selected for over-expression in Arabidopsis: *COMT1* and *ELI3-2* encode enzymes involved in the phenylpropanoid pathway, while *VTC2* encodes a mannose-1-phosphate guanylyltransferase active in the ascorbic acid (AsA) biosynthetic pathway.

8. *Plutella* bioassays with *vtc2* null mutants indicated that a functional AsA pathway is required for UV-B-mediated resistance in *B. napus*.
9. Removal of functional COMT1 and ELI3-2 does not affect UV-B-mediated resistance against *Plutella* in Arabidopsis, although bioassays with the *fah1-7* mutant revealed that this pathway is involved in UV-B-mediated resistance.
10. A UV-B-treated *35S*pro:3xHA-COMT1 Arabidopsis line was less susceptible to *Plutella* than UV-B-treated wild-type plants, suggesting that hyper-activation of the phenylpropanoid pathway in Arabidopsis enhances UV-B-mediated resistance against *Plutella.*

The main findings from this project (Figure 7-1) have contributed to our knowledge on the molecular mechanisms of UV-B-mediated plant resistance against pests, and future research will hopefully expand our understanding on the intricate interplay between these two signalling pathways in enhancing plant tolerance to invertebrate herbivores.

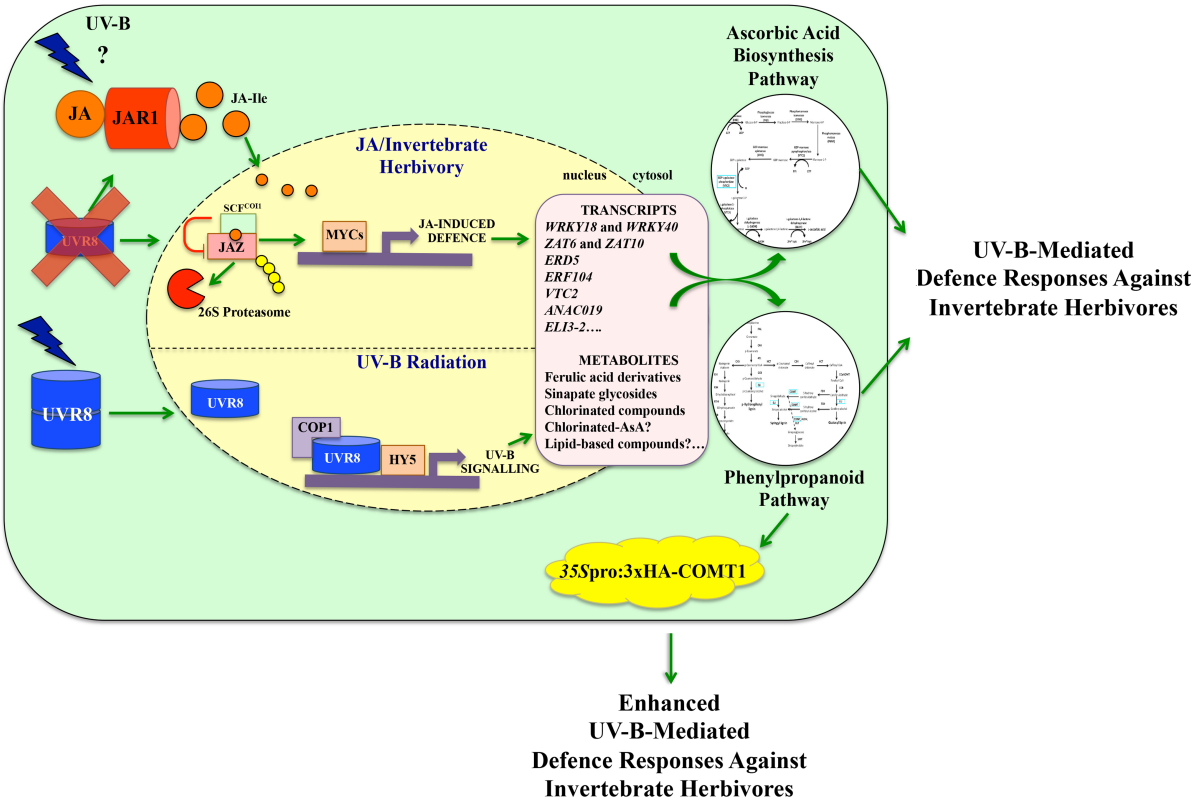

Figure 7-1: Schematic representation of the main findings from this project and the putative role of the phenylpropanoid pathway in mediating UV-B-enhanced plant defence responses. The use of Arabidopsis mutants impaired in JAR1 or UVR8 function revealed that UV-B-mediated plant defence is dependent on functional JAR1, which promotes the formation of JA derivatives such as JA-Ile, but is independent of the UV-B photoreceptor, UVR8. It remains unknown if UV-B directly targets the formation of JA-derivatives or if it operates upstream or downstream of JAR1, however it seems that the production of JA-derivatives, such as JA-Ile, via JAR1 is essential for mediating UV-B-mediated plant defence against invertebrate pests. Transcriptomic and metabolomic studies identified various genes and compounds commonly regulated by UV-B radiation and invertebrate herbivory (pink box). Experiments with Arabidopsis mutants impaired in the expression of gene products involved in the phenylpropanoid and ascorbic acid biosynthesis pathways suggest that they are involved in mediating plant defence against *Plutella* and slug herbivores, while bioassays with an Arabidopsis line over-expressing a putative *B. napus COMT1* gene found heightened levels of UV-B-mediated defence responses against *Plutella* larvae, indicating that the phenylpropanoid pathway is important in mediating plant defence responses against invertebrate pests.

7.7 Future research

Progress has been made in investigating the molecular mechanisms of UV-B mediated herbivore resistance in *B. napus*, however further research is required to address the many questions that still remain over the convergence between UV-B- and herbivore-induced signalling pathways in plants.

The first objective is to confirm where in the JA pathway UV-B responses integrate by conducting invertebrate bioassays with Arabidopsis mutants affected in JA signalling upstream of the JAR1 protein. Despite a previous study reporting no increased levels of JA in UV-B-treated *N. attenuata* plants (Demkura et al., 2010), it would be interesting to examine invertebrate feeding preferences on -/+UV-B-treated *aos* and *lox2* mutants impaired in JA biosynthesis, to investigate if UV-B influences the JA biosynthetic pathway to regulate UV-B-mediated resistance in Arabidopsis. Hopefully, these bioassays will provide invaluable insight into how these two signalling pathways cross-communicate with one another to enhance plant tolerance to pests.

Data obtained from the transcriptomic and metabolomic studies was extensive, and as such could not be completely interpreted during this project. It is therefore of great importance to continue analysing these findings and to repeat the metabolomics when possible with more concentrated samples, to gain more information on the overlap between UV-B- and herbivore-induced responses in *B. napus.* If possible, Arabidopsis mutant and transgenic lines impaired in expression of some of the putative transcription factors identified as being commonly regulated by UV-B and invertebrate herbivory should be obtained for further study, to assess if the encoded products have any role in regulating UV-B-mediated resistance. Such studies will include comparing the expression of various wound-response genes in these lines to wild-type plants following -/+UV-B treatment, while also conducting invertebrate bioassays with -/+UV-B-treated plants to investigate any effects of removing or enhancing levels of these genes in Arabidopsis on slug and *Plutella* feeding preferences. As no studies have previously compared changes in the *B. napus* transcriptome and metabolome following treatment with UV-B radiation, MeJA application or invertebrate herbivory, all the information extracted from these datasets is novel, and will be invaluable in driving future projects investigating UV-B-mediated resistance in plants. Likewise, knowledge of the genetic and biochemical changes elicited by slug herbivory on *B. napus* will be of extreme interest to fellow researchers investigating the mechanisms of plant-pest interactions, as the lack of research being conducted on this important agricultural pest has limited our understanding on plant

defence responses against them, and how we can use these endogenous mechanisms to devise novel methods of slug control.

Finally, continued analysis of the Arabidopsis transgenic lines over-expressing putative *B. napus* orthologues of *COMT1, ELI3-2* and *VTC2* will be important in assessing any roles the encoded products may have in UV-B-mediated resistance. Homozygous *35S*pro:GFP-ELI3-2 and *35S*pro:GFP-VTC2 lines are currently being generated from segregating lines, and will hopefully be ready for analysis and use in invertebrate bioassays in the near future. It will be important to assess invertebrate feeding preferences between -/+UV-B-treated plants of the same genotype as well as between the over-expressing lines and Col-0 plants following exposure to the same light treatments, to allow conclusions to be drawn on the effects of over-expressing these genes on the susceptibility of Arabidopsis to invertebrate herbivory. Further bioassays with additional *35S*pro:3xHA-COMT1 lines should also be conducted to assess if the heightened resistance described in Chapter 6 is due to over-expression of this gene in Arabidopsis, or if it is simply a result of where this gene has been inserted in the Arabidopsis genome. If over-expression of these genes is found to increase Arabidopsis resistance against *Plutella* and/or slugs, then the molecular basis for this enhanced resistance needs to be elucidated by using a variety of analytical techniques to assess both the physical properties and the genetic and biochemical profiles of these transgenic lines. Such techniques include thin layer chromatography, to provide a semi-quantitative overview of the abundance of phenylpropanoid compounds in -/+UV-B-treated Col-0, *35S*pro:3xHA-COMT1 and *35S*pro:GFP-ELI3-2 lines, the Maüle histochemical staining technique to assess the degree of lignification in the same over-expressing lines along with any subsequent changes in the structural aspects of these plants, the ascorbate oxidase assay to measure levels of AsA in the *35S*pro:GFP-VTC2 transgenic lines (Rao and Ormrod, 1995), and of course an omics-based approach to compare differences at the transcriptional and metabolomic levels of these plants to the progenitor line.

These future studies will be essential for building upon the foundations laid down by this project, and will hopefully be invaluable in providing greater insight into the molecular basis of herbivore resistance in members of the Brassicaceae family.

Appendices

Appendix 1

Annotation Cluster 1	Enrichment Score: 8.82	Count	PValue	FDR
GOTERM_CC_FAT	GO:0005618~cell wall	77	5.62E-11	7.20E-08
GOTERM_CC_FAT	GO:0030312~external encapsulating structure	77	1.14E-10	1.46E-07
GOTERM_CC_FAT	GO:0009505~plant-type cell wall	38	5.33E-07	6.83E-04
Annotation Cluster 2	**Enrichment Score: 5.32**	**Count**	**PValue**	**FDR**
GOTERM_BP_FAT	GO:0009628~response to abiotic stimulus	113	5.15E-08	8.46E-05
GOTERM_BP_FAT	GO:0006970~response to osmotic stress	45	1.66E-05	2.73E-02
GOTERM_BP_FAT	GO:0009651~response to salt stress	40	1.25E-04	2.05E-01
Annotation Cluster 3	**Enrichment Score: 4.80**	**Count**	**PValue**	**FDR**
GOTERM_BP_FAT	GO:0016053~organic acid biosynthetic process	53	2.99E-08	4.92E-05
GOTERM_BP_FAT	GO:0046394~carboxylic acid biosynthetic process	53	2.99E-08	4.92E-05
GOTERM_BP_FAT	GO:0006633~fatty acid biosynthetic process	23	8.90E-05	1.46E-01
GOTERM_BP_FAT	GO:0006631~fatty acid metabolic process	25	1.06E-03	1.73E+00
GOTERM_BP_FAT	GO:0008610~lipid biosynthetic process	36	1.19E-02	1.78E+01
Annotation Cluster 4	**Enrichment Score: 4.68**	**Count**	**PValue**	**FDR**
GOTERM_MF_FAT	GO:0004674~protein serine/threonine kinase activity	95	2.53E-07	3.83E-04
GOTERM_BP_FAT	GO:0006468~protein amino acid phosphorylation	99	8.40E-07	1.38E-03
GOTERM_BP_FAT	GO:0006796~phosphate metabolic process	112	2.04E-06	3.35E-03
GOTERM_BP_FAT	GO:0006793~phosphorus metabolic process	112	2.14E-06	3.52E-03
GOTERM_MF_FAT	GO:0004672~protein kinase activity	99	7.19E-06	1.09E-02
GOTERM_BP_FAT	GO:0016310~phosphorylation	103	7.56E-06	1.24E-02
GOTERM_MF_FAT	GO:0032559~adenyl ribonucleotide binding	181	1.49E-05	2.25E-02
GOTERM_MF_FAT	GO:0005524~ATP binding	177	3.54E-05	5.35E-02
GOTERM_MF_FAT	GO:0001882~nucleoside binding	188	6.11E-05	9.25E-02
GOTERM_MF_FAT	GO:0032555~purine ribonucleotide binding	193	6.93E-05	1.05E-01
GOTERM_MF_FAT	GO:0032553~ribonucleotide binding	193	6.93E-05	1.05E-01
GOTERM_MF_FAT	GO:0030554~adenyl nucleotide binding	187	7.12E-05	1.08E-01
GOTERM_MF_FAT	GO:0001883~purine nucleoside binding	187	7.12E-05	1.08E-01
GOTERM_MF_FAT	GO:0017076~purine nucleotide binding	199	2.87E-04	4.34E-01
GOTERM_MF_FAT	GO:0000166~nucleotide binding	221	6.28E-03	9.10E+00
Annotation Cluster 5	**Enrichment Score: 4.61**	**Count**	**PValue**	**FDR**

GOTERM_BP_FAT	GO:0009617~response to bacterium	37	1.15E-07	1.89E-04
GOTERM_BP_FAT	GO:0042742~defense response to bacterium	29	1.57E-06	2.58E-03
GOTERM_BP_FAT	GO:0006952~defense response	70	7.94E-02	7.43E+01
Annotation Cluster 6	**Enrichment Score: 4.36**	**Count**	**PValue**	**FDR**
GOTERM_BP_FAT	GO:0010033~response to organic substance	120	1.60E-10	2.62E-07
GOTERM_BP_FAT	GO:0009719~response to endogenous stimulus	102	1.37E-09	2.25E-06
GOTERM_BP_FAT	GO:0009725~response to hormone stimulus	82	2.62E-05	4.31E-02
GOTERM_BP_FAT	GO:0007242~intracellular signaling cascade	69	3.32E-04	5.43E-01
GOTERM_BP_FAT	GO:0009755~hormone-mediated signalling	43	4.33E-04	7.09E-01
GOTERM_BP_FAT	GO:0032870~cellular response to hormone stimulus	43	4.33E-04	7.09E-01
GOTERM_BP_FAT	GO:0009873~ethylene mediated signalling pathway	19	7.71E-03	1.19E+01
GOTERM_BP_FAT	GO:0000160~two-component signal transduction system (phosphorelay)	22	1.20E-02	1.80E+01
GOTERM_BP_FAT	GO:0009723~response to ethylene stimulus	24	1.92E-02	2.73E+01
Annotation Cluster 7	**Enrichment Score: 3.50**	**Count**	**PValue**	**FDR**
GOTERM_BP_FAT	GO:0018130~heterocycle biosynthetic process	20	1.56E-04	2.56E-01
GOTERM_BP_FAT	GO:0044271~nitrogen compound biosynthetic process	50	1.60E-04	2.62E-01
GOTERM_BP_FAT	GO:0009309~amine biosynthetic process	25	5.36E-04	8.76E-01
GOTERM_BP_FAT	GO:0008652~cellular amino acid biosynthetic process	23	7.22E-04	1.18E+00
Annotation Cluster 8	**Enrichment Score: 3.24**	**Count**	**PValue**	**FDR**
GOTERM_BP_FAT	GO:0009266~response to temperature stimulus	40	5.09E-05	8.35E-02
GOTERM_BP_FAT	GO:0009409~response to cold	29	1.33E-04	2.19E-01
GOTERM_BP_FAT	GO:0009408~response to heat	14	2.75E-02	3.68E+01
Annotation Cluster 9	**Enrichment Score: 3.11**	**Count**	**PValue**	**FDR**
GOTERM_MF_FAT	GO:0005529~sugar binding	19	2.25E-04	3.40E-01
GOTERM_MF_FAT	GO:0030246~carbohydrate binding	24	2.69E-03	4.00E+00
Annotation Cluster 10	**Enrichment Score: 2.88**	**Count**	**PValue**	**FDR**
GOTERM_CC_FAT	GO:0048046~apoplast	45	5.74E-06	7.35E-03
Annotation Cluster 11	**Enrichment Score: 2.80**	**Count**	**PValue**	**FDR**
GOTERM_BP_FAT	GO:0005976~polysaccharide metabolic process	31	6.13E-06	1.01E-02
GOTERM_BP_FAT	GO:0044042~glucan metabolic process	22	1.19E-04	1.95E-01

GOTERM_BP_FAT	GO:0044264~cellular polysaccharide metabolic process	22	1.57E-04	2.58E-01
GOTERM_BP_FAT	GO:0006073~cellular glucan metabolic process	18	6.07E-04	9.92E-01
GOTERM_MF_FAT	GO:0016762~xyloglucan:xyloglucosyl transferase activity	7	9.89E-03	1.40E+01
Annotation Cluster 12	**Enrichment Score: 2.77**	**Count**	**PValue**	**FDR**
GOTERM_MF_FAT	GO:0050403~trans-zeatin O-beta-D-glucosyltransferase activity	4	1.69E-03	2.52E+00
GOTERM_MF_FAT	GO:0050502~cis-zeatin O-beta-D-glucosyltransferase activity	4	1.69E-03	2.52E+00
Annotation Cluster 13	**Enrichment Score: 2.71**	**Count**	**PValue**	**FDR**
GOTERM_BP_FAT	GO:0007166~cell surface receptor linked signal transduction	21	9.66E-04	1.58E+00
GOTERM_BP_FAT	GO:0007169~transmembrane receptor protein tyrosine kinase signalling pathway	17	2.73E-03	4.39E+00
GOTERM_BP_FAT	GO:0007167~enzyme linked receptor protein signalling pathway	17	2.73E-03	4.39E+00
Annotation Cluster 14	**Enrichment Score: 2.60**	**Count**	**PValue**	**FDR**
GOTERM_CC_FAT	GO:0031224~intrinsic to membrane	185	1.35E-03	1.71E+00
GOTERM_CC_FAT	GO:0016021~integral to membrane	152	4.89E-03	6.09E+00
Annotation Cluster 15	**Enrichment Score: 2.37**	**Count**	**PValue**	**FDR**
GOTERM_BP_FAT	GO:0031407~oxylipin metabolic process	8	2.54E-03	4.09E+00
GOTERM_BP_FAT	GO:0009694~jasmonic acid metabolic process	7	2.79E-03	4.49E+00
GOTERM_BP_FAT	GO:0031408~oxylipin biosynthetic process	7	5.94E-03	9.33E+00
GOTERM_BP_FAT	GO:0009695~jasmonic acid biosynthetic process	6	8.21E-03	1.27E+01
Annotation Cluster 16	**Enrichment Score: 2.07**	**Count**	**PValue**	**FDR**
GOTERM_BP_FAT	GO:0009737~response to abscisic acid stimulus	29	3.17E-03	5.09E+00
GOTERM_BP_FAT	GO:0009738~abscisic acid mediated signalling	10	2.33E-02	3.21E+01
Annotation Cluster 17	**Enrichment Score: 2.00**	**Count**	**PValue**	**FDR**
GOTERM_BP_FAT	GO:0052542~callose deposition during defense response	6	2.64E-03	4.26E+00
GOTERM_BP_FAT	GO:0052386~cell wall thickening	6	3.42E-03	5.48E+00
GOTERM_BP_FAT	GO:0052545~callose localization	6	4.36E-03	6.92E+00
GOTERM_BP_FAT	GO:0033037~polysaccharide localization	6	5.45E-03	8.59E+00
GOTERM_BP_FAT	GO:0052482~cell wall thickening during defense response	5	1.07E-02	1.62E+01
GOTERM_BP_FAT	GO:0052544~callose deposition in cell wall during defense response	5	1.07E-02	1.62E+01

GOTERM_BP_FAT	GO:0052543~callose deposition in cell wall	5	1.65E-02	2.39E+01
Annotation Cluster 18	**Enrichment Score: 1.85**	**Count**	**PValue**	**FDR**
GOTERM_MF_FAT	GO:0046527~glucosyltransferase activity	16	1.13E-02	1.58E+01
GOTERM_MF_FAT	GO:0035251~UDP-glucosyltransferase activity	14	1.78E-02	2.39E+01
Annotation Cluster 19	**Enrichment Score: 1.83**	**Count**	**PValue**	**FDR**
GOTERM_BP_FAT	GO:0044036~cell wall macromolecule metabolic process	10	1.75E-03	2.84E+00
GOTERM_BP_FAT	GO:0010383~cell wall polysaccharide metabolic process	5	8.41E-03	1.29E+01
GOTERM_BP_FAT	GO:0045491~xylan metabolic process	4	2.12E-02	2.96E+01
GOTERM_BP_FAT	GO:0010410~hemicellulose metabolic process	4	2.12E-02	2.96E+01
Annotation Cluster 20	**Enrichment Score: 1.81**	**Count**	**PValue**	**FDR**
GOTERM_BP_FAT	GO:0009743~response to carbohydrate stimulus	22	4.38E-03	6.96E+00
Annotation Cluster 21	**Enrichment Score: 1.69**	**Count**	**PValue**	**FDR**
GOTERM_BP_FAT	GO:0006576~biogenic amine metabolic process	11	1.60E-03	2.59E+00
GOTERM_BP_FAT	GO:0042430~indole and derivative metabolic process	9	2.15E-03	3.47E+00
GOTERM_BP_FAT	GO:0042434~indole derivative metabolic process	9	2.15E-03	3.47E+00
GOTERM_BP_FAT	GO:0042435~indole derivative biosynthetic process	8	4.19E-03	6.67E+00
GOTERM_BP_FAT	GO:0000162~tryptophan biosynthetic process	6	4.36E-03	6.92E+00
GOTERM_BP_FAT	GO:0046219~indolalkylamine biosynthetic process	6	4.36E-03	6.92E+00
GOTERM_BP_FAT	GO:0042401~biogenic amine biosynthetic process	8	6.56E-03	1.02E+01
GOTERM_BP_FAT	GO:0006568~tryptophan metabolic process	6	8.21E-03	1.27E+01
GOTERM_BP_FAT	GO:0006586~indolalkylamine metabolic process	6	8.21E-03	1.27E+01
GOTERM_BP_FAT	GO:0046417~chorismate metabolic process	8	1.11E-02	1.67E+01
GOTERM_BP_FAT	GO:0009073~aromatic amino acid family biosynthetic process	8	1.11E-02	1.67E+01
GOTERM_BP_FAT	GO:0009072~aromatic amino acid family metabolic process	9	1.74E-02	2.51E+01
GOTERM_BP_FAT	GO:0043648~dicarboxylic acid metabolic process	10	2.15E-02	3.00E+01
Annotation Cluster 22	**Enrichment Score: 1.62**	**Count**	**PValue**	**FDR**
GOTERM_BP_FAT	GO:0034637~cellular carbohydrate biosynthetic process	23	1.03E-03	1.69E+00

GOTERM_BP_FAT	GO:0016051~carbohydrate biosynthetic process	28	1.21E-03	1.97E+00
GOTERM_BP_FAT	GO:0030243~cellulose metabolic process	10	1.05E-02	1.60E+01
GOTERM_BP_FAT	GO:0000271~polysaccharide biosynthetic process	12	3.94E-02	4.84E+01
Annotation Cluster 23	**Enrichment Score: 1.57**	**Count**	**PValue**	**FDR**
GOTERM_BP_FAT	GO:0009414~response to water deprivation	18	2.18E-02	3.04E+01
GOTERM_BP_FAT	GO:0009415~response to water	18	3.33E-02	4.26E+01
Annotation Cluster 24	**Enrichment Score: 1.43**	**Count**	**PValue**	**FDR**
GOTERM_BP_FAT	GO:0006020~inositol metabolic process	5	1.34E-02	1.99E+01
GOTERM_BP_FAT	GO:0019751~polyol metabolic process	7	2.12E-02	2.97E+01
Annotation Cluster 25	**Enrichment Score: 1.41**	**Count**	**PValue**	**FDR**
GOTERM_BP_FAT	GO:0042430~indole and derivative metabolic process	9	2.15E-03	3.47E+00
GOTERM_BP_FAT	GO:0042434~indole derivative metabolic process	9	2.15E-03	3.47E+00
GOTERM_BP_FAT	GO:0019760~glucosinolate metabolic process	7	3.63E-02	4.55E+01
GOTERM_BP_FAT	GO:0016143~S-glycoside metabolic process	7	3.63E-02	4.55E+01
GOTERM_BP_FAT	GO:0019757~glycosinolate metabolic process	7	3.63E-02	4.55E+01
GOTERM_BP_FAT	GO:0016137~glycoside metabolic process	10	4.74E-02	5.50E+01
Annotation Cluster 26	**Enrichment Score: 1.39**	**Count**	**PValue**	**FDR**
GOTERM_BP_FAT	GO:0042538~hyperosmotic salinity response	7	2.96E-02	3.90E+01
Annotation Cluster 27	**Enrichment Score: 1.32**	**Count**	**PValue**	**FDR**
GOTERM_BP_FAT	GO:0006575~cellular amino acid derivative metabolic process	29	2.46E-03	3.96E+00
GOTERM_BP_FAT	GO:0042398~cellular amino acid derivative biosynthetic process	21	6.90E-03	1.08E+01
GOTERM_BP_FAT	GO:0019748~secondary metabolic process	37	9.53E-03	1.46E+01
GOTERM_BP_FAT	GO:0019438~aromatic compound biosynthetic process	22	1.04E-02	1.58E+01
Annotation Cluster 28	**Enrichment Score: 1.29**	**Count**	**PValue**	**FDR**
GOTERM_BP_FAT	GO:0009063~cellular amino acid catabolic process	7	3.63E-02	4.55E+01
GOTERM_BP_FAT	GO:0046395~carboxylic acid catabolic process	10	4.45E-02	5.26E+01
GOTERM_BP_FAT	GO:0016054~organic acid catabolic process	10	4.45E-02	5.26E+01
GOTERM_BP_FAT	GO:0009310~amine catabolic process	7	4.80E-02	5.54E+01

Annotation Cluster 29	Enrichment Score: 1.26	Count	PValue	FDR
GOTERM_BP_FAT	GO:0018130~heterocycle biosynthetic process	20	1.56E-04	2.56E-01
GOTERM_BP_FAT	GO:0033014~tetrapyrrole biosynthetic process	8	2.16E-02	3.02E+01
GOTERM_BP_FAT	GO:0015995~chlorophyll biosynthetic process	6	4.08E-02	4.96E+01
GOTERM_BP_FAT	GO:0006779~porphyrin biosynthetic process	7	4.80E-02	5.54E+01
Annotation Cluster 30	**Enrichment Score: 1.23**	**Count**	**PValue**	**FDR**
GOTERM_MF_FAT	GO:0050162~oxalate oxidase activity	3	9.35E-03	1.33E+01
GOTERM_CC_FAT	GO:0044421~extracellular region part	7	2.68E-02	2.94E+01
Annotation Cluster 31	**Enrichment Score: 1.19**	**Count**	**PValue**	**FDR**
GOTERM_BP_FAT	GO:0043401~steroid hormone mediated signalling	5	5.64E-02	6.15E+01
GOTERM_BP_FAT	GO:0009742~brassinosteroid mediated signalling	5	5.64E-02	6.15E+01
GOTERM_BP_FAT	GO:0048545~response to steroid hormone stimulus	5	5.64E-02	6.15E+01
GOTERM_BP_FAT	GO:0009741~response to brassinosteroid stimulus	6	1.01E-01	8.27E+01
Annotation Cluster 32	**Enrichment Score: 1.17**	**Count**	**PValue**	**FDR**
GOTERM_BP_FAT	GO:0022610~biological adhesion	4	6.78E-02	6.85E+01
GOTERM_BP_FAT	GO:0007155~cell adhesion	4	6.78E-02	6.85E+01
Annotation Cluster 33	**Enrichment Score: 1.15**	**Count**	**PValue**	**FDR**
GOTERM_BP_FAT	GO:0048585~negative regulation of response to stimulus	10	1.28E-02	1.90E+01
GOTERM_BP_FAT	GO:0010104~regulation of ethylene mediated signalling pathway	4	3.37E-02	4.31E+01
GOTERM_BP_FAT	GO:0070297~regulation of two-component signal transduction	4	3.37E-02	4.31E+01
Annotation Cluster 34	**Enrichment Score: 1.15**	**Count**	**PValue**	**FDR**
GOTERM_BP_FAT	GO:0009081~branched chain family amino acid metabolic process	6	4.08E-02	4.96E+01
Annotation Cluster 35	**Enrichment Score: 1.14**	**Count**	**PValue**	**FDR**
GOTERM_CC_FAT	GO:0046658~anchored to plasma membrane	9	3.23E-02	3.44E+01
Annotation Cluster 36	**Enrichment Score: 1.12**	**Count**	**PValue**	**FDR**
GOTERM_BP_FAT	GO:0019853~L-ascorbic acid biosynthetic process	5	4.82E-03	7.63E+00
GOTERM_BP_FAT	GO:0019852~L-ascorbic acid metabolic process	5	4.82E-03	7.63E+00

Annotation Cluster 37	Enrichment Score: 1.10	Count	PValue	FDR
GOTERM_CC_FAT	GO:0005788~endoplasmic reticulum lumen	6	8.27E-03	1.01E+01
GOTERM_CC_FAT	GO:0044432~endoplasmic reticulum part	11	3.52E-02	3.68E+01
Annotation Cluster 38	**Enrichment Score: 1.06**	**Count**	**PValue**	**FDR**
GOTERM_BP_FAT	GO:0010374~stomatal complex development	5	4.99E-02	5.69E+01
Annotation Cluster 39	**Enrichment Score: 1.03**	**Count**	**PValue**	**FDR**
GOTERM_BP_FAT	GO:0045087~innate immune response	24	3.94E-02	4.84E+01
GOTERM_BP_FAT	GO:0009626~plant-type hypersensitive response	7	4.00E-02	4.88E+01
GOTERM_BP_FAT	GO:0006955~immune response	25	4.37E-02	5.20E+01
GOTERM_BP_FAT	GO:0034050~host programmed cell death induced by symbiont	7	4.38E-02	5.21E+01
Annotation Cluster 40	**Enrichment Score: 1.03**	**Count**	**PValue**	**FDR**
GOTERM_MF_FAT	GO:0003979~UDP-glucose 6-dehydrogenase activity	3	1.80E-02	2.40E+01
Annotation Cluster 41	**Enrichment Score: 1.02**	**Count**	**PValue**	**FDR**
GOTERM_CC_FAT	GO:0009941~chloroplast envelope	39	6.39E-03	7.89E+00
GOTERM_CC_FAT	GO:0009526~plastid envelope	39	1.31E-02	1.56E+01
Annotation Cluster 42	**Enrichment Score: 1.00**	**Count**	**PValue**	**FDR**
GOTERM_BP_FAT	GO:0007018~microtubule-based movement	12	3.50E-03	5.59E+00
GOTERM_BP_FAT	GO:0007017~microtubule-based process	14	1.93E-02	2.74E+01
GOTERM_MF_FAT	GO:0003777~microtubule motor activity	9	3.58E-02	4.24E+01
Annotation Cluster 43	**Enrichment Score: 0.99**	**Count**	**PValue**	**FDR**
GOTERM_BP_FAT	GO:0009821~alkaloid biosynthetic process	4	3.37E-02	4.31E+01
GOTERM_BP_FAT	GO:0009820~alkaloid metabolic process	8	4.79E-02	5.54E+01
Annotation Cluster 44	**Enrichment Score: 0.95**	**Count**	**PValue**	**FDR**
GOTERM_MF_FAT	GO:0008483~transaminase activity	9	1.08E-02	1.52E+01
GOTERM_MF_FAT	GO:0016769~transferase activity, transferring nitrogenous groups	9	4.16E-02	4.75E+01
Annotation Cluster 45	**Enrichment Score: 0.50**	**Count**	**PValue**	**FDR**
GOTERM_BP_FAT	GO:0016052~carbohydrate catabolic process	20	2.25E-02	3.12E+01
GOTERM_BP_FAT	GO:0009820~alkaloid metabolic process	8	4.79E-02	5.54E+01

Appendix 1: Annotation clusters and GO terms ($p \geq 0.05$) of Brassica 95K Unigenes possessing at least a 2-fold change in expression (RPKM ≥ 3) following treatment with UV-B radiation, MeJA treatment, slug herbivory or *Plutella* herbivory (Chapter 4, section 4.4.2).

Appendix 2

CN	Peak ID	Proposed KEGG EF ([M-H]$^-$)	Putative EF ([M-H]$^-$)	Putative Metabolite Details
1	d4d89811f1d34fd991c73ef9482f705ff7ed22b7	N/A	N/A	Background noise.
2	4be2e3386d169cee75ff115af02ef44a08b99cab	N/A	$C_{14}H_{29}O_7Cl$	Cl-containing.
3	34a642e0e558cd149db973b7d2e47fe55bd3926c	N/A	N/A	N/A
4	cbef867e70c11aa41873f072f336d892120ae8a	$C_{15}H_{22}O_9$	$C_{15}H_{22}O_9$	Low abundance
5	d3a5a3b787d9ba97436e08810102f6481488900f	N/A	$C_{14}H_{14}O_9$	Low abundance; possible 3-O-Galloylshikimic acid.
6	f94412ca20dfe5fe66b76ddb0bcbe4bd53fb887b	N/A	N/A	Peak found alongside **CN11**; no further information available.
7	beed99533c1f566bb92051a4fb336b64c2a4d77f	$C_6H_8O_7$	N/A	
8	9950036e2a18cfaaac7b98dacab412a64d0c6fc0	$C_6H_8O_7$	N/A	
9	1870659f7e5f1ec5a929c0bf5eeb00276012aac1	N/A	N/A	
10	146fb934548370b0f0679c14f5686c159854c3e2	$C_{17}H_{20}O_9$	$C_{17}H_{20}O_9$	5-O-Feruloyquinic acid.
11	b2d8a112c08c6bee5db8e48536abc4964bae9c3d	$C_{23}H_{31}ClO_6$	N/A	Three isomers closely eluting together prevented further analysis; may benefit from a lipidomics approach.
12	e5ac0aa06a7423485a9d17475da681b01e412976	N/A	N/A	
13	6a9a0c0a90de7a21f8db69b7cb5e966e70ea3c76	$C_{16}H_{14}F_3N_5O$	$C_{17}H_{19}NO_7$	Proposed modified phenolic acid glycoside.
14	93a0f0afc6d49c5cdd0885c79395495b7180ae3a	$C_{23}H_{29}NO_{12}$	N/A	Low abundance and difficult to characterise.
15	343af0de67b652d72d93f87241c8e9102513df18	N/A	$C_{14}H_{24}O_{12}S$	Resembles **U5**; separated by CH_2 group.
16	bc68c1662edb0fe3407e79ad80b0a07f2bf521df	N/A	N/A	
17	a4e9a45e774d44e86fcd085e6143ba54ee030b99	N/A	N/A	
18	65df8c42314d7674703b512415ebc472e559da03	N/A	$C_{20}H_{36}O_9$	Could be fragment of **UV7.**
19	b0581fa770835b3ca19c099b0f605a13178861b1	N/A	$C_{20}H_{36}O_9$	Could be fragment of **UV7.**
20	8c7083b2619c22449b8c4661e4e2f3effd46d6d1	N/A	N/A	Two isomers of feruoylquinic acids; related to **CN10.**
21	d46099442d52a6a450023557ab2d4ffbcfe7130a	N/A	$C_{14}H_{27}O_8Cl$	Cl-containing.
22	dd6732d753662aea40a092ff82c92956e33cc375	N/A	$C_{18}H_{35}O_8Cl$	Cl-containing.
23	89cae35458308264f3ff9a7d9fc129e7be3e5e7c	N/A	N/A	
24	d874162097dd03b65cde97bf08f2192e47592840	N/A	N/A	Background noise.
25	a31ec0a01ddd31b262a95d9d00f831943f1a2d55	N/A	$C_{18}H_{20}N_4OS_3$	Unknown, but responsive to *Plutella* and MeJA.
26	068272b6a942cd7b5750625097646843ab10878b	$C_5H_4O_3$	N/A	
UV1	ef87b37a6a47e28ef48e00f8c1d67adf2144c276	N/A	N/A	
UV2	a7a599f4816545be19d1b193dbcb965560e553cf	$C_5H_6O_4$	N/A	
UV3	d4d4826247e578cd6ff53e82b8662d144846510d	N/A	N/A	
UV4	46cf893181b60e4739b8aef02100f50857aa3085	N/A	N/A	
UV5	697ec4157edae798751ca615666d93f79cdaae1a	$C_{19}H_{18}N_4O_8$	$C_{15}H_{26}O_{12}S$	Possesses sulphated, acylated sore stucture, likely attached to

				aliphatic chain. Related to **CN15.**
UV6	a8abf5f9dcffdb700d4126636df1844d150bcc3a	$C_{10}H_{10}O_5$	$C_{10}H_{10}O_5$	Hydroxyferulic acid methyl ester.
UV7	66a23a170e3de3103c3b3e7cd639db58c439cf01	$C_{17}H_{22}O_{10}$	$C_{17}H_{22}O_{10}$	Potential sinapoyl-glycoside analogue.
UV8	a8969a1e28455240eeed8ed33304fc53da36b8e9	N/A	N/A	
UV9	d5824375cd3a57906f7fb48e5200913900a0013f	N/A	N/A	
UV10	3b2f757efe9b677c7a965fea6473b3dbd734df7e	N/A	N/A	
UV11	5e848267cb2983dc3e685809470b679172d8201b	N/A	N/A	Low abundance and difficult to characterise.
UV12	d666d013a17b49d29f0df53b595831fd7ee44ccb	N/A	N/A	
UV13	983b8f7f3a8b7edd4728b204eb63a80bedb4f3ba	N/A	N/A	
UV14	38b06a55b5c6f6a078053c1816dea58d0b0cbf97	N/A	N/A	
UV15	a01c5e618d4cf1c7e3535bdb4b85f0a4a46bc921	N/A	N/A	
UV16	f8a48d0b80752e52e356da2fdb57e38eb05d7f28	N/A	N/A	
UV17	3948a3c1b98588d09e1e2d43356b782f6abf1a16	N/A	N/A	
UV18	21bb76d7e052be6a2e125a108dc3f577ee6ff3d1	$C_{12}H_{18}O_{11}$	N/A	Potential fragment of **UV20.**
UV19	15974bb2bb7ec64e0e558b30e7e597ba4fc06ea6	N/A	N/A	
UV20	7dcb10d09876c0d75c99231f09854dfad0f26eaa	N/A	$C_{21}H_{26}O_{11}NCl$	Potential chloride-indole-AsA-related compound.
UV21	2ebe664589041fb7e0d5a1405eeba887ddd91a8d	N/A	N/A	
UV22	0caec0214f40d8dda6902212bd8ecf790eb133ed	N/A	$C_{16}H_{19}NO_7Cl$	Potential chloride-indole-AsA-related compound.
UV23	44eefe590af9c51f0931ad3285f00d9b856251b3	N/A	N/A	
UV24	b1ac3cc004a47dbadb4c7df89d6a17978e4de0b9	N/A	N/A	
S1	639f39431e9b6c7dd0b1bed88cab39078b63fe16	H_3PO_4	N/A	
S2	33c4ed6bacba09ede9d701475b5dd344b2121442	N/A	N/A	
S3	483a8de227f706a1f75439208f4461869ec59604	N/A	N/A	
S4	1962d27cb3bac39098d18f21ff6fe3bcf645fa1d	$C_4H_8O_3$	N/A	
S5	a92625f902e071f7565e7fb420afaf469e4ffc66	$C_3H_4O_4$	N/A	
S6	2d7426de893f1cdf28a944baa23761657f4e289b	N/A	N/A	Isomer of **S12.**
S7	0d6f55cc09785ca55a51823bd0f7dd631c84ff62	N/A	N/A	
S8	31468ff43b32d123bd4874d6118f2d2cb837154b	N/A	N/A	
S9	34d0880f09efd560d91a2d149cf1f87cb3f1d38b	N/A	N/A	
S10	27ba93d24b65c1a27706c2358ce24bda038f8560	N/A	N/A	
S11	b10638de56192fe34a0c0e25468c5ca267084d5a	N/A	N/A	
S12	6c26acd98ab860fb9d2a68a62faab39a0821ba1e	N/A	N/A	
S13	66c9624fc02b34cb62ca05179dba3074b3d7e4fe	N/A	$C_{16}H_{29}O_8$	Potential lipid-based compound.
S14	3b2df96f694c26bcbc228ba049f7eb1cbcb628f9	N/A	N/A	
S15	7a0038eb0112d361cb2735c48f818bc0d4d60c98	N/A	N/A	
S16	15f1664bcc5f90984743c9438fc95f72085fb9de	N/A	N/A	Caffeic acid-containing compound, with phosphosugary group.
S17	cca60b0267019d7cd8c3ee6bbc48cebeb428bac0	N/A	N/A	
S18	a967417449e903031e038390f572522529141eaf	N/A	$C_{20}H_{35}O_9$	Same elution profile as **S19**; potential lipid-based compound?

S19	4395530ea9668f04629b92585ff9663349500b2a	N/A	N/A	Same elution profile as **S18**; potential lipid-based compound?
P1	cd5fc8f9978823300ab78c112a13f34bcc44eb51	N/A	N/A	
P2	0faa38b8834cb76bda98c80761ad29eabdc79a88	$C_{16}H_{18}O_8$	N/A	
P3	ca4d04ea4249515a0c6a655ffcba130fbb52172f	N/A	N/A	
MJ1	0e1e7e1dfa9b1ef521246283e92f8c0e0dee88e1	N/A	$C_{11}H_{21}O_{12}P$	
MJ2	feb29328e22fb3f48207d1088bb751cf24b51390	$C_8H_8O_2$	N/A	Potential fragment of a larger parental ion.
MJ3	61314b395b2c648ce688647ebc5fb24dc681ce92	N/A	N/A	
MJ4	5a0b1b6dc602ae0376b826eb970638c04093f8ee	N/A	N/A	
MJ5	92dfc75b64a1348ae99288c07984132af47c8920	N/A	$C_{20}H_{34}O_9Cl$	Low abundance and difficult to characterise.
MJ6	df64200b03a56fbad93e525326eb6ffb485b782	N/A	N/A	
MJ7	379623150f51cf185b64ce3793656aebb4577fe3	$C_{18}H_{28}O_9$	N/A	
MJ8	670d7b64ea45bb4b2aff2a64bb72822ef8932104	$C_{16}H_{20}N_2O_{10}S_2$	$C_{16}H_{20}N_2O_{10}S_2$	hydroxyglucobrassicin.
MJ9	88b40e6e89f1ac0465de73545ce5b9df3d3a7017	N/A	N/A	Background noise.
MJ10	e67b9dffad1317a4d21fa6cf58ad6513cbf74a90	$C_{12}H_{20}O_4$	N/A	
MJ11	f15d369a8ba39e9a9c212221bf5459a2da272f43	$C_{12}H_{18}O_4$	N/A	
MJ12	fdc18ec1c1cd21f8cac8d4a0087a9a7a4eb5e396	N/A	N/A	
MJ13	78f94a5aebc73fd46623a328afb650b06d577e9a	$C_{18}H_{27}NO_6$	N/A	
MJ14	4cc56ca424d05647eaeb604f807904912b90779a	N/A	N/A	
MJ15	0ce79c0113fff3c1db4aee3aaf362ee077e8d823	$C_{12}H_{18}O_4$	N/A	
MJ16	440e313127a2124ad64a34673186d1901b83c220	$C_{18}H_{28}O_9$	N/A	
MJ17	73ddd845856379c2003ff3ccd07669b035733ef0	$C_{12}H_{18}O_3$	N/A	

Appendix 2: List of *B. napus* compounds found to accumulate in response to UV-B radiation, invertebrate herbivory or MeJA treatment. Table listing the compounds accumulating in response to at least one treatment by ≥ 1.5-fold with adjusted *p*-value ≤ 0.05. Peak IDs assigned to each compound during peak analysis. Putative elemental formulas (EFs; $[M-H]^-$) calculated by KEGG and from manual investigations are presented where available, and a brief description of putative characteristics of select compounds is provided based on fragmentation data and chemical characteristics of the compound. CN, compound number (Chapter 5, section 5.3).

REFERENCES

A-H-MACKERNESS, S., SURPLUS, S. L., BLAKE, P., JOHN, C. F., BUCHANAN-WOLLASTON, V., JORDAN, B. R. & THOMAS, B. 1999. Ultraviolet-B-induced stress and changes in geneexpression in Arabidopsis thaliana: role of signallingpathways controlled by jasmonic acid, ethylene andreactive oxygen species. *Plant, Cell and Environment,* 22**,** 1413-1423.

A.-H.-MACKERNESS, S., JOHN, C. F., JORDAN, B. & THOMAS, B. 2001. Early Signaling Components in Ultraviolet-B Responses: Distinct Roles for Different Reactive Oxygen Species and Nitric Oxide. *FEBS Letters***,** 237-242.

AGRAWAL, A. A. & KURASHIGE, N. S. 2003. A Role for Isothiocyanates in Plant Resistance Against the Specialist Herbivore *Pieris rapae*. *Journal of Chemical Ecology,* 29**,** 1403-1415.

AHMAD, M., JARILLO, J. A., SMIRNOVA, O. & CASHMORE, A. R. 1998. The CRY1 Blue Light Photoreceptor of Arabidopsis Interacts with Phytochrome A In Vitro. *Molecular Cell,* 1**,** 939-948.

ALEXIEVA, V., SERGIEV, I., MAPELLI, S. & KARANOV, E. 2001. The Effect of Drought and Ultraviolet Radiation on Growth and Stress Markers in Pea and Wheat. *Plant, Cell and Environment,* 24**,** 1337-1344.

ALI, J. G. & AGRAWAL, A. A. 2012. Specialist versus generalist insect herbivores and plant defense. *Trends in Plant Science,* 17**,** 293-302.

ANTTILA, U., JULKUNEN-TIITTO, R., ROUSI, M., YANG, S., RANTALA, M. J. & RUUHOLA, T. 2010. Effects of Elevated Ultraviolet-B Radiation on a Plant–Herbivore Interaction. *Oecologia,* 164**,** 163-175.

APHALO, P. J., BALLARÉ, C. L. & SCOPEL, A. L. 1999. Plant-plant signalling, the shade-avoidance response and competition. *Journal of Experimental Botany,* 50**,** 1629-1634.

ARGUESO, C. T., RAINES, T. & KIEBER, J. J. 2010. Cytokinin signaling and transcriptional networks. *Current Opinion in Plant Biology,* 13**,** 533-539.

BALLARÉ, C. L., BARNES, P. W. & FLINT, S. D. 1995. Inhibition of Hypocotyl Elongation by Ultraviolet-B Radiation in De-Etiolating Tomato Seedlings. I. The Photoreceptor. *Physiologia Plantarum,* 93**,** 584-592.

BALLARÉ, C. L., SCOPEL, A. L., STAPLETON, A. E. & YANOVSKY, M. J. 1996. Solar Ultraviolet-B Radiation Affects Seedling Emergence, DNA Integrity, Plant Morphology, Growth Rate, and Attractiveness to Herbivore lnsects in Datura ferox'. *Plant Physiology,* 112**,** 161-170.

BALLARÉ, C. L. 2014. Light Regulation of Plant Defense. *Annual Review of Plant Biology,* 65**,** 335-363.

BARAH, P., WINGE, P., KUSNIERCZYK, A., TRAN, D. H. & BONES, A. M. 2013. Molecular Signatures in Arabidopsis thaliana in Response to Insect Attack and Bacterial Infection. *PLoS ONE,* 8.

BARI, R. & JONES, J. D. G. 2009. Role of Plant Hormones in Plant Defence Responses. *Plant Molecular Biology,* 69**,** 473-488.

BARNES, P. W., BALLARE, C. L. & CALDWELL, M. M. 1996. Photomorphogenic Effects of UV-B Radiation on Plants: Consequences for Light Competition. *Journal of Plant Physiology,* 148**,** 15-20.

BELL, E., CREELMAN, R. A. & MULLET, J. E. 1995. A chloroplast lipoxygenase is required for wound-induced jasmonic acid accumulation in Arabidopsis. *Proceedings of the National Academy of Sciences,* 92**,** 8675-8679.

BERROCAL-LOBO, M., MOLINA, A, & SOLANO, R. 2002. Constitutive Expression of ETHYLENE-RESPONSE-FACTOR1 in Arabidopsis Confers Resistance to Several Necrotrophic Fungi. *The Plant Journal*, 29, 23-32.

BIDART-BOUZAT, M. G. & KLIEBENSTEIN, D. 2011. An Ecological Genomic Approach Challenging the Paradigm of Differential Plant Responses to Specialist Versus Generalist Insect Herbivores. *Oecologia,* 167**,** 677-689.

BOCCALANDRO., H. E., MAZZA, C. A., MAZZELLA, M. A., CASAL, J. J. & BALLARÉ, C. L. 2001. Ultraviolet B Radiation Enhances a Phytochrome-B-Mediated Photomorphogenic Response in Arabidopsis. *Plant Physiology,* 126**,** 780-788.

BOSTOCK, R. M. 2005. Signal Crosstalk and Induced Resistance: Straddling the Line Between Cost and Benefit. *Annual Review of Phytopathology,* 43**,** 545-580.

BRIGGS, W. R. & HUALA, E. 1999. Blue-Light Photoreceptors In Higher Plants. *Annual Review of Cell and Developmental Biology,* 15**,** 33-62.

BRIGGS, W. R. & CHRISTIE, J. M. 2002. Phototropins 1 and 2: Versatile Plant Blue-Light Receptors. *TRENDS in Plant Science,* 7**,** 204-210.

BRITT, A. B., CHEN, J. J., WYKOFF, D. & MITCHELL, D. 1993. A UV-Sensitive Mutant of Arabidopsis Defective in the Repair of Pyrimidine-Pyrimidinone(6-4) Dimers. *Science,* 261**,** 1571-1574.

BRITT, A. B. 2004. Repair of DNA Damage Induced by Solar UV. *Photosynthesis Research,* 81**,** 105-112.

BROEKGAARDEN, C., VOORRIPS, R. E., DICKE, M. & VOSMAN, B. 2011. Transcriptional Responses Of Brassica Nigra To Feeding By Specialist Insects Of Different Feeding Guilds. *Insect Science,* 18**,** 259-272.

BROSCHE, M. & STRID, A. 2003. Molecular events following perception of ultraviolet-B radiation by plants. *Physiologia Plantarum,* 117**,** 1-10.

BROWN, B. A., CLOIX, C., JIANG, G. H., KAISERLI, E., HERZYK, P., KLIEBENSTEIN, D. J. & JENKINS, G. I. 2005. A UV-B-specific signaling component orchestrates plant UV protection. *Proceedings of the National Academy of Sciences USA,* 102**,** 18225-18230.

BROWN, B. A. & JENKINS, G. I. 2008. UV-B Signaling Pathways with Different Fluence-Rate Response Profiles Are Distinguished in Mature Arabidopsis Leaf Tissue by Requirement for UVR8, HY5, and HYH. *Plant Physiology,* 146**,** 576-588.

BRUCE, T. J. A. & PICKETT, J. A. 2007. Plant Defence Signalling Induced by Biotic Attacks. *Current Opinion in Plant Biology,* 10**,** 387-392.

BU, Q., JIANG, H., LI, C.-B., ZHAI, Q., ZHANG, J., WU, X., SUN, J., XIE, Q. & LI, C. 2008. Role of the Arabidopsis Thaliana NAC Transcription Factors ANAC019 and ANAC055 in Regulating Jasmonic Acid-Signaled Defense Responses. *Cell Research,* 18**,** 756-767.

BURMEISTER, W. P., COTTAZ, S., ROLLIN, P., VASELLA, A. & HENRISSAT, B. 2000. High Resolution X-ray Crystallography Shows That Ascorbate Is a Cofactor for Myrosinase and Substitutes for the Function of the Catalytic Base. *The Journal Of Biological Chemistry,* 275**,** 39385-39393.

BUSTIN, S. A., BENES, V., GARSON, J. A., HELLEMANS, J., HUGGETT, J., KUBISTA, M., MUELLER, R., NOLAN, T., PFAFFL, W. F., SHIPLEY, G. L., VANDESOMPELE, J. & WITTWER, C. T. 2009. The MIQE Guidelines: Minimum Information for Publication of Quantitative Real-Time PCR Experiments. *Clinical Chemistry,* 55**,** 611-622.

CALDWELL, M. M. & FLINT, S. D. 1994. Stratospheric Ozone Reduction, Solar Uv-B Radiation And Terrestrial Ecosystems. *Climate Change,* 28**,** 375-394.

CAMERA, S. L., GOUZERH, G., DHONDT, S., HOFFMANN, L., FRITIG, B., LEGRAND, M. & HEITZ, T. 2004. Metabolic Reprogramming in Plant Innate Immunity: The Contributions of Phenylpropanoid And Oxylipin Pathways. *Immunological Reviews,* 198**,** 267-284.

CAPUTO, C., RUTITZKY, M, & BALLARÉ, C. L. 2006. Solar ultraviolet-B radiation alters the attractiveness of Arabidopsis plants to diamondback moths (Plutella xylostella L.): impacts on oviposition and involvement of the jasmonic acid pathway. *Oecologia,* 149**,** 81-90.

CASATI, P., CAMPI, M., MORROW, D. J., FERNANDES, J. F. & WALBOT, V. 2011. Transcriptomic, Proteomic and Metabolomic Analysis of UV-B Signaling in Maize. *BMC Genomics,* 12.

CASHMORE, A. R., JARILLO, J. A., WU, Y.-J. & LIU, D. 1999. Cryptochromes: Blue Light Receptors for Plants and Animals. *Science,* 284**,** 760-765.

CECCHINI, N. M., MONTEOLIVA, M. I. & ALVAREZ, M. E. 2011. Proline Dehydrogenase Contributes to Pathogen Defense in Arabidopsis. *Plant Physiology,* 155**,** 1947-1959.

CERRUDO, I., KELLER, M. M., CARGNEL, M. D., DEMKURA, P. V., DE WIT, M., PATITUCCI, M. S., PIERIK, R., PIETERSE, C. M. J. & BALLARE, C. L. 2012. Low Red/Far-Red Ratios Reduce Arabidopsis Resistance to Botrytis cinerea and Jasmonate Responses via a COI1-JAZ10-Dependent, Salicylic Acid-Independent Mechanism. *Plant Physiology,* 158**,** 2042-2052.

CHALHOUB, B., DENOEUD, F., LIU, S., PARKIN, I. A. P., TANG, H., WANG, X., CHIQUET, J., BELCRAM, H., TONG, C., SAMANS, B., CORRÉA, M., DA SILVA,

C., JUST, J., FALENTIN, C., KOH, C. S., LE CLAINCHE, I., BERNARD, M., BENTO, P., NOEL, B., LABADIE, K., ALBERTI, A., CHARLES, M., ARNAUD, D., GUO, H., DAVIAUD, C., ALAMERY, S., JABBARI, K., ZHAO, M., EDGER, P. P., CHELAIFA, H., TACK, D., LASSALLE, G., MESTIRI, I., SCHNEL, N., LE PASLIER, M.-C., FAN, G., RENAULT, V., BAYER, P. E., GOLICZ, A. A., MANOLI, S., LEE, T.-H., THI, V. H. D., CHALABI, S., HU, Q., FAN, C., TOLLENAERE, R., LU, Y., BATTAIL, C., SHEN, J., SIDEBOTTOM, C. H. D., WANG, X., CANAGUIER, A., CHAUVEAU, A., BÉRARD, A., DENIOT, G., GUAN, M., LIU, Z., SUN, F., LIM, Y. P., LYONS, E., TOWN, C. D., BANCROFT, I., WANG, X., MENG, J., MA, J., PIRES, J. C., KING, G. J., BRUNEL, D., DELOURME, R., RENARD, M., AURY, J.-M., ADAMS, K. L., BATLEY, J., SNOWDON, R. J., TOST, J., EDWARDS, D., ZHOU, Y., HUA, W., SHARPE, A. G., PATERSON, A. H., GUAN, C. & WINCKER, P. 2014. Early allopolyploid evolution in the post-Neolithic Brassica napus oilseed genome. *Science,* 345**,** 950-953.

CHALKER-SCOTT, L. 1999. Environmental Significance of Anthocyanins in Plant Stress Responses. *Photochemistry and Photobiology,* 70**,** 1-9.

CHEN, M. & CHORY, J. 2011. Phytochrome Signaling Mechanisms and the Control of Plant Development. *Trends in Cell Biology,* 21**,** 664-671.

CHEN, M.-S. 2008. Inducible Direct Plant Defense Against Insect Herbivores: A Review. *Insect Science,* 15**,** 101-114.

CHESNEY, J. A., MAHONEY JR, J. M. & EATON, J. M. 1991. A Spectrophotometric Assay for Chlorine-Containing Compounds. *Analytical Biochemistry* 196**,** 262-266.

CHIANG, Y.-H., ZUBO, Y. O., TAPKEN, W., KIM, H. J., LAVANWAY, A. M., HOWARD, L., PILON, M., KIEBER, J. J. & SCHALLER, G. E. 2012. Functional Characterization of the GATA Transcription Factors GNC and CGA1 Reveals Their Key Role in Chloroplast Development, Growth, and Division in Arabidopsis. *Plant Physiology,* 160**,** 332-348.

CHICO, J. M., CHINI, A., FONSECA, S. & SOLANO, R. 2008. JAZ Repressors Set the Rhythm in Jasmonate Signaling. *Current Opinion in Plant Biology,* 11**,** 486-494.

CHINI, A., FONSECA, S., FERNANDEZ, G., ADIE, B., CHICO, J. M., LORENZO, O., GARCIA-CASADO, G., LOPEZ-VIDRIERO, I., LOZANO, F. M., PONCE, M. R., MICOL, J. L. & SOLANO, R. 2007. The Jaz Family of Repressors is the Missing Link in Jasmonate Signalling. *Nature,* 448**,** 666-673.

CHRISTIANSON, J. A., DENNIS, E. S., LLEWELLYN, D. J. & WILSON, I. W. 2010. ATAF NAC transcription factors: Regulators of plant stress signaling. *Plant Signaling & Behavior,* 5**,** 428-434.

CHRISTIE, J. M. & JENKINS, G. I. 1996. Distinct UV-B and UV-A/Blue Light Signal Transduction Pathways lnduce Chalcone Synthase Gene Exptession in Arabidopsis Cells. *Plant Cell,* 8**,** 1555-1567.

CHRISTIE, J. M. 2007. Phototropin Blue-Light Receptors. *Annual Review of Plant Biology,* 58**,** 21-45.

CHRISTIE, J. M., ARVAI , A. S., BAXTER, K. J., HEILMANN, M., PRATT, A. J., O'HARA, A., KELLY, S. M., HOTHORN, M., SMITH, B. O., HITOMI, K., JENKINS, G. I. & GETZOFF, E. D. 2012. Plant UVR8 Photoreceptor Senses UV-B by Tryptophan-Mediated Disruption of Cross-Dimer Salt Bridges. *science,* 335**,** 1492-1496.
CONKLIN, P. L., WILLIAMS, E. H. & LAST, R. L. 1996. Environmental Stress Sensitivity of an Ascorbic Acid-Deficient Arabidopsis Mutant. *Proceedings of the National Academy of Sciences,* 93**,** 9970-9974.

CONKLIN, P. L. & BARTH, C. 2004. Ascorbic Acid, A Familiar Small Molecule Intertwined In The Response Of Plants To Ozone, Pathogens, And The Onset Of Senescence. *Plant, Cell and Environment,* 27**,** 959-970.

DAAYF, F., ONGENA, M., BOULANGER, R., EL HADRAMI, I. & BELANGER, R. R. 2000. Induction of Phenolic Compounds in two Cultivars of Cucumber by Treatment of Healthy and Powdery Mildew-Infected Plants with Extracts of *Reynoutria sachalinensis*. *Journal of Chemical Ecology,* 26**,** 1579-1593.

DAVIS, A. M., HALL, A., MILLAR, A., DARRAH, C. & DAVIS, S. J. 2009. Protocol: Streamlined sub-protocols for floral-dip transformation and selection of transformants in Arabidopsis thaliana. *Plant Methods,* 5.

DE VOS, R. C. H., MOCO, S., LOMMEN, A., KEURENTJES, J. J. B., BINO, R. J. & HALL, R. D. 2007. Untargeted large-scale plant metabolomics using liquid chromatography coupled to mass spectrometry. *NATURE PROTOCOLS,* 2**,** 778-791.

DELESSERT, C., KAZAN, K., WILSON, I. W., VAN DER STRAETEN, D., MANNERS, J., DENNIS, E. S. & DOLFERUS, R. 2005. he transcription factor ATAF2 represses the expression of pathogenesis-related genes in Arabidopsis. *The Plant Journal,* 43**,** 745-757.

DEMARSY, E. & FANKHAUSER, C. 2009. Higher Plants use LOV to Perceive Blue Light. *Current Opinion in Plant Biology,* 12**,** 69-74.

DEMKURA, P. V., ABDALA, G., BALDWIN, I. T. & BALLARE, C. B. 2010. Jasmonate-Dependent and -Independent Pathways Mediate Specific Effects of Solar Ultraviolet B Radiation on Leaf Phenolics and Antiherbivore Defense. *Plant Physiology,* 152.

DEMKURA, P. V. & BALLARÉ, C. L. 2012. UVR8 Mediates UV-B-Induced Arabidopsis Defense Responses against Botrytis cinerea by Controlling Sinapate Accumulation. *Molecular Plant* 5**,** 642-652.

DERVINIS, C., FROST, C. J., LAWRENCE, S. D., NOVAK, N. G. & DAVIS, J. M. 2010. Cytokinin Primes Plant Responses to Wounding and Reduces Insect Performance. *Journal of Plant Growth Regulation,* 29**,** 289-296.

DEVOTO, A., ELLIS, C., MAGUSIN, A., CHANG, H.-S., CHILCOTT, C., ZHU, T. & TURNER, J. G. 2005. Expression Profiling Reveals COI1 to be a Key Regulator of Genes Involved in Wound- and Methyl Jasmonate-Induced Secondary Metabolism, Defence, and Hormone Interactions. *Plant Molecular Biology,* 58**,** 497-513.

DIXON, R. A., ACHNINE, L., KOTA, P., LIU, C.-J., REDDY, M. S. S. & WANG, L. 2002. The Phenylpropanoid Pathway And Plant Defence— A Genomics Perspective. *Molecular Plant Pathology,* 3**,** 371-390.

DOMBRECHT, B., XUE, G. P., SPRAGUE, S. J., KIRKEGAARD, J. A., ROSS, J. J., REID, J. B., FITT, G. P., SEWELAM, N., SCHENK, P. M., MANNERS, J. M. & KAZAN, K. 2007. MYC2 Differentially Modulates Diverse Jasmonate-Dependent Functions in Arabidopsis. *The Plant Cell,* 19**,** 2225-2245.

EHLTING, J. R., CHOWRIRA, S. G., MATTHEUS, N., AESCHLIMAN, D. S., ARIMURA, G.-I. & BOHLMANN, J. 2008. Comparative transcriptome analysis of Arabidopsis thaliana infested by diamond back moth (Plutella xylostella) larvae reveals signatures of stress response, secondary metabolism, and signalling. *BMC Genomics,* 9.

ENGVILD, K. C. 1986. Chlorine-Containing Natural Compounds in Higher Plants. *Phytochemistry,* 25**,** 781-791.

ERB, M., MELDAU, S. & HOWE, G. A. 2012. Role of Phytohormones in Insect-Specific Plant Reactions. *TRENDS in Plant Science,* 17**,** 250-259.

FABRO, G., KOVÁCS, I., PAVET, V., SZABADOS, L. & ALVAREZ, M. E. 2004. Proline Accumulation and AtP5CS2 Gene Activation Are Induced by Plant-Pathogen Incompatible Interactions in Arabidopsis. *Molecular Plant-Microbe Interactions,* 17**,** 343-350.

FALK, K. L., KÄSTNER, J., BODENHAUSEN, N., SCHRAMM, K., PAETZ, C., VASSÃO, D. G., REICHELT, M., VON KNORRE, D., BERGELSON, J., ERB, M., GERSHENZON, J. & MELDAU, S. 2014. The role of glucosinolates and the jasmonic acid pathway in resistance of Arabidopsis thaliana against molluscan herbivores. *Molecular Ecology,* 23**,** 1188-1203.

FARMER, E. E. & RYAN, C. A. 1990. Interplant Communication: Airborne Methyl Jasmonate Induces Synthesis of Proteinase Inhibitors in Plant Leaves. *Proceedings of the National Academy of Sciences,* 87**,** 7713-7716.

FARMER, E. E. & RYAN, C. A. 1992. Octadecanoid Precursors of Jasmonic Acid Activate the Synthesis of Wound-Inducible Proteinase Inhibitors. *The Plant Cell,* 4**,** 129-134.

FAVORY, J. J., STEC, A., GRUBER, H., RIZZINI, L., ORAVECZ, A., FUNK, M., ALBERT, A., CLOIX, C., JENKINS, G. I., OAKELEY, E. J., SEIDLITZ, H. K., NAGY, F. & ULM, R. 2009. Interaction of COP1 and UVR8 regulates UV-B-induced photomorphogenesis and stress acclimation in Arabidopsis. *EMBO,* 28**,** 591-601.

FELLENBERG, C., VAN OHLEN, M., HANDRICK, V. & VOGT, T. 2012. The role of CCoAOMT1 and COMT1 in Arabidopsis anthers. *Planta,* 236**,** 51-61.

FEYS, B. J. F., BENEDETTI, C. E., PENFOLD, C. N. & TURNER, J. G. 1994. Arabidopsis Mutants Selected for Resistance to the Phytotoxin Coronatine Are Male Sterile, lnsensitive to Methyl Jasmonate, and Resistant to a Bacterial Pathogen. *The Plant Cell,* 6**,** 751-759.

FIEHN, O., KOPKA, J., TRETHEWEY, R. N. & WILLMITZER, L. 2000. Identification of Uncommon Plant Metabolites Based on Calculation of Elemental Compositions Using Gas Chromatography and Quadrupole Mass Spectrometry. *Analytical Chemistry,* 72**,** 3573-3580.

FLINT, S. D., JORDAN, P. W. & CALDWELL, M. M. 2008. Plant Protective Response To Enhanced Uv-B Radiation Under Field Conditions: Leaf Optical Properties And Photosynthesis. *Photochemistry and Photobiology,* 41**,** 95-99.

FOGGO, A., HIGGINS, S., WARGENT, J. J. & COLEMAN, R. A. 2007. Tri-trophic consequences of UV-B exposure: plants, herbivores and parasitoids. *Oecologia,* 154**,** 505-512.

FRANKLIN, K. A. 2009. Light and Temperature Signal Crosstalk in Plant Development. *Current Opinion in Plant Biology,* 12**,** 63-68.

FROHNMEYER, H., BOWLER, C. & SCHAFER, E. 1997. Evidence for Some Signal Transduction Elements Involved in UV-Light-Dependent Responses in Parsley Protoplasts. *Journal of Experimental Botany,* 48**,** 739-750.

FROHNMEYER, H., LOYALL, L., BLATT, M. R. & GRABOV, A. 1999. Millisecond UV-B Irradiation Evokes Prolonged Elevation of Cytosolic-Free Ca2+ and Stimulates Gene Expression in Transgenic Parsley Cell Cultures. *The Plant Journal,* 20**,** 109-117.

FROHNMEYER, H. & STAIGER, D. 2003. Ultraviolet-B Radiation-Mediated Responses in Plants. Balancing Damage and Protection. *Plant Physiology,* 113**,** 1420-1428.

GAO, Q. & ZHANG, L. 2008. Ultraviolet-B-Induced Oxidative Stress and Antioxidant Defense System Responses in Ascorbate-Deficient *vtc1* Mutants of *Arabidopsis thaliana*. *Journal of Plant Physiology,* 165**,** 138-148.

GERHARDT, K. E., WILSON, M. L. & GREENBERG, B. M. 2005. Ultraviolet Wavelength Dependence of Photomorphological and Photosynthetic Responses in Brassica napus and Arabidopsis thaliana. *Photochemistry and Photobiology,* 81**,** 1061-1068.

GITZ, D. C. & LIU-GITZ, L. 2003. How do UV Photomorphogenic Responses Confer Water Stress Tolerance? *Photochemistry and Photobiology,* 78**,** 529-534.

GITZ, D. C., LIU-GITZ, L., BRITZ, S. J. & SULLIVAN, J. H. 2005. Ultraviolet-B Effects On Stomatal Density, Water-Use Efficiency, And Stable Carbon Isotope Discrimination In Four Glasshouse-Grown Soybean (Glyicine Max) Cultivars. *Environmental and Experimental Botany,* 53.

GOUJON, T., SIBOUT, R., POLLET, B., MABA, B., NUSSAUME, L., BECHTOLD, N., LU, F., RALPH, J., MILA, I., BARRIERE, Y., LAPIERRE, C. & JOUANIN, L. 2003. A new Arabidopsis thaliana Mutant Deficient in the Expression of O-Methyltransferase Impacts Lignins and Sinapoyl Esters. *Plant Molecular Biology,* 51**,** 973-989.

GRANT, G. G. & LANGEVIN, D. 2002. Structure-Activity Relationships of Phenolic and Nonphenolic Aromatic Acids as Oviposition Stimuli for the Spruce Budworm, *Choristoneura Fumiferana* (Lepidoptera: Tortricidae). *IOBC wprs Bulletin,* 25.

GRIBBLE, G. W. 1998. Naturally Occurring Organohalogen Compounds. *Accounts of Chemical Research,* 31**,** 141-152.

GRIBBLE, G. W. 1999. The diversity of Naturally Occurring Organobromine Compounds. *Chemical Society Reviews,* 28**,** 335-346.

GUO, D., CHEN, F., WHEELER, J., WINDER, J., SELMAN, S., PETERSON, M. & DIXON, R. A. 2001. Improvement of in-rumen Digestibility of Alfalfa Forage by Genetic Manipulation of Lignin O-Methyltransferases. *Transgenic Research,* 10**,** 457-464.

JUNG, H.G. & VOGEL, K. P. 1986. Influence of lignin on digestibility of forage cell wall material. *Journal of Animal Science,* 62**,** 1703-1712.

HALPIN, C., KNIGHT, M. E., FOXON, G. E., CAMPBELL, M. M., BOUDET, A. M., BOON, J. J., CHABBERT, B., TOLLIER, M.-T. & SCHUCH, W. 1994. Manipulation of lignin quality by downregulation of cinnamyl alcohol dehydrogenase. *The Plant Journal,* 6**,** 339-350.

HARBORNE, J. B. & WILLIAMS, C. A. 2000. Advances in Flavonoid Research Since 1992. *Phytochemistry,* 55**,** 481-504.

HASEGAWA, S., SOGABE, Y., ASANO, T., NAKAGAWA, T., NAKAMURA, H., KODAMA, H., OHTA, H., YAMAGUCHI, K., MUELLER, M. J. & NISHIUCHI, T. 2011. Gene expression analysis of wounding-induced root-to-shoot communication in Arabidopsis thalianapce_2274 705..716. *Plant, Cell and Environment,* 34**,** 705-716.

HE, Y., FUKUSHIGE, H., HILDEBRAND, D. F. & GAN, S. 2002. Evidence Supporting a Role of Jasmonic Acid in Arabidopsis Leaf Senescence. *Plant Physiology,* 128**,** 876-884.

HEIDEL, A. J. & BALDWIN, I. T. 2004. Microarray Analysis of Salicylic Acid- and Jasmonic Acid- Signalling in Responses of *Nicotiana attenuata* to Attack yy Insects from Multiple Feeding Guilds. *Plant, Cell and Environment,* 27**,** 1362-1373.

HEIJDE, M., BINKERT, M., YIN, R., ARES-ORPEL, F., RIZZINI, L., VAN DE SLIJKE, E., PERSIAU, G., NOLF, J., GEVAERT, K., DE JAEGER, G. & ULM, R. 2013. Constitutively Active UVR8 Photoreceptor Variant in Arabidopsis. *Proceedings of the National Academy of Sciences,* 110**,** 20326-20331.

HOLMES, M. G. & KEILLER, D. R. 2002. Effects of Pubescence and Waxes on the Reflectance of Leaves in the Ultraviolet and Photosynthetic Wavebands: A Comparison of a Range of Species. *Plant, Cell and Environment,* 25**,** 85-93.

HOPKINS, R. J., VAN DAM, N. M. & VAN LOON, J. J. A. 2009. Role of Glucosinolates in Insect-Plant Relationships and Multitrophic Interactions. *Annual Review of Entomology,* 54**,** 57-83.

HOU, X., LEE, L. Y. C., XIA, K., YAN, Y. & YU, H. 2010. DELLAs Modulate Jasmonate Signaling via Competitive Binding to JAZs. *Developmental Cell,* 19**,** 884-894.

HOWE, G. A. & JANDER, G. 2008. Plant Immunity to Insect Herbivores. *Annual Review of Plant Biology,* 59**,** 41-66.

HUANG, D. W., SHERMAN, B. T. & LEMPICKI, R. A. 2009. Systematic and integrative analysis of large gene lists using DAVID bioinformatics resources. *NATURE PROTOCOLS,* 4**,** 44-57.

HUANG, J.-C., PIATER, L. A. & DUBERY, I. A. 2012. The Nac Transcription Factor Gene ANAC072 Is Differentially Expressed In Arabidopsis Thaliana In Response To Microbe-Associated Molecular Pattern (MAMP) Molecules. *Physiological and Molecular Plant Pathology,* 80**,** 19-27.

HUANG, X. & RENWLCK, J. A. A. 1994. Relative Activities of Glucosinolates as Oviposition Stimulants for *Pieris Rapae* and *P. Napi Oleracea*. *Journal of Chemical Ecology,,* 20**,** 1025-1037.

HULL, A. K., REKHA, V. & CELENZA, J. L. 2000. Arabidopsis cytochrome P450s that catalyze the first step of tryptophan-dependent indole-3-acetic acid bio- synthesis. *Proceedings of the National Academy of Sciences USA,* 97**,** 2379-2384.

IKONEN, A., TAHVANAINEN, J. & ROININEN, H. 2001. Chlorogenic Acid as an Antiherbivore Defence of Willows Against Leaf Beetles. *Entomologia Experimentalis et Applicata,* 99**,** 47-54.

INOUEA, S.-I., KINOSHITA, T., TAKEMIYA, A., DOIB, M. & SHIMAZAKIA, K.-I. 2008. Leaf Positioning of Arabidopsis in Response to Blue Light. *Molecular Plant,* 1**,** 15-26.

IZAGUIRRE, M. M., SCOPEL, A. L., BALDWIN, I. T. & BALLARE, C. L. 2003. Convergent Responses to Stress. Solar Ultraviolet-B Radiation and Manduca sexta Herbivory Elicit Overlapping Transcriptional Responses in Field-Grown Plants of Nicotiana longiflora. *Plant Physiology,* 132**,** 1755-1767.

IZAGUIRRE, M. M., MAZZA, C. A., BIONDINI, M., BALDWIN, I. T. & BALLARE, C. L. 2006. Remote sensing of future competitors: Impacts on plant defenses. *PNAS,* 103**,** 7170-7174.

IZAGUIRRE, M. M., MAZZA, C. A., SVATOS, A., BALDWIN, I. T. & BALLARÉ, C. L. 2007. Solar Ultraviolet-B Radiation and Insect Herbivory Trigger Partially Overlapping Phenolic Responses in Nicotiana attenuata and Nicotiana longiflora. *Annals of Botany,* 99**,** 103-109.

JANSEN, M. A. K., GABA, V. & GREENBERG, B. M. 1998. Higher Plants and UV-B Radiation: Balancing Damage, Repair and Acclimation. *TRENDS in Plant Science,* 3**,** 131-135.

JENKINS, G. I., LONG, J. C., WADE, H. K., SHENTON, M. R. & BIBIKOVA, T. N. 2001. UV and Blue Light Signalling: Pathways Regulating Chalcone Synthase Gene Expression in Arabidopsis. *New Phytologist,* 151**,** 121-131.

JENKINS, G. I. 2009. Signal Transduction in Responses to UV-B Radiation. *Annual Review of Plant Biology,* 60**,** 407-431.

JENKINS, G. I. 2014. The UV-B Photoreceptor UVR8: From Structure to Physiology. *The Plant Cell,* 26**,** 21-37.

JIAO, Y., LAU, O. S. & DENG, X. W. 2007. Light-regulated transcriptional networks in higher plants. *Nature Reviews Genetics,* 8**,** 217-230.

JIN, H., COMINELLI, E., BAILEY, P., PARR, A., MEHRTENS, F., JONES, J., TONELLI, C., WEISSHAAR, B. & MARTIN, C. 2000. Transcriptional Repression by AtMYB4 Controls Production of UV-Protecting Sunscreens in Arabidopsis. *The EMBO Journal,* 19**,** 6150-6161.

JOHNSON, G. & SCHAAL, L. A. 1952. Relation of Chlorogenic Acid to Scab Resistance in Potatoes. *Science,* 115**,** 627-629.

JONES, J. D. G. & DANGL, J. L. 2006. The Plant Immune System. *Nature,* 444**,** 323-329.

JUNG, C., LYOU, S. H., YEU, S., KIM, M. A., RHEE, S., KIM, M., LEE, J. S., CHOI, Y. D. & CHEONG, J.-J. 2007. Microarray-based screening of jasmonate-responsive genes in Arabidopsis thaliana. *Plant Cell Reports,* 26**,** 1053-1063.

KAISERLI, E. & JENKINS, G. I. 2007. UV-B Promotes Rapid Nuclear Translocation of the Arabidopsis UV-B–Specific Signaling Component UVR8 and Activates Its Function in the Nucleus. *The Plant Cell,* 19**,** 2662-2673.

KAMI, C., LORRAIN, S., HORNITSCHEK, P. & FANKHAUSER, C. 2010. Chapter Two – Light-Regulated Plant Growth and Development. *Current Topics in Developmental Biology,* 91**,** 29-66.

KÄSTNER, J., VON KNORRE, D., HIMANSHU, H., ERB, M., BALDWIN, I. & MELDAU, S. 2014. Salicylic Acid, a Plant Defense Hormone, Is Specifically Secreted by a Molluscan Herbivore. *PLoS ONE,* 9.

KAVI-KISHOR, P. B., SANGAM, S. S., AMRUTHA, R. N., SRI LAXMI, P., NAIDU, K. R., RAO, K. R. S. S., RAO, S., REDDY, K. J., THERIAPPAN, P. & SREENIVASULU, N. 2005. Regulation of proline biosynthesis, degradation, uptake and transport in higher plants: Its implications in plant growth and abiotic stress tolerance. *CURRENT SCIENCE,* 88**,** 424-438.

KEMPEMA, L. A., CUI, X., HOLZER, F. M. & WALLING, L. L. 2007. Arabidopsis Transcriptome Changes in Response to Phloem-Feeding Silverleaf Whitefly Nymphs. Similarities and Distinctions in Responses to Aphids. *Plant Physiology,* 143**,** 849-865.

KESARWANI, M., YOO, J. & DONG, X. 2007. Genetic Interactions of TGA Transcription Factors in the Regulation of Pathogenesis-Related Genes and Disease Resistance in Arabidopsis. *Plant Physiology,* 144**,** 336-346.

KESSLER, A. & BALDWIN, I. T. 2002. Plant Responses to Insect Herbivory: The Emerging Molecular Analysis. *Annual Review of Plant Biology,* 53**,** 299-328.

KIEDROWSKI, S., KAWALLECK, P., HAHLBROCK, K., SOMSSICH, I. E. & DANGL, J. L. 1992. Rapid activation of a novel plant defense gene is strictly dependent on the Arabidopsis RPM1 disease resistance locus. *EMBO,* 11**,** 4677-4684.

KILIAN, J., WHITEHEAD, D., HORAK, J., WANKE, D., WEINL, S., BATISTIC, O., D'ANGELO, C., BORNBERG-BAUER, E., KUDLA, J. & HARTER, K. 2007. The Atgenexpress Global Stress Expression Data Set: Protocols, Evaluation And Model Data Analysis Of Uv-B Light, Drought And Cold Stress Responses. *The Plant Journal* 50**,** 347-363.

KIM, B. C., TENNESSEN, D. J. & LAST, R. L. 1998 UV-B-induced photomorphogenesis in Arabidopsis thaliana. *The Plant Journal* 15**,** 667–674.

KIM, S.-J., KIM, K.-W., CHO, M.-H., FRANCESCHI, V. R., DAVIN, L. B. & LEWIS, N. G. 2007. Expression of cinnamyl alcohol dehydrogenases and their putative homologues during Arabidopsis thaliana growth and development: Lessons for database annotations? *Phytochemistry,* 68**,** 1957-1974.

KIM, W.-Y., FUJIWARA, S., SUH, S.-S., KIM, J., KIM, Y., HAN, L., DAVID, K., PUTTERILL, J., NAM, H. G. & SOMERS, D. E. 2007. ZEITLUPE is a Circadian Photoreceptor Stabilized by GIGANTEA in Blue Light. *Nature Letters,* 449**,** 356-362.

KINOSHITA, T., DOI, M., SUETSUGU, N., KAGAWA, T., WADA, M. & SHIMAZAKI, K.-I. 2001. phot1 and phot2 Mediate Blue Light Regulation of Stomatal Opening. *Letters to Nature,* 414**,** 656-660.

KLIEBENSTEIN, D. J., LIM, J. E., LANDRY, L. G. & LAST, R. L. 2002. Arabidopsis UVR8 Regulates Ultraviolet-B Signal Transduction and Tolerance and Contains Sequence Similarity to Human Regulator of Chromatin Condensation 1. *Plant Physiology,* 130**,** 234-243.

KODA, Y. & KIKUTA, Y. 1994. Wound-Induced Accumulation of Jasmonic Acid in Tissues of Potato Tubers. *Plant Cell Physiology,* 35**,** 751-756.

KOEPPE, D. E., ROHRBAUGH, L. M. & WENDER, S. H. 1969. The Effect of Varying U.V. Intensities on the Concentration of Scopolin and Caffeoylquinic Acids in Tobacco and Sunflower. *Phytochemistry,* 8**,** 889-896.

KONIG, S., FEUSSNER, K., KAEVER, A., LANDESFEIND, M., THUROW, C., KARLOVSKY, P., GATZ, C., POLLE, A. & FEUSSNER, I. 2014. Soluble Phenylpropanoids Are Involved In The Defense Response Of Arabidopsis Against Verticillium Longisporum. *New Phytologist,* 202**,** 823-837.

KOORNNEEF, A. & PIETERSE, C. M. J. 2008. Cross Talk in Defense Signaling. *Plant Physiology,* 146**,** 839-844.

KUHLMANN, F. & MULLER, C. 2009a. Development-dependent effects of UV radiation exposure on broccoli plants and interactions with herbivorous insects. *Environmental and Experimental Botany,* 66**,** 61-68.

KUHLMANN, F. & MULLER, C. 2009b. UV-B impact on aphid performance mediated by plant quality and plant changes induced by aphids. *Plant Biology,* 12**,** 676-684.

KUHLMANN, F. & MULLER, C. 2011. *Impacts of Ultraviolet Radiation on Interactions Between Plants and Herbivorous Insects: A Chemo-Ecological Perspective*, Springer.

KUHNERT, N., JAISWAL, R., MATEI, M. F., SOVDAT, T. & DESHPANDE, S. 2010. How to Distinguish Between Feruloyl Quinic Acids and Isoferuloyl Quinic Acids by Liquid Chromatography/ Tandem Mass Spectrometry. *Rapid Communications In Mass Spectrometry,* 24**,** 1575-1582.

KUSANO, M., TOHGE, T., FUKUSHIMA, A., KOBAYASHI, M., HAYASHI, N., OTSUKI, H., KONDOU, Y., GOTO, H., KAWASHIMA, M., MATSUDA, F., NIIDA, R., MATSUI, M., SAITO, K. & FERNIE, A. R. 2011. Metabolomics Reveals Comprehensive Reprogramming Involving Two Independent Metabolic Responses of Arabidopsis to UV-B Light. *The Plant Journal,* 67**,** 354-369.

KUŚNIERCZYK, A., TRAN, D. H. T., WINGE, P., JØRSTAD, T. S., REESE, J. C., TROCZYŃSKA, J. & BONES, A. M. 2011. Testing the importance of jasmonate signalling in induction of plant defences upon cabbage aphid (Brevicoryne brassicae) attack. *BMC Genomics,* 12.

LAGARIAS, J. C. & RAPOPORT, H. 1980. Chromopeptides from Phytochrome. The Structure and Linkage of the PR Form of the Phytochrome Chromophore. *Journal of the American Chemical Society,* 102**,** 4821-4828.

LANDRY, L. C., CHAPPLE, C. C. S. & LAST, R. L. 1995. Arabidopsis Mutants Lacking Phenolic Sunscreens Exhibit Enhanced Ultraviolet-B lnjury and Oxidative Damage. *Plant Physiology,* 109**,** 1159-1166.

LATTANZIO, V. & CARDINALI, A. 2006. Role of Polyphenols in the Resistance Mechanisms of Plants Against Fungal Pathogens and Insects. *Phytochemistry,* 37/661**,** 23-67.

LAVOLA, A., JULKUNEN-TIITTOS, R., APHALO, P., DE LA ROSA, T. & LEHTO, T. 1997. The Effect of U.V.-B Radiation on U.V.-Absorbing Secondary Metabolites in Birch Seedlings Grown under Simulated Forest Soil Conditions. *New Phytologist,* 137**,** 617-621.

LAVOLA, A. 1998. Accumulation of Flavonoids and Related Compounds in Birch Induced by UV-B Irradiance. *Tree Physiology,* 18**,** 53-58.

LAWRENCE, S. D., NOVAK, N. G., JONES, R. W., FARRAR, J. R. R. & BLACKBURN, M. B. 2014. Herbivory responsive C2H2 zinc finger transcription factor protein StZFP2 from potato. *Plant Physiology and Biochemistry,* 80**,** 226-233.

LEITNER, M., BOLAND, W. & MITHÖFER, A. 2005. Direct and Indirect Defences Induced by Piercing-Sucking and Chewing Herbivores in *Medicago truncatula*. *New Phytologist,* 167**,** 597-606.

LEON, J., ROJO, E. & SANCHEZ-SERRANO, J. J. 2001. Wound Signalling in Plants. *Journal of Experimental Botany,* 52**,** 1-9.

LEVIN, D. A. 1976. The Chemical Defenses of Plants to Pathogens and Herbivores. *Annual Review of Ecology and Systematics,* 7**,** 121-159.

LI, J., OU-LEE, T.-M., RABA, R., AMUNDSON, R. G. & LAST, R. L. 1993. Arabidopsis Flavonoid Mutants are Hypersensitive to UV-6 lrradiation. *The Plant Cell,* 5**,** 171-179.

LI, Q.-H. & YANG, H.-Q. 2007. Cryptochrome Signaling in Plants. *Photochemistry and Photobiology,* 83**,** 94-101.

LI, X.-L., YANG, X., HU, Y.-X., YU, X.-D. & LI, Q. L. 2014. A Novel NAC Transcription Factor From Suaeda Liaotungensis K. Enhanced Transgenic Arabidopsis Drought, Salt, And Cold Stress Tolerance. *Plant Cell Reports,* 33**,** 767-778.

LIANG, Y.-S., CHOI, Y. H., KIM, H. K., LINTHORST, H. J. M. & VERPOORTE, R. 2006a. Metabolomic Analysis of Methyl Jasmonate Treated *Brassica rapa* Leaves by 2-Dimensional NMR Spectroscopy. *Phytochemistry,* 67**,** 2503-2511.

LIANG, Y.-S., KIM, H. K., LEFEBER, A. W. M., ERKELENS, C., CHOI, Y. H. & VERPOORTE, R. 2006b. Identification of Phenylpropanoids in Methyl Jasmonate Treated *Brassica rapa* Leaves Using Two-Dimensional Nuclear Magnetic Resonance Spectroscopy. *Journal of Chromatography A,* 1112**,** 148-155.

LIM, E.-K., LI, Y., PARR, A., JACKSON, R., ASHFORD, D. A. & BOWLES, D. J. 2001. Identification of Glucosyltransferase Genes Involved in Sinapate Metabolism and Lignin Synthesis in Arabidopsis. *THE JOURNAL OF BIOLOGICAL CHEMISTRY,* 276**,** 4344-4349.

LIN, C. 2000. Plant Blue-Light Receptors. *TRENDS in Plant Science,* 5**,** 337-342.

LIN, C., AHMAD, M. & CASHMORE, A. R. 2002. Arabidopsis Cryptochrome 1 is a Soluble Protein Mediating Blue Light-Dependent Regulation of Plant Growth and Development. *The Plant Journal,* 10**,** 893-902.

LINSTER, C. L., GOMEZ, T. A., CHRISTENSEN, K. C., ADLER, L. N., YOUNG, B. D., BRENNER, C. & CLARKE, S. G. 2007. Arabidopsis VTC2 Encodes a GDP-L-Galactose Phosphorylase, the Last Unknown Enzyme in the Smirnoff-Wheeler Pathway to Ascorbic Acid in Plants. *Journal Of Biological Chemistry,* 282**,** 18879-18885.

LISCUM, E., HODGSON, D. W. & CAMPBELL, T. J. 2003. Blue Light Signaling through the Cryptochromes and Phototropins. So That's What the Blues Is All About. *Plant Physiology,* 133**,** 1429-1436.

LOIS, R. 1994. Accumulation of UV-absorbing flavonoids induced by UV-B radiation in Arabidopsis thaliana L. I. Mechanisms of UV-resistance in Arabidopsis. *Planta,* 194.

LORENZO, O., PIQUERAS, R., SÁNCHEZ-SERRANO, J. J. & SOLANO, R. 2003. ETHYLENE RESPONSE FACTOR1 Integrates Signals from Ethylene and Jasmonate Pathways in Plant Defense. *The Plant Cell,* 15**,** 165-178.

LORENZO, O., CHICO, J. M., SANCHEZ-SERRANO, J. J. & SOLANO, R. 2004. JASMONATE-INSENSITIVE1 Encodes a MYC Transcription Factor Essential to Discriminate between Different Jasmonate-Regulated Defense Responses in Arabidopsis. *The Plant Cell,* 16**,** 1938-1950.

MAEDA, K., KIMURA, S., DEMURA, T., TAKEDA, J. & OZEKI, Y. 2005. DcMYB1 acts as a Transcriptional Activator of the Carrot Phenylalanine Ammonia-Lyase Gene (*DcPAL1*) in Response to Elicitor Treatment, UV-B Irradiation and the Dilution Effect. *Plant Molecular Biology,* 59**,** 739-752.

MAHMOUD, S. S. & CROTEAU, R. B. 2002. Strategies for Transgenic Manipulation of Monoterpene Biosynthesis in Plants. *TRENDS in Plant Science,* 7**,** 366-373.

MARQUEZ, L. A., DUNFORD, H. B. & VAN WART, H. 1989. Kinetic Studies on the Reaction of Compound II of Myeloperoxidase with Ascorbic Acid. *The Journal of Biological Chemistry,* 265**,** 5666-5670.

MAZZA, C. A., IZAGUIRRE, M. M., ZAVALA, J., SCOPEL, A. L. & BALLARE, C. L. 2002. Insect perception of ambient ultraviolet-B radiation. *Ecology Letters,* 5**,** 722-726.

MAZZA, C. A., IZAGUIRRE, M. M., CURIALE, J. & BALLARE, C. L. 2009. A look into the invisible: ultraviolet-B sensitivity in an insect (Caliothrips phaseoli) revealed through a behavioural action spectrum. *Proceedings of the Royal Society B,* 282.

MCKENZIE, R. L., BJÖRN, L. O., BAIS, A. & ILYASD, M. 2003. Changes in biologically active ultraviolet radiation reaching the Earth's surface. *Photochemical & Photobiological Sciences,* 2**,** 5-15.

MEWIS, I., TOKUHISA, J. G., SCHULTZ, J. C., APPEL, H. M., ULRICHS, C. & GERSHENZON, J. 2006. Gene Expression and Glucosinolate Accumulation in *Arabidopsis Thaliana* in Response to Generalist and Specialist Herbivores of Different Feeding Guilds and the Role of Defense Signaling Pathways. *Phytochemistry,* 67**,** 2450-2462.

MEWIS, I., SCHREINER, M., NGUYEN, C. N., KRUMBEIN, A., ULRICHS, C., LOHSE, M. & ZRENNER, R. 2012. UV-B Irradiation Changes Specifically the Secondary Metabolite Profile in Broccoli Sprouts: Induced Signaling Overlaps with Defense Response to Biotic Stressors. *Plant Cell Physiology,* 53**,** 1546-1560.

MIKKELSEN, M. D., HANSEN, C. H., WITTSTOCK, U. & HALKIER, B. A. 2000. Cytochrome P450 CYP79B2 from Arabidopsis Catalyzes the Conversion of Tryptophan to Indole-3-acetaldoxime, a Precursor of Indole Glucosinolates and Indole-3-acetic Acid. *THE JOURNAL OF BIOLOGICAL CHEMISTRY,* 275**,** 33712-33717.

MIKKELSEN, M. D., PETERSEN, B. L., GLAWISCHNIG, E., JENSEN, A. B., ANDREASSON, E. & HALKIER, B. A. 2003. Modulation of CYP79 Genes and Glucosinolate Profiles in Arabidopsis by Defense Signaling Pathways. *Plant Physiology,* 131**,** 298-308.

MITHEN, R. 2001. Glucosinolates – Biochemistry, Genetics and Biological Activity. *Plant Growth Regulation,* 34**,** 91-103.

MITHOFER, A. & BOLAND, W. 2012. Plant Defense Against Herbivores: Chemical Aspects. *Annual Review of Plant Biology,* 64**,** 431-450.

MITTLERA, R., KIM, Y., SONG, L., COUTU, J., COUTU, A., CIFTCI-YILMAZ, S., LEE, H., STEVENSON, B. & ZHU, J.-K. 2006. Gain- and loss-of-function mutations in Zat10 enhance the tolerance of plants to abiotic stress. *FEBS Letters,* 580**,** 6537-6542.

MIYAZAKI, Y., TAKASE, T. & KIYOSUE, T. 2015. ZEITLUPE Positively Regulates Hypocotyl Elongation at Warm Temperature Under Light in *Arabidopsis thaliana*. *Plant Signaling & Behavior,* 10.

MONDE, K., SATOH, H., NAKAMURA, M., TAMURA, M. & TAKASUGI, M. 1998. Organochlorine Compounds from a Terrestrial Higher Plant: Structures and Origin of Chlorinated Orcinol Derivatives from Diseased Bulbs of Lilium maximowiczii. *Journal of Natural Products,* 61**,** 913-921.

MORALES, L. O., TEGELBERG, R., BROSCHE, M., KEINÄNEN, M., LINDFORS, A. & APHALO, P. J. 2010. Effects of Solar UV-A and UV-B Radiation on Gene Expression and Phenolic Accumulation in *Betula pendula* Leaves. *Tree Physiology,* 30**,** 923-934.

MORALES, L. O., BROSCHÉ, M., VAINONEN, J., JENKINS, G. I., WARGENT, J. J., SIPARI, N., STRID, A., LINDFORS, A. V., TEGELBERG, R. & P.J., A. 2013. Multiple Roles for UV RESISTANCE LOCUS8 in Regulating Gene Expression and Metabolite Accumulation in Arabidopsis under Solar Ultraviolet Radiation. *Plant Physiology,* 161**,** 744-759.

MORAN, P. J. & THOMPSON, G. A. 2001. Molecular Responses to Aphid Feeding in Arabidopsis in Relation to Plant Defense Pathways. *Plant Physiology,* 125**,** 1074-1085.

MULLER-MOULE, P. 2008. An Expression Analysis of the Ascorbate Biosynthesis Enzyme VTC2. *Plant Molecular Biology,* 68**,** 31-41.

NAKAGAWA, T., KUROSE, T., HINO, T., TANAKA, K., KAWAMUKAI, M., NIWA, Y., TOYOOKA, K., MATSUOKA, K., JINBO, T. & KIMURA, T. 2007. Development of Series of Gateway Binary Vectors, pGWBs, for Realizing Efficient Construction of Fusion Genes for Plant Transformation. *Journal of Bioscience and Bioengineering,* 104**,** 34-41.

NOMURA, H., KOMORI, T., UEMURA, S., KANDA, Y., SHIMOTANI, K., NAKAI, K., FURUICHI, T., TAKEBAYASHI, K., SUGIMOTO, T., SANO, S., SUWASTIKA, I. N., FUKUSAKI, E., YOSHIOKA, H., NAKAHIRA, Y. & SHIINA, T. 2012. Chloroplast-mediated activation of plant immune signalling in Arabidopsis. *Nature Communications,* 3.

NORVAL, M., CULLEN, A. P., DE GRUIJL, F. R., LONGSTRETH, J., TAKIZAWA, Y., LUCAS, R. M., NOONANG, F. P. & VAN DER LEUN, J. C. 2007. The effects on human health from stratospheric ozone depletion and its interactions with climate change. *Photochemical & Photobiological Sciences,* 6**,** 232-251.

NUNES-NESI, A., CARRARI, F., LYTOVCHENKO, A., SMITH, A. M. O., LOUREIRO, M. E., RATCLIFFE, R. G., SWEETLOVE, L. J. & FERNIE, A. R. 2005. Enhanced Photosynthetic Performance and Growth as a Consequence of Decreasing Mitochondrial Malate Dehydrogenase Activity in Transgenic Tomato Plants. *Plant Physiology,* 137**,** 611-622.

O'DONNELL, P. J., CALVERT, C., ATZORN, R., WASTERNACK, C., LEYSER, H. M. O. & BOWLES, D. J. 1996. Ethylene as a Signal Mediating the Wound Response of Tomato Plants. *Science,* 274**,** 1914-1917.

O'HARA, A. & JENKINS, G. I. 2012. In Vivo Function of Tryptophans in the Arabidopsis UV-B Photoreceptor UVR8. *The Plant Cell,* 24**,** 3755-3766.

OHNISHI, T., SUGAHARA, S., YAMADA, T., KIKUCHI, K., YOSHIBA, Y., HIRANO, H. Y. & TSUTSUMI, N. 2005. OsNAC6, a member of the NAC gene family, is induced by various stresses in rice. *Genes & Genetic Systems,* 80**,** 135-139.

ORAVECZ, A., BAUMANN, A., MÁTÉ, Z., BRZEZINSKA, A., MOLINIER, J., OAKELEY, E. J., ÁDÁM, E., SCHÄFER, E., NAGY, F. & R, ULM. 2006. CONSTITUTIVELY PHOTOMORPHOGENIC1 Is Required for the UV-B Response in Arabidopsis. *The Plant Cell,* 18**,** 1975-1990.

OSTERLUND, M. T., WEI, N. & DENG, X. W. 2000. The Roles of Photoreceptor Systems and the COP1-Targeted Destabilization of HY5 in Light Control of Arabidopsis Seedling Development. *Plant Physiology,* 124**,** 1520-1524.

PANDEY, S. P., ROCCARO, M., SCHON, M., LOGEMANN, E. & SOMSSICH, I. E. 2010. Transcriptional reprogramming regulated by WRKY18 and WRKY40 facilitates powdery mildew infection of Arabidopsis. *The Plant Journal,* 64**,** 912-923.

PASTORI, G. M. & FOYER, C. H. 2002. Common Components, Networks, and Pathways of Cross- Tolerance to Stress. The Central Role of "Redox" and Abscisic Acid-Mediated Controls. *Plant Physiology,* 129**,** 460-468.

PENG, M., HUDSON, D., SCHOFIELD, A., TSAO, R., YANG, R., GU, H., BI, Y. M. & ROTHSTEIN, S. J. 2008. Adaptation of Arabidopsis to nitrogen limitation involves induction of anthocyanin synthesis which is controlled by the NLA gene. *Journal of Experimental Botany,* 59**,** 2933-2944.

PENNINCKX, I. A. M. A., THOMMA, B. P. H. J., BUCHALA, A., MÉTRAUX, J.-P. & BROEKAERT, W. F. 1998. Concomitant Activation of Jasmonate and Ethylene Response Pathways Is Required for Induction of a Plant Defensin Gene in Arabidopsis. *The Plant Cell,* 10**,** 2103-2113.

POKORNY, R., KLAR, T., HENNECKE, U., CARELL, T., BATSCHAUER, A. & ESSEN, L.-O. 2008. Recognition and Repair of UV Lesions in Loop Structures of Duplex DNA by DASH-Type Cryptochrome. *Proceedings of the National Academy of Sciences,* 105**,** 21023-21027.

POSCHENRIEDER, C., TOLRÀ, R. & BARCELÓ, J. 2006. Can metals defend plants against biotic stress? *TRENDS in Plant Science,* 11**,** 288-295.

QUIRANTES-PINÉ, R., FUNES, L., MICOL, V., SEGURA-CARRETERO, A. & FERNÁNDEZ-GUTIÉRREZ, A. 2009. High-Performance Liquid Chromatography with Diode Array Detection Coupled to Electrospray Time-Of-Flight and Ion-Trap Tandem Mass Spectrometry to Identify Phenolic Compounds from a Lemon Verbena Extract. *Journal of Chromatography A,* 1216**,** 5391-5397.

RALPH, J., LAPIERRE, C., MARITA, J. M., KIM, H., LU, F., HATFIELD, R. D., RALPH, S., CHAPPLE, C., FRANKE, R., HEMM, M. R., VAN DOORSSELAER, J., SEDEROF, R. R., O'MALLEY, D. M., SCOTT, J. T., MACKAY, J. J., YAHIAOUI, N., BOUDET, A. M., PEAN, M., PILATE, G., JOUANIN, L. & BOERJAN, W. 2001. Elucidation of New Structures in Lignins of CAD- and COMT-Deficient Plants by NMR. *Phytochemistry,* 57**,** 993-1003.

RALPH, S. G., YUEH, H., FRIEDMANN, M., AESCHLIMAN, D., ZEZNIK, J. A., NELSON, C. C., BUT- TERFIELD, Y. S. N., KIRKPATRICK, R., LIU, J., JONES, S. J. M., MARRA, M. A., DOUGLAS, C. J., RIT- LAND, K. & BOHLMANN, J. 2006. Conifer defence against insects: Microarray gene expression profiling of Sitka spruce (Picea sitchensis) induced by mechanical wound- ing or feeding by spruce budworms (Choristoneura occidentalis) or white pine wee- vils (Pissodes strobi) reveals large-scale changes of the host transcriptome. *Plant Cell and Environment,* 29**,** 1545-1570.

RAVIV, M. & ANTIGNUS, Y. 2004. UV Radiation Effects on Pathogens and Insect Pests of Greenhouse-Grown Crops. *Photochemistry and Photobiology,* 79**,** 219-226.

REHRIG, E. M., APPEL, H. M., JONES, A. D. & SCHULTZ, J. C. 2014. Roles For Jasmonate- And Ethylene-Induced Transcription Factors In The Ability Of Arabidopsis To Respond Differentially To Damage Caused By Two Insect Herbivores. *Frontiers in Plant Science,* 5.

RENWICK, J. A. A. & LOPEZ, K. 1999. Experience-Based Food Consumption by Larvae of *Pieris rapae*: Addiction to Glucosinolates? *Entomologia Experimentalis et Applicata,* 91**,** 51-58.

REYMOND, P. & FARMER, E. E. 1998. Jasmonate and Salicylate as Global Signals for Defense Gene Expression. *Current Opinion in Plant Biology,* 1**,** 404-411.

REYMOND, P., WEBER, H., DAMOND, M. & FARMER, E. E. 2000. Differential Gene Expression in Response to Mechanical Wounding and Insect Feeding in Arabidopsis. *The Plant Cell,* 12**,** 707-719.

REYMOND, P., BODENHAUSEN, N., VAN POECKE, R. M. P., KRISHNAMURTHY, V., DICKE, M. & FARMER, E. E. 2004. A Conserved Transcript Pattern in Response to a Specialist and a Generalist Herbivore. *The Plant Cell,* 16**,** 3123-3147.

RISCHER, H., ORESIC, M., SEPPANEN-LAAKSO, T., KATAJAMAA, M., LAMMERTYN, F., ARDILES-DIAZ, W., VAN MONTAGU, M. C. E., INZE, D., OKSMAN-CALDENTEY, K.-M. & GOOSSENS, A. 2006. Gene-to-Metabolite Networks for Terpenoid Indole Alkaloid Biosynthesis in Catharanthus roseus Cells. *Proceedings of the National Academy of Sciences,* 103**,** 5614-5619.

RIZZINI, L., FAVORY, J. J., CLOIX, C., FAGGIONATO, D., O'HARA, A., KAISERLI, E., BAUMEISTER, R., SCHÄFER, E., NAGY, F., JENKINS, G. I. & ULM, R. 2011. Perception of UV-B by the Arabidopsis UVR8 Protein. *Science,* 332**,** 103-106.

ROBERT-SEILANIANTZ, A., NAVARRO, L., BARI, R. & JONES, J. D. G. 2007. Pathological hormone imbalances. *Current Opinion in Plant Biology,* 10**,** 372-379.

ROBERTS, M. R. & PAUL, N. D. 2006. Seduced by the dark side: integrating molecular and ecological perspectives on the influence of light on plant defence against pests and pathogens. *New Phytologist,* 170**,** 677-699.

ROCKWELL, N. C., SU, Y.-S. & LAGARIAS, J. C. 2006. Phytochome Structure and Signaling Mechanisms. *Annual Review of Plant Biology,* 57**,** 837-858.

ROJO, E., LEÓN, J. & SÁNCHEZ-SERRANO, J. J. 1999. Cross-Talk between Wound Signalling Pathways Determines Local Versus Systemic Gene Expression in *Arabidopsis thaliana*. *The Plant Journal,* 20**,** 135-142.

ROUSSEAUX, M. C., BALLARE, C. L., SCOPEL, A. L., SEARLES, P. S. & CALDWELL, M. M. 1998. Solar ultraviolet-B radiation affects plant-insect interactions in a natural ecosystem of Tierra del Fuego (southern Argentina). *Oecologia,* 116**,** 528-535.

ROUSSEAUX, M. C., SCOPEL, A. L., SEARLES, P. S., CALDWELL, M. M., SALA, O. E. & BALLARE, C. L. 2001. Responses to Solar Ultraviolet-B Radiation in a Shrub-Dominated Natural Ecosystem of Tierra del Fuego (Southern Argentina). *Global Change Biology,* 7**,** 467-478.

ROUSSEAUX, M. C., JULKUNEN-TIITTO, R., SEARLES, P. S., SCOPEL, A. L., APHALO, P. J. & BALLARÉ, C. L. 2004. Solar UV-B radiation affects leaf quality and insect herbivory in the southern beech tree Nothofagus antarctica. *Oecologia,* 138**,** 505-512.

RUEGGER, M., MEYER, K., CUSUMANO, J. C. & CHAPPLE, C. 1999. Regulation of Ferulate-5-Hydroxylase Expression in Arabidopsis in the Context of Sinapate Ester Biosynthesis. *Plant Physiology,* 119**,** 101-110.

RYAN, C. A. 1990. PROTEASE INHIBITORS IN PLANTS: Genes for Improving Defenses Against Insects and Pathogens. *Annual Review of Phytopathology,* 28**,** 425-449.

SASAKI-SEKIMOTO, Y., TAKI, N., OBAYASHI, T., AONO, M., MATSUMOTO, F., SAKURAI, N., SUZUKI, H., HIRAI, M. Y., NOJI, M., SAITO, K., MASUDA, T., TAKAMIYA, K.-I., SHIBATA, D. & OHTA, H. 2005. Coordinated activation of metabolic pathways for antioxidants and defence compounds by jasmonates and their roles in stress tolerance in Arabidopsis. *The Plant Journal,* 44**,** 653-668.

SAXENA, D. & STOTZKY, G. 2001. Bt corn has a higher lignin content than non-bt corn. *American Journal of Botany,* 88**,** 1704-1706.

SCHALLER, F. 2001. Enzymes of the Biosynthesis of Octadecanoid-Derived Signalling Molecules. *Journal of Experimental Botany,* 52**,** 11-23.

SCHLAEPPI, K., BODENHAUSEN, N., BUCHALA, A., MAUCH, F. & REYMOND, P. 2008. The Glutathione-Deficient Mutant pad2-1 Accumulates Lower Amounts of Glucosinolates and is More Susceptible to the Insect Herbivore Spodoptera Littoralis. *The Plant Journal,* 55**,** 774-786.

SCHMELZER, E., KRÜGER-LEBUS, S. & HAHLBROCK, K. 1989. Temporal and Spatial Patterns of Gene Expression around Sites of Attempted Funga1 lnfection in Parsley Leaves. *The Plant Cell,* 1**,** 993-1001.

SCHMITTGEN, T. D. & LIVAK, K. J. 2008. Analyzing real-time PCR data by the comparative CT method. *Nature Protocols,* 3**,** 1101-1108.

SCHWANDER, H., MAYER, B., RUGGABER, A., ALBOLD, A., SECKMEYER, G. & KOEPKE, P. 1999. Method To Determine Snow Albedo Values In The Ultraviolet For Radiative Transfer Modeling. *APPLIED OPTICS* 38**,** 3869-3875.

SENTHIL-KUMAR, M. & MYSORE, K. S. 2012. Ornithine-delta-aminotransferase and proline dehydrogenase genes play a role in non-host disease resistance by regulating pyrroline-5-carboxylate metabolism-induced hypersensitive response. *Plant, Cell and Environment,* 35**,** 1329-1343.

SEO, H. S., SONG, J. T., CHEONG, J.-J., LEE, Y.-H., LEE, Y. W., HWANG, I., LEE, J. S. & CHOI, Y. D. 2001. Jasmonic Acid Carboxyl Methyltransferase: A Key Enzyme for Jasmonate-Regulated Plant Responses. *Proceedings of the National Academy of Sciences,* 98**,** 4788-4793.

SERHAN, C. N., GOTLINGER, K., HONG, S. & ARITA, M. 2004. Resolvins, Docosatrienes, and Neuroprotectins, Novel Omega-3-Derived Mediators, and their Aspirin-Triggered Endogenous Epimers: An Overview of their Protective Roles in Catabasis. *Prostaglandins & Other Lipid Mediators,* 73**,** 155-172.

SHADLE, G. L., WESLEY, S. V., KORTH, K. L., CHEN, F., LAMB, C. & DIXON, R. A. 2003. Phenylpropanoid Compounds and Disease Resistance in Transgenic Tobacco with Altered Expression of L-Phenylalanine Ammonia-Lyase. *Phytochemistry,* 64**,** 153-161.

SHI, H., WANG, X., YE, T., CHEN, F., DENG, J., YANG, P., ZHANG, Y. & CHAN, Z. 2014. The Cys2/His2-type zinc finger transcription factor ZAT6 modulates biotic and abiotic stress responses by activating salicylic acid-related genes and CBFs in Arabidopsis. *Plant Physiology,* 165**,** 1367-1379.

SHINKLE., J. R., ATKINS, A. K., HUMPHREY, E. E., RODGERS, C. W., WHEELER, S. L. & BARNES, P. W. 2004. Growth and Morphological Responses to Different UV Wavebands in Cucumber (*Cucumis Sativum*) and Other Dicotyledonous Seedlings. *PHYSIOLOGIA PLANTARUM,* 120**,** 240-248.

SHIRLEY, B. W., KUBASEK, W. L., STORZ, G., BRUGGEMANN, E., KOORNNEEF, M., AUSUBEL, F. M. & GOODMAN, H. M. 1995. Analysis of Arabidopsis Mutants Deficient in Flavonoid Biosynthesis. *The Plant Journal,* 8**,** 659-671.

SMIRNOFF, N. & WHEELER, G. L. 2000. Ascorbic Acid in Plants: Biosynthesis and Function. *Critical Reviews in Biochemistry and Molecular Biology,* 35**,** 291-314.

SPOEL, S. H., JOHNSON, J. S. & DONG, X. 2007. Regulation of Tradeoffs Between Plant Defenses Against Pathogens with Different Lifestyles. *Proceedings of the National Academy of Sciences,* 104**,** 18842-18847.

STASWICK, P. E. & TIRYAKI, I. 2004. The Oxylipin Signal Jasmonic Acid Is Activated by an Enzyme That Conjugates It to Isoleucine in Arabidopsis. *The Plant Cell,* 16**,** 2117-2127.

STOTZ, H. U., PITTENDRIGH, B. R., KROYMANN, J., WENIGER, K., FRITSCHE, J., BAUKE, A. & MITCHELL-OLDS, T. 2000. Induced Plant Defense Responses against Chewing Insects. Ethylene Signaling Reduces Resistance of Arabidopsis against Egyptian Cotton Worm But Not Diamondback Moth. *Plant Physiology,* 124**,** 1007-1017.

STOUT, J. & CHAPPLE, C. 2004. Chapter Three: The Phenylpropanoid Pathway in Arabidopsis: Lessons Learned from Mutants in Sinapate Ester Biosynthesis. *Recent Advances in Phytochemistry,* 38**,** 39-67.

STRACKE, R., ISHIHARA, H., HUEP, G., BARSCH, A., MEHRTENS, F., NIEHAUS, K. & WEISSHAAR, B. 2007. Differential Regulation of Closely Related R2R3-Myb Transcription Factors Controls Flavonol Accumulation in Different Parts of the *Arabidopsis thaliana* Seedling. *The Plant Journal,* 50**,** 660-677.

STRACKE, R., FAVORY, J.-J., GRUBER, H., BARTELNIEWOEHNER, L., BARTELS, S., BINKERT, M., FUNK, M., WEISSHAAR, B. & ULM, R. 2010a. The Arabidopsis bzip Transcription Factor HY5 Regulates Expression of the *PFG1/MYB12* Gene in Response to Light and Ultraviolet-B Radiation. *Plant, Cell and Environment,* 33**,** 88-103.

STRACKE, R., JAHNS, O., KECK, M., TOHGE, T., NIEHAUS, K., FERNIE, A. R. & WEISSHAAR, B. 2010b. Analysis of PRODUCTION OF FLAVONOL GLYCOSIDES-dependent flavonol glycoside accumulation in Arabidopsis thaliana plants reveals MYB11-, MYB12- and MYB111-independent flavonol glycoside accumulation. *New Phytologist,* 188**,** 985-1000.

STRATMANN, J. W., STELMACH, B. A., WEILER, E. W. & RYAN, C. A. 2000. UVB/UVA Radiation Activates a 48 kDa Myelin Basic Protein Kinase and Potentiates Wound Signaling in Tomato Leaves. *Photochemistry and Photobiology,* 71**,** 116-123.

STRID, Å., CHOW, W. S. & ANDERSON, J. M. 1994. UV-B Damage and Protection at the Molecular Level in Plants. *Photosynthesis Research,* 39**,** 475-489.

SUZA, W. P., AVILA, C. A., CARRUTHERS, K., KULKARNI, S., GOGGIN, F. L. & LORENCE, A. 2010. Exploring the Impact of Wounding and Jasmonates on Ascorbate Metabolism. *Plant Physiology and Biochemistry,* 48**,** 337-350.

TAIZ, L. & ZEIGER, E. 2002. Photosynthesis: Physiological and Ecological Considerations. *Plant physiology. Sinauer Associates: Sunderland, MA. 3rd ed.***,** 172-174.

TAKEMIYA, A., INOUE, S.-I., DOI, M., KINOSHITA, T. & SHIMAZAKI, K.-I. 2005. Phototropins Promote Plant Growth in Response to Blue Light in Low Light Environments. *The Plant Cell,* 17**,** 1120-1127.

TAKEUCHI, Y., IKEDA, S. & KASA, H. 1993. Dependence on Wavelength and Temperature of Growth Inhibition Induced by UV-B Irradiation. *Plant Cell Physiology* 34**,** 913-917

TATTINI, M., GALARDI, C., PINELLI, P., MASSAI, R., REMORINI, D. & AGATI, G. 2004. Differential Accumulation of Flavonoids and Hydroxycinnamates in Leaves of Ligustrum Vulgare Under Excess Light and Drought Stress. *New Phytologist,* 163**,** 547-561.

THINES, B., KATSIR, L., MELOTTO, M., NIU, Y., MANDAOKAR, A., LIU, G., NOMURA, K., HE, S. Y., HOWE, G. A. & BROWSE, J. 2007. JAZ Repressor Proteins are Targets of the SCFcoi1 Complex During Jasmonate Signalling. *Nature,* 448**,** 661-666.

THOMPSON, G. A. & GOGGIN, F. L. 2006. Transcriptomics and Functional Genomics of Plant Defence Induction by Phloem-Feeding Insects. *Journal of Experimental Botany,* 57**,** 755-766.

TILBROOK, K., ARONGAUS, A. B., BINKERT, M., HEIJDE, M., YIN, R. & ULM, R. 2013. The UVR8 UV-B Photoreceptor: Perception, Signaling and Response. *The Arabidopsis Book/American Society of Plant Biologists.*

TRAPNELL, C., ROBERTS, A., GOFF, L., PERTEA, G., KIM, D., KELLEY, D. R., PIMENTEL, H., SALZBERG, S. L., RINN, J. L. & PACHTER, L. 2012. Differential gene and transcript expression analysis of RNA-seq experiments with TopHat and Cufflinks. *NATURE PROTOCOLS,* 7**,** 562-579.

TRICK, M., CHEUNG, F., DROU, N., FRASER, F., LOBENHOFER, E. K., HURBAN, P., MAGUSIN, A., TOWN, C. D. & BANCROFT, I. 2009. A newly-developed community microarray resource for transcriptome profiling in Brassica species enables the confirmation of Brassica-specific expressed sequences. *BMC Plant Biology,* 9.

TZAFRIR, I., PENA-MURALLA, R., DICKERMAN, A., BERG, M., ROGERS, R., HUTCHENS, S., SWEENEY, T. C., MCELVER, J., AUX, G., PATTON, D. & MEINKE, D. 2004. Identification of Genes Required for Embryo Development in Arabidopsis. *Plant Physiology,* 135**,** 1206-1220.

U, N. 1935. Genome analysis in Brassica with special reference to the experimental formation of B. napus and peculiar mode of fertilization. *Japan. J. Bot,* 7**,** 389-452.

ULM, R., BAUMANN, A., ORAVECZ, A., MATE, Z., ADAM, E., OAKELEY, E. J., SCHAFER, E. & NAGY, F. 2004. Genome-wide analysis of gene expression reveals function of the bZIP transcription factor HY5 in the UV-B response of Arabidopsis. *PNAS,* 101**,** 1397-1402.

VAN DER HOOFT, J. J. J., AKERMI, M., ÜNLÜ, F. Y., MIHALEVA, V., ROLDAN, V. G., BINO, R. J., DE VOS, R. C. H. & VERVOORT, J. 2012. Structural Annotation and Elucidation of Conjugated Phenolic Compounds in Black, Green, and White Tea Extracts. *Journal of Agricultural and Food Chemistry,* 60**,** 8841-8850.

VAN DER HOOFT, J. J. J., DE VOS, R. C. H., RIDDER, L., VERVOORT, J. & BINO, R. J. 2013. Structural Elucidation of Low Abundant Metabolites in Complex Sample Matrices. *Metabolomics,* 9**,** 1009-1018.

VANDENBORRE, G., SMAGGHE, G. & VAN DAMME, E. J. M. 2011. Plant lectins as defense proteins against phytophagous insects. *Phytochemistry,* 72**,** 1538-1550.

VANE, J. R. 2000. The Mechanism of Action of Anti-Inflammatory Drugs. *Advances in Eicosanoid Research (Ernst Schering Research Foundation Workshop),* 31**,** 1-23.
VICK, B. A. & ZIMMERMAN, D. C. 1984. Biosynthesis of Jasmonic Acid by Several Plant Species. *Plant Physiology,* 75**,** 458-461.

VIJAYAN, P., SHOCKEY, J., LÉVESQUE, C. A., COOK, R. J. & BROWSE, J. 1998. A Role for Jasmonate in Pathogen Defense of Arabidopsis. *Proceedings of the National Academy of Sciences,* 95**,** 7209-7214.

VOELCKEL, C. & I.T., BALDWIN. 2004. Generalist And Specialist Lepidopteran Larvae Elicit Different Transcriptional Responses In Nicotiana Attenuata, Which Correlate With Larval FAC Profiles. *Ecology Letters,* 7**,** 770-775.

VOGT, T. 2010. Phenylpropanoid Biosynthesis. *Molecular Plant,* 3**,** 2-20.

VOS, M. D., VAN OOSTEN, V. R., VAN POECKE, R. M. P., VAN PELT, J. A., POZO, M. J., MUELLER, M. J., BUCHALA, A. J., MÉTRAUX, J.-P., VAN LOON, L. C., DICKE, M. & PIETERSE, C. M. J. 2005. Signal Signature and Transcriptome Changes of Arabidopsis During Pathogen and Insect Attack. *Molecular Plant-Microbe Interactions,* 18**,** 923-937.

WANG, H., HAO, J., CHEN, X., HAO, Z., WANG, X., LOU, Y., PENG, Y. & GUO, Y. 2007. Overexpression of Rice WRKY89 Enhances Ultraviolet B Tolerance and Disease Resistance in Rice Plants. *Plant Molecular Biology,* 65**,** 799-815.

WARREN, J. M., BASSMAN, J. H., FELLMAN, J. K., MATTINSON, D. S. & EIGENBRODE, S. 2003. Ultraviolet-B Radiation Alters Phenolic Salicylate and Flavonoid Composition of *Populus trichocarpa* Leaves. *Tree Physiology,* 23**,** 527-535.

WASTERNACK, C. & PARTHIER, B. 1997. Jasmonate-signalled plant gene expression. *TRENDS in Plant Science,* 2**,** 302-307.

WEI, X., ZHANG, X., SHEN, D., WANG, H., WU, Q., LU, P., QIU, Y., SONG, J., ZHANG, Y. & LI, X. 2013. Transcriptome Analysis of Barbarea vulgaris Infested with Diamondback Moth (Plutella xylostella) Larvae. *PLoS ONE,* 8.

WHETTEN, R. & SEDEROFF, R. 1991. Genetic engineering of wood. *Forest Ecology and Management,* 43**,** 301-316.

WIDARTO, H. T., VAN DER MEIJDEN, E., LEFEBER, A. W. M., ERKELENS, C., KIM, H. K., CHOI, Y. H. & VERPOORTE, R. 2006. Metabolomic Differentiation of *Brassica rapa* Following Herbivory by Different Insect Instars using Two-Dimensional Nuclear Magnetic Resonance Spectroscopy. *Journal of Chemical Ecology,* 32**,** 2417-2428.

WILLIS, J. C., BOHAN, D. A., CHOI, Y. H., CONRAD, K. F. & SEMENOV, M. A. 2006. Use of an Individual-Based Model to Forecast the Effect of Climate Change on the Dynamics, Abundance and Geographical Range of the Pest Slug Deroceras Reticulatum in the UK. *Global Change Biology,* 12**,** 1643-1657.

WINKEL, B. S. J. 2006. The Biosynthesis of Flavonoids. *The Science of Flavonoids***,** 71-95.

WINKEL-SHIRLEY, B. 2002. Biosynthesis of flavonoids and effects of stress. *Current Opinion in Plant Biology* 5**,** 218-223.
WIRSING, L., NAUMANN, K. & VOGT, T. 2011. Arabidopsis Methyltransferase Fingerprints by Affinity-Based Protein Profiling. *Analytical Biochemistry,* 408**,** 220-225.

WITTSTOCK, U. & GERSHENZON, J. 2002. Constitutive Plant Toxins and Their Role in Defense Against Herbivores and Pathogens. *Current Opinion in Plant Biology,* 5**,** 300-307.

WU, D., HU, Q., YAN, Z., CHEN, W., YAN, C., HUANG, X., ZHANG, J., YANG, P., DENG, H., WANG, J., DENG, X. W. & SHI, Y. 2012. Structural basis of ultraviolet-B perception by UVR8. *Nature,* 484**,** 214-219.

XU, Y. H., WANG, J. W., WANG, S., WANG, J. Y. & CHEN, X. Y. 2004. *Plant Physiology,* 135**,** 507-515.

YANG, Y. & ANDERSON, E. J. 1999. Antimicrobial Activity of a Porcine Myeloperoxidase Against Plant Pathogenic Bacteria and Fungi. *Journal of Applied Microbiology,* 86**,** 211-220.

YAO, K., DE LUCA, V. & BRISSON, N. 1995. Creation of a Metabolic Sink for Tryptophan Alters the Phenylpropanoid Pathway and the Susceptibility of Potato to Phytophthora infestans. *The Plant Cell,* 7**,** 1787-1799.

ZALLER, J. G., SEARLES, P. S., M,, ROUSSEAUX, C., FLINT, S. D., CALDWELL, M. M., SALA, O., BALLARÉ, C. L. & SCOPEL, A. L. 2003. Solar ultraviolet-B radiation can affect slug feeding preference for some plant species native to a fen ecosystem in Tierra del Fuego, Argentina. *Plant Ecology,* 169.

ZANG, Y.-X., KIM, H. U., KIM, J. A., LIM, M.-H., JIN, M., LEE, S. C., KWON, S.-J., LEE, S.-I., HONG, J. K., PARK, T.-H., MUN, J.-H., SEOL, Y.-J., HONG, S.-B. & PARK, B.-S. 2009. Genome-Wide Identification of Glucosinolate Synthesis Genes in *Brassica rapa*. *FEBS Journal,* 276**,** 3559-3574.

ZAVALA, J. A., SCOPEL, A. L. & BALLARÉ, C. L. 2001. Effects of Ambient UV-B Radiation on Soybean Crops: Impact on Leaf Herbivory by *Anticarsia Gemmatalis*. *Plant Ecology,* 156**,** 121-130.

ZHENG, Z., QAMAR, S. A., CHEN, Z. & MENGISTE, T. 2006. Arabidopsis WRKY33 transcription factor is required forresistance to necrotrophic fungal pathogens. *The Plant Journal,* 48**,** 592-605.

ZHU-SALZMAN, K., SALZMAN, R. A., AHN, J. E. & KOIWA, H. 2004. Transcriptional Regulation of Sorghum Defense Determinants against a Phloem-Feeding Aphid. *Plant Physiology,* 134**,** 420-431.

ZIMMERMAN, D. C. & FENG, P. 1978. Characterization of a Prostaglandin-Like Metabolite of Linolenic Acid Produced by a Flaxseed Extract. *Lipids,* 13**,** 313-316.

ZOLMAN, B. K., YODER, A. & BARTEL, B. 2000. Genetic Analysis of Indole-3-butyric Acid Responses in Arabidopsis thaliana Reveals Four Mutant Classes. *Genetics,* 156**,** 1323-1337.